

Effective Shoulder Design and Maintenance



Final Report June 2007

Sponsored by
the Iowa Highway Research Board
(IHRB Project TR-531)
and
the Iowa Department of Transportation
(CTRE Project 05-198)



IOWA STATE
UNIVERSITY

About the PGA

The mission of the Partnership for Geotechnical Advancement is to increase highway performance in a cost-effective manner by developing and implementing methods, materials, and technologies to solve highway construction problems in a continuing and sustainable manner.

Disclaimer Notice

The contents of this report reflect the views of the authors, who are responsible for the facts and the accuracy of the information presented herein. The opinions, findings and conclusions expressed in this publication are those of the authors and not necessarily those of the sponsors.

The sponsors assume no liability for the contents or use of the information contained in this document. This report does not constitute a standard, specification, or regulation.

The sponsors do not endorse products or manufacturers. Trademarks or manufacturers' names appear in this report only because they are considered essential to the objective of the document.

Non-discrimination Statement

Iowa State University does not discriminate on the basis of race, color, age, religion, national origin, sexual orientation, gender identity, sex, marital status, disability, or status as a U.S. veteran. Inquiries can be directed to the Director of Equal Opportunity and Diversity, (515) 294-7612.

Technical Report Documentation Page

1. Report No. IHRB Project TR-531		2. Government Accession No.		3. Recipient's Catalog No.	
4. Title and Subtitle Effective Shoulder Design and Maintenance				5. Report Date June 2007	
				6. Performing Organization Code	
7. Authors David White, Mohamed Mekkawy, Charles Jahren, Duane Smith, and Muhannad Suleiman				8. Performing Organization Report No. CTRE Project 05-198	
9. Performing Organization Name and Address Center for Transportation Research and Education Iowa State University 2711 South Loop Drive, Suite 4700 Ames, IA 50010-8664				10. Work Unit No. (TRAIS)	
				11. Contract or Grant No.	
12. Sponsoring Organization Name and Address Iowa Highway Research Board Iowa Department of Transportation 800 Lincoln Way Ames, IA 50010				13. Type of Report and Period Covered Final Report	
				14. Sponsoring Agency Code	
15. Supplementary Notes					
16. Abstract Granular shoulders are an important element of the transportation system and are constantly subjected to performance problems due to wind- and water-induced erosion, rutting, edge drop-off, and slope irregularities. Such problems can directly affect drivers' safety and often require regular maintenance. The present research study was undertaken to investigate the factors contributing to these performance problems and to propose new ideas to design and maintain granular shoulders while keeping ownership costs low. This report includes observations made during a field reconnaissance study, findings from an effort to stabilize the granular and subgrade layer at six shoulder test sections, and the results of a laboratory box study where a shoulder section overlying a soft foundation layer was simulated. Based on the research described in this report, the following changes are proposed to the construction and maintenance methods for granular shoulders: <ul style="list-style-type: none"> • A minimum CBR value for the granular and subgrade layer should be selected to alleviate edge drop-off and rutting formation. • For those constructing new shoulder sections, the design charts provided in this report can be used as a rapid guide based on an allowable rut depth. The charts can also be used to predict the behavior of existing shoulders. • In the case of existing shoulder sections overlying soft foundations, the use of geogrid or fly ash stabilization proved to be an effective technique for mitigating shoulder rutting. 					
17. Key Words edge drop-off—geogrid—granular shoulders—rutting—shoulder stabilization				18. Distribution Statement No restrictions.	
19. Security Classification (of this report) Unclassified.		20. Security Classification (of this page) Unclassified.		21. No. of Pages 294	22. Price NA

EFFECTIVE SHOULDER DESIGN AND MAINTENANCE

**Final Report
June 2007**

Principal Investigator

David J. White

Associate Professor of Civil, Construction, and Environmental Engineering
Iowa State University

Co-Principal Investigators

Charles T. Jahren

Associate Professor of Civil, Construction, and Environmental Engineering
Iowa State University

Muhannad T. Suleiman

Lecturer in Civil, Construction, and Environmental Engineering
Iowa State University

Research Assistant

Mohamed Mekkawy
Iowa State University

Sponsored by
the Iowa Highway Research Board
(IHRB Project TR-531)

Preparation of this report was financed in part
through funds provided by the Iowa Department of Transportation
through its research management agreement with the
Center for Transportation Research and Education,
CTRE Project 05-198.

Center for Transportation Research and Education

Iowa State University

2711 South Loop Drive, Suite 4700

Ames, IA 50010-8664

Phone: 515-294-8103

Fax: 515-294-0467

www.ctre.iastate.edu

TABLE OF CONTENTS

ACKNOWLEDGMENTS	XVII
EXECUTIVE SUMMARY.....	XIX
INTRODUCTION.....	1
Research Objectives.....	1
Research Plan.....	1
LITERATURE REVIEW.....	3
Introduction.....	3
Shoulder Types	3
Initial Construction and Maintenance Costs	5
Current Shoulder Practices	5
Iowa DOT Specification Review	7
Common Shoulder Problems	10
Subgrade Stabilization	12
Granular Shoulder Stabilization.....	18
FIELD RECONNAISSANCE	29
Introduction.....	29
District 1.....	30
District 2.....	35
District 3.....	57
Summary of Findings from Field Reconnaissance	70
Key Findings from Field Reconnaissance.....	72
VEHICLE TIRE-AGGREGATE INTERACTION	73
SHOULDER TEST SECTIONS.....	78
Test Section No. 1: S.S. Polymer, Highway 122, Clear Lake, IA.....	78
Test Section No. 2: Foamed Asphalt, I-35.....	89
Test Section No. 3: Soybean Oil Soapstock, Highway 18, Rudd, IA	99
Test Section No. 4: Portland Cement, 16th St., Ames, IA.....	107
Test Section No. 5: Fly Ash, Highway 34, Batavia, IA	116
Test Section No. 6: Geosynthetic Stabilization, Highway 218, Nashua, IA.....	142
Key Findings from All Shoulder Test Sections	164
LABORATORY EVALUATION OF STABILIZERS.....	167
Introduction.....	167
Test Procedures.....	167
Test Results.....	168
Summary and Conclusions.....	168
Recommendations.....	171
LABORATORY BOX STUDY.....	172
Introduction.....	172

Test Setup.....	172
Finite Element Analysis	177
Materials	177
Test Results.....	180
Summary and Conclusions.....	195
SHOULDER DESIGN CHARTS	198
ECONOMIC EVALUATIONS OF SHOULDER MAINTENANCE AND CONSTRUCTION	202
Sources of Cost Information	202
Maintenance Costs	204
Construction (Investment) Costs.....	211
Economic Evaluation (Life-Cycle Costs)	226
Observations from Economic Analysis.....	239
Cost of Granular Layer Stabilizers.....	240
SUMMARY AND CONCLUSIONS	243
Relevant Research.....	243
Field Reconnaissance.....	243
Test Sections	244
Laboratory Evaluation of Stabilizers	246
Laboratory Box Study	247
Shoulder Design Charts	247
RECOMMENDATIONS	249
Shoulder Construction	249
Shoulder Reconstruction.....	249
Edge Drop-Off	249
REFERENCES	250
APPENDIX A. SAMPLE CALCULATION OF WEIGHTED AVERAGE CBR VALUES FOR THE GRANULAR AND SUBGRADE LAYERS	A-1
APPENDIX B. PROJECT MEETINGS	B-1
APPENDIX C. FINITE ELEMENT ANALYSIS FOR LABORATORY BOX STUDY	C-1

LIST OF FIGURES

Figure 1. Iowa DOT granular shoulder section (modified from Iowa DOT Standard Road Plan RH-37D).....	6
Figure 2. Common granular shoulder problems	10
Figure 3. Selection of stabilizer (Chu et al. 1955)	13
Figure 4. Tensar BX1100 geogrid (image scale 1:2.5)	15
Figure 5. Gradation envelope for foamed asphalt mixes (modified from Muthen 1998).....	19
Figure 6. Gradation requirement for cement stabilized base course (modified from Department of the Army, the Navy, and the Air Force 1994).....	21
Figure 7. Samples of Soiltec and S.S. polymers	26
Figure 8. Samples of soybean oil soapstock	28
Figure 9. Shoulder drop-off along the shoulder section of Hwy 164, October 27, 2005.....	30
Figure 10. Severe water erosion along the pavement edge, June 16, 2005.....	31
Figure 11. Shoulder section at U.S. 30 milepost 151.95 E.B., September 2, 2006	32
Figure 12. Grain size distribution of granular shoulder material (M.P. 151.95 E.B.)	32
Figure 13. Granular shoulder section on U.S. 30 (milepost 156.0 W.B.), September 2, 2006.....	33
Figure 14. Grain size distribution of granular shoulder material (M.P. 156.0 W.B.).....	33
Figure 15. Granular shoulder section on U.S. 30 (milepost 160.25 E.B.), September 2, 2006	34
Figure 16. Grain size distribution of granular shoulder material (M.P. 160.25 E.B.)	34
Figure 17. Granular shoulder section following a paved bridge approach shoulder, Hwy 18 milepost 184.55 E.B., July 26, 2005	36
Figure 18. Three-inch shoulder drop-off, Hwy 18 milepost 184.55 E.B., July 26 2005.....	36
Figure 19. Elevation profile relative to the pavement edge, Hwy 18 milepost 184.55 E.B.....	37
Figure 20. DCP test results, Hwy 18 milepost 184.55 E.B.....	38
Figure 21. Outside granular shoulder section on Hwy 18 milepost 196.14 E.B., July 26, 2005 ...	39
Figure 22. Elevation profile relative to the pavement edge (before blading), Hwy 18 milepost 196.14 E.B.	39
Figure 23. Maintenance of shoulder section, July 26, 2005.....	40
Figure 24. DCP test results, Hwy 18 milepost 196.14 E.B.....	40
Figure 25. Granular shoulder section stabilized with soybean oil, May 10, 2006	41
Figure 26. Grain size distribution of the shoulder granular material, Hwy 18 W.B.....	42
Figure 27. Crushed limestone samples stabilized with soybean oil collected for SEM analysis...42	
Figure 28. SEM image of limestone rock stabilized with soybean oil (x200 magnification).....43	
Figure 29. Magnified SEM image of the highlighted area in Figure 28, showing the soybean oil and organic fibers (x600 magnification).....	43
Figure 30. Magnified image showing the organic fibers (x2000 magnification).....	44
Figure 31. Elevation profile relative to the pavement edge, Hwy 18 W.B.	44
Figure 32. DCP test results, Hwy 18 W.B.	45
Figure 33. Granular shoulder section located on a super-elevated curve on Hwy 65 milepost 198.3 N.B., July 26, 2005	46
Figure 34. Shoulder drop-off adjacent to the pavement on Hwy 65 milepost 198.3 N.B., July 26, 2005	46
Figure 35. Elevation profile relative to the pavement edge, Hwy 65 milepost 198.3 N.B.	47
Figure 36. DCP test results, Hwy 65 milepost 198.3 N.B.	47
Figure 37. Granular shoulder section at exit ramp of Hwy 65 onto Hwy 27, May 10, 2006.....	48
Figure 38. Shoulder edge drop-off on Hwy 65 exit ramp to Hwy 27, May 10 2006	49

Figure 39. Shoulder rutting caused by soft subgrade and absence of granular layer on Hwy 65 exit ramp to Hwy 27, May 10, 2006	49
Figure 40. Grain size distribution of granular and subgrade layers, Hwy 65 exit ramp to Hwy 27	50
Figure 41. Elevation profile relative to the pavement edge, Hwy 65 exit ramp to Hwy 27.....	50
Figure 42. DCP test results, Hwy 65 exit ramp to Hwy 27.....	51
Figure 43. Granular shoulder section on Hwy 122, July 26, 2005.....	52
Figure 44. Cross slope damage at the intersection with Larke Ave. on Hwy 122, July 26, 2005..	52
Figure 45. Elevation profiles relative to the pavement edge, Hwy 122	53
Figure 46. DCP test results, Section 1, 200 ft. east of Hwy 122.....	53
Figure 47. Granular shoulder section maintained with asphalt millings on Hwy 20 milepost 242 E.B., September 23, 2006.....	54
Figure 48. Four in. shoulder drop-off on Hwy 20 milepost 242 E.B., September 23, 2006.....	55
Figure 49. Grain size distribution analysis for granular material, Hwy 20 milepost 242 E.B.	55
Figure 50. Elevation profile relative to the pavement edge, Hwy 20 milepost 242 E.B.....	56
Figure 51. DCP test results, Hwy 20 milepost 242 E.B.....	56
Figure 52. Granular shoulder section (southbound shoulder looking north) on Hwy IA 12 Station 1080+00', October 14, 2005.....	57
Figure 53. Granular shoulder with RAP material on Hwy IA 12 Station 1080+00', October 14, 2005.....	58
Figure 54. Grain size distribution of the shoulder granular material, Hwy IA 12 Station 1080+00'	58
Figure 55. Elevation profile of the shoulder section relative to the pavement, Hwy IA 12 Station 1080+00'	59
Figure 56. DCP test results, Hwy IA 12 Station 1080+00'	59
Figure 57. Granular shoulder section on Hwy IA 3 St. 940 E.B., October 14, 2005.....	60
Figure 58. Granular shoulder section on Hwy IA 3 St. 940 W.B., October 14, 2005.....	61
Figure 59. Grain size distribution analysis for shoulder materials, Hwy IA 3 St. 940	61
Figure 60. Elevation profile of shoulder section relative to the pavement, Hwy IA 3 St. 940 W.B.	62
Figure 61. Performing DCP test at the westbound shoulder, October 14, 2005	62
Figure 62. DCP test results, Hwy IA 3 St. 940	63
Figure 63. Granular shoulder section on Hwy 9 St. 135+00' W.B., October 14, 2005	64
Figure 64. Elevation profile of the shoulder section relative to the pavement edge, Hwy 9 St. 135+00' W.B.....	64
Figure 65. Grain size distribution analysis for Hwy 9 St. 135+00' W.B.: (a) sample obtained from shoulder section, (b) sample obtained from stockpile	65
Figure 66. DCP test results, Hwy 9 St. 135+00' W.B	65
Figure 67. Granular shoulder section on Hwy 71 crossing Hwy 10 S.B., October 14, 2005.....	66
Figure 68. Grain size distribution analysis of the shoulder material, Hwy 71 crossing Hwy 10 S.B.....	66
Figure 69. Elevation profile of the shoulder section relative to the pavement, Hwy 71 crossing Hwy 10 S.B.....	67
Figure 70. DCP test results, Hwy 71 crossing Hwy 10 S.B.....	67
Figure 71. Shoulder section with 4 ft. of HMA and 4 ft. of blended limestone and crushed concrete on Hwy 60 St. 149+00', October 14, 2005.....	68
Figure 72. Grain size distribution analysis, Hwy 60 St. 149+00'	69

Figure 73. Elevation profile of shoulder section relative to the pavement, Hwy 60 St. 149+00' ..	69
Figure 74. DCP test results, Hwy 60 St. 149+00'	70
Figure 75. Variability plot for edge drop-offs with distance from white line to pavement edge...	71
Figure 76. Aggregate shoulder section on State Ave., August 19, 2005	73
Figure 77. High-speed video camera demonstration, August 19, 2005	74
Figure 78. High-speed video camera placed at the side of the road, August 19, 2005	75
Figure 79. Images captured by a stationary high-speed camera showing aggregate displacement at different times after coming in contact with the tire	76
Figure 80. Screenshot of the software used to monitor aggregate trajectory	77
Figure 81. Aggregate trajectory relative to the direction of vehicle travel	77
Figure 82. Erosion of the granular shoulder adjacent to the pavement edge on Hwy 122, April 18, 2005	79
Figure 83. Elevation profiles relative to the pavement edge, Hwy 122	79
Figure 84. Grain size distribution analysis, Hwy 122	80
Figure 85. S.S. polymer topically applied to the granular shoulder, April 28, 2005	80
Figure 86. Compacting the shoulder section after three topical applications, April 28, 2005.....	81
Figure 87. DCP test results, (a) inside the stabilized area and (b) outside the stabilized area.....	82
Figure 88. Delamination of the bonded granular material under the impact of traffic, June 11, 2005	82
Figure 89. Elevation profile relative to the pavement edge collected at (a) 50 ft. and (b) 300 ft. from the beginning of the section	83
Figure 90. Crushed limestone added to areas with high edge drop-off on Hwy 122, July 26, 2005	84
Figure 91. Measured penetration depth of S.S. polymer for upper bound gradation.....	85
Figure 92. Unconfined compression test conducted on S.S. polymer-stabilized sample	86
Figure 93. Unconfined compressive strength results for unsoaked samples	86
Figure 94. Disintegrated specimen after soaking for four hours.....	87
Figure 95. Fly ash added to the granular material on I-35 milepost 150 northbound, September 1, 2005	89
Figure 96. Full depth reclamation of FA on I-35 milepost 150 northbound, September 1, 2005	90
Figure 97. FA surface sealed using chip seal on I-35 milepost 150 northbound, September 1, 2005	90
Figure 98. Optimum moisture content and maximum dry density determined by standard Proctor test, I-35 milepost 150 northbound.....	91
Figure 99. Variation of field moisture content with depth along the shoulder section, I-35 milepost 150 northbound	92
Figure 100. Variation of field dry density with depth along the shoulder section, I-35 milepost 150 northbound.....	92
Figure 101. DCP test results showing strength gain with time, I-35 milepost 150 northbound ...	93
Figure 102. Edge drop-off caused by failure of foamed asphalt-stabilized section, July 25, 2006.....	94
Figure 103. Asphalt patch placed on the deteriorated shoulder adjacent to a horizontal curve, I-35 milepost 150 northbound, July 7, 2006	95
Figure 104. Vacuum saturation test conducted on granular material stabilized with foamed asphalt	96
Figure 105. Failure of foamed asphalt stabilized sample during wet-dry testing	97

Figure 106. Percent volume change caused by freeze-thaw cycles.....	97
Figure 107. Percent mass loss during freeze-thaw cycles.....	98
Figure 108. Shoulder on Hwy 18 milepost 202.50 near Rudd, IA, May 10 2006	99
Figure 109. Grain size distribution analysis, Hwy 18 milepost 202.50 WB.....	100
Figure 110. Tilling of a 3 ft. section adjacent to the pavement, August 22, 2006.....	101
Figure 111. Applying Feed Energy soybean oil to the shoulder section, August 22, 2006	101
Figure 112. Mixing Feed Energy soybean oil with shoulder granular material, August 22, 2006.....	102
Figure 113. Compacting the stabilized section using a pneumatic roller on Hwy 18 milepost 202.50 Rudd, IA, on August 22, 2006	102
Figure 114. Distributor plugging after separation of emulsion and soybean oil, August 22, 2006.....	103
Figure 115. Placing crushed limestone material over the stabilized area, August 22, 2006.....	103
Figure 116. Elevation profile relative to the pavement edge, Hwy 18 milepost 202.50 W.B.	104
Figure 117. Asphalt millings placed at the shoulder test section and a 2 in. edge drop-off developed after two months, October 10, 2006	104
Figure 118. DCP test results, Hwy 18 milepost 202.50 W.B.	105
Figure 119. Three-inch edge drop-off after eight month on Hwy 18 milepost 202.50 near Rudd, IA, on June 23, 2006.....	105
Figure 120. Edge drop-off and wash boarding along the pavement edge on 16th St. Ames, IA, on September 6, 2006.....	107
Figure 121. Grain size distribution analysis of granular material from 16th St. Ames, IA	108
Figure 122. Blading of the shoulder section on 16th St. in Ames, IA, September 26, 2006	109
Figure 123. Truck carrying a water tank ahead of shoulder reclaimer, September 26, 2006.....	109
Figure 124. Spreading of cement over the reclaimed test section, September 26, 2006.....	110
Figure 125. Mixing the cement with the granular material, September 26, 2006.....	110
Figure 126. Compaction of stabilized section using smooth drum roller, September 26, 2006..	111
Figure 127. Hard granular surface formed seven days after construction, October 3, 2006.....	112
Figure 128. Development of wash boarding towards the end of the section (seven days after construction), October 3, 2006.....	112
Figure 129. Variation of CIV profile with time, 16th St. Ames, IA	113
Figure 130. Significant edge drop-off observed after four months on 16th St. Ames, IA, December 30, 2006	113
Figure 131. Three-inch edge drop-off adjacent to pavement after eight months, May 18, 2007	114
Figure 132. Subgrade material, September 22, 2005.....	116
Figure 133. Severe rutting at the shoulder section, Milepost 207.8-90' Westbound, September 22, 2005	117
Figure 134. Closer image of the shoulder rutting shown in Figure 133, September 22, 2005	117
Figure 135. Summary of CBR values collected at Highway 34, September 22, 2005	118
Figure 136. Determining shoulder elevations relative to the pavement, September 22, 2005	118
Figure 137. Elevation profiles relative to the pavement edge, September 22, 2005.....	119
Figure 138. Results of XRD for the clay material	121
Figure 139. Grain size distribution of the clay subgrade material, Highway 34, Batavia, IA	122
Figure 140. pH meter used to determine the pH of stabilized clay.....	122
Figure 141. Results of the pH test conducted for the subgrade clay mixed with varying percentages of fly ash.....	123

Figure 142. Fly ash set time testing	123
Figure 143. Results of fly ash set time for three batches	124
Figure 144. Vacuum saturation apparatus.....	124
Figure 145. Stabilized samples under saturation for one hour.....	125
Figure 146. Unconfined compression test.....	125
Figure 147. Unconfined compressive strength after seven-day cure	126
Figure 148. Semi trailer bottom dump truck spreading fly ash on top of subgrade layer, October 31, 2005.....	127
Figure 149. Mixing fly ash with subgrade soil using a road reclaimer, October 31, 2005	127
Figure 150. Water truck used to increase moisture content of clay-fly ash mixture, October 31, 2005.....	128
Figure 151. Motor grader used to recover windrowed aggregate, October 31, 2005.....	128
Figure 152. Smooth wheel roller used to compact the crushed limestone layer, October 31, 2005.....	129
Figure 153. DCP test results with time at (a) 3.0 ft. and (b) 6.0 ft. from pavement edge.....	131
Figure 154. DCP test results after seven months, June 8, 2006.....	133
Figure 155. Plate load test results, June 8, 2006.....	134
Figure 156. Plate load test results, October 10, 2006	135
Figure 157. Plate load test results, May 4, 2007	136
Figure 158. Higher rut depth observed along the control section after one month from shoulder reconstruction, November 23, 2005	137
Figure 159. Performance of shoulder section after seven months, June 8 2006.....	137
Figure 160. Stabilized shoulder along the exit ramp showing no rut under heavy traffic load, June 8, 2006.....	138
Figure 161. No shoulder rutting observed after 19 months, May 14, 2007	138
Figure 162. Newly constructed granular shoulder section, October 17, 2006	139
Figure 163. Shoulder rutting developed along wheel path with repetitive loading, October 17, 2006.....	139
Figure 164. About 3 in. of rut developed after six passes.....	140
Figure 165. Results of DCP testing at (a) 3 ft., (b) 6 ft., and (c) 12 ft. from pavement edge	140
Figure 166. Severe rutting along the inside shoulder, June 1, 2006	142
Figure 167. Profile of rut depth measured inside the wheel path and CIV measured at 2 ft. from pavement edge, June 1, 2006	143
Figure 168. DCP results conducted at several locations along inside shoulder, June 1, 2006	144
Figure 169. Moisture-density relationship for subgrade material	145
Figure 170. Proposed test sections.....	147
Figure 171. Motor grader removing the contaminated granular layer, June 23, 2006.....	147
Figure 172. Placing virgin aggregate next to the test section, June 23, 2006	148
Figure 173. Skid loader leveling the subgrade, June 23, 2006	148
Figure 174. Pneumatic roller used to compact the subgrade, June 23, 2006	149
Figure 175. Cutting the geogrids to 8 ft. wide sections, June 23, 2006.....	149
Figure 176. Rolling the BX 1200 geogrid over the soft subgrade layer, June 23, 2006.....	150
Figure 177. Overlapping geogrids in the direction of aggregate spreading, June 23, 2006.....	150
Figure 178. Spreading the new crushed limestone over the geogrid, June 23, 2006	151
Figure 179. Compacting the granular layer using a pneumatic roller, June 23, 2006.....	151
Figure 180. Exposed edges of the geogrid after construction was completed, June 23, 2006.....	152

Figure 181. Development of shoulder rutting one month after shoulder construction, July 25, 2006.....	154
Figure 182. No rutting at the test section stabilized with BX1200, July 25, 2006	154
Figure 183. Plate load test conducted at the inside shoulder, July 25, 2006.....	155
Figure 184. Plate load test results immediately after construction, June 23, 2006.....	156
Figure 185. Plate load test results three months after construction, September 27, 2006	157
Figure 186. Plate load test results ten months after construction, April 17, 2007	158
Figure 187. Profile of CIV with time	159
Figure 188. Profile of CIV with distance from the pavement edge	160
Figure 189. DCP results before and after stabilization, Highway 218, Nashua, IA.....	161
Figure 190. Exposed BX4100 geogrid, October 24, 2006.....	162
Figure 191. Exposed geogrid about 8 ft. from the pavement edge, April 17, 2007.....	162
Figure 192. Axial compression test	170
Figure 193. Soapstock-stabilized samples after vacuum saturation test.....	170
Figure 194. Summary of compressive strength results	171
Figure 195. Schematic of the laboratory apparatus setup	173
Figure 196. Photographs of the laboratory test setup.....	174
Figure 197. Applying a static load to compact the soil.....	175
Figure 198. Applying cyclic loading to the soil using a 6 in. plate.....	175
Figure 199. Measuring the reaction beam deflection.....	176
Figure 200. Magnitude of beam deflection with applied loads.....	176
Figure 201. Grain size distribution analysis for the granular material used in the laboratory box testing.....	178
Figure 202. Relationship between moisture content and dry unit weight for the granular material used in the laboratory box testing.....	178
Figure 203. Grain size distribution for the RAP material	179
Figure 204. Soil displacement with increasing number of cycles, control test.....	181
Figure 205. Soil displacement with increasing number of cycles, BX1200 (not anchored).....	182
Figure 206. Unanchored geogrid pulled to the center of the box under the impact of cyclic loading.....	183
Figure 207. Soil displacement with increasing number of cycles, BX1200 (partially anchored).....	184
Figure 208. Soil displacement with increasing number of cycles, BX1200	185
Figure 209. Soil displacement with increasing number of cycles, BX1100	187
Figure 210. Soil displacement with increasing number of cycles, BX4100	188
Figure 211. Soil displacement with increasing number of cycles, Woven geotextile	190
Figure 212. Soil displacement with increasing number of cycles, nonwoven geotextile	191
Figure 213. RAP material overlying soft subgrade soil.....	192
Figure 214. Soil displacement with increasing number of cycles, BX1200 with RAP	193
Figure 215. Soil displacement with increasing number of cycles, OGS class C fly ash.....	194
Figure 216. Summary of cumulative measured soil displacement for all tests.....	196
Figure 217. Comparison of measured and predicted soil displacement.....	196
Figure 218. Relationship between subgrade CBR and expected granular shoulder rut depth.....	199
Figure 219. Influence of the granular layer CBR value on the magnitude of rut depth.....	200
Figure 220. Influence of granular layer thickness on the magnitude of rut depth.....	200
Figure 221. Influence of axle load on the magnitude of rut depth.....	201
Figure 222. Typical aggregate shoulder	208

Figure 223. Annual maintenance cost for a typical aggregate shoulder.....	208
Figure 224. Partially paved HMA shoulder	214
Figure 225. Construction costs for two ft. partially paved HMA shoulder.....	214
Figure 226. Construction costs for four ft. partially paved HMA shoulder	215
Figure 227. Shoulder repair using foamed asphalt with HMA overlay	217
Figure 228. Annual maintenance cost for foamed asphalt with HMA overlay.....	217
Figure 229. Full-width paved shoulders	220
Figure 230. Annual maintenance costs for full-width HMA shoulders	220
Figure 231. Annual maintenance costs for full-width PCC shoulders.....	221
Figure 232. Polymer grid repair	224
Figure 233. Annual maintenance costs for geogrid repair	224
Figure 234. Maintenance of shoulder sections using fly ash	225
Figure 235. Annual maintenance costs for fly ash shoulder repair	225
Figure 236. Benefit-cost analysis for aggregate shoulders.....	229
Figure 237. Present worth analysis for aggregate shoulders	229
Figure 238. Benefit-cost analysis for 2 ft. partially paved HMA shoulder	230
Figure 239. Present worth analysis for 2 ft. partially paved HMA shoulder	230
Figure 240. Benefit-cost analysis for 4 ft. partially paved HMA shoulder	231
Figure 241. Present worth analysis for 4 ft. partially paved HMA shoulder	231
Figure 242. Benefit-cost analysis for foamed asphalt and HMA overlay	232
Figure 243. Present worth analysis for foamed asphalt and HMA overlay	232
Figure 244. Benefit-cost analysis for full-width HMA shoulders.....	233
Figure 245. Present worth analysis for full-width HMA shoulders	233
Figure 246. Benefit-cost analysis for full-width PCC shoulders	234
Figure 247. Present worth analysis for full-width PCC shoulders.....	234
Figure 248. Benefit-cost analysis for polymer grid repair	235
Figure 249. Present worth analysis for polymer grid repair.....	235
Figure 250. Benefit-cost analysis for fly ash repair	236
Figure 251. Present worth analysis for fly ash repair.....	236
Figure A.1. Sample calculation of weighted average CBR values for the granular and subgrade layers	A-1
Figure C.1. Finite element model of the laboratory box	C-1
Figure C.2. Boundary conditions of the finite element model.....	C-2
Figure C.3. Modeling (a) flexible and (b) rigid loading plate.....	C-3
Figure C.4. Finite element model with a rigid wall	C-4
Figure C.5. Finite element model with compressible layer	C-5
Figure C.6. Enlarged finite element model representing field conditions	C-5
Figure C.7. Effective stress distribution under flexible and rigid plates.....	C-6
Figure C.8. Soil displacement resulting from applying a static load over rigid and flexible plates	C-7
Figure C.9. Vertical soil displacement measured at the model boundary.....	C-7
Figure C.10. Effective stress distribution for the finite element models	C-8

LIST OF TABLES

Table 1. Summary of granular and paved shoulder costs in Iowa for calendar year 2000 (Souleyrette et al. 2001)	5
Table 2. Paved shoulder practices in Iowa and neighboring states (Souleyrette et al. 2001)	6
Table 3. Iowa DOT specification review	8
Table 4. Summary of drop-off standards for several states (Nordlin et al. 1976).....	11
Table 5. Summary of laboratory and field test sections (Berg et al. 2000).....	16
Table 6. Foamed asphalt content (Ruckel et al. 1982).....	20
Table 7. Optimal binder content range (Bowering and Martin 1976).....	20
Table 8. Recommended cement Contents for various soil types (Fang 1990).....	22
Table 9. Summary of field reconnaissance	29
Table 10. Soil properties of the aggregate samples obtained at U.S. 30.....	35
Table 11. Relationship between UCS and CBR	38
Table 12. Range of field values for granular shoulder parameters	70
Table 13. Results of FA durability testing	96
Table 14. Chemical composition of the clay and OGS fly ash materials.....	121
Table 15. Engineering properties of the subgrade and granular materials.....	122
Table 16. Average CBR value with time in the upper 8 in.	132
Table 17. E values calculated for shoulder sections after seven months	135
Table 18. Summary of E values measured with time from shoulder reconstruction	136
Table 19. Engineering properties of subgrade and granular materials.....	145
Table 20. Mechanical properties and costs of the selected geogrids	146
Table 21. Summary of E values determined from plate load testing.....	159
Table 22. Summary of laboratory test procedures	168
Table 23. Summary of laboratory test results	169
Table 24. Engineering properties of the selected geosynthetics	179
Table 25. Soil properties before and after the test, control test	180
Table 26. Soil properties before and after the test, BX1200 Geogrid (not anchored)	182
Table 27. Soil properties before and after the test, BX1200 Geogrid (partially anchored)	184
Table 28. Soil properties before and after the test, BX1200 Geogrid.....	185
Table 29. Summary of predicted and measured soil displacement for the BX1200 geogrid reinforced tests	186
Table 30. Soil properties before and after the test, BX1100 Geogrid.....	186
Table 31. Soil properties before and after the test, BX4100 Geogrid.....	188
Table 32. Comparison among measured soil displacements for the three biaxial geogrid types	188
Table 33. Soil properties before and after the test, woven geotextile.....	189
Table 34. Soil properties before and after the test, nonwoven geotextile.....	191
Table 35. Soil properties before and after the test, BX1200 with RAP.....	192
Table 36. Soil properties before and after the test, OGS class C fly ash	194
Table 37. Summary of soil properties measured before and after each test.....	197
Table 38. Summary of maintenance and construction costs	204
Table 39. Maintenance costs for typical aggregate shoulders.....	205
Table 40. Shoulder maintenance costs from 2002 to 2006.....	207
Table 41. Cost estimate for soft shoulder maintenance	210
Table 42. Construction costs for partially paved shoulders	213

Table 43. Cost estimate for foamed AC with HMA overlay	216
Table 44. Cost Estimate for full-width paved shoulder construction	219
Table 45. Cost estimate for geogrid and fly ash shoulder repairs	229
Table 47. Calculations for present worth of the expenditures	238
Table 48. Cost per mile for stabilized construction without the cost of the stabilizing agent	240
Table 49. Cost per gallon for products used in laboratory study of granular material stabilization	241
Table 50. Estimated cost per mile for stabilized construction including stabilizing agent.....	241
Table C.1. Summary of material properties	C-2

ACKNOWLEDGMENTS

The Iowa Department of Transportation and the Iowa Highway Research Board sponsored this study under contract TR-531. Numerous people assisted the authors in identifying shoulder sections for investigation. The technical steering committee helped refine the research tasks and provided suggestions. The authors would like to thank the Iowa DOT personnel and materials suppliers who lent their assistance throughout the project.

Input and review comments were provided by the Technical Advisory Committee members: Mark Nahra, John Vu, William Zitterich, Kent Nicholson, James Berger, Roy Gelhaus, Francis Todey, Michael Heitzman, Keith Norris, and Mark Black. Jim Howley of Tensar, Inc. provided the geogrid materials used in the field and laboratory study.

EXECUTIVE SUMMARY

The present study was undertaken to investigate the performance problems associated with granular shoulders and to propose new ideas for designing and maintaining granular shoulders while keeping ownership costs low. This research encompassed a variety of activities regarding granular shoulders, including reviewing shoulder construction practices and performance problems reported in literature, carrying out a field reconnaissance to observe common granular shoulder problems, constructing and monitoring several test sections with selected granular and subgrade stabilizers, and conducting laboratory studies to evaluate dust suppressant products that claim to stabilize granular layers, as well as chemical and mechanical stabilizers for the subgrade layer. Further, a cost estimate analysis was conducted to contemplate possible improvements and repairs for aggregate shoulders. Based on this research, shoulder design charts are provided that can be used in selecting appropriate design parameters for shoulder construction and that can provide a basis for QA/QC. The main conclusions determined from this research study are summarized below.

Relevant Research

Several types of shoulders are reported in literature, including (1) earth, (2) granular, (3) blotter, (4) cold recycled asphalt, (5) asphalt, and (6) portland cement. For granular shoulders, which are the focus of this research, the most serious types of deterioration include rutting and edge drop-off. They most often occur within the first two ft. from the pavement edge due to settlement of the shoulder, degradation of the granular material, wind or water erosion, and/or vehicle off-tracking.

The initial construction costs for granular shoulders can be about 70% of the construction costs for paved shoulders. However, maintenance costs for granular shoulders are much higher than those of paved shoulders. The maintenance costs generally do not exceed the initial savings in construction costs.

Field Reconnaissance

Several good and poor granular shoulder sections were inspected in three districts: 1, 2, and 3. The two major problems observed were edge drop-off and subgrade layers with a California bearing ratio (CBR) less than 10. Approximately two-thirds of the inspected sites had an edge drop-off greater than 1.5 in., 40% had a slope greater than 4%, and 50% had a subgrade CBR value less than 10. Additionally, the grain size distribution with distance from the pavement edge was measured at three sections. The results show that the fines content increases as distance from the pavement edge increases. Changes in fines content most likely occur due to wind or water erosion and/or vehicle off-tracking. A high-speed video camera demonstration in which a truck was driven over a shoulder section at 40 mph showed that vehicle off-tracking elevates and displaces aggregate in the opposite direction of vehicle travel.

Test Sections

Six granular shoulder sections were selected to test chemical and mechanical stabilization products. The test sections were either experiencing edge drop-off or severe rutting. The granular layers of four test sections were chemically stabilized using either S.S. polymer, foamed asphalt, dustlock soybean oil, or portland cement. A soft subgrade layer was stabilized using class C fly ash and three geogrids at two test sections.

Test Section No. 1, S.S. Polymer

Test section 1 was stabilized with about 700 gallons of S.S. polymer, applied using topical applications. The polymer, which was diluted at a ratio of 3:1 by volume, penetrated to a depth of 0.5 in., forming a granular film that was detached after 30 days. The section performed inadequately, and the 6 to 12 in. strip adjacent to the pavement edge showed signs of delamination. Monitoring the section revealed no increase in the CBR values at the upper 15 in. A laboratory study showed that using granular material that complies with the lower bound of the gradation curve specified by Iowa DOT resulted in a higher S.S. polymer penetration depth. Further durability testing and evaluation using diluted S.S. polymer (e.g., 7:1 or 9:1) is needed.

Test Section No. 2, Foamed Asphalt

This section was reconstructed using full-depth reclamation to a depth of 12 in. of foamed asphalt and 3% to 4% class C fly ash. The section was monitored by conducting DCP tests with time, which revealed an increase in the CBR value from 0.4 to 59 in the upper 10 in. A laboratory study showed that vacuum saturating samples that were stabilized with foamed asphalt reduced their compressive strength by about 20%. Further, freeze-thaw testing showed that foamed asphalt can expand by 18%; however, the percent mass loss due to freeze-thaw cycles was satisfactory. Edge drop-off and shoulder distresses started to develop along the pavement edge after approximately one year. Foamed asphalt was successful in improving the properties of the shoulder section for a short duration. For longer durations, the stabilized section showed significant signs of distress near the pavement edge.

Test Section No. 3, Soybean Oil

This shoulder section was experiencing edge drop-off between 3 and 4 in. deep. The test section was 340 ft. long by 2 ft. wide by 6 in. deep and was stabilized using feed energy soybean oil. Two applications at a rate of 0.7 gal/yd² were placed and mixed with the granular material to a depth of 6 in. Due to the separation of the oil and the emulsion, the distributor became plugged and a final topical application was not carried out. Elevation profiles measured with time revealed that the feed energy soybean oil did not mitigate the redevelopment of the edge drop-off. Dynamic cone penetrometer (DCP) tests also revealed no CBR increase in the upper 8 in. of the stabilized test section. After 8 months, a 3 in. edge drop-off along the pavement edge was measured.

Test Section No. 4, Portland Cement

This section, which was located on 16th St. in Ames, IA, was experiencing edge drop-off and washboarding near the pavement edge. A 200 ft. long by 1.5 ft. wide test section was constructed by mixing 10% portland cement with the granular material to a depth of 6 in. Monitoring the section revealed that the first 100 ft. of the section performed adequately and exhibited a hard cemented surface, whereas washboarding and erosion were observed along the second 100 ft., after 7 days. Clegg impact value (CIV) profiles demonstrated significant improvement after 7 and 14 days. No additional strength gain was measured after 28 days. CIVs outside the stabilized area were generally lower than those measured near the pavement edge. Edge drop-offs and erosion were observed along the stabilized area after four months. After eight months, the edge drop-off further progressed to a depth of about 3 in.

Test Section No. 5, Fly Ash

This shoulder section was overlying a subgrade layer with a CBR of about 2. Significant shoulder rutting was noted. The test section was 8 miles long and 8 ft. wide. The shoulder section was reconstructed by windrowing the upper 6 in. of crushed limestone and mixing 15% to 20% class C fly ash with the upper 12 in. of the subgrade clay. The mix was compacted using a pad foot roller and the limestone was reclaimed and compacted using a smooth wheel roller. DCP and plate load tests were conducted to document the performance of the section. DCP tests demonstrated an increase of CBR values with time. Similarly, plate load tests showed an increase in E with time. Fly ash stabilization was successful in improving both the short- and long-term performance of the shoulder section.

Preliminary testing conducted at the new Highway 34 bypass (within this test section) revealed low CBR values for the underlying earth shoulder fill and subgrade layers. If similar conditions exist at other locations, future maintenance problems from severe rutting may be a concern.

Test Section No. 6, Geosynthetics

This test section was undergoing severe rutting due to the bearing capacity failure of the subgrade. A test section, which was about 1,020 ft. long, was constructed by placing three biaxial geogrids at the interface between the granular and subgrade layers. The control section started to develop rutting after one month, whereas the stabilized sections showed no signs of shoulder rutting. Plate load tests, DCP tests and CIV tests were regularly conducted to monitor the section performance. Plate load tests showed a significant difference in E between the stabilized and the control section. Further, the E value increased with time. CIVs were highest near the pavement, since the thickness of the rock layer was highest. CIVs measured outside the stabilized area were low, indicating soft shoulder conditions. CBR values, determined from DCP testing, increased for the upper 8 in. after three months. All geogrids considerably improved the performance of the shoulder test section and eliminated rutting. After ten months, the geogrids at 8 ft. from the pavement edge, where the overlying granular layer was 1 to 2 in. thick, were exposed. Exposure of the grid may lead to tearing or UV degradation and loss of reinforcement benefits.

Laboratory Evaluation of Stabilizers

A laboratory study was conducted to evaluate the use of two polymer emulsion products, portland cement, and a soybean oil product in stabilizing the shoulder granular layer. For each stabilizer, six standard Proctor samples were prepared. Three samples were tested in compression, while the other three were subjected to vacuum saturation followed by compression testing. The average ultimate compression strength (UCS) of S.S. polymer-stabilized samples was about 445 psi and decreased to 76 psi after vacuum saturation, while the average UCS of Soiltac polymer-stabilized samples was about 1,118 psi. Vacuum saturating the samples resulted in an average compressive strength of about 252 psi. The average UCS of portland cement-stabilized samples was about 694 psi and decreased to 254 psi after vacuum saturation. Dustlock soybean oil-stabilized samples demonstrated an average UCS of about 706 psi and decreased to 623 psi when subjected to vacuum saturation. This was the smallest strength reduction compared to the other stabilizers tested, which makes sense because soybean oil is a water-repellent product. All four products showed potential in successfully stabilizing the granular layer. More durability testing and pilot studies are needed before implementation.

Laboratory Box Study

To test several mechanical and chemical stabilization methods, a laboratory box study was conducted that simulated a shoulder section overlying a subgrade with low CBR values (between 3 and 5). The laboratory apparatus consisted of a loading frame, reaction beam, and a hydraulic actuator. A steel box (2 ft. x 2 ft. x 2 ft.) was used to contain the soil, and was loaded using a 6 in. diameter loading plate. Cyclic loading with three loading stages was used to study the performance of the laboratory model under selected mechanical and chemical stabilization techniques.

At each stage, a pressure was applied and sustained for 5,000 cycles at a frequency of 1 Hz. These pressures were 40, 80, and 120 psi. The control test showed the highest cumulative soil displacement, which was about 11.2 in. at 15,000 cycles. The CBR and lightweight deflectometer values of the subgrade soil typically increased after each test due to soil densification. No considerable change was noted in the strength properties of the granular layer. The BX1200 geogrid reduced soil displacement by about 75% compared to the control test, while the BX1100 and BX4100 geogrids alleviated soil displacement by about 70% compared to the control test. All geogrids used did not prevent aggregate from punching through the subgrade layer. The approximate punching depth was 1 in. The woven and nonwoven geotextiles reduced soil displacement by about 70% percent compared to the control test. The performance of the nonwoven geotextile, however, started to decrease at the third loading stage while soil displacement increased rapidly. Both woven and nonwoven geotextiles were successful in separating the granular and subgrade layers. Using both recycled asphalt pavement material and the BX1200 geogrid resulted in a reduction in soil displacement that was three times lower than the control test. The soil displacement was 50% higher than when using crushed limestone. Stabilizing the subgrade soil with 20% fly ash resulted in the lowest soil displacement. Fly ash stabilization reduced soil displacement by 40% percent compared Test No. 4 (BX1200 with

crushed limestone). The recorded soil displacement was also six times lower than the control test.

Shoulder Design Charts

Shoulder design charts were developed to help mitigate the shoulder rutting that arises from bearing capacity failure in the subgrade layer. The chart, which is based on the CBR value of the subgrade layer and rut depth, was developed from the semi-empirical method proposed by Giroud and Han (2004) and from an equation for calculating rut depth proposed by the U.S. Army Corps of Engineers in 1989. The developed design chart can be a rapid tool for designing new granular shoulder, providing a basis for QA/QC, and predicting the behavior of existing shoulders. Field and laboratory rut depth measurements were used to validate the developed chart. The measured rut depths are in a relatively good agreement with the predicted chart values.

Recommendations

As a result of the research described in this report, the following are proposed on a pilot study basis:

- For edge drop-off shoulder sections, it is recommended that researchers evaluate the use of mixing polymer emulsion products such as S.S. polymer or Soiltac polymer with the granular layer.
- Investigate the effects of other soybean oil products such as dustlock soybean oil, since this products had previous success in stabilizing the shoulder section near Garner, IA and showed good performance in the laboratory study.

Shoulder Construction

- A minimum weighted average CBR value for the earth shoulder fill and the subgrade layers up to a depth of 20 in. should be about 12. The weighted average CBR value for the granular layer should not be less than 10.
- DCP test and Clegg impact test are rapid tools that can be used in the field to verify the CBR values during shoulder construction.
- The provided design charts can be used as a design guide for constructing new shoulders. By selecting an appropriate CBR value for each layer, and by estimating the expected traffic levels and loads, the allowable rut depth can be controlled. The design charts can also be used for QA/QC.

Shoulder Reconstruction

- In the case of shoulder rutting due to bearing capacity failure of the subgrade, it is proposed that fly ash or geogrid stabilization be used. The percentage of fly ash and moisture content added should be determined from laboratory testing. The geogrid should be placed at the interface of the subgrade and granular layer. The overlying granular layer should have a uniform thickness of about 6 to 8 in.

INTRODUCTION

Shoulders are an important element of the highway system, providing space for emergency stops, a recovery zone for errant vehicles, structural support for the pavement, drainage, improved sight distance, a passage for bicyclists, and increased roadway width to accommodate agricultural vehicles. Although constructing granular shoulders is initially less expensive than constructing paved shoulders (by up to 70%), granular shoulders often add expense later because they require relatively frequent maintenance and have performance problems (Price 1990). Such performance problems include erosion, rutting, edge drop-off, and slope irregularities. Current maintenance procedures for granular shoulders in Iowa typically involve shoulder regrading, placing additional material, and recompaction. These maintenance and repair problems are costly and require investigation so that the factors that contribute to these problems are better understood. The overall goal of this research was to improve the performance of granular shoulders while keeping ownership costs low.

Research Objectives

The objectives of this research were as follows:

- Identify practices for design, construction, and maintenance of granular shoulders that result in reduced rutting and edge drop-off, improved safety, reduced maintenance costs, and extended performance life, with recommendations specific to Iowa materials and conditions.
- Document several granular shoulder sites where poor and good performance has been observed in order to better understand the factors contributing to shoulder problems.
- On a pilot study basis, evaluate and compare the performance of several test sections using chemical stabilization (e.g., fly ash and cement) and mechanical reinforcement (e.g., geogrid) techniques, including application of waste and recycled materials in construction (e.g., limestone screenings, recycled concrete, or recycled asphalt).
- Perform a cost/benefit analysis to investigate owner costs of alternative systems.

Research Plan

This research project was designed to include a literature review, field reconnaissance of problematic shoulder sections, documentation of construction and performance of six test sections, a specially designed laboratory box study to simulate longer term repetitive loading, cost estimation and analysis for shoulder repair maintenance, and recommended construction and maintenance alternatives for granular shoulder sections.

The literature review focuses on identifying shoulder types, associated distresses, previous studies related to shoulder performance, current shoulder practices in Iowa and other states, and initial construction and maintenance costs. A summary of some stabilization products and techniques that can be applied to granular shoulders is also presented.

Field investigations were conducted to document shoulder problems observed across Iowa and to evaluate maintenance and repair techniques. Preliminary field testing was carried out at each shoulder section to determine the factors contributing to the problem. The researchers consulted with district maintenance engineers on a state-wide basis to document problems, including the frequency of maintenance, types of granular materials used, and the effects of budget limitations on maintenance and repair practices.

Several shoulder test sections were constructed and monitored to examine the effects of selected stabilizers on the performance of granular shoulder sections. Four test sections were constructed to evaluate the performance of stabilizers on the granular layer. Stabilizers included liquid polymer stabilizer, foamed asphalt with fly ash, soybean oil, and portland cement. Two test sections were stabilized by treating the material underlying the granular layer. One test section with soft underlying subgrade soil was stabilized using ASTM class C fly ash mixed to 12 in. At another site, three geogrid reinforcement products were evaluated by placing the geogrid at the interface between the subgrade and the granular layer. The results from field and laboratory testing for each test section are presented in this report.

Because not all of the identified shoulder materials and stabilizers could be evaluated in the field, a specially designed laboratory box study was conducted. Stabilization techniques included the use of woven and nonwoven geotextiles, geogrids, and fly ash. Further, granular materials including crushed limestone and recycled asphalt pavement (RAP) were used. The laboratory apparatus consisted of a loading frame, reaction beam, a hydraulic actuator, and a specially fabricated steel box to contain the soil. Three incremental cyclic loads were applied, each sustained for 5,000 cycles at a frequency of 1 Hz. The soil displacement history measured for each combination of granular material and stabilization method is presented in this report.

A cost estimate analysis was carried out to evaluate the various maintenance and stabilization alternatives identified in the study. Alternatives such as full and partial paving of the shoulder and adding aggregate are compared. In addition, the cost of the stabilization alternatives used for each test section are compared.

Lastly, recommendations are proposed for construction, repair, and maintenance of granular shoulders, which will improve performance by reducing shoulder rutting and edge drop-off formation. However, some aspects of the recommendations need further testing before full implementation.

LITERATURE REVIEW

Introduction

Shoulders can vary from only 2 ft. on minor rural roads to about 12 ft. on major roads (Humphreys and Parham 1994). According to NCHRP Synthesis No. 63, desirable features of shoulders include clear delineation between travel lanes and shoulders, adequate cross-slope for good drainage, enough width for emergency use and for guardrail installation, structural stability, and low total and construction costs.

Shoulder Types

Shoulders can consist of earth, stabilized material, or surface-treated materials (Butt et al. 1997). The following paragraphs describe some of the various types of shoulders and their corresponding performance problems.

Earth Shoulders

Typically, earth shoulders are native soil, unstabilized or without turf cover. Ideally, their soil is naturally well-graded and rainfall amounts are low. These shoulders may be satisfactory for light traffic (Butt et al. 1997).

Granular Shoulders

Granular shoulders are normally used for low-volume traffic roadways. Aggregate mix design, compaction technique, and construction methods are key factors in achieving a proper aggregate shoulder (Butt et al. 1997). The Iowa State Patrol fatal crash investigation officers reported that deficient granular shoulders are a major contribution to many of Iowa's fatal crashes. The most serious types of granular shoulder deterioration include rutting and edge drop-off, which often occur within 2 ft. of the pavement edge (Souleyrette et al. 2001). A detailed discussion of rut development is located in a subsequent section, but the major factors that contribute to rutting and edge drop-off include the following:

- Settlement of the shoulder
- Degradation of the granular material
- Erosion caused by surface drainage
- High traffic volume
- Off-tracking by wide vehicles

Price (1990) further reported noticeable problems where the pavement edge meets the gravel shoulder. These problems include water running off the pavement, which causes soft spots in the shoulder and accelerated rutting.

Blotter Shoulders

Blotter shoulders are normally a combination of a thin bituminous mix placed upon an existing granular shoulder. This process is reportedly effective in reducing water infiltration into the granular material, keeping the aggregate in place (Butt et al. 1997). Common distresses observed at blotter shoulders are block cracking, longitudinal and transverse cracking, and edge cracking.

Cold Recycled Asphalt Shoulders

Cold recycled asphalt shoulders are produced by a process in which existing bituminous shoulders are reworked on the roadway. Pulverizing equipment is used to produce recycled asphalt that can be used as a base course material with the addition of an emulsion or a recycling agent (Souleyrette et al. 2001).

Asphalt Concrete Shoulders

When placed adjacent to a portland cement concrete (PCC) pavement, asphalt concrete (AC) shoulders create a lane-shoulder joint that can be difficult to seal. This is because of the different thermal properties of the two materials. An unsealed lane-shoulder joint can result in water infiltration, leading to shoulder separation. In this configuration, the AC shoulder does not provide structural support to the pavement. If placed adjacent to an AC pavement, the cold joint can be eliminated; however, if the shoulder does not have the same structural design (surface and base layer thickness), the movement at this joint can be significant. Common AC shoulder distresses are shoulder drop-off, alligator cracking, block cracking, and longitudinal and transverse cracking (Souleyrette et al. 2001).

Portland Cement Concrete Shoulders

In addition to increased service life, one of the major advantages in using PCC shoulders is the reduction of pavement stress, due to the shoulder support for the mainline. Distresses that occur in PCC shoulders are similar to those that can occur in the mainline pavement, such as transverse cracking, faulting, and corner and joint spalling (Butt et al. 1997). According to Souleyrette et al. (2001), roadways with paved shoulders are generally much safer than similar roadways without paved shoulders. The opportunity to install rumble strips on paved shoulders further improves motorist safety. Shoulder rumble strips can reduce run-off-road crashes by 20% to 50% (Souleyrette et al. 2001). Rumble strips are also more cost-effective than other safety improvements, such as guardrails and slope flattening. However, paved shoulders are not always the proper solution, since previous studies have shown that partially paved shoulders are only cost-effective if traffic volumes do not exceed 1,500–2000 vehicles per day (VPD), while full-width paved shoulders are not cost-effective on roads with traffic volumes less than 3,000 VPD. In 1995, the Iowa DOT determined that a 3 ft. paved shoulder became cost effective with an average daily traffic (ADT) exceeding 2,100 (Souleyrette et al. 2001).

Initial Construction and Maintenance Costs

Comparing the cost of constructing and maintaining granular shoulders to that of paved shoulders in Colorado, Price (1990) found that granular shoulders cost 70% of the initial costs of paved shoulders. However, maintenance costs for granular shoulders are much higher than those of paved shoulders. Granular shoulder maintenance costs generally do not exceed the initial savings in construction costs. Table 1 summarizes the initial and maintenance costs of two-lane granular versus paved shoulders for the calendar year 2000 in Iowa. Maintenance functions for granular shoulders averaged \$4,794,000/year, or about \$259/lane-mile, while the maintenance cost of paved shoulders averaged \$329,000/year, or about \$76/lane-mile (Souleyrette et al. 2001). A study by Engineering Research and International, Inc. (1997), which investigated shoulder surfacing in South Dakota, arrived at a similar conclusion, that gravel shoulders are cheaper to construct but more expensive to maintain on an annual basis.

Table 1. Summary of granular and paved shoulder costs in Iowa for calendar year 2000 (Souleyrette et al. 2001)

Shoulder type	Cost type	Width	Cost (\$)
Paved (ACC)	Initial	3 ft	53,469 / mile
Granular	Initial	3 ft	13,376 / mile
Paved (ACC)	Initial	6 ft	106,938 / mile
Granular	Initial	6 ft	26,752 / mile
Paved (ACC)	Restoration	-	5.69 / s.y.
Granular	Restoration	-	1.43 /s.y.

Current Shoulder Practices

An overview of the shoulder practices in Iowa and neighboring states was conducted to better understand the criteria for choosing paved versus unpaved shoulders. In Iowa, all interstate shoulders are paved. Expressway shoulders are granular unless the design year ADT exceeds 10,000, at which point paved shoulders are to be constructed. The painted edge line for National Highway System (NHS) roadways are offset 4 ft. from the pavement edge with a 4 ft. partially paved shoulder. On non-NHS routes, shoulders are designed to be 10 ft. granular shoulders that can be reduced to 6 or 8 ft. if the yearly ADT is less than 3,000. Iowa's 3R standards do not include adding paved shoulders to existing routes (Souleyrette et al. 2001). Figure 1 shows a typical Iowa Department of Transportation (DOT) granular shoulder section. The granular shoulder material used is either Type A gravel, which is crushed stone or a gravel-limestone mixture, or Type B, which is a uniform mixture of coarse and fine particles produced by crushing limestone, dolomite, or quartzite (Iowa DOT Standard Specifications 2005). The maximum aggregate size for both types is 3/4 in. Table 2 provides a summary of paved shoulder practices in Iowa and neighboring states. According to survey reported by NCHRP Synthesis No. 63, the predominant slope for shoulders is 4% or 1/2 in./ft.

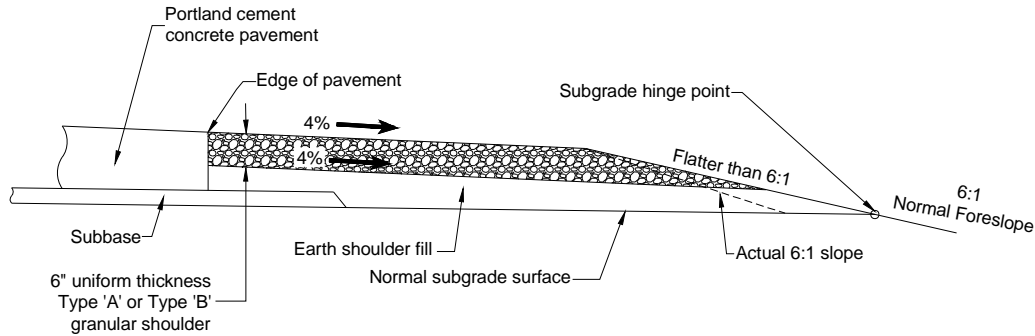


Figure 1. Iowa DOT granular shoulder section (modified from Iowa DOT Standard Road Plan RH-37D)

Table 2. Paved shoulder practices in Iowa and neighboring states (Souleyrette et al. 2001)

State	Total shoulder width/shoulder width paved		
	Rural multi-lane highways	Two-lane highways	Miscellaneous
Iowa	Right 10 ft./4ft. Left 6ft./4ft. Greater than 10,000 ADT consider full-width paved shoulder	NHS 10 ft./4 ft. Non NHS: ADT > 3,000 10 ft./4 ft. ADT < 3,000 8 ft./2 ft.	4 ft. paved shoulder on 3R projects Rumble strips on full-width paved shoulder and 2 ft. PCC shoulder 6 ft. paved shoulder typically provided where bike paths are include on primary highway system
Illinois	Right 10-12 ft./8-12 ft. Left 6ft./4-6 ft.	Principal arterial 10 ft./10 ft. Minor arterial 10 ft./4 ft.	3R improvement: 3 ft. paved shoulder if ADT > 3,000 1-2 ft. paved shoulder if ADT < 3,000 Rumble strips on freeways and expressways or high accident locations
Minnesota	Right 11.5 ft./10 ft. Left 5.5-11.5 ft./4-10 ft.	ADT > 2,000 9.5-11.5 ft./8-10 ft. ADT < 2,000 4-8 ft./1.5 ft./min	Min. 4 ft. paved shoulder if bike usage anticipated Rumple strips on paved shoulders greater than 4 ft.
Wisconsin	Right 10 ft./8-10 ft. Left 6-10 ft./3-10 ft.	ADT > 1,250 6-10 ft./3 ft./min.	Min. 5 ft. paved shoulder if bike ADT > 25 bicycles per day Rumble strips on most paved shoulders
South Dakota	Right 8/8 ft. Left 4/4 ft.	ADT > 2,500 8/8 ft. ADT < 2,500 28 ft. pavement	Rumble strips on all paved shoulders
Nebraska	Right 10 ft./8 ft. Left 6 ft./4 ft.	Priority system 10 ft./8 ft. ADT > 3,000 8 ft./8 ft. ADT < 3,000 28 ft. pavement	Rumble strips on all paved shoulders located to facilitate bikes
Missouri	Right 10 ft./4ft. Left 6ft./4ft. Greater than 10,000 ADT consider full-width paved shoulder	NHS 10 ft./4 ft. Non NHS: ADT > 3,000 10 ft./4 ft. ADT < 3,000 8 ft./2 ft.	4 ft. paved shoulder on 3R projects Rumble strips on full-width paved shoulder and 2 ft. PCC shoulder 6 ft. paved shoulder typically provided where bike paths are include on primary highway system

Iowa DOT Specification Review

The following Iowa DOT specifications were reviewed for recent changes that would affect shoulder design and maintenance. The review included the following sections:

- 2121, Granular Shoulders
- 2122, Paved Shoulders
- 2123, Earth Shoulders
- 2213, Base Widening
- 2302, Portland Cement Concrete Pavement Widening
- 2308, Bituminous Fog Seal
- 4120, Granular Surfacing Materials

Iowa DOT specifications are modified every six months, in October and April, with a general supplemental (GS) specification that is sequentially numbered, starting with 1001 on October 2, 2001. Previous specifications followed that same pattern; however, a new database approach to maintaining specifications was initiated at that time which has provided a more streamlined approach to tracking specification changes since that date.

Mr. Dan Harness of the Iowa DOT Specifications Section provided a spreadsheet that listed all specification changes since October 2, 2001. The research team reviewed the specifications and analyzed the changes, providing remarks that are listed in Table 3. Most of the changes were editorial changes that simplify construction contract administration by specifying the use of planned quantities for measurement and by streamlining wording in “basis of payment” sections. Word choice was improved in Section 4120, Granular Surfacing Materials.

One of the more significant items was a change to ensure that higher quality earth fill is placed under shoulders. This improvement occurred with GS 1002 on April 30, 2002. Apparently, this change was made to reduce the difficulties that were being experienced with soft shoulders, as described elsewhere in this report. In addition to this change, hot mix asphalt base materials and mix design requirements were raised from 300,000 to 1,000,000 equivalent single-axle loads (ESAL).

Table 3. Iowa DOT specification review

Section 2121, Granular Shoulders			
Article	GS	Change	Remark
2121.05, A	01002	Replace the first sentence and add new second and third sentences	Require select or suitable soil for earth shoulder fill
2121.06, A	01008	Replace the first sentence of the third paragraph	Allow steel vibratory rollers in addition to pneumatic rollers
2121.06, B	01008	Replace the first sentence of the second paragraph	Allow steel vibratory rollers in addition to pneumatic rollers
2121.07, B	01007	Add a new third sentence and replace the sixth sentence	Define fillet width in terms of additional pavement thickness and delete prohibition of dropoffs on both sides of roadway.
2121.07, C	01004	Add a new article	Require full width shoulder to grade for winter shutdown
2121.08	01007	Replace the second paragraph	Require planned quantity as basis of payment
2121.09	01002	Add a new last paragraph	Accommodate "place only" and recycled material situations
2121.09	01003	Add units into last paragraph	Clarify situation above
2121.09	01007	Delete the first paragraph	Editorial (Basis of Payment)
2121.09, A, 2	01007	Replace the entire article	Editorial (Basis of Payment)
Section 2122, Paved Shoulders			
Article	GS	Change	Remark
2122.02 A	1002	New Article	Increase ESALS from 300,000 to 1,000,000 for HMA base mixture
2123.02	01002	Replace the second sentence and add a new third sentence	Require select or suitable soil for earth shoulder fill
Section 2123, Earth Shoulders			
Article	GS	Change	Remark
2123.02	01002	Replace the second sentence and add a new third sentence	Require select or suitable soil for earth shoulder fill
2123.04, A	01005	Replace the first paragraph	Require planned quantity as method of measurement
2123.04, B	01005	Replace the first sentence	Require planned quantity as method of measurement
2123.05	01005	Delete the first paragraph	Editorial (Basis of Payment)
2123.05, A	01005	Replace the first sentence	Editorial (Basis of Payment)
2123.05, B	01005	Replace the first sentence	Editorial (Basis of Payment)

Table 3. Specification review (continued)

Section 2213, Base Widening			
Article	GS	Change	Remark
2213.01	01006	Delete the indented paragraph	Editorial
2213.01	01011	Delete "and the following provisions" form the end of the last sentence of the first paragraph	Editorial
2213.07	01007	Replace "Article 2303.03, A, 2" with "Article 2303.03, B, 2" in the second indented paragraph	Accommodate change in article designation in HMA Construction Specification
2213.08, A	01007	Replace "Article 2303.03, D" with "Article 2303.03, E" in the third paragraph and replace the second sentence of the fifth paragraph	Accommodate change in article designation in HMA Construction Specification
2213.09	01007	Replace "Article 2303.03, C" with "Article 2303.03, D" in the fourth paragraph	Accommodate change in article designation in HMA Construction Specification
2213.14	01005	Repace the entire article	Require planned quantity other change in method of measurement
2213.14	01007	Replace the entire article	Require planned quantity other change in method of measurement
2213.14, D	01001	Replace the entire article	Require planned quantity other change in method of measurement
2213.14, D, 2	01012	Change to plan quantity	Require planned quantity other change in method of measurement
2213.14, G	01001	Replace the entire article	Require planned quantity other change in method of measurement
2213.14, H	01001	Add a new article	Require planned quantity other change in method of measurement
2213.15	01005	Replace the entire article	Editorial (Basis of Payment)
2213.15, D	01001	Replace the entire article	Editorial (Basis of Payment)
2213.15, F	01002	Replace the title and article	Editorial (Basis of Payment)
2213.15, G	01001	Replace the entire article	Editorial (Basis of Payment)
2213.15, H	01001	Add a new article	Editorial (Basis of Payment)

Common Shoulder Problems

Figure 2 shows the frequent problems occurring in granular shoulder sections. Frequent granular shoulder problems include edge drop-off, shoulder rutting, erosion by water or wind, irregular slope, and settlement of the subgrade soil.

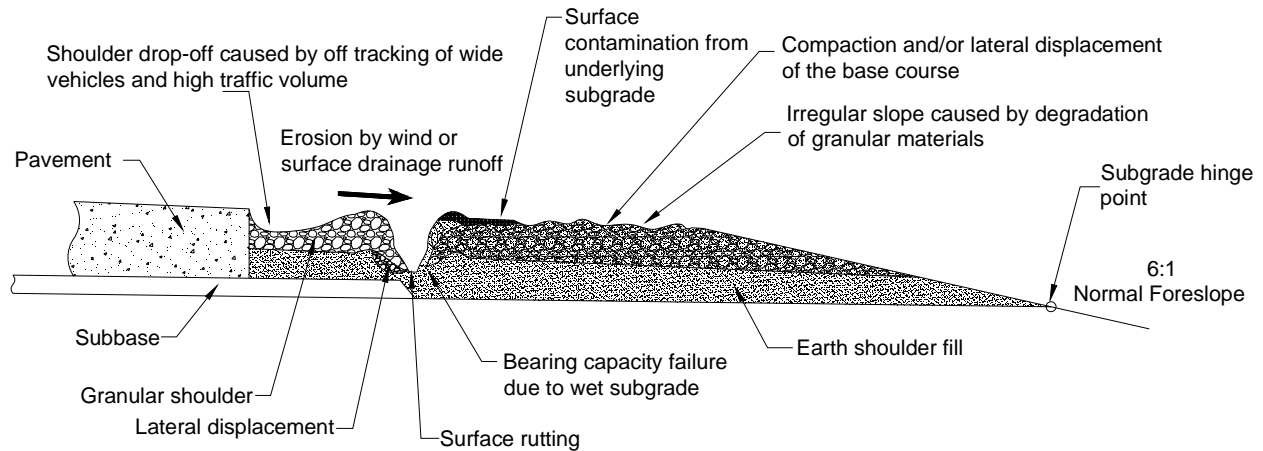


Figure 2. Common granular shoulder problems

Shoulder Rutting and Edge Drop-offs

According to Fannin and Sigurdsson (1996), where traffic is channelized a rut is defined as the distance between the initial elevation of the surface before trafficking and the lower point in the rut beneath the wheel. Where traffic is not channelized, an erratic pattern of ruts develops, which can be defined as the distance between adjacent high and low spots of the base course thickness (Giroud and Han 2004a). Vertical drop-offs found along the edge of the pavement can lead a driver to overcorrect upon reentry onto the paved surface. This overcorrection may cause the vehicle to cross into opposing traffic or leave the opposite side of the roadway. According to Wagner and Kim (2004), shoulder drop-offs have been observed more frequently along the inside of horizontal curves.

A recent study by Hallmark et al. (2006) investigated the relationship between edge drop-off and road characteristics. The results show that edge drop-offs of 2.5 in. or greater are most likely to occur at narrow shoulders (shoulder widths less than 3.0 ft.). Shoulder sections with widths varying from 3 to 7.25 ft. are most likely to exhibit shoulder drop-off when the grade is higher than 4.8%. Edge drop-offs higher than 3 in. were encountered at sections with narrow lanes (less than 11.6 ft.). This study, however, did not find evidence that shoulder sections near horizontal curves and mailboxes have higher proportions of edge drop-off. The authors attributed that to frequent maintenance and a higher level of treatments.

For low-volume road design, AASHTO (2001) design guidelines allow rut depths from 0.5 to 3 in., while in the case of unpaved access roads rut depth greater than 3 in. is acceptable. In 1976, a

study was conducted by the California Department of Transportation that documented the allowable edge drop-offs for shoulders according to five state DOTs (Nordlin et al. 1976). Table 4 presents a summary of the findings.

Table 4. Summary of drop-off standards for several states (Nordlin et al. 1976)

State	Drop-off standard
California	<ul style="list-style-type: none"> • Repair drop-offs greater than 1.5 in. or when edge failure becomes apparent
Illinois	<ul style="list-style-type: none"> • No published standards but attempts to keep shoulders flush with pavement • Posts warning signs to alert traffic to shoulder construction
New York	<ul style="list-style-type: none"> • 2 in. maximum drop-off on state highways (DHV = 200) • 1.5 in. maximum drop-off on state highways (DHV = 200-500) • 1 in. maximum drop-off on express ways (DHV > 500)
Oregon	<ul style="list-style-type: none"> • Requires shoulders to be flush with traveled way • Considering change in standards to permit up to 2 in. drop-off
Texas	<ul style="list-style-type: none"> • No published standards but try to limit drop-off to 2-3 inches
Washington	<ul style="list-style-type: none"> • Requires shoulders to be flush with traveled way • Drop-offs greater than 3 in. should be filled with stabilized material

Note: DHV = design hourly volume

According to Giroud and Han (2004a), surface rutting occurs due to one or more of the following mechanisms:

- Compaction of the base course aggregate and/or subgrade soil under repeated traffic loading
- Bearing capacity failure in the base course or subgrade due to normal and shear stresses induced by initial traffic
- Bearing capacity failure in the base course or subgrade after repeated traffic loads, which can result in progressive deterioration of the base course, reduction in effective base course thickness due to base course contamination by the subgrade soil, a reduction in the ability of the base course to distribute traffic loads to the subgrade, or a decrease in subgrade strength due to pore pressure buildup or disturbance
- Lateral displacement of base course and subgrade material due to the accumulation of incremental plastic strains induced by each load cycle

High Traffic Speed and Traffic Volume

A study by Berthelot and Carpentier (2003) examining the gravel loss characteristics demonstrated that high traffic speeds and high traffic volumes contribute to gravel loss. Therefore, off-tracking of vehicles onto the shoulder section contributes to the gravel loss near the pavement edge, which increases the edge drop-offs. In the same study, it was reported that gravel samples retrieved from the road surface along the wheel paths were cleared of surface gravel almost immediately under the impact of heavy trucks. In addition, the coarse gravel

particles were pushed to the center of the lane and the outside of the wheel paths within a few truck passes. Furthermore, between 5% and 43% of the coarse-size particles were ground to sand-size particles. Once the wheel tracks are formed, the water infiltration rate is reduced compared to the non-tracked portion. This, in turn, increases the surface runoff and thus causes greater erosion, even though ruts are not present. When a rut does form, runoff is prevented from flowing across the shoulder and is confined to the rut. The confined flow causes additional erosion (Foltz 1996).

Dust Emission

Another factor that contributes to rut development along the pavement edge, as well as degradation of the shoulder section, is dust emission. Emission rates from unpaved shoulders were studied by Moosmuller et al. (1998). It was determined that paved roads with unpaved shoulders are among the largest dust emitting road types. Emissions from unpaved shoulders are attributed to aerodynamic forces caused by high-speed, high-profile vehicles such as tractor-trailers. The main constituents of these dust particles are oxides of silicon, iron, aluminum, and calcium compounds. Jones et al. (2001) showed that loss of fines is not only a safety hazard, but also contributes to increased gravel loss and the need for more frequent maintenance. The loss of fines from the unpaved structure's surface leads initially to a reduction in surface layer cohesion and subsequently its disintegration. This disintegration also increases surface irregularity, and eventually it starts the process of longitudinal rutting (Jones et al. 1984). To reduce dust emission from granular surfaces in Iowa, Bergeson et al. (1990) suggested the use of granular material graded on the fine side of the Iowa DOT Class A gradation for granular surfaces and shoulders. This gradation is believed to have sufficient fines (No. 40 to No. 200 sieve) to act as a binder for the coarser particles, which in turn promotes the formation of a strong surface. In their study to control fugitive dust, Bergeson and Brocka (1996) suggested treating unpaved roads with bentonite. Their study demonstrated that 70% dust reduction can be achieved at a 9% bentonite treatment level. This reduction is caused by the interaction between the negatively charged clay particles in bentonite and the positively charged limestone, which creates agglomeration of fine particles and causes the fine particles to stick to larger limestone particles. Bergeson and Brocka (1996) reported that dust reduction was observed over extended periods (i.e., greater than two seasons).

Pavement Overlays

Asphalt overlay is another common source of drop-off at the pavement edge (Humphreys and Parham 1994). Roadways are often resurfaced without restoring the adjacent shoulders to bring them up to the resurfaced roadway level.

Subgrade Stabilization

The following sections discuss general guidelines for selecting stabilization methods and methods for incorporating geosynthetics into shoulder construction to help the shoulder withstand heavier and repetitive traffic loads.

General Stabilization Guidelines

Figure 3 shows a chart developed by Chu et al. (1955) for stabilizer selection. Using data from grain size distribution and Atterberg limits test, the appropriate soil stabilizer can be selected. According to Glogowski et al. (1992), whenever lime and cement are selected, fly ash can be added to improve performance. The following factors should also be taken into consideration during selection of a suitable stabilizer:

- Fly ash type (class C, class F, carbon content, calcium oxide content)
- Lime type (hydrated lime, quick lime)
- Proportion of stabilizer to soil
- Ratio of lime to fly ash
- Age of mixture (the rate of strength gain varies with soil and stabilizer types and can continue for years)
- Temperature (pozzolanic reactions are retarded at temperatures below 40°F)
- Dry density and moisture content of compacted mixture

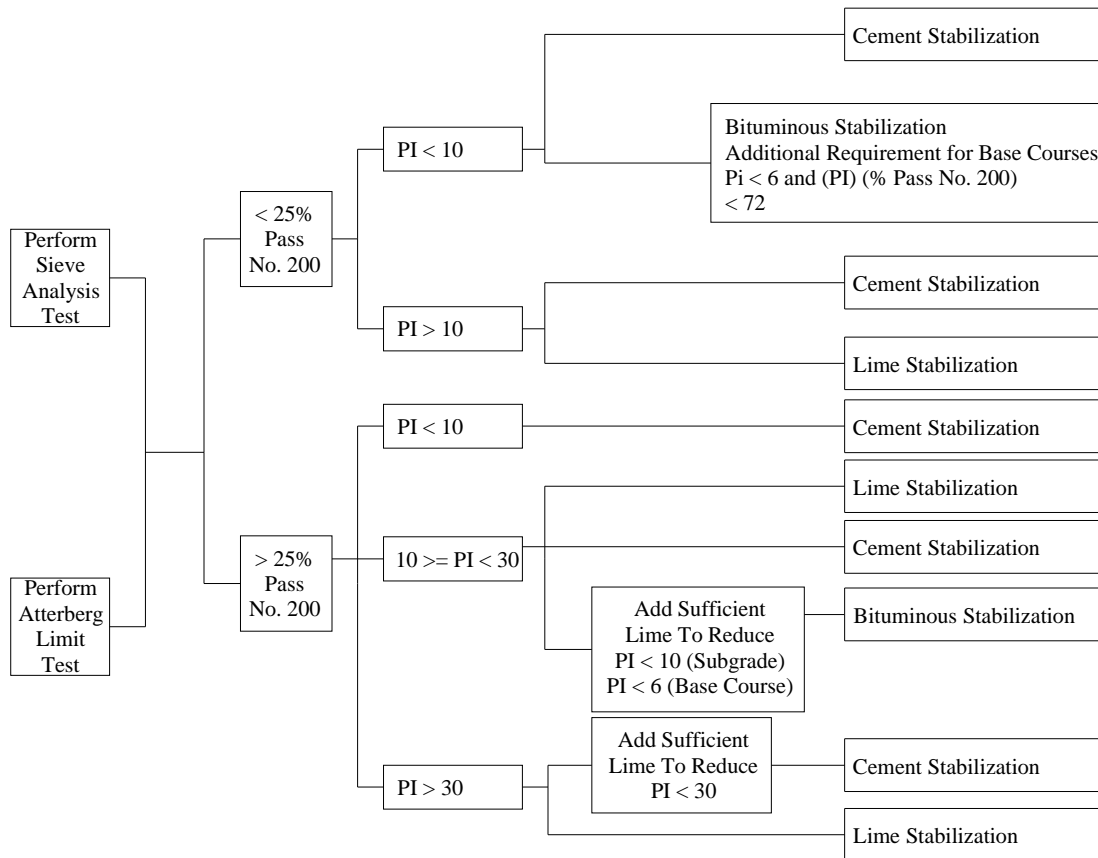


Figure 3. Selection of stabilizer (Chu et al. 1955)

Geosynthetics

During the past few decades, the use of geosynthetics to reinforce unpaved structures has markedly increased. Geosynthetics, which are typically placed at the interface between the base course and the subgrade, can carry higher traffic volumes and can prevent lateral movement of the base aggregate, stiffening the layer so it distributes wheel loads over a greater area of the subgrade (Tensar Earth Technologies, Inc. 1996). According to Berg et al. (2000), Giroud and Han (2004a), and Powell et al. (1999), the following benefits of using geosynthetics in roadways have been identified:

- Reduction of the intensity of stress on the subgrade
- Increase of the bearing capacity of the subgrade
- Prevention of the subgrade fines from pumping into the base
- Prevention of the contamination of the base materials, allowing for more open-graded, free draining aggregates
- Reduction of the depth of excavation required for the removal of unsuitable subgrade materials
- Reduction of the thickness of the aggregate layer required to stabilize the subgrade
- Minimized disturbance of the subgrade during construction
- Minimized maintenance and extended pavement life
- Prevention of the development and growth of local shear zones, allowing the subgrade to support stresses close to the plastic limit while acting as if it is still in the elastic limit

Two types of geosynthetics are typically used: geotextiles and geogrids. Nonwoven geotextiles have been mainly used for separation of the base course aggregate and the subgrade. Geogrids and woven geotextiles have been used as a reinforcement to increase resistance to traffic loadings (Giroud and Noiray 1981).

Three fundamental reinforcement mechanisms have been identified involving the use of geogrids: (1) lateral restraint, (2) improved bearing capacity, and (3) tensioned membrane effect. Lateral restraint refers to the interlocking and confinement of aggregate during loading, restricting the lateral flow of the material. This increases the modulus of the base course material, which thus increases the vertical stress distribution applied to the subgrade. Improved bearing capacity is achieved by shifting the failure envelope from the weaker subgrade to the stiffer base course. The tensioned membrane effect is based upon the concept of an improved vertical stress distribution resulting from tensile stress in a deformed membrane. In early research stages, the tensioned membrane effect was believed to govern the reinforcement mechanism. However, later research demonstrated that reinforcement benefits are obtained without significant deformation and that lateral restraint is the primary reinforcement mechanism, followed by the improved bearing capacity concept (U.S. Army Corps of Engineers 2003). Figure 4 shows a biaxial geogrid commonly used for soil reinforcement.



Figure 4. Tensar BX1100 geogrid (image scale 1:2.5)

Some geogrids have demonstrated superior performance in the laboratory by providing better interlock with the aggregate base material (Fannin and Sigurdsson 1996). Geogrids may interlock with aggregates if there is an appropriate relationship between the aperture size and the aggregate particle size. The effectiveness of the interlocking, however, depends on the in-plane stiffness of the geogrid and the stability of the geogrid ribs and junctions. Therefore, the interlocking mechanisms for unpaved structures are different for geotextiles and geogrids.

There are two benefits of interlocking between the geogrid and the base course aggregate. First, lateral movement of the base course aggregate is reduced and, as a result, no outward shear stresses are transmitted to the subgrade. Second, the bottom confined surface of the base course provides a rough surface that resists lateral movement of the subgrade, which generates inward shear stresses. According to results of the theory of plasticity, outward shear stresses decrease the bearing capacity, while inward shear stresses increase the bearing capacity. The stresses induced by vehicular loads tend to be oriented outward (Giroud and Han 2004a). The presence of outward shear stresses can reduce the bearing capacity to as little as one half of the value of purely vertical loading. When geosynthetics are used, the outward shear stresses are picked up by the reinforcement, which is put into tension, and purely vertical loads are transmitted to the subgrade, mobilizing its full bearing capacity (Milligan et al. 1989).

Separation of subgrade and base course materials appears to be very important for the thinnest base course layer, where the geotextile outperforms the geogrid. However, the geogrid outperforms the geotextile on the thicker base course layer, where reinforcement rather than separation dominates (Fannin and Sigurdsson 1996).

The benefits from using geosynthetics can be expressed in terms of traffic benefit ratio (TBR). TBR is defined as the ratio of the number of cycles necessary to reach a given rut depth for a test section containing reinforcement to the number of cycles necessary to reach the same rut depth for an unreinforced section with the same base course thickness and subgrade properties. Base course reduction (BCR) can also be used to express the added value of using geosynthetics. The BCR is expressed as a percentage savings of the unreinforced base course thickness. TBR and BCR field and laboratory results were found to vary significantly, which may be attributed to the many variables affecting the results of a particular test (Berg et al. 2000). Table 5 presents a summary of the significant variability encountered in previous field and laboratory studies.

Table 5. Summary of laboratory and field test sections (Berg et al. 2000)

	TBR	BCR
Geotextiles		
Range	1–220	22–33%
Typical values	1.5–10	
Geogrid/Geotextile composite		
Range	0.8–670	30–50%
Typical values	1.5–70	

Giroud and Noiray (1981) presented a design method for unpaved roads in 1981. The method was widely used, since it combined a theoretical analysis with an empirical formula deduced from full-scale tests on aggregate roads as a function of soil properties and traffic. The method considered the subgrade and the geotextile modulus to determine the required thickness of an aggregate layer for a given number of passes of a particular vehicle. Their assumptions are the same as those normally used for stress distribution and bearing capacity calculations in foundation engineering (Holtz and Sivakugan 1987).

Even though the Giroud and Noiray’s (1981) paper is recognized as a significant attempt to understand the mechanics of unpaved structures, several researchers have criticized this method. Fannin and Sigurdsson (1996), in their research study on unpaved roads, concluded that the analytical approach of Giroud and Noiray (1981) significantly overpredicts the number of passes required to develop a 5 cm rut, and the approach is only applicable to unpaved structures that do not exhibit compaction of the base course. In addition, the method presents an unnecessary emphasis on firm anchorage (Fannin and Sigurdsson 1996; Milligan et al. 1989). As discussed above, lateral restraint has been identified as the primary reinforcement mechanism; anchorage of the reinforcement is viewed as less important. The design method therefore does not take into account the interlocking mechanism of the geogrid-base course layer, which makes it unsuitable for geogrid reinforcement design.

Another older method, presented by Steward et al. (1977) and adopted by the U.S. Forest Service, does not account for traffic, quantify the anticipated rut depth, or account for different properties of geosynthetics. Furthermore, this method is only applicable for a base course California bearing ratio (CBR_{bc}) greater than 80 over very soft subgrade soils, which is rarely encountered in the field (Giroud and Han 2004b; Tensar Earth Technologies, Inc. 1996).

In this study, the design method presented by Giroud and Han (2004a and 2004b) is adopted for designing geogrid reinforced shoulder sections. The improved Giroud and Han (2004a) method is based on theoretical development and experimental calibration that more accurately predicts the behavior of unpaved structures. This method considers the mechanical properties of geogrids. The influence of geogrids is accounted for by two factors: the bearing capacity factor (N_c), which implies interlock between the geogrid and the base course materials, and the aperture stability modulus (J), which is linked to the increase in the stress distribution angle. The design method also accounts for the quality of the base course materials, the variation in the stress distribution angle with the number of load cycles, and the influence of rut depth. Only failure of subgrade soil is considered in this method. The subgrade is assumed to be saturated and have low permeability (i.e., it behaves in an undrained manner) (Giroud and Han 2004a; Tensar Earth Technologies, Inc. 1996). The limitations of the Giroud-Han method are the following:

- The method was only validated for Tensar biaxial geogrids and geotextiles products.
- Only an aperture stability modulus of less than or equal to 0.8 mN° can be used.
- Tensioned membrane effect is not taken into account.

Using field and laboratory data from previous studies, Giroud and Han (2004b) developed and calibrated Equation (1) for calculating base course thickness.

$$h = \frac{0.868 + (0.661 - 1.006J^2) \left(\frac{r}{h}\right)^{1.5} \log N}{f_E} X \left[\sqrt{\frac{P/(\pi r^2)}{mN_c f_c CBR_{sg}}} - 1 \right] r \quad (1)$$

Where, h = required base course thickness (m); J = geogrid aperture stability modulus (mN°); N = number of axel passages; P = wheel load (kN); r = radius of equivalent tire contact area (m); m = bearing capacity mobilization coefficient; N_c = bearing capacity factor; f_c = factor equal to 30 kPa; and CBR_{sg} = CBR of subgrade soil. For unreinforced unpaved roads, $J = 0$ and $N_c = 3.14$. For geotextile-reinforced unpaved roads, $J = 0$ and $N_c = 5.14$. For geogrid-reinforced unpaved roads, $J > 0$ and $N_c = 5.71$. The bearing capacity mobilization coefficient, m , is defined using Equation (2).

$$m = \left(\frac{s}{f_s}\right) \left\{ 1 - \xi \exp\left[-\omega\left(\frac{r}{h}\right)^n\right] \right\} \quad (2)$$

Where, s = rut depth (mm) and f_s = factor equal to 75 mm rut depth. The variables ξ , ω , and n are parameters equal to 0.9, 1.0, and 2, respectively, according to calibration using experimental data. The bearing capacity mobilization coefficient, m , cannot be greater than unity. If m is greater than 1, the base course thickness must be increased or a smaller allowable rut depth selected.

To calculate the required base course thickness for specific site conditions, a series of iterations is performed. For the first iteration, Equation (2) is used to calculate the bearing capacity mobilization coefficient using an assumed base course thickness. The base course thickness, h , is then calculated using Equation (1) and compared to the assumed h value. The calculated h is then used for the second iteration. The iterative process is repeated until the assumed base course thickness equals the calculated value.

Granular Shoulder Stabilization

The subsequent sections discuss base course stabilization techniques, which can alleviate edge drop-offs, erosion, and disintegration of granular material under the impact of traffic.

Foamed Asphalt

Foamed asphalt (FA), also known as foamed bitumen or expanded asphalt, refers to a mixture of pavement construction aggregate and foamed bitumen. The FA is produced by a process in which water is injected into the hot bitumen, resulting in immediate foaming. The injected water turns into vapor, which is trapped in thousands of tiny bubbles. The bitumen expands to approximately 15 times its original volume, forming foam. In this state, the bitumen has a high surface area and extremely low viscosity. The bitumen has to be mixed with aggregate in its foamed state before it dissipates and resumes its original properties (Kendall et al. 2001; Muthen 1998).

The potential of FA for use as a soil binder was first realized in 1956 by Dr. Csanyi, at Iowa State University's Engineering Experiment Station. He demonstrated the effectiveness of stabilizing marginal local aggregates such as gravel, sand, and loess soils (Asi 2001). Unpaved roads that were stabilized using FA in South Africa show excellent performance after eight years, despite the heavy traffic (Collings et al. 2004). The following advantages of FA are well documented (Asi 2001 and Muthen 1998):

- FA increases the shear strength of granular materials. The strength characteristics approach those treated with cement, but FA is more flexible and fatigue resistant.
- FA can be used with a wider range of aggregate types than other cold mix processes.
- FA is time efficient because it can be compacted immediately and can carry traffic almost right after compaction.
- FA conserves energy because only bitumen needs to be heated.
- Evaporation of volatiles from the mix are avoided; therefore, the process is environmentally friendly.
- FA can be constructed in adverse weather conditions, such as cold weather or light rain, without affecting its workability or quality.
- FA offers a cheaper means of incorporating asphalt into untreated soils than emulsified asphalt.

The disadvantages of FA are that (1) it is moisture susceptible because of the large void content, (2) its design methodology is relatively new, and (3) FA mix is not abrasion resistant (Muthen

1998). Using higher binder content, 1%–2% lime, or 1.5%–2% cement can decrease the permeability and increase the mix stiffness and early strength development (Kendall et al. 2001, Lee and Kim 2003, and Asi 2001).

Characterization of Foamed Asphalt

FA is characterized in terms of expansion ratio and half-life. The expansion ratio is defined as the ratio between the maximum volume achieved in the foam state and the final volume of the binder once the foam has dissipated. The half-life is the time, in seconds, between the moment the foam achieves maximum volume and the moment it has dissipated to half the maximum volume. The quantity of water used and the temperature at which the foam is produced are important factors that affect the half-life and expansion ratio of the foam. Higher temperature and water quantity will increase the expansion ratio and decrease the half-life. Higher expansion foam will result in higher strength, greater cohesion, and increased coating of the aggregate (Muthen 1998).

Recommended Aggregate Gradation

Foamed asphalt works with a range of aggregate gradation. The Iowa DOT gradation requirement for granular shoulders and the gradation requirement for aggregates that can be stabilized with FA, according to Muthen (1998), are shown in Figure 5. The figure indicates that FA is a good candidate for stabilizing granular shoulders in Iowa based on specified gradation. If necessary, grading can be adjusted by adding fines or coarse material so that the final gradation conforms to the gradation envelope. The percentage of fines is recommended to be a minimum of 5%. Generally, both the gradation and the plasticity index (PI) should be determined. Materials with PI greater than 12 should be treated with lime to reduce the PI (Muthen 1998; Lee and Kim 2003).

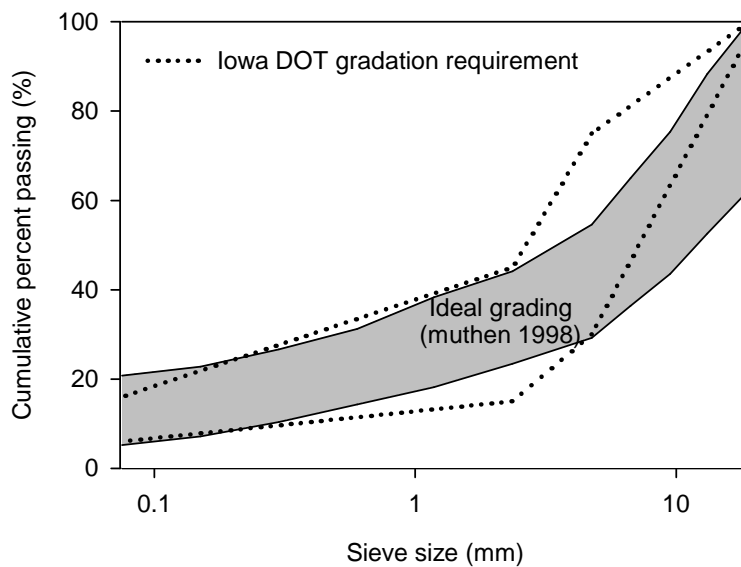


Figure 5. Gradation envelope for foamed asphalt mixes (modified from Muthen 1998)

Foamed Asphalt Content

Previous research suggests the use of 3.5% binder for 5% fines content and up to 5% binder for 20% fines content. In general, the finer the aggregate, the more FA needed. In addition, previous research has found that slightly more asphalt content is needed for FA mixtures than the optimum amount for emulsion (Lee and Kim 2003). Table 6 and Table 7 show the recommended FA content, as reported by Ruckel et al. (1982) and Bowering and Martin (1976). Too much binder will act as a lubricant, which will decrease the strength and the stability of the mix.

Table 6. Foamed asphalt content (Ruckel et al. 1982)

% passing No. 4 sieve	% passing No. 200 sieve	Foamed asphalt content (%)
< 50 (gravels)	3-5	3.0
	5-7.5	3.5
	7.5-10	4.0
	>10	4.5
>50 (sands)	3-5	4.5
	5-7.5	4.0
	7.5-10	4.5
	>10	5.0

Table 7. Optimal binder content range (Bowering and Martin 1976)

Soil type	Binder (%)	Additional
Well graded clean gravel	2.0-2.5%	
Well graded marginally clayey/silty gravel	2.0-2.5%	
Poorly graded marginally clayey gravel/silty gravel	2.0-2.5%	
Clayey gravel	4.0-6.0%	Lime modification
Well graded clean sand	4.0-5.0%	Filler
Well graded marginally silty sand	2.5-4.0%	
Poorly graded marginally silty sand	3.0-4.5%	Low penetration of bitumen and filler
Poorly graded clean sand	2.5-5.0%	Filler
Silt sand	2.5-4.5%	
Silty clayey sand	4.0%	Possibly lime
Clayey sand	3.0-4.0%	Lime modification

Portland Cement Stabilization

Portland cement (PC)-stabilized soil is a mixture of pulverized soil material and measured amounts of PC and water compacted at high density. It is primarily used as a base course for roads, airports, shoulders, and parking areas (Portland Cement Association 1979). There are three types of cement stabilized soils (Fang 1990):

1. PC soil contains sufficient cement to produce a hard and durable construction material and only enough moisture to satisfy the hydration requirement for cement and soil and to provide lubrication for compaction. It is commonly used for stabilizing the road bases of flexible and rigid pavements.
2. Cement modified soil (CMS) is a semi-hardened mixture of soil and cement with relatively small quantities of cement added to granular soils. The mixture reduces plasticity and volume change and increases the bearing capacity of the soil. It is often used for erosion and frost protection.
3. Plastic PC soil is a hardened product but contains, at the time of placement, sufficient water to produce consistency similar to plastering mortar. It is used primarily in the lining of ditches and trenches and in the protection of such surfaces against erosion.

The soil portion of the PC-stabilized soil mixture can be any combination of sand, silt, clay, and gravel. In addition, old granular base roads, with or without their bituminous surfaces, can be recycled to make good soil-cement. However, soils with a granular breaking skeleton and sufficient fines to partly fill the voids without interference from grain-to-grain contact (approximately 10% to 35% of non-plastic fines) require the least amount of cement for adequate hardening (Portland Cement Association 1979; Fang 1990). Figure 6 shows the gradation requirement for a cement-stabilized base course and the Iowa DOT gradation requirement for granular shoulders. A segment of the Iowa DOT shoulder gradation requirement matches the gradation requirement for cement-stabilized base courses. In addition, the percentage of fines (material passing the No. 200 sieve) is within the suggested limits.

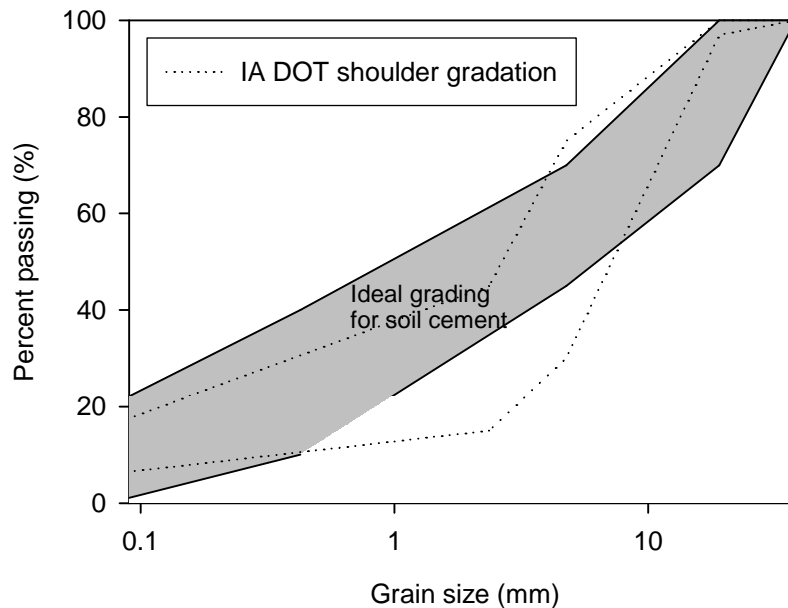


Figure 6. Gradation requirement for cement stabilized base course (modified from Department of the Army, the Navy, and the Air Force 1994)

According to the Portland Cement Association (1979), using PC-stabilized soil converts the unpaved structure to a hard, slab-like material, which does not consolidate further under traffic or rut or shove during spring thaws. In addition, PC-stabilized soil can bridge weak local subgrade

areas and is little affected by freezing and thawing. PC-stabilized shoulders are stable under all weather conditions, do not consolidate under traffic, resist erosion and growth of vegetation, and provide rapid runoff of surface water. However, deicing salts are harmful to PC-stabilized shoulders and should be drained away as rapidly as possible. Unlike PC-stabilized soil, CMS is not intended to withstand freeze-thaw and wet-dry cycles. CMS shoulders, which have been found to eliminate edge rut, are always surfaced with bituminous material (Portland Cement Association 1979).

The majority of performance problems occurring in cement-stabilized granular materials are related to shrinkage cracking. Although the cracks themselves do not present a structural problem, they often accelerate degradation by allowing water infiltration (Fang 1990). PC-stabilized soil shrinks as a result of hydration and moisture loss. Generally, materials containing higher fines content exhibit higher shrinkage potential than coarser material. Limiting the plasticity of soil, blending low shrinkage cement with fly ash, and using expansive cement were found to be effective methods for reducing shrinkage (Guthrie et al. 2002).

A previous study by Guthrie et al. (2002) showed that using 3% cement is sufficient to meet the compressive strength, durability, and moisture susceptibility requirements for stabilizing aggregate base material. Table 8 shows typical cement requirements for various soil types.

Table 8. Recommended cement Contents for various soil types (Fang 1990)

AASHTO soil classification	Unified soil classification	Normal range of cement requirements		Cement content for moisture- density test, % by weight	Cement contents for wet-dry and freeze-thaw tests, % by weight
		% by volume	% by weight		
A-1-a	GW, GP, GM, SW, SP, SM	5-7	3-5	5	3-5-7
A-1-b	GM, GP, SM, SP	7-9	5-8	6	6-4-8
A-2	GM, GC, SM, SC	7-10	5-9	7	5-7-9
A-3	SP	8-12	7-11	9	7-9-11
A-4	CL, ML	8-12	7-12	10	8-10-12
A-5	ML, MH, CH	8-12	8-13	10	8-10-12
A-6	CL, CH	10-14	9-15	12	10-12-14
A-7	MH, CH	10-14	10-16	13	11-13-15

Limestone Screenings

Limestone screenings, being a byproduct of aggregate production, are typically less expensive than other rock gradations. Limestone screenings have a maximum particle size of 3/8 in. and may contain as little as 20% to more than 40% passing the No. 200 sieve. Generally, the Unified Soil Classification System (USCS) of this material is SM (silty sand), and the AASHTO

classification is A-2-4 silty, clayey gravel and sand. The optimum moisture contents for limestone screenings typically range from about 9% to about 22%.

Recently, the principal investigator of this project completed a study (White et al. 2005b) investigating the possibility of using limestone screenings as a structural layer in road construction. A test section was constructed at an access road into a new sand production facility located about 10 miles east of Cedar Rapids and 1 mile north of U.S. Highway 30 on Old River Road. The section had a combination of cement kiln dust (CKD) and class C fly ash stabilized limestone screenings overlying manufactured sand. The stabilized layer was about 12 in. thick. The section was covered with 4 to 6 in. of crushed limestone as a wearing surface. Falling weight deflectometer results suggested that stabilized limestone screenings can perform as a structural layer in road construction. After 20 months, visual inspections show that the section is performing well under daily traffic, and there are no signs of rutting.

Concurrent to the field testing, a laboratory study was conducted in which stabilizers such as PC, CKD, and class C fly ash were used to stabilize the limestone screenings. The findings of this laboratory study indicate that stabilized limestone screenings could be a good contender as an alternative shoulder material (for more details on this laboratory study, refer to White et al. 2005b).

Calcium Chloride

Calcium chloride is a material produced from natural brine deposits found underground and is usually processed in three forms: pellets, flakes, or liquid. It is primarily used for dust control and base stabilization for unpaved roads. There are two important characteristics of calcium chloride that enable it to stabilize unpaved structures. First, calcium chloride is hygroscopic, since it attracts moisture from the atmosphere and the surrounding environment and resists evaporation. Second, calcium chloride is deliquescent, meaning that the solid form can dissolve into a liquid by absorbing moisture from the atmosphere and the surroundings. When compared to pure water, calcium chloride solution has a stronger moisture film, higher surface tension, lower vapor pressure, and lower freezing point. These properties enable it to keep the unpaved surface damp, and to keep dust or small particles in place. As a result, the coarse particles tend to stay in place, alleviating their abrasive action. Because the material stays in place, the frequency of blading can be reduced by 25% to 75% (Kirchner and Gall 1991).

Previous research and field tests showed many benefits of calcium chloride. Adding the proper amount of calcium chloride to granular material will result in a greater density than would be achieved by water alone. The stronger film moisture formed by calcium chloride improves lubrication allowing the aggregate to slide easily as they are mechanically compacted. In addition, calcium chloride works to inhibit evaporation and therefore maintain optimum moisture for a longer period. Calcium chloride also depresses the freezing point of water which helps the granular material resist frost heave in winter (Kirchner and Gall 1991). Calcium chloride was used on a road in Clayton County, Iowa where 700 tons of rock was added twice a year. After the section was treated with calcium chloride, no rock was added for 3 years, and 4,200 tons of rock was saved (Public Works Journal Corporation 1980).

The percentage of calcium chloride needed to stabilize unpaved structures is generally 1% to 2.5% of the dry weight of aggregate, which is higher than the percentage needed for dust control (Monlux 2003). The application rate for calcium chloride mixed with soil varies from 0.27 to 0.5 gal/yd². For topical applications, the application rate is about 0.1 gal/yd² (Bushman et al. 2004 and Kirchner and Gall 1991).

Calcium chloride works best with well-graded gravel, with fines content ranging from 12% to 18%. Calcium chloride does not perform well if the percentage of fines is less than 10% (Kirchner and Gall 1991). Further, it is best applied after seasonal spring rains when there is ample moisture in the ground (Monlux 2003).

According to Kirchner and Gall (1991), calcium chloride costs 41% to 46% and 83% less than lignosulfonate and oil emulsion stabilizers, respectively. The construction cost of in-place calcium chloride, as reported by Monlux (2003), ranges from \$4,000/mile to \$6,000/mile, depending on the application rate, project location, structure width, and mixing depth. Calcium chloride is considered cost-effective when compared to the combined costs of construction, blading maintenance, and replacement of aggregate for an unstabilized section.

Magnesium Chloride

Magnesium chloride is a salt with properties that are useful for chemical stabilization of granular surfaces. The main properties of magnesium chloride, as reported by Thenoux and Vera (2003), are (1) solubility in water, (2) deliquescence, which allows magnesium chloride to absorb moisture when relative humidity is above 32%, (3) the vapor pressure of magnesium chloride is less than that of water at any temperature and relative humidity, allowing for better compaction, and (4) magnesium chloride increases surface tension up to 45%, which reduces evaporation and results in erosion resistance. The stabilization mechanism of magnesium chloride depends on humidity absorption and retention, which is related to the period of time the absorbed moisture is retained in the soil. In addition, under low-humidity conditions, magnesium chloride crystallizes in the road surface, cementing the fine particles. This forms a hard crust that resists the abrasive action of traffic and reduces deterioration rate (Thenoux and Vera 2003).

The rate of application of magnesium chloride documented in the literature varies from 0.5 to 0.7 gal/yd² (Kirchner and Gall 1991; Bushman et al. 2004). Bushman et al. (2004) recommend 0.1 gal/yd² for topical applications and a 1 part magnesium chloride to 3.8 parts water for a dilution rate for both blending and topical applications.

Even though the stabilization mechanism of magnesium chloride is similar to that of calcium chloride, at temperatures higher than 71°F and at relative humidities lower than 31% magnesium chloride begins to lose its capabilities, whereas calcium chloride does not. In addition, leaching of magnesium chloride occurs at high moisture contents (Kirchner and Gall 1991; Bolander 1999).

The cost of magnesium and calcium chlorides are about equal; however, calcium chloride is a more effective stabilizer, especially at high temperatures and low humidities. Therefore, on an application basis, magnesium chloride can cost about twice as much (Kirchner and Gall 1991).

Polymer Emulsion

Many commercially available polymer emulsion products are used as dust suppressants. This section focuses on two products commonly used for dust and erosion control. These products, which have a milky white appearance, as shown in Figure 7, are *Soil Sement*[®] (henceforth referred to as S.S. polymer) and *Soiltac*[®] (henceforth referred to as Soiltac polymer).

S.S. polymer, which has a pH ranging from 4.0 to 9.5, saturates the soil, coating each particle. The polymers then bond to create a solid mass. According to Bushman et al. (2004), a highly durable surface is created that will endure the stresses of climatic extremes and heavy vehicle traffic. Additional aggregate may be added, particularly if the soil contains clay, to improve water drainage. S.S. polymer usually dries in 2 to 3 hours and cures in 24 to 36 hours. A study by Bushman et al. (2004) that investigated stabilization methods for unpaved roads suggested the following sequence for applying S.S. polymer:

- Dilute the S.S. polymer and blend with the soil to a depth of 6 in. using a reclaimer
- Compact the treated material
- Regrade the stabilized section with a motor grader to provide proper crown
- Perform final compaction
- Apply liquid S.S. polymer topically to the entire stabilized section

It was also reported that the dilution of S.S. polymer was 1 part concentrate to 1.8 parts water for both the mixing and the topical applications. The application rates were 0.7 and 0.1 gal/yd² for the mixing and the topical applications, respectively (Bushman et al. 2004). According to personnel from Midwest Industrial Supply, Inc., S.S. polymer dilution ranges from 9:1 to 15:1 by volume for most applications. In the case of granular shoulders, the recommended application rate is about 2.9 gal/yd². S.S. polymer costs about \$8/gal. excluding shipping and application.

The manufacturer of Soiltac polymer describes the product as a polymer-based emulsion, which, when applied, penetrates through the soil to form a protective barrier with a rigid and stable base. The penetration depth for topical applications varies between 0.125 to 2 in. depending on soil type. Soiltac polymer works best with non-plastic soils with a uniform grain size distribution. The pH of Soiltac polymer ranges from 4.5 to 6.0, with boiling and freezing points equal to 212° F and 32° F, respectively. To stabilize a 6 in. deep shoulder, the recommended application rate is 0.36 gal/yd² with a dilution rate equal to $\gamma_{opt} - \gamma_{in situ}$. Such application should last from 12 to 24 months before maintenance is required. Soiltac polymer costs about \$5/gal., excluding shipping and application.

Bergmann (2000) reported that polymers are not considered to be long-term stabilizers. When used to stabilize low-volume roads or trails, it is necessary to do a maintenance application coat

every two to three years because the products will break down due to environmental conditions (NAVFAC 1998).

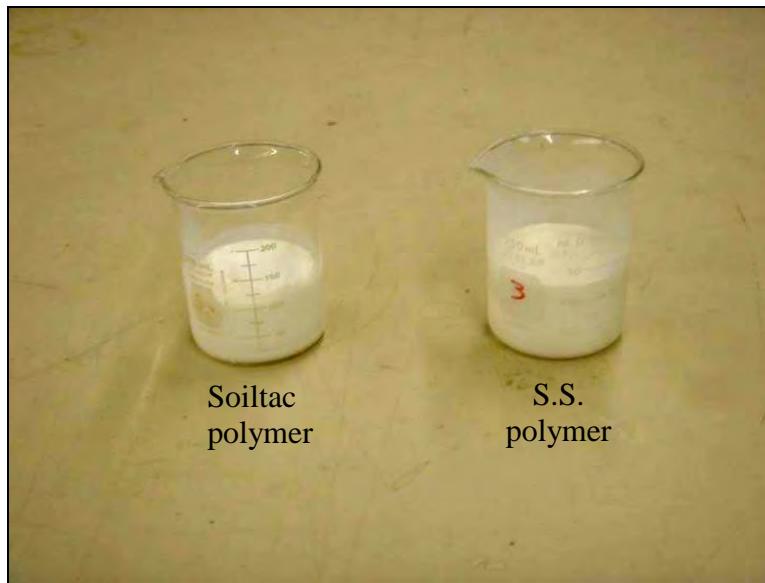


Figure 7. Samples of Soiltac and S.S. polymers

Lignosulfonates

Lignosulfonates consist of a glue found mainly in trees. During the pulping process at the wood mill, lignosulfonates are removed from the pulp and flushed into tanks or lagoons. The chemicals added during the pulping process determine whether it is a calcium, sodium, or ammonium lignosulfonate. The liquid is typically sold in a 50% suspended solid solution (Cook 2002; Bolander 1999).

Previous studies in stabilizing granular shoulders and unpaved roads demonstrated that blending the granular material with lignosulfonates at a depth of 4 to 8 in. is necessary to provide flexibility, hygroscopic tendencies, and permanent fix to the granular surface (Cook 2002; Bushman et al. 2004). Bushman et al. (2004) further recommended an additional topical application to improve the granular surface performance. Application rates documented in past research ranged from 0.8 to 1.0 gal/yd², while the dilution rate was one part lignosulfonate to one part water (Bolander 1999; Bushman et al. 2004).

The performance of lignosulfonates in stabilizing granular material in the field varied in the literature. In New York, lignosulfonate was uniformly blended with shoulder granular material at a rate of 8 gal./ton using a pugmill. The material was laid down and compacted in a 3 ft. wide shoulder. Two and a half years later, the shoulder material did not show any signs of erosion or distress. Another study in Niagara County, New York, reported similar results (Cook 2002). In contrast to the previous studies, Bolander (1999) demonstrated that lignosulfonates increase strength in warm, dry climates only, and as moisture content increased, strength decreased. Furthermore, lignosulfonate-stabilized granular specimens showed poor durability performance

under both wet-dry and freeze-thaw cycles. As moisture content increases, erosion and leaching of lignosulfonates takes place due to the lignosulfonate's high solubility, causing strength degradation. When compared with calcium chloride, lignosulfonates cost between 1.41 to 1.46 times more to achieve the same level of performance (Santoni et al. 2001; Kirchner and Gall 1991).

Soybean Oil

Soybean oil is typically used as a dust suppressant. The product proves to be an effective, locally grown, environmentally safe, economical dust control and road stabilizer. Soybean oil acts as a binding agent and stabilizes the road by keeping the dust particles bound together (Morgan et al. 2005).

Soybean oil is a by-product of the soybean oil industry. The original by-product is processed twice, once to acquire products that can be used in the feed industry and a second time to remove unwanted stems and parts of soybeans. The end result is an emulsion of the by-product. The emulsion is then added to a small amount of soybean oil. The availability of the soybean oil varies depending on the market and can be difficult to obtain at certain times (Morgan et al. 2005).

Two soybean oil products were investigated during the course of this study. The first product (referred to in this report as Feed Energy soybean oil) was supplied by the Feed Energy Company based in Des Moines, Iowa. This product is difficult for suppliers to store and transport. The product has to be kept at a constant temperature of 155° F and continuously or periodically agitated. As the product becomes cooler, it gets thicker, making transport and pumping difficult. This product also cannot be pumped using blade pumps, because the blades of the pump shear the product, giving it a peanut butter-like consistency. If the product is not agitated continuously or periodically, the soybean oil settles to the bottom and the emulsion is left on top (Morgan et al. 2005). The suppliers recommend two topical applications at a rate of 0.70 gal/yd² for a 100% solution, which costs around \$0.4/gal.

The second product, which is also a by-product of the soybean oil refining process, is *Dustlock*[®] (henceforth referred to as dustlock soybean oil). It was supplied by Boer & Sons, Inc. in Boyden, Iowa. The manufacturer of this product is Environmental Dust Control, Inc. in Currie, Minnesota. According to the supplier, the product, excluding shipping and field application, costs about \$2/gal. Unlike the soapstock product produced by Feed Energy Company, this product does not need continuous agitation, since the oil and emulsion do not separate, and resembles residual fuel oils. Figure 8 shows a sample of both soapstock soybean oil products.

The soapstock has an odor within the first few weeks after application that some individuals find offensive. The odor usually dissipates within a few weeks. Currently, soapstock producers are researching additives that will reduce or remove the offensive odor as well as improve dust control effectiveness (Lohnes and Coree 2002).

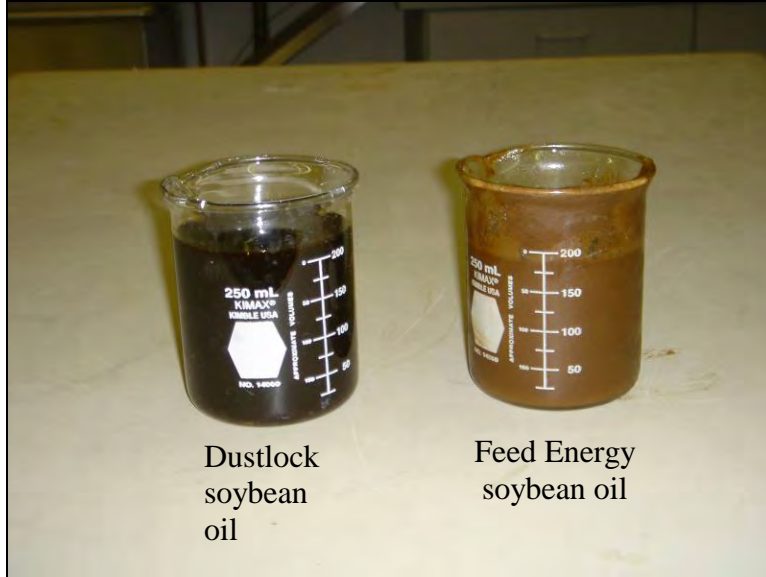


Figure 8. Samples of soybean oil soapstock

FIELD RECONNAISSANCE

Introduction

Field investigations were conducted across Iowa to document shoulder problems and evaluate maintenance and repair techniques. Visual inspections and testing were conducted at several shoulder sections in Districts 1, 2, and 3. Table 9 provides a summary of the problems observed at the investigated shoulder sections. Detailed descriptions of the shoulder sections are discussed in the subsequent sections.

Table 9. Summary of field reconnaissance

Location		District	Granular shoulder material	Edge line offset (in.)	Shoulder drop-off (in.)	Comments
Hwy 146	Outside	1	Crushed limestone	24	4	-
East 64	Outside	1	Crushed limestone	3	11	Severe water erosion
Hwy 30 – M.P. 151.95 E.B.	Outside	1	Crushed limestone	6	2	Wind/traffic erosion
Hwy 30 – M.P. 156.0 W.B.	Outside	1	Crushed limestone	25	0	-
Hwy 30 – M.P. 160.25 E.B.	Outside	1	Crushed limestone	25	2.5	Wind/traffic erosion
Hwy 18 – M.P. 184.55 E.B.	Inside	2	Crushed limestone	6	3.0	Shoulder drop-off after a bridge approach slab
Hwy 18 – M.P. 196.14 E.B.	Outside	2	Crushed limestone	24	1.5	Wide shoulder – migration of aggregate due to traffic
Hwy 18 W.B. 0.5 miles from Hwy 69	Outside	2	Crushed limestone	19	1.25	12” next to the pavement is stabilized with soy oil
Hwy 65 – M.P. 198.3 N.B.	Outside	2	Crushed limestone	24	2.25	Super-elevated curve. Water erosion
Hwy 65 off ramp to Hwy 27 (M.P. 193 E.B.)	Outside	2	Crushed limestone	2	3.5	Severe rutting and at 14 ft. from the pavement edge. Soft subgrade
Hwy 122 EB	Outside	2	Crushed limestone	3	2	-
Hwy 20 EB	Outside	2	Crushed limestone and HMA	3.5	4	-
Hwy IA 12 St. 1080+00’ N.B.	Outside	3	Crushed limestone blended with HMA	28.5	1.25	2 year old section

Table 9. Summary of field reconnaissance (continued)

Location	District	Granular shoulder material	Edge line offset (in.)	Shoulder drop-off (in.)	Comments
Hwy IA 3 Station 940 W.B.	Outside 3	Quartzite maintained with crushed concrete	3	2.25	Wet subgrade and wet subdrain outlet
Hwy 9 St. 135+00' E.B.	Outside 3	65% HMA + quartzite and class C gravel	2	0	Wide shoulder – migration of aggregate Due to traffic
Hwy 71 Crossing Hwy 10	Outside 3	Crushed limestone	6	0.5	Erosion due to traffic
Hwy 60 St. 149+00'	Outside 3	Blend of crushed limestone, recycled concrete, HMA	27	0.25	A 4 ft. asphalt patch was placed along the pavement edge

District 1

Highway 146

The inspected section was about 0.5 miles south of U.S. 30 in Marshall County, IA. The outside shoulder section is comprised of crushed limestone and is about 3 ft. wide. The distance between the edge line and the pavement edge is 24 in. The shoulder drop-off was about 4 in., as shown in Figure 9. The reason for the shoulder drop-off formation is the addition of an asphalt overlay, which increased the pavement elevation relative to the shoulder elevation.



Figure 9. Shoulder drop-off along the shoulder section of Hwy 164, October 27, 2005

Highway E64

The inspected shoulder section is located on highway E64 in Tama County, IA. The shoulder section is approximately 0.5 miles east of U.S. 63. The granular material used at this section is crushed limestone. The edge line is 3 in. from the pavement edge. The section, which is located at the down slope of a super-elevated curve, was experiencing severe erosion due to water migration along the pavement edge. The rut depth was about 11 in. (Figure 10).

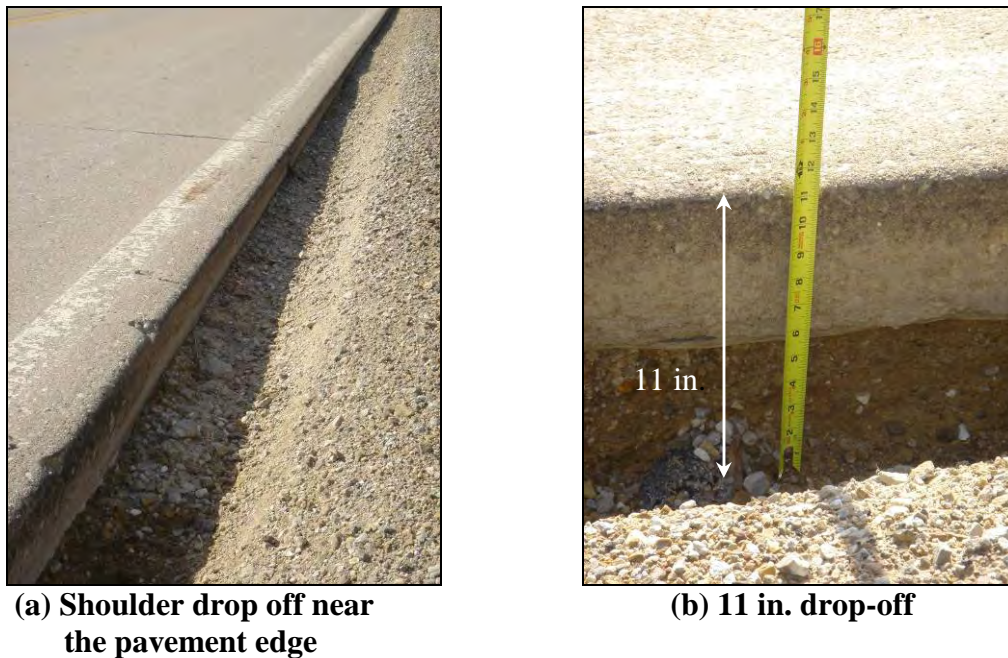


Figure 10. Severe water erosion along the pavement edge, June 16, 2005

Highway U.S. 30

Three shoulder sections on U.S. 30 were inspected to document the changes in gradation of the granular material as distance from the pavement edge increased. The shoulder sections are located at mileposts 151.95 E.B., 156.0 W.B., and 160.25 E.B. Changes in gradation are primarily caused by migration of aggregate away from the pavement due to off-tracking of vehicles and due to wind induced by high-profile vehicles.

The first shoulder section (milepost 151.95 E.B.) is about 8 ft. wide and is comprised of crushed limestone, as shown in Figure 11. The edge line is 6 in. from the pavement edge. A 2 in. drop-off was measured at this section. Aggregate samples were collected at 0, 24, and 36 in. from the pavement edge, and grain size analysis was conducted. The results of the grain size analysis, shown in Figure 12, indicate that the granular material gets coarser with increasing distance from the pavement. The soil properties of the collected samples are shown in Table 10.



Figure 11. Shoulder section at U.S. 30 milepost 151.95 E.B., September 2, 2006

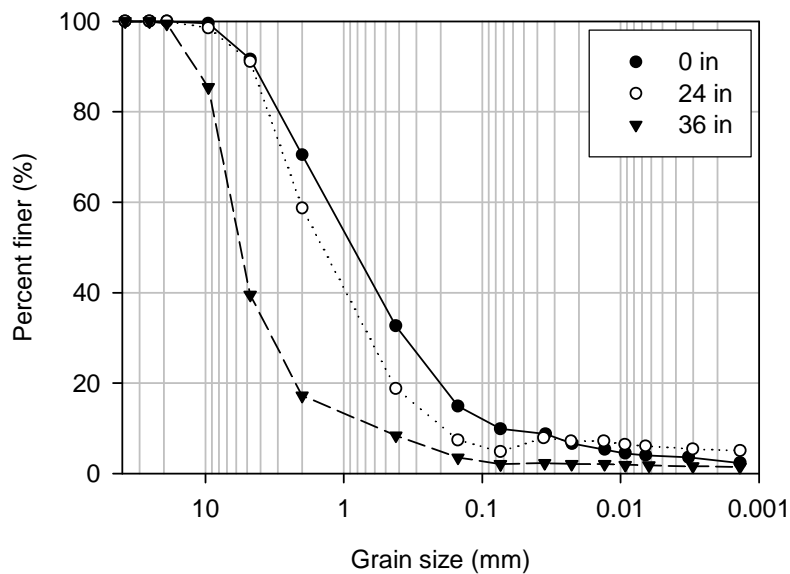


Figure 12. Grain size distribution of granular shoulder material (M.P. 151.95 E.B.)

The second shoulder section inspected on U.S. 30 (milepost 156.0 W.B.) was about 8 ft. wide. The edge line is 25 in. from the pavement edge, and, unlike the first section, there is no shoulder drop-off (Figure 13). However, the crushed limestone on the surface was observed to be loose. Aggregate samples were collected for grain size analysis every 1 ft. from the pavement edge up to a distance of 5 ft. The results of the grain size analysis, which are shown in Figure 14, reveal that the percentage of fines increases gradually with distance from the pavement edge. The loss of fines reduces cohesion of the surface layer, resulting in loose, coarse aggregate. If not maintained, this section can undergo longitudinal rutting. The soil properties of the samples collected are shown in Table 10



Figure 13. Granular shoulder section on U.S. 30 (milepost 156.0 W.B.), September 2, 2006

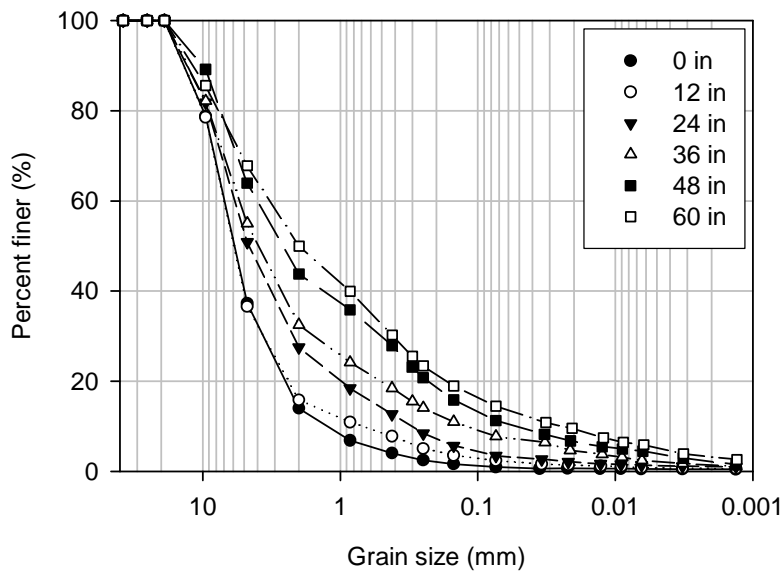


Figure 14. Grain size distribution of granular shoulder material (M.P. 156.0 W.B.)

The third shoulder section investigated on U.S. 30 (milepost 160.25 E.B.) was about 8 ft. wide. The edge line is 25 in. from the pavement edge, and the shoulder drop-off was measured to be 2.5 in. (Figure 15). A visible wheel path was noted about 3 ft. from the pavement edge. Further, the area adjacent to the pavement was cleared of surface gravel. This was reflected in the grain size analysis results, which were conducted on samples collected every 1 ft. up to a distance of 5 ft. from the pavement edge (Figure 16). The soil properties of the samples collected are shown in Table 10. The samples collected at 0 and 12 in. have less coarse gravel, whereas the sample collected at 24 in. has coarser gravel, than the sample collected at 36 in.



Figure 15. Granular shoulder section on U.S. 30 (milepost 160.25 E.B.), September 2, 2006

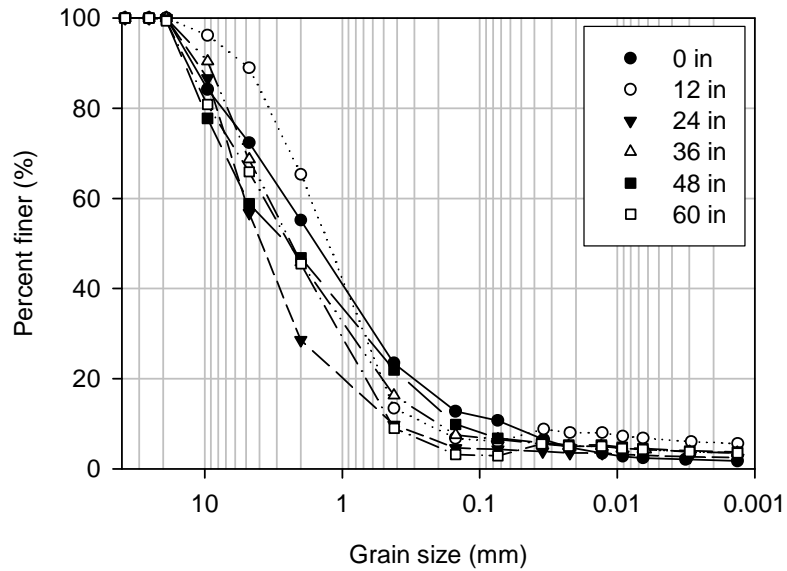


Figure 16. Grain size distribution of granular shoulder material (M.P. 160.25 E.B.)

Table 10. Soil properties of the aggregate samples obtained at U.S. 30

Mile post	Distance from pavement (in.)	D ₁₀	D ₃₀	D ₆₀	C _u	C _c	%P _{#4}	%P ₂₀₀	USCS	AASHT
									class.	O
151.95 E.B.	0	0.074	0.35	1.4	18.9	1.18	91.6	9.9	SW-SM	A-1-b
	24	0.2	0.65	2.1	10.5	1.01	91.1	6.1	SW-SM	A-1-b
	36	0.55	3.2	6.5	11.8	2.86	39.5	2.1	GW	A-1-a
156.0 W.B.	0	1.3	3.9	7.0	5.4	1.67	37.3	0.9	GW	A-1-a
	12	0.79	3.9	7.0	8.8	2.75	36.5	2.3	GW	A-1-a
	24	0.3	2.1	6.0	20	2.45	50.9	3.4	SW	A-1-a
	36	0.13	1.8	5.5	42.3	4.5	55.0	7.7	SP-SM	A-1-a
	48	0.06	0.5	4.0	66	1.04	63.9	11.3	SW-SM	A-1-b
	60	0.024	0.43	3.2	133	2.4	67.8	14.4	SM	A-1-b
160.25 E.B.	0	0.074	0.59	2.7	36.4	1.7	72.4	10.7	SW-SM	A-1-b
	12	0.25	0.7	2.7	10.8	0.7	88.9	6.0	SP-SM	A-1-b
	24	0.43	2.1	5.0	11.6	2.05	56.5	4.3	SW	A-1-a
	36	0.21	0.85	3.5	16.6	0.98	68.6	6.5	SP-SM	A-1-a
	48	0.16	0.7	5.0	31.3	0.61	58.8	6.7	SP-SM	A-1-a
	60	0.45	1.0	3.9	8.7	0.56	65.8	2.8	SP	A-1-a

District 2

Highway 18, Milepost 184.55 E.B.

The inside shoulder section investigated is about 6 ft. wide. The granular material was composed of crushed limestone, and the edge line was 6 in. from the pavement edge. The granular shoulder is after a paved bridge approach shoulder, as shown in Figure 17. The shoulder drop-off at this section, which was measured to be 3 in. (Figure 18), can be attributed to the rapid change from paved to unpaved shoulder, which can cause off-tracking of vehicles onto the granular shoulder. With high speeds and high traffic volumes, surface deterioration is expected.

The elevation profile relative to the pavement edge was determined. Elevation measurements were collected every 3 in. up to a distance of 5 ft. from the pavement (Figure 19). In addition to the 3 in. drop-off, the elevation profile shows that the shoulder slope is 10%, which is steeper than the 4% slope specified by the Iowa DOT. The shoulder slope is calculated by determining the elevation difference between the first and last point of the profile.



Figure 17. Granular shoulder section following a paved bridge approach shoulder, Hwy 18 milepost 184.55 E.B., July 26, 2005

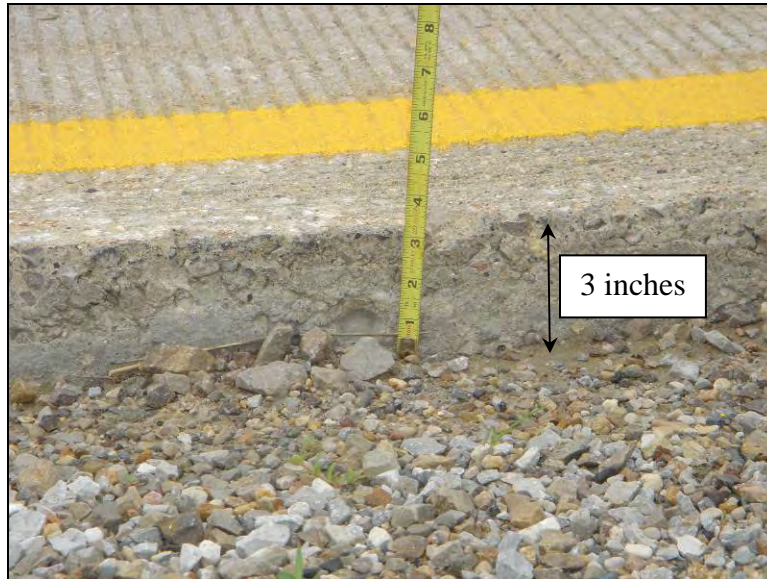


Figure 18. Three-inch shoulder drop-off, Hwy 18 milepost 184.55 E.B., July 26 2005

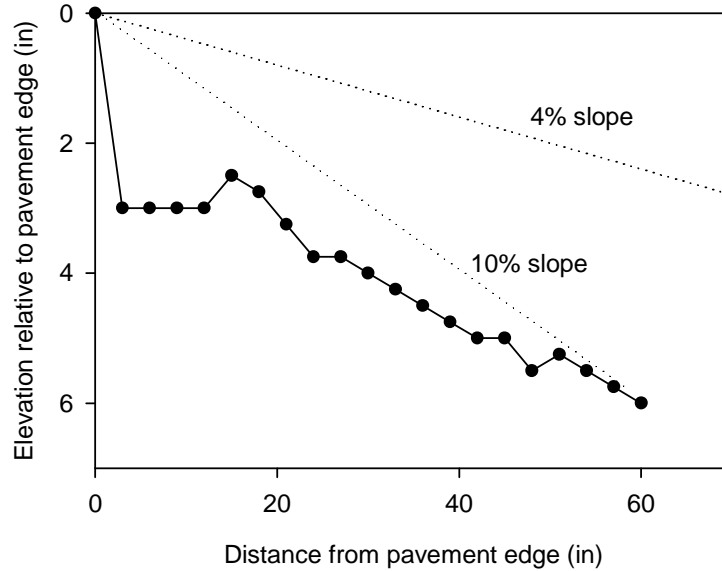


Figure 19. Elevation profile relative to the pavement edge, Hwy 18 milepost 184.55 E.B.

For the Highway 18 test section, dynamic cone penetrometer (DCP) tests were conducted according to ASTM D6951 (Standard Test Method for Use of the Dynamic Cone Penetrometer in Shallow Pavement Applications) at 14 and 70 in. away from the pavement edge (Figure 20). In this report, the CBR value for the granular layer was determined by calculating the weighted average for the upper 8 in. For the subgrade layer, the CBR value reported is a weighted average of CBR values between 8 and 20 in. deep. The weighted average calculation method is used throughout this report to evaluate strength and determine a representative CBR value for each layer. A sample calculation for determining a CBR weighted average is shown in Appendix A. Table 11 shows the relationship between unconfined compressive strength (UCS) and CBR values, as well as the ways both of these relate to the consistency of clay material. The correlation between UCS and clay consistency was developed by Das (2006), while the correlation between UCS and CBR was reported by Burnham and Johnson (1993).

At 14 in. from the pavement edge, the CBR values for the granular and subgrade layers are 3 and 39, respectively, indicating a weak granular layer. At 70 in., the CBR values for the granular and subgrade layers are 16 and 13, respectively, indicating a stiff subgrade layer.

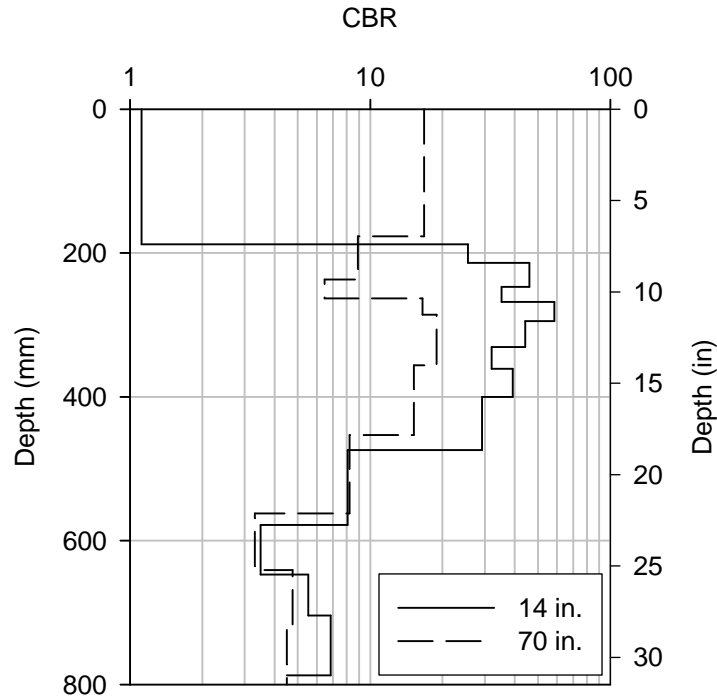


Figure 20. DCP test results, Hwy 18 milepost 184.55 E.B.

Table 11. Relationship between UCS and CBR

UCS (psi)	CBR	Consistency
0-4	0-4	Very soft
4-7	4-7	Soft
7-15	7-10	Medium
15-29	10-21	Stiff
29-58	21-42	Very stiff
>58	>42	Hard

Highway 18 Milepost 196.14 E.B.

At this location the outside shoulder section is about 14 ft. wide and the shoulder consists of crushed limestone. The edge line is 24 in. from the pavement edge (Figure 21). The shoulder width appears to be greater than typical shoulder sections (8 to 10 ft.) due to the migration of aggregate under the impact of traffic.



Figure 21. Outside granular shoulder section on Hwy 18 milepost 196.14 E.B., July 26, 2005

The elevation profile relative to the pavement edge was determined, as shown in Figure 22. The profile shows an edge drop-off of 1.5 in. Further, the shoulder had an irregular surface, with a slope of about 5%. During inspection, the shoulder section was being bladed (Figure 23) to reduce the surface irregularity. Since the edge drop-off was not severe, aggregate was neither added nor reclaimed beyond the typical 10 ft. shoulder width. DCP tests were conducted at 14.5 and 96 in. from the pavement edge. A weighted average CBR of 19 and 39 was calculated for the granular layer and subgrade, respectively (Figure 24).

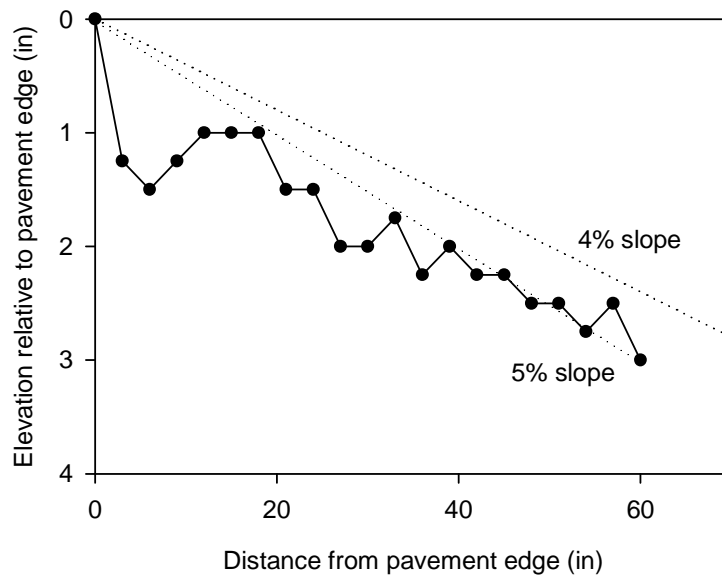


Figure 22. Elevation profile relative to the pavement edge (before blading), Hwy 18 milepost 196.14 E.B.



(a) Blading of shoulder surface



(b) Shoulder surface after blading

Figure 23. Maintenance of shoulder section, July 26, 2005

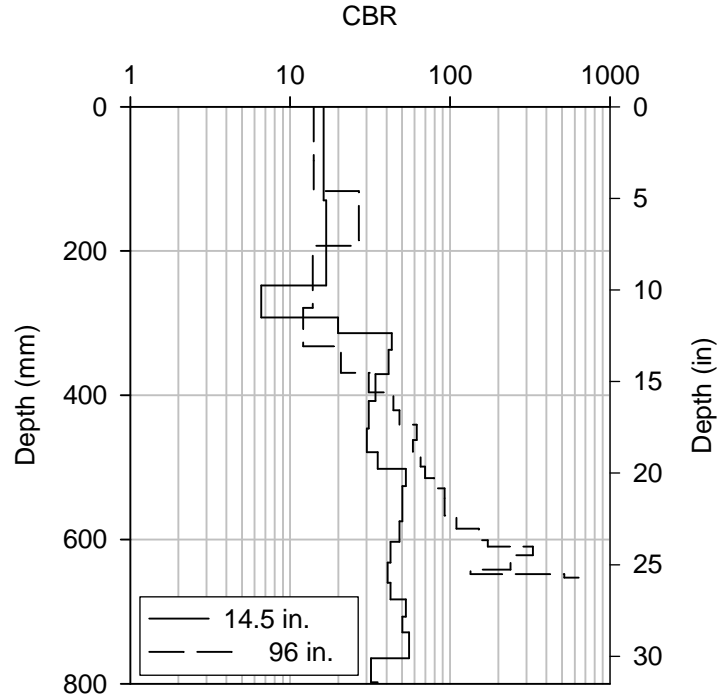


Figure 24. DCP test results, Hwy 18 milepost 196.14 E.B.

Highway 18 W.B. (0.5 Miles from Hwy 69)

The outside granular shoulder section, near Garner, IA, is about 10 ft. wide. The granular material consists of crushed limestone, and the edge line is about 7 in. from the pavement edge. The lane width adjacent to this section is 11 ft. The 12 in. adjacent to the pavement were stabilized with dustlock soybean oil, as shown in Figure 25. The original width of the stabilized area was 36 in.; however, with time the stabilized area deteriorated to the current width. Dustlock soybean oil was applied at this shoulder section in 2001, and, according to the District 2

Operation Manager, no maintenance work has been required since the application of the soybean oil. There are no records of the construction procedures or the addition rate.

Five samples were collected from the shoulder at 12 in. intervals from the pavement edge up to a distance of 5 ft. for grain size distribution analysis. The results, which are shown in Figure 26, reveal no significant differences in grain size distribution. In addition to the granular samples, a sample of the stabilized material (Figure 27) was obtained and analyzed using scanning electron microscopy (SEM). The SEM images show the penetration of the soybean oil through the granular layer (depicted as dark regions in the SEM image), as well as the presence of fibers (Figure 28 and Figure 29). These fibers were probably an original component of the soybean oil product (Figure 30) and could potentially contribute to the stabilization of the granular material. The SEM images reveal that both the oil and the fibers are rich in oxygen and carbon, indicating an organic chemical compound. The limestone rock is composed mainly of magnesium, silica, and calcium, as well as traces of potassium and alumina.

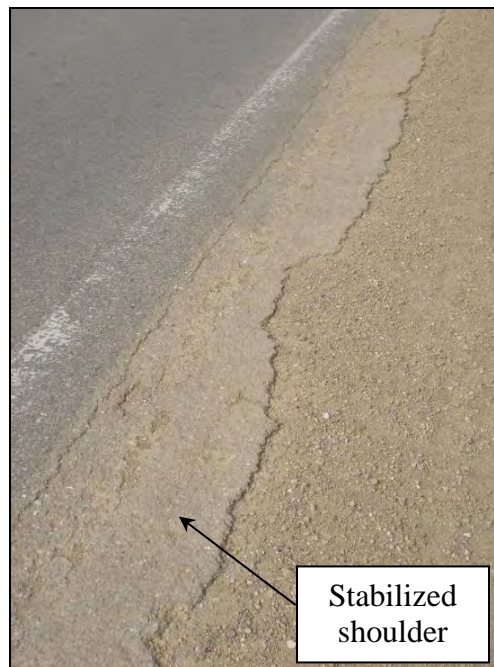


Figure 25. Granular shoulder section stabilized with soybean oil, May 10, 2006

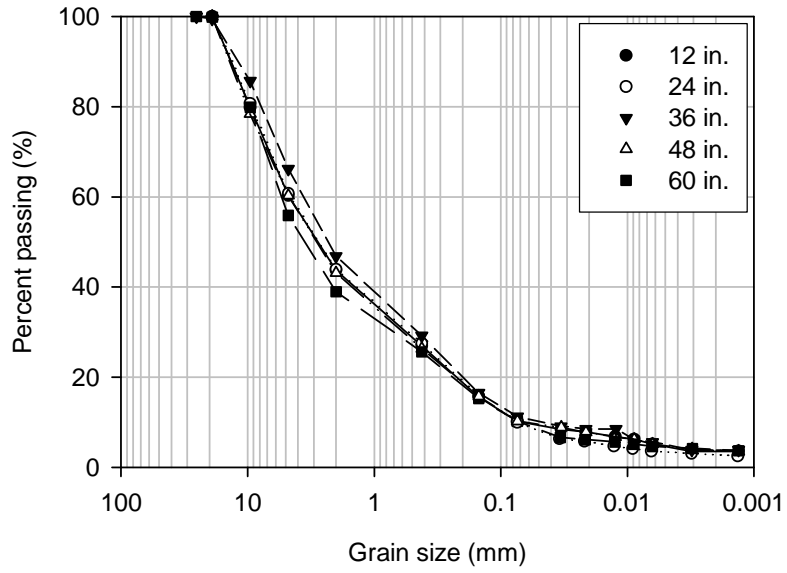


Figure 26. Grain size distribution of the shoulder granular material, Hwy 18 W.B.



Figure 27. Crushed limestone samples stabilized with soybean oil collected for SEM analysis

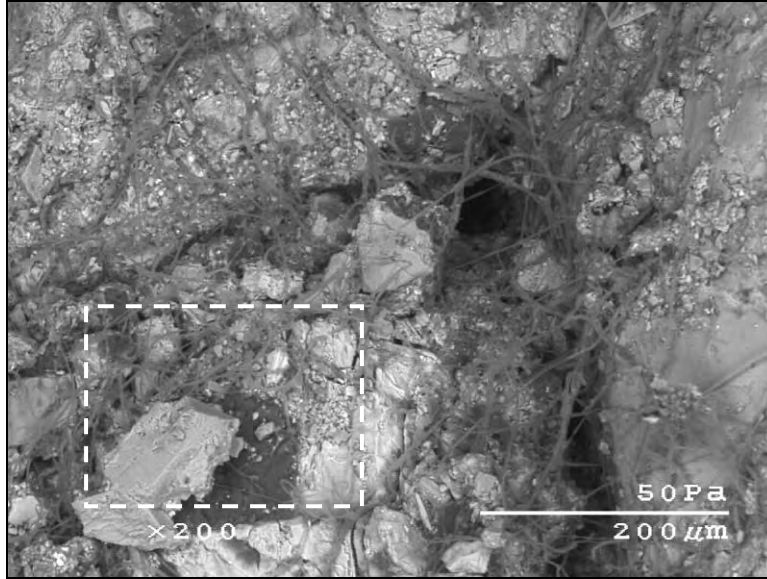


Figure 28. SEM image of limestone rock stabilized with soybean oil (x200 magnification)

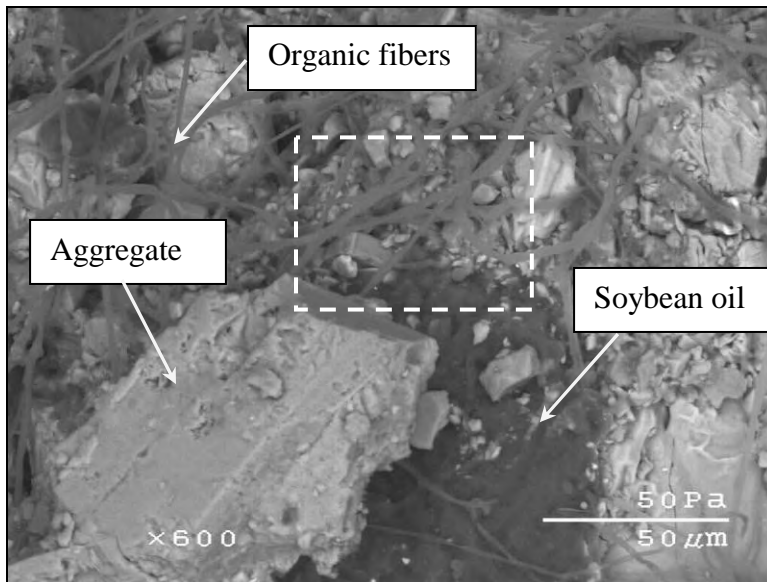


Figure 29. Magnified SEM image of the highlighted area in Figure 28, showing the soybean oil and organic fibers (x600 magnification)

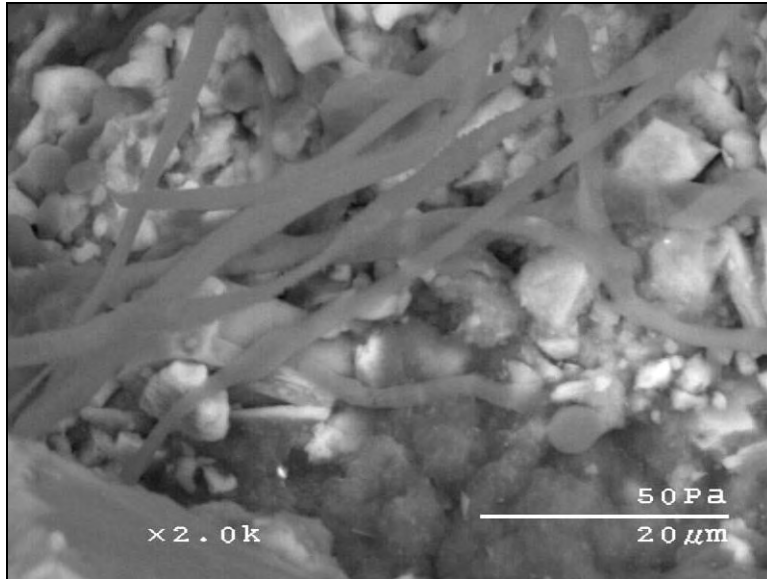


Figure 30. Magnified image showing the organic fibers (x2000 magnification)

The elevation profile of the shoulder section was determined relative to the pavement elevation (Figure 31). The edge drop-off adjacent to the stabilized area is about 1.25 in. and the overall slope of the section is about 4%, which is in agreement with the Iowa DOT requirement. A DCP test was conducted at 36 in. from the pavement edge (Figure 32). The CBR value for the upper 8 in. is 5, which may be attributed to loose material in the upper layer. The strength increases significantly in the underlying 12 in. (CBR of 83).

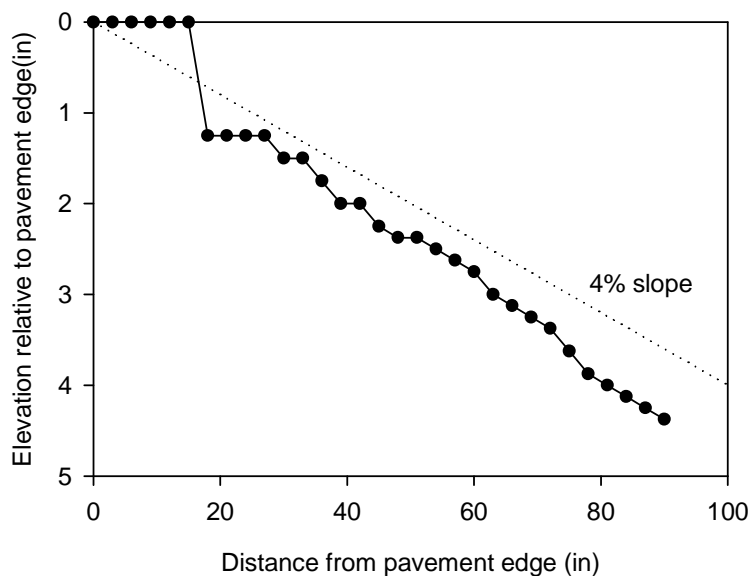


Figure 31. Elevation profile relative to the pavement edge, Hwy 18 W.B.

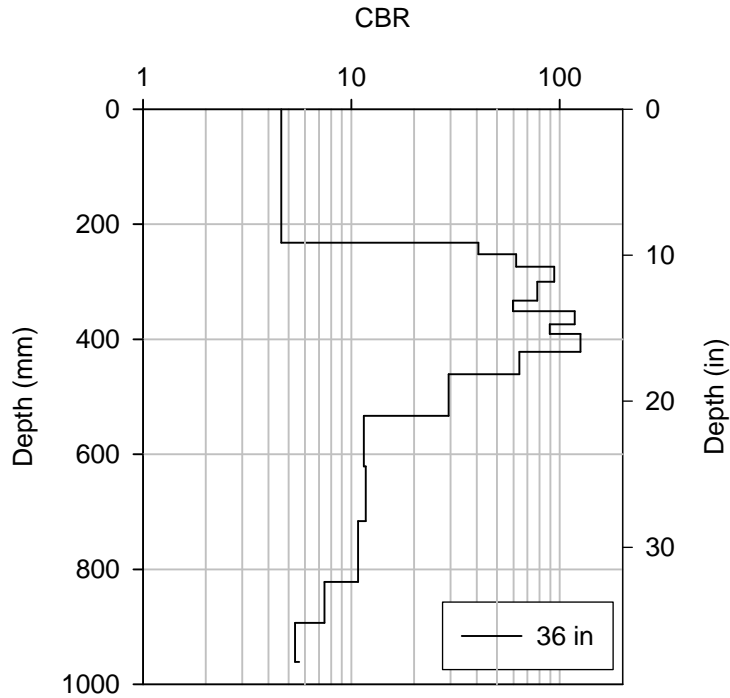


Figure 32. DCP test results, Hwy 18 W.B.

Highway 65 Milepost 198.3 N.B.

This shoulder section is about 10 ft. wide and consists of crushed limestone. The section is located on a super-elevated curve (Figure 33). The edge line is 24 in. from the pavement edge. The shoulder drop-off was about 2.25 in. (Figure 34).

The elevation profile of the shoulder section was determined relative to the pavement edge, as shown in Figure 35. The profile shows the shoulder drop-off, which is confined to the area adjacent to the pavement. Apart from the rutted area, the shoulder slope is in agreement with the 4% slope required by Iowa DOT. DCP testing was conducted at 15 in. from the pavement edge (Figure 36). The CBR of both the granular and subgrade layers are 182 and 218, respectively.



Figure 33. Granular shoulder section located on a super-elevated curve on Hwy 65 milepost 198.3 N.B., July 26, 2005



Figure 34. Shoulder drop-off adjacent to the pavement on Hwy 65 milepost 198.3 N.B., July 26, 2005

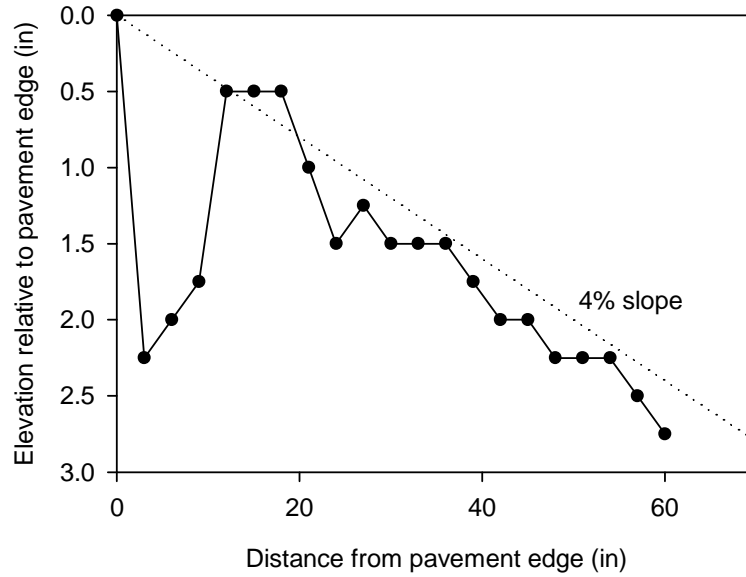


Figure 35. Elevation profile relative to the pavement edge, Hwy 65 milepost 198.3 N.B.

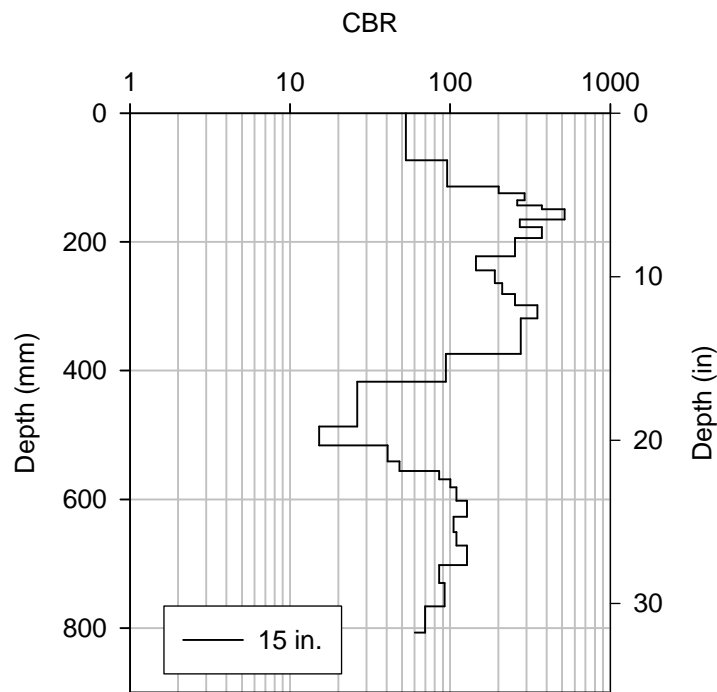


Figure 36. DCP test results, Hwy 65 milepost 198.3 N.B.

Highway 65 Exit Ramp to Highway 27 (Milepost 193 E.B.)

The outside shoulder section is located on the exit ramp of Highway 65 onto Highway 27 (Figure 37). The shoulder section is 14 ft. wide, and the edge line is 2 in. from the pavement edge. The granular material at this shoulder section is crushed limestone. Figure 38 shows the shoulder drop-off, which was 3 in. Due to the absence of the granular layer and the exposure of the soft

subgrade layer at a distance of 12 to 14 ft. from the pavement edge, the section was undergoing rutting caused by heavy traffic loadings, as evidenced by the tire marks (Figure 39).

A soil sample was obtained from both the crushed limestone and the subgrade material for grain size distribution analysis (Figure 40). The limestone and the subgrade materials are classified as SP-SM (poorly graded sand with silt) according to USCS (A-1-b according to AASHTO) and CL (lean clay) (A-6), respectively. The elevation profile relative to the pavement edge was determined, as shown in Figure 41. The profile, which extended a distance of 7.5 ft, shows that the maximum shoulder drop-off is 3.5 in. at 9 in. from the pavement edge, and the overall slope of the section is about 4%. Three DCP tests were conducted. The first test was conducted inside the shoulder drop-off at 3 in. from the pavement, the second test was conducted outside the shoulder drop-off at 3.1 ft. from the pavement, and the third test was conducted on the subgrade at 14 ft. from the pavement (Figure 42). The CBR of the granular layer was 62 and 152 at 3 in. and 3.1 ft, respectively. At 14 ft. from the pavement edge, the CBR was about 2.

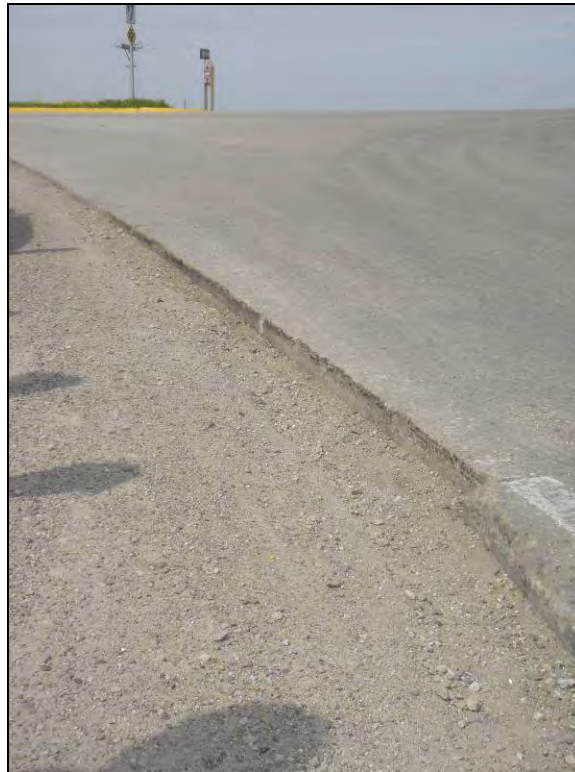


Figure 37. Granular shoulder section at exit ramp of Hwy 65 onto Hwy 27, May 10, 2006



Figure 38. Shoulder edge drop-off on Hwy 65 exit ramp to Hwy 27, May 10 2006



Figure 39. Shoulder rutting caused by soft subgrade and absence of granular layer on Hwy 65 exit ramp to Hwy 27, May 10, 2006

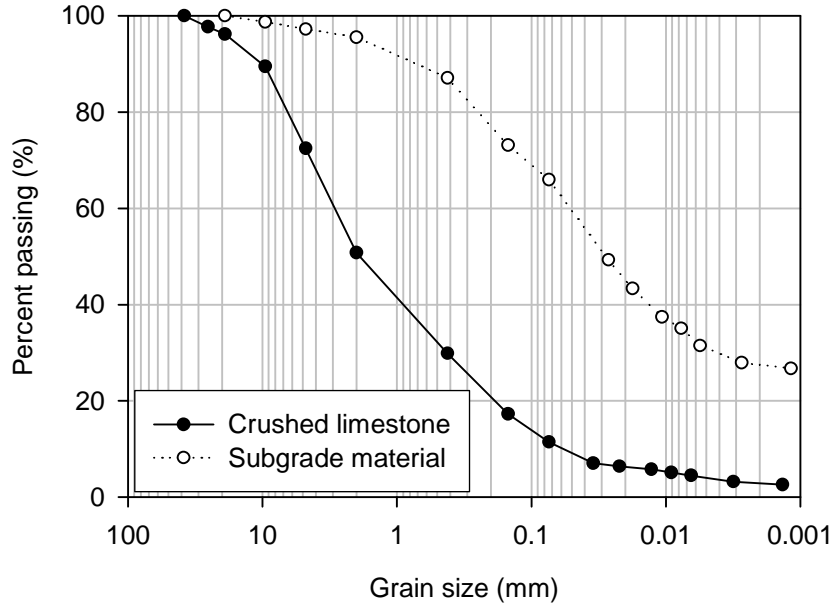


Figure 40. Grain size distribution of granular and subgrade layers, Hwy 65 exit ramp to Hwy 27

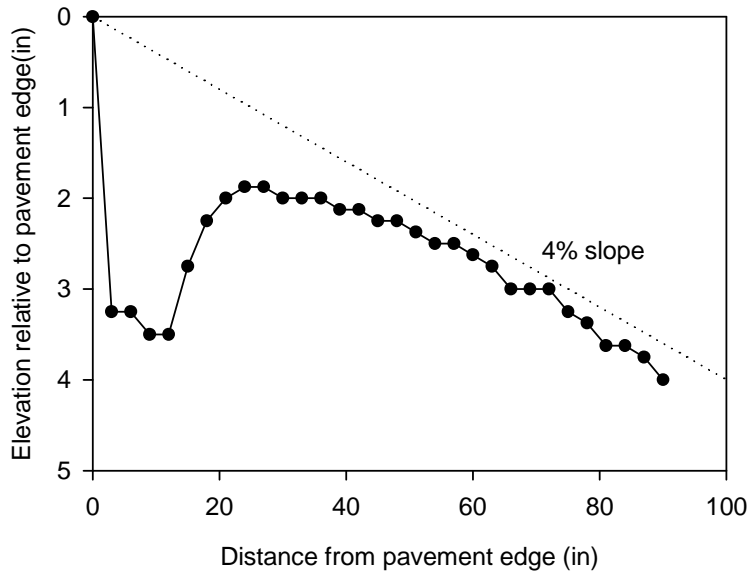


Figure 41. Elevation profile relative to the pavement edge, Hwy 65 exit ramp to Hwy 27

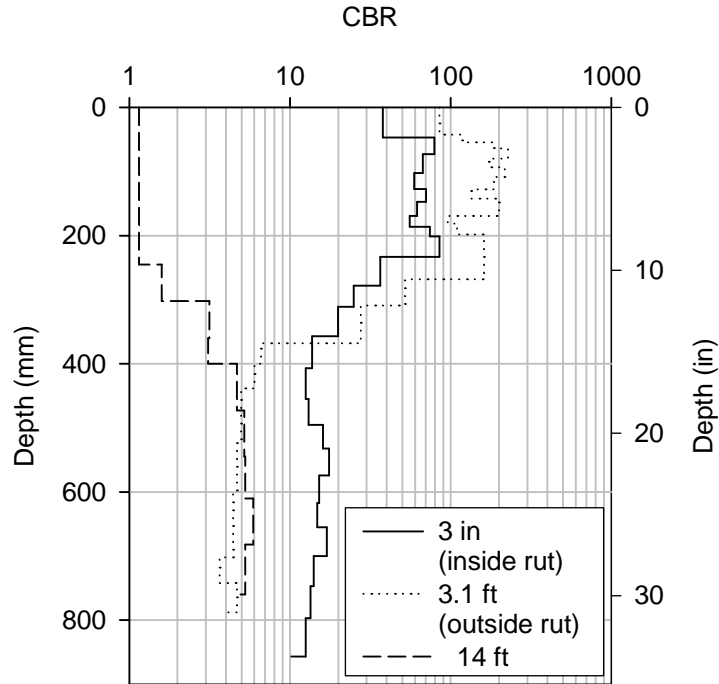


Figure 42. DCP test results, Hwy 65 exit ramp to Hwy 27

Highway 122 (Intersection with Larke Ave.)

Two sections were inspected at Highway 122. The first section, which is about 200 ft. east of Larke Ave., is 14 ft. wide with crushed limestone (Figure 43). The distance between the edge line and the pavement edge is 3 in. The second section is at the intersection of Highway 122 and Larke Ave. Significant rutting was observed in the second section, as shown in Figure 44.

The elevation profiles of both shoulder sections were determined relative to the pavement edge, as shown in Figure 45. The elevation profile of the first section reveals a 2 in. edge drop-off and a 7% slope, which is higher than the 4% slope specified by the Iowa DOT. The elevation profile of the second section shows shoulder rutting of about 4.25 in.

DCP tests were conducted at 26 and 96 in. from the pavement edge (Figure 46). At 26 in., the CBR of the granular layer was 77. The CBR value of the underlying subgrade was 39. At 96 in., the CBR values for the granular and subgrade layers were 70 and 12, respectively.



Figure 43. Granular shoulder section on Hwy 122, July 26, 2005



Figure 44. Cross slope damage at the intersection with Larke Ave. on Hwy 122, July 26, 2005

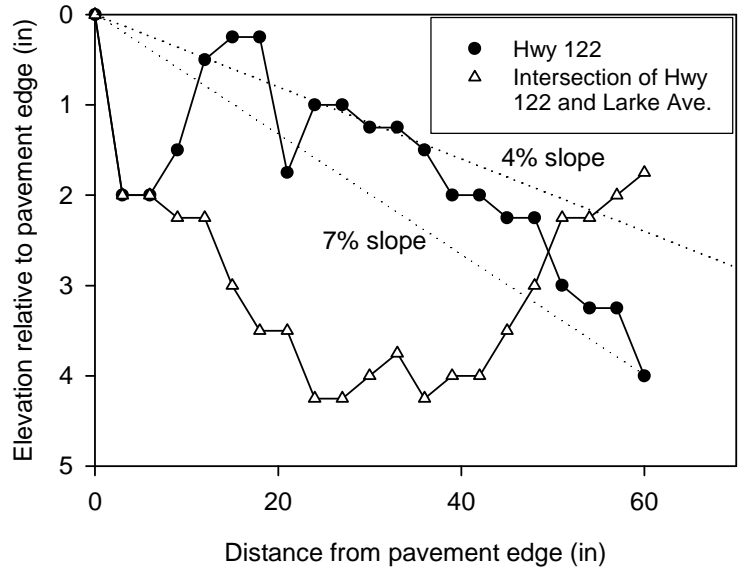


Figure 45. Elevation profiles relative to the pavement edge, Hwy 122

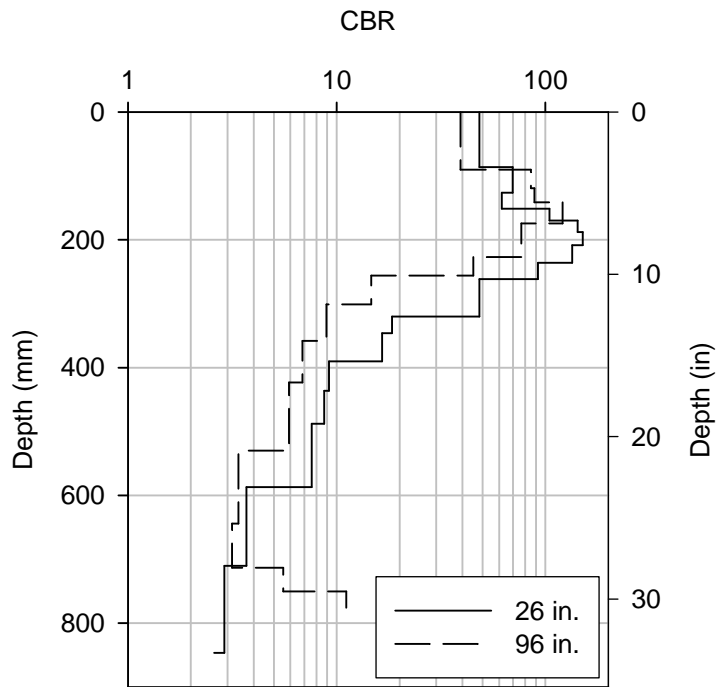


Figure 46. DCP test results, Section 1, 200 ft. east of Hwy 122

Highway 20 Milepost 242 E.B.

This shoulder section is 10 ft. wide and consists of crushed limestone with asphalt millings on the surface. The asphalt millings were placed to compensate for the frequent loss of rock and the chronic edge drop-off problem (Figure 47). The edge line is about 3.5 in. from the pavement edge. The edge drop-off, probably caused by vehicle off-tracking, was equal to 4 in. (Figure 48).

A sample was collected from the granular layer for grain size distribution analysis (Figure 49). The material is classified as GP (poorly graded gravel; A-1-a). An elevation profile relative to the pavement edge was collected, as shown in Figure 50. The profile shows the 4 in. drop-off next to the pavement edge and a 10% slope. DCP tests were conducted at 1 and 9 ft. from the pavement edge (Figure 51). The CBR values for the granular layer at 1 and 9 ft. were 76 and 32, respectively. The average CBR values for the subgrade layer at 1 and 9 ft. were 8 and 16, respectively.



Figure 47. Granular shoulder section maintained with asphalt millings on Hwy 20 milepost 242 E.B., September 23, 2006



Figure 48. Four in. shoulder drop-off on Hwy 20 milepost 242 E.B., September 23, 2006

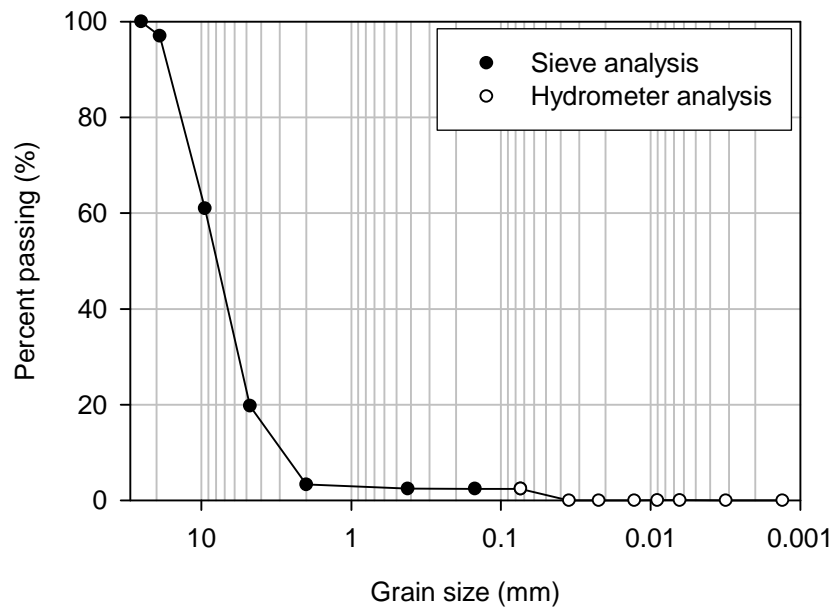


Figure 49. Grain size distribution analysis for granular material, Hwy 20 milepost 242 E.B.

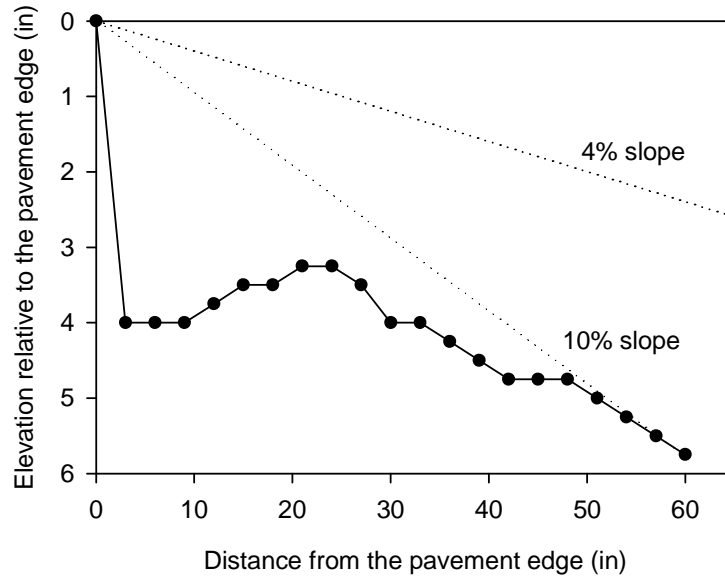


Figure 50. Elevation profile relative to the pavement edge, Hwy 20 milepost 242 E.B.

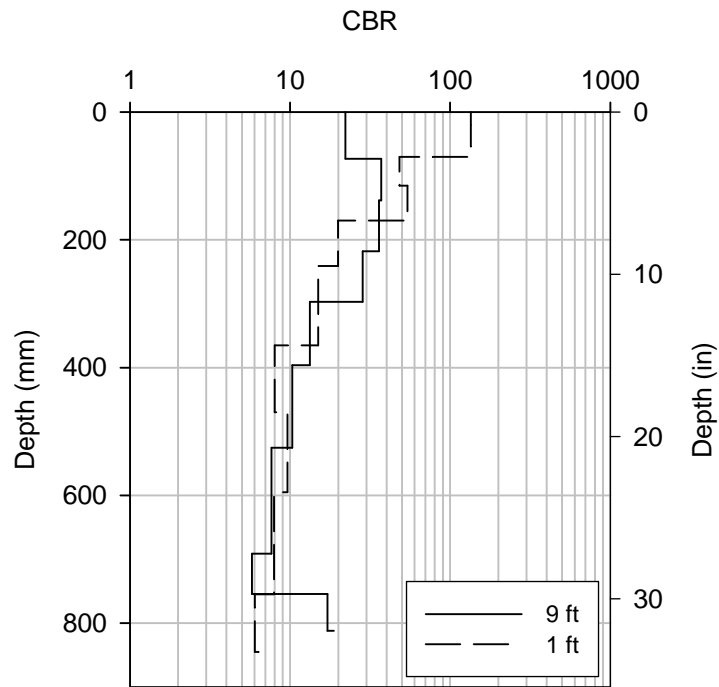


Figure 51. DCP test results, Hwy 20 milepost 242 E.B.

District 3

Highway IA 12 St. 1080+00' N.B.

This shoulder section was constructed in 2004 as part of a major pavement repair. The shoulder width is about 6 ft. Rumble strips were constructed adjacent to the southbound shoulder only (Figure 52). The shoulder granular layer consists of crushed limestone and RAP material (Figure 53).

A sample of the shoulder material was obtained for grain size distribution analysis (Figure 54). The shoulder material is classified as SP-SM (poorly graded sand with silt; A-1-a). The elevation profile of the section relative to the pavement revealed an edge drop-off of 1.5 in. Further, the shoulder has a 6% slope (Figure 55). DCP tests were performed at 1.25 and 4 ft. from the pavement edge. As shown in Figure 56, the CBR value for the granular layer (i.e., the upper 8 in.) was 25. For the subgrade layer, the CBR value was about 9.



Figure 52. Granular shoulder section (southbound shoulder looking north) on Hwy IA 12 Station 1080+00', October 14, 2005



Figure 53. Granular shoulder with RAP material on Hwy IA 12 Station 1080+00', October 14, 2005

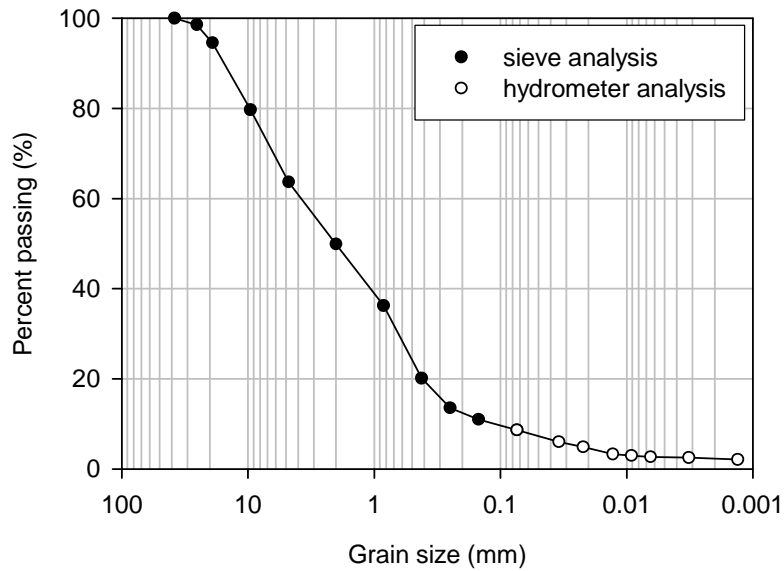


Figure 54. Grain size distribution of the shoulder granular material, Hwy IA 12 Station 1080+00'

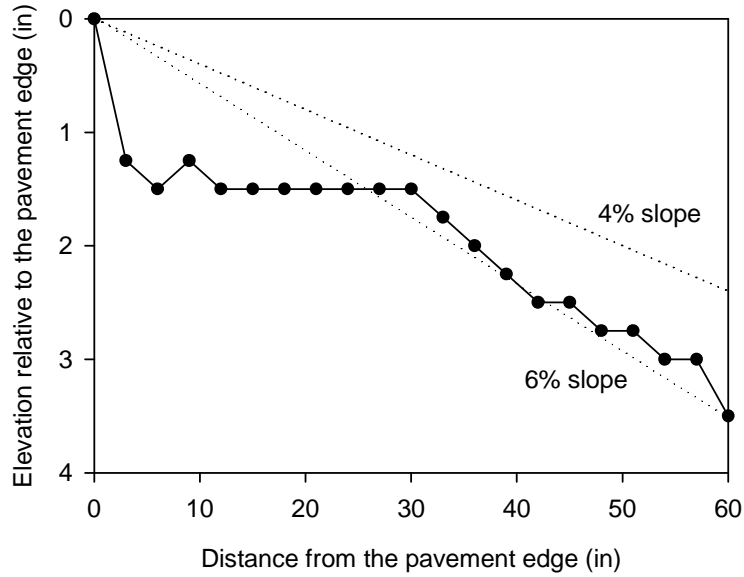


Figure 55. Elevation profile of the shoulder section relative to the pavement, Hwy IA 12 Station 1080+00'

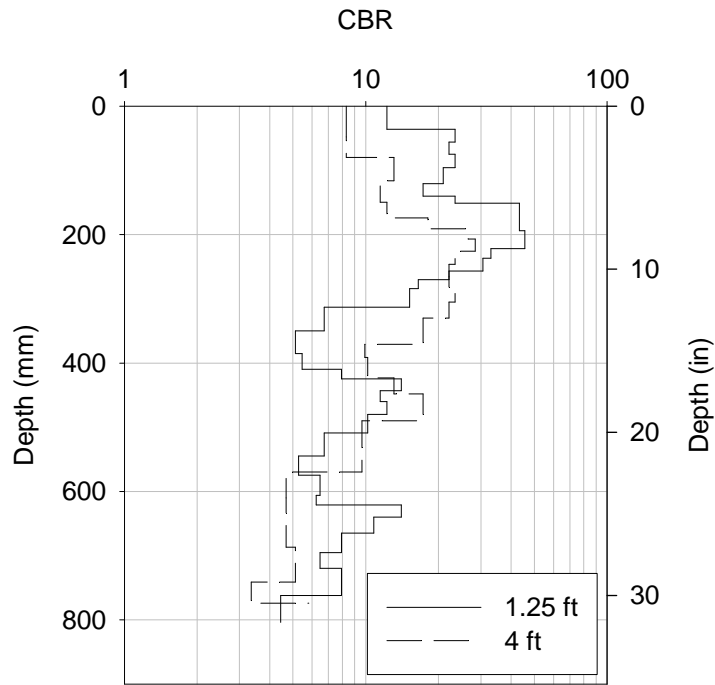


Figure 56. DCP test results, Hwy IA 12 Station 1080+00'

Highway IA 3 Station 940

The eastbound and westbound shoulders on Highway IA 3 Station 940 were inspected. The eastbound shoulder, shown in Figure 57, is a quartzite granular shoulder maintained using crushed concrete. The shoulder is about 12 ft. wide, and the edge line is located along the

pavement edge. The westbound shoulder, shown in Figure 58, is a quartzite granular shoulder and is about 12 ft. wide. The edge line is 3 in. from the pavement edge. The edge drop-off at the westbound shoulder is approximately 2.25 in. According to the District 3 maintenance manager, the eastbound shoulder requires more maintenance than the westbound shoulder, as well as the addition of crushed concrete material.

Soil samples were collected from each shoulder for grain size distribution analysis (Figure 59). The eastbound material contained a higher percentage of sand and fine material (material passing the No. 4 sieve and the No. 200 sieve). The samples from the eastbound and westbound shoulders are classified as SP-SM (poorly graded sand with silt; A-1-a) and GW (well-graded gravel; A-1-a). The elevation profile relative to the pavement was measured in the westbound shoulder, as shown in Figure 60. The profile shows a shoulder drop-off equal to 2.25 in. and a 6% slope. DCP tests were conducted on both shoulders, as shown in Figure 61. The CBR values for the shoulder granular layer at the eastbound and westbound shoulders are 33 and 41, respectively. The CBR values calculated for the subgrade layer at the eastbound and westbound shoulders are 6 and 9, respectively (Figure 62). Upon visual inspection, the in situ moisture content of the subgrade was higher at the eastbound shoulder, and the subdrain outlet was wet.



Figure 57. Granular shoulder section on Hwy IA 3 St. 940 E.B., October 14, 2005



Figure 58. Granular shoulder section on Hwy IA 3 St. 940 W.B., October 14, 2005

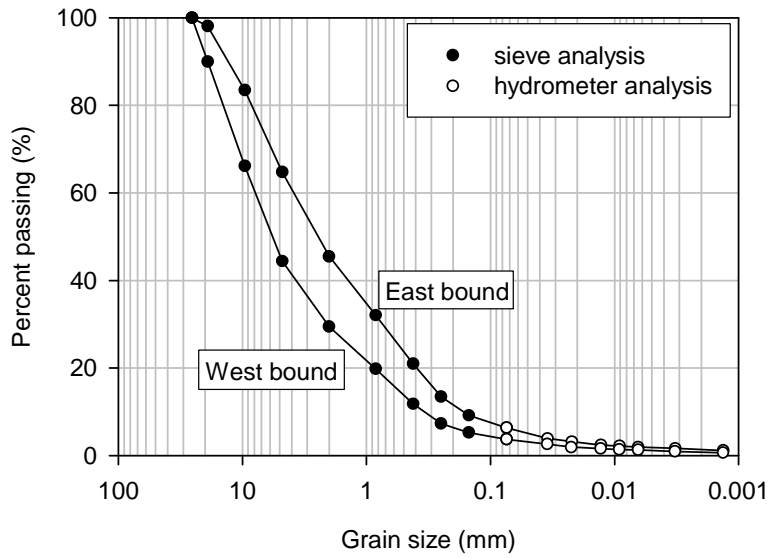


Figure 59. Grain size distribution analysis for shoulder materials, Hwy IA 3 St. 940

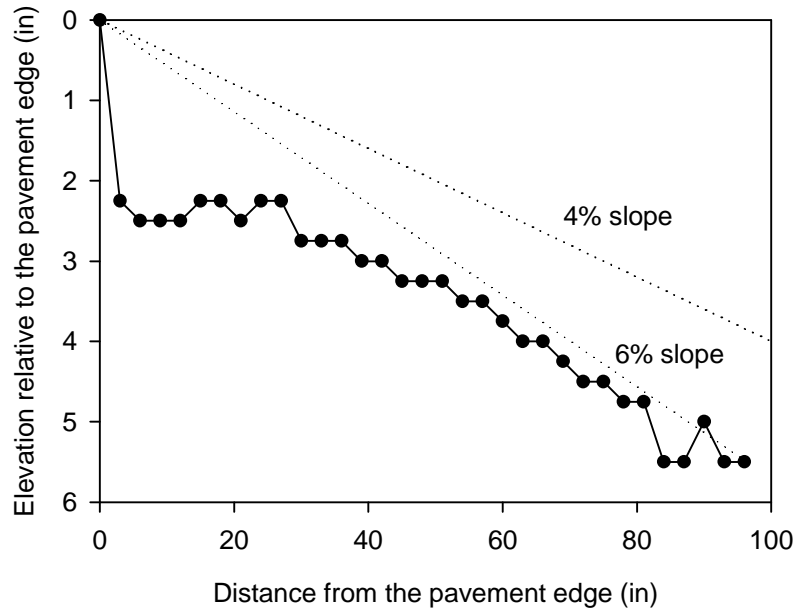


Figure 60. Elevation profile of shoulder section relative to the pavement, Hwy IA 3 St. 940 W.B.



Figure 61. Performing DCP test at the westbound shoulder, October 14, 2005

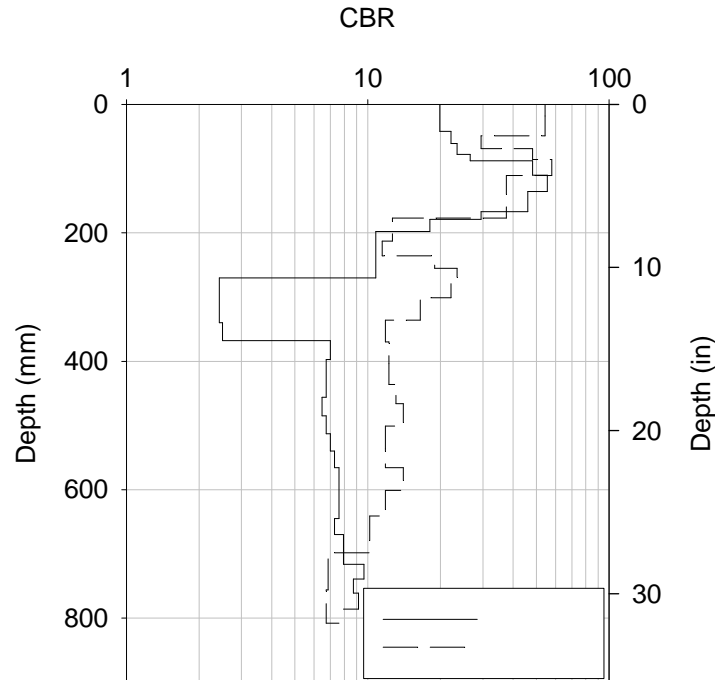


Figure 62. DCP test results, Hwy IA 3 St. 940

Highway 9 Station 135+00' E.B.

This shoulder section is 10 ft. wide and the edge line is 2 in. from the pavement edge. The shoulder, which was originally an earth shoulder, has a 3 in. deep granular layer. According to the district engineer, the granular layer consists of 65% asphalt millings plus quartzite and class C gravel (Figure 63).

The elevation profile of the shoulder section relative to the pavement was measured, revealing an edge drop-off of 1.5 in. and a shoulder slope of 11% (Figure 64). Soil samples were obtained from the shoulder section and from a quartzite stockpile present at the site for grain size distribution analysis. The new quartzite material was later added to the shoulder section to correct the slope. The grain size distribution curve shows that the soil sample collected from the shoulder material is gap-graded and contains a relatively low percentage of fine material (Figure 65). The soil samples from the shoulder and stockpile are classified as GP (poorly graded gravel; A-1-a) and SM (silty sand; A-1-b). One DCP test was carried out at 12 in. from the pavement edge. The CBR of the granular layer was about 48 (Figure 66). The CBR of the underlying subgrade layer was 10.



Figure 63. Granular shoulder section on Hwy 9 St. 135+00' W.B., October 14, 2005

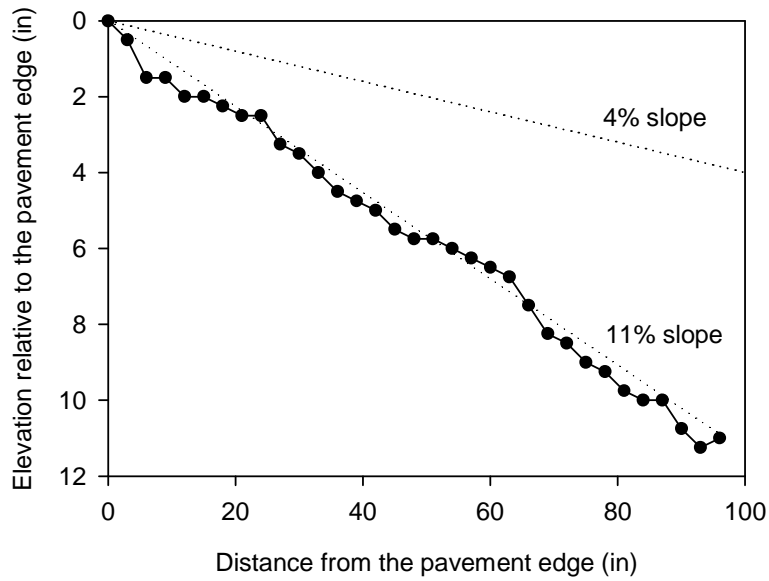


Figure 64. Elevation profile of the shoulder section relative to the pavement edge, Hwy 9 St. 135+00' W.B

A soil sample was collected from the shoulder section to conduct grain size distribution analysis (Figure 68). The material is classified as SW-SM (well-graded sand with silt; A-1-b). The elevation profile of the shoulder section relative to the pavement edge was measured. The results, shown in Figure 69, reveal a shoulder drop-off of 0.5 in. and a shoulder slope of approximately 4%. A DCP test, performed at 2 ft. from the pavement edge, showed CBR values for the granular and subgrade layers of about 81 and 7, respectively (Figure 70).



Figure 67. Granular shoulder section on Hwy 71 crossing Hwy 10 S.B., October 14, 2005

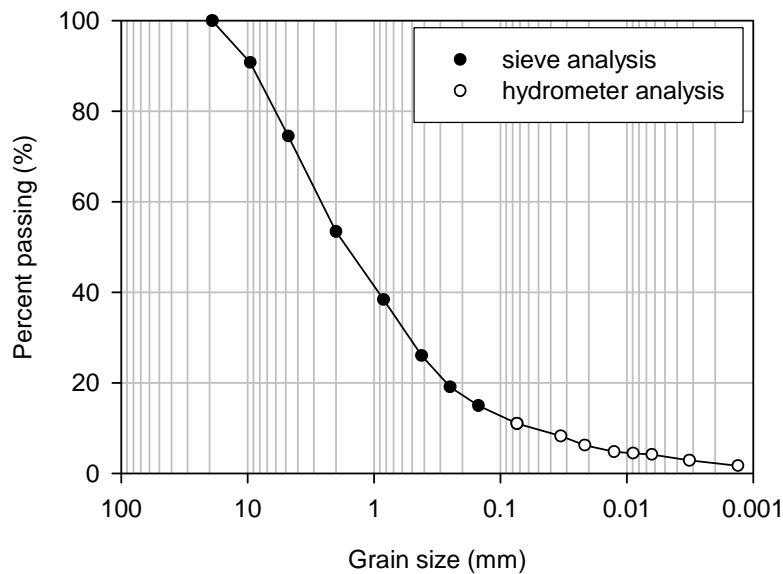


Figure 68. Grain size distribution analysis of the shoulder material, Hwy 71 crossing Hwy 10 S.B.

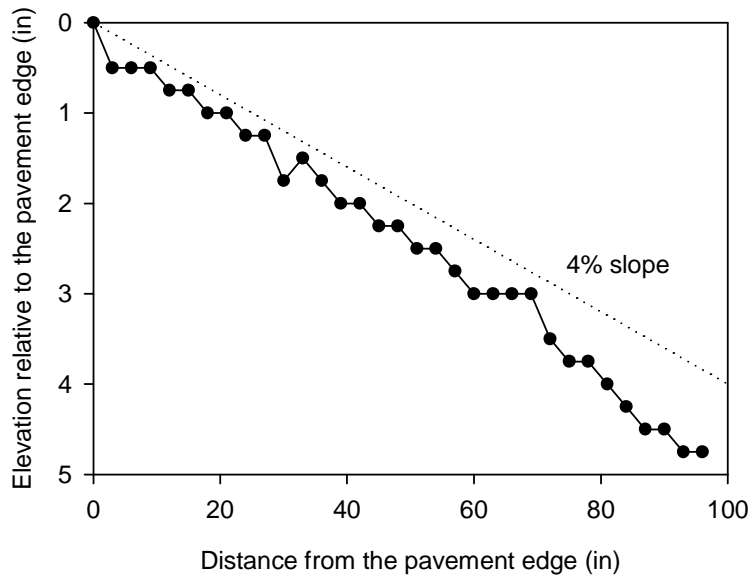


Figure 69. Elevation profile of the shoulder section relative to the pavement, Hwy 71 crossing Hwy 10 S.B.

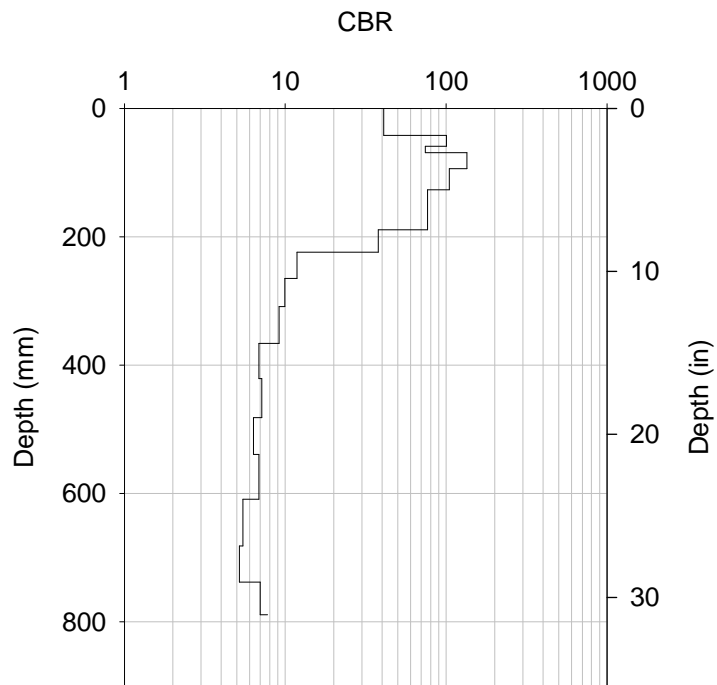


Figure 70. DCP test results, Hwy 71 crossing Hwy 10 S.B.

Highway 60 Station 149+00'

This partially paved shoulder section is approximately 12 ft. wide. The 4 ft. adjacent to the pavement were paved using HMA to stop a chronic edge rut problem at this section. The rest of the shoulder is composed of a crushed limestone-crushed concrete blend (Figure 71). The width of the pavement is 14 ft., and the edge line is 16 in. from the pavement edge.

A sample of the shoulder material was collected for grain size distribution analysis (Figure 72). The material is classified as SP-SM (poorly graded sand with silt; A-1-a). The elevation profile, shown in Figure 73, was measured relative to the pavement. The edge drop-off adjacent to the paved shoulder is 1.5 in. and the overall slope of the shoulder section is about 4%. A DCP test was conducted at 27 in. from the paved shoulder edge (Figure 74). The CBR values of the granular and the subgrade layers are 7 and 4, respectively.



Figure 71. Shoulder section with 4 ft. of HMA and 4 ft. of blended limestone and crushed concrete on Hwy 60 St. 149+00', October 14, 2005

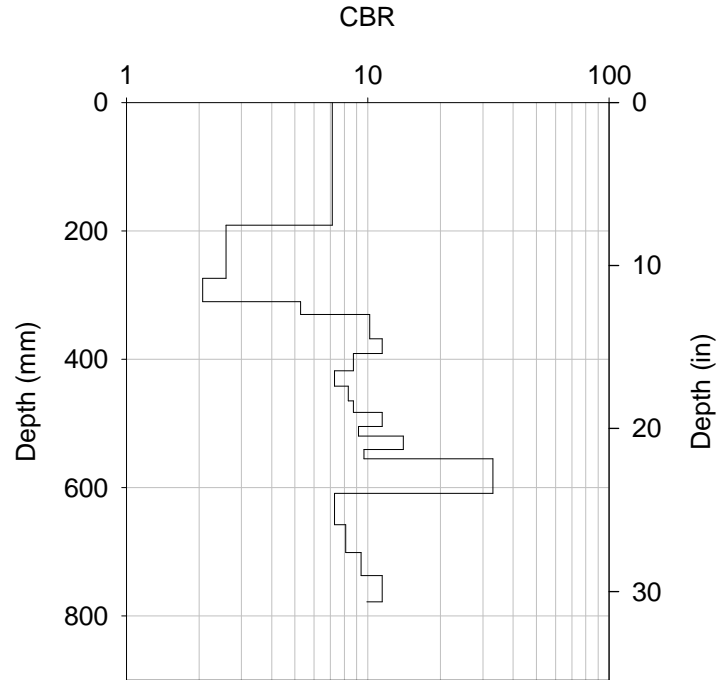


Figure 74. DCP test results, Hwy 60 St. 149+00'

Summary of Findings from Field Reconnaissance

Comparison of Field Measurements to Design Specifications

Table 12 summarizes the range of field values for parameters used either to design or initiate maintenance for granular shoulders. The reported range of field values included good and problematic shoulder sections. The data show that the range of field values for shoulder slopes and percentage of fines, in some instances, exceeded the Iowa DOT design requirements. Further, several important parameters, such as CBR values for granular and subgrade layers, are not currently part of the Iowa DOT shoulder design method. This can allow shoulders to be constructed over soft foundation soils, as observed in several shoulder sections.

Table 12. Range of field values for granular shoulder parameters

Parameter	Iowa DOT design requirement	Range of field values			Standard deviation	No. of measurements
		Minimum	Maximum	Average		
Slope (%)	4	4	11	6	3	12
CBR _{SG} (%)	*	7	182	58	57	16
CBR _{GL} (%)	*	4	218	32	54	15
% fines	6–16	2	14	7.0	4	29
Edge drop-off (in.)	0	0	11	3.0	3	17

* No reported design criteria or specification

Relationship between Edge Drop-Off and Edge Line Location

Certain road conditions, such as edge line location and the presence of slopes and horizontal curves, are said to trigger the formation of shoulder edge drop-off. A simple field study was conducted to investigate the effect of edge line location on the magnitude of the edge drop-off. Fifty granular shoulder sections were inspected, and at each section the following information was collected:

- Location
- Number of highway lanes
- Presence of slopes and/or horizontal curves
- Magnitude of edge drop-off
- Location of edge line
- Type of granular shoulder material

Figure 75 summarizes the results collected from all sections. Even though it is reasonable to assume that the larger the offset distance, the less likely off-tracking will occur, there is not enough evidence from the data collected to support that edge drop-off formation will also decrease. This is because vehicle off-tracking is not the only factor governing the formation of edge drop-off. Other factors such as the presence of horizontal curves and slopes, traffic volume, erosion from surface runoff, type of granular material, and percentage of fines can also contribute to edge drop-off formation. Further, spot edge drop-off measurements, such as the ones collected in this study, are less likely to yield conclusive results. Significant variability, however, was observed where the distance from the white line to the pavement edge ranged from 2 to 3 in. Less variability was noted at larger distances. A further improvement to this study is to collect edge drop-off data at predetermined intervals along each shoulder section.

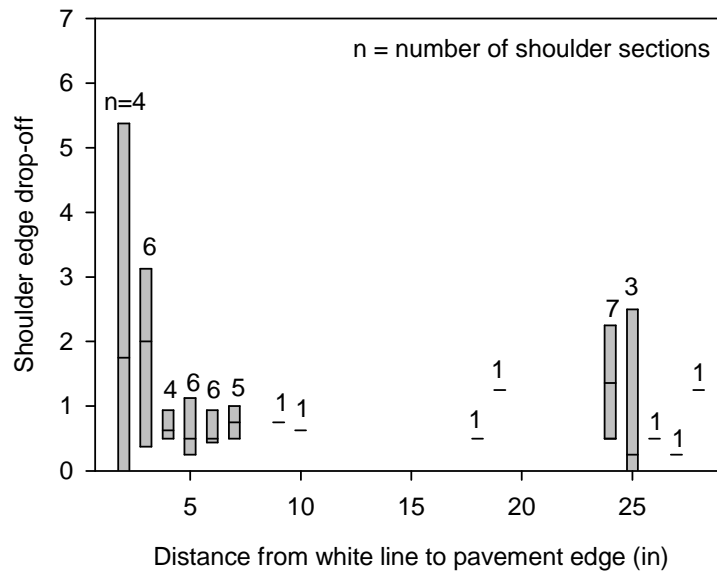


Figure 75. Variability plot for edge drop-offs with distance from white line to pavement edge

Key Findings from Field Reconnaissance

- Unpaved shoulders are comprised mainly of crushed limestone, quartzite material, RAP, or recycled concrete.
- The two major problems observed during field reconnaissance are edge drop-off and a soft subgrade layer.
- Approximately two-thirds of the number of inspected sites had an edge drop-off greater than 1.5 in.
- About 40% of the shoulder sections had a slope higher than the 4% specified by the Iowa DOT.
- About half of the shoulder sections had a subgrade CBR value less than 10.
- Wind induced by high-profile vehicles displaces fines, yielding a coarser granular material gradation.
- One shoulder section stabilized with soybean oil in District 2 showed good performance and did not require any maintenance for six years.
- Spot edge drop-off measurements at 50 granular shoulder sites did not reveal a conclusive relationship between the distance from the white line to the pavement edge and the magnitude of edge drop-off.
- Granular shoulders are maintained by adding virgin or recycled material, reclaiming displaced rock adjacent to the shoulder, and shoulder blading. Between 1 and 1.5 in. edge drop-off is the threshold for initiating maintenance. Shoulders are generally maintained two times in the summer and once in the fall before the ground freezes.

VEHICLE TIRE-AGGREGATE INTERACTION

The shoulder sections investigated during the field reconnaissance showed that aggregate migration away from the pavement edge under the impact of traffic is an important factor in the formation of edge drop-offs. An approach was then conceived to study vehicle tire-aggregate interaction for unpaved shoulders. This was accomplished by observing the trajectory of aggregates using a high-speed camera.

A granular shoulder section on State Ave. in Ames, IA, was selected to be monitored using the special high-speed camera. The granular material consisted of crushed limestone. The shoulder width was about 10 ft. wide and the white line was 2 in. from the pavement edge (Figure 76).



Figure 76. Aggregate shoulder section on State Ave., August 19, 2005

To capture the vehicle tire-aggregate behavior, three observations were conducted of a pickup truck driven on the northbound shoulder at a constant 40 mph. For the first two passes, the high-speed camera was attached to the front of the truck, as shown in Figure 77. The captured video showed aggregate elevated and displaced away from the pavement edge (Figure 77c). In the third attempt, the high-speed camera was placed at the side of road (Figure 78).



(a) Camera fixed to the front of the pickup truck



(b) Closer image of the high-speed camera



(c) Image captured using the high-speed video camera

Figure 77. High-speed video camera demonstration, August 19, 2005

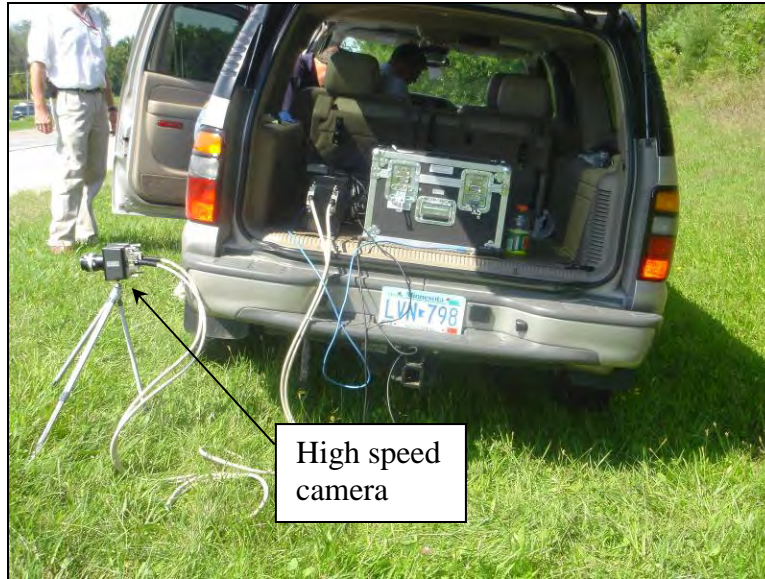


Figure 78. High-speed video camera placed at the side of the road, August 19, 2005

Figure 79 shows a series of images captured at different times using the high-speed camera after the aggregate had come in contact with the tire. The figure shows that aggregates are elevated after coming in contact with the vehicle tire. The trajectories of three aggregates (highlighted in Figure 79) were measured using a special software viewer (Figure 80). The software viewer enables the user to record x-y coordinates at a given time interval. By recording the coordinates of the tire diameter in the viewer and scaling it to the actual tire dimension, the aggregate trajectories can be calculated. The results, shown in Figure 81, indicate that aggregates are elevated upward and pushed in the opposite direction of the traveling vehicle. The time 0.0 seconds in the figure represents the time at which the front wheel was directly over the monitored aggregates.

Repeated off-tracking of vehicles will thus eventually clear the shoulder surface of aggregate and cause edge drop-off, which is consistent with the gradation measurements conducted during the field reconnaissance.

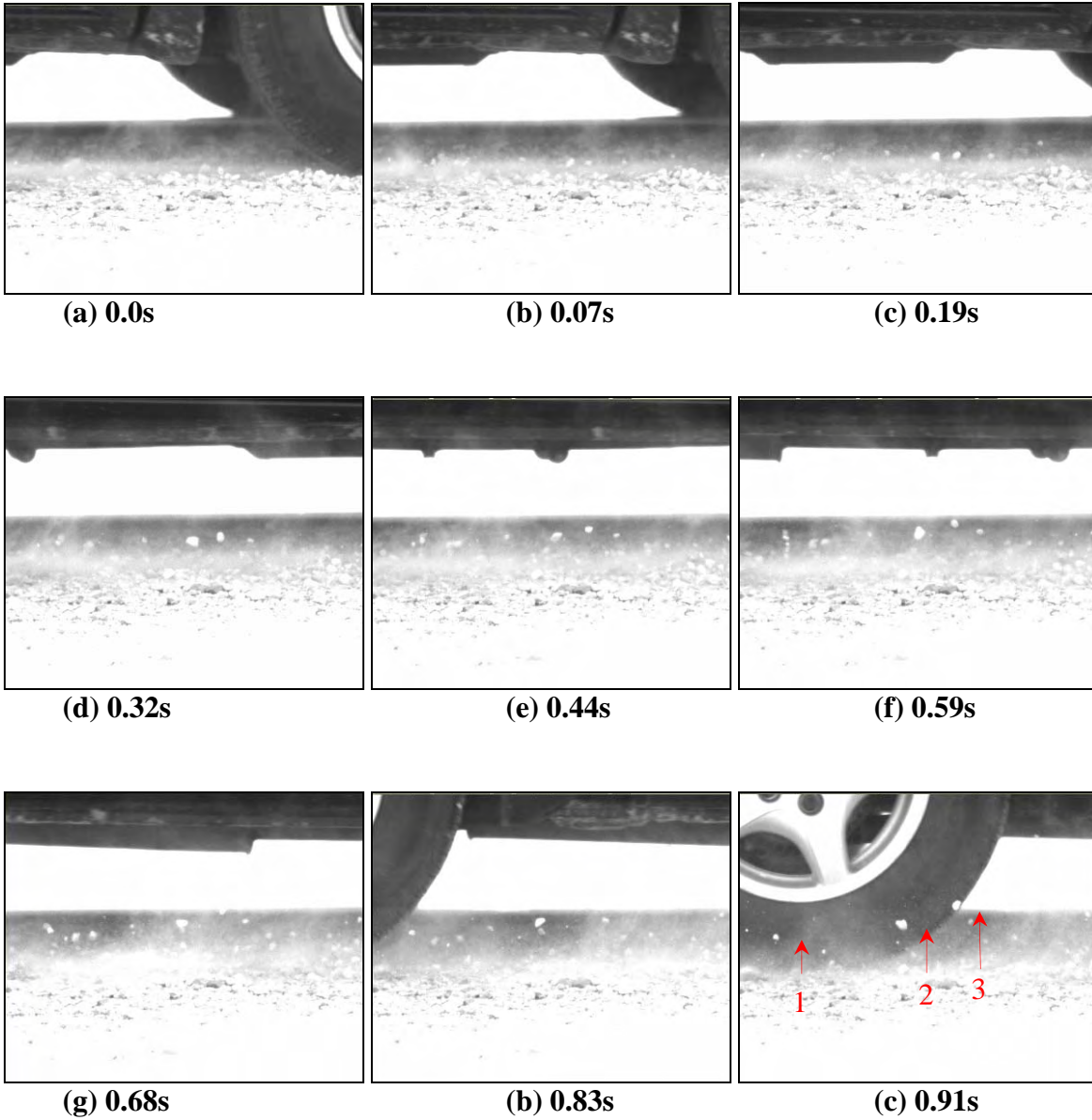


Figure 79. Images captured by a stationary high-speed camera showing aggregate displacement at different times after coming in contact with the tire

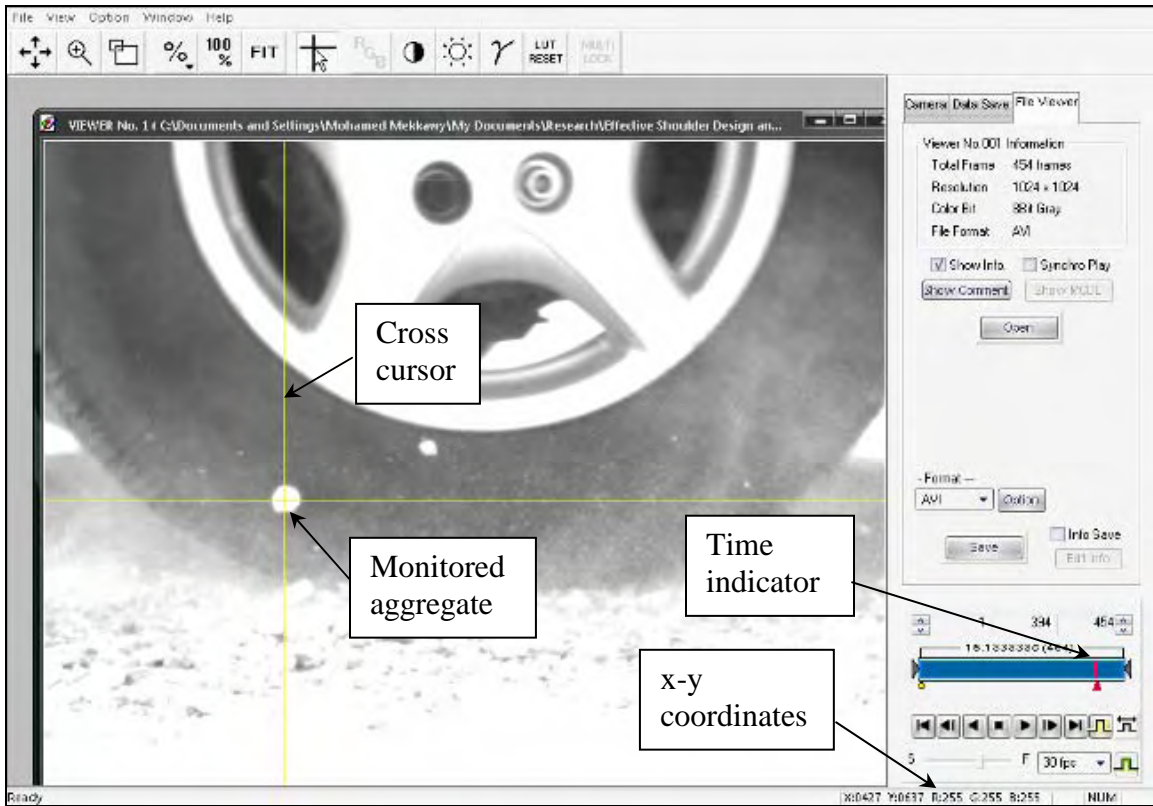


Figure 80. Screenshot of the software used to monitor aggregate trajectory

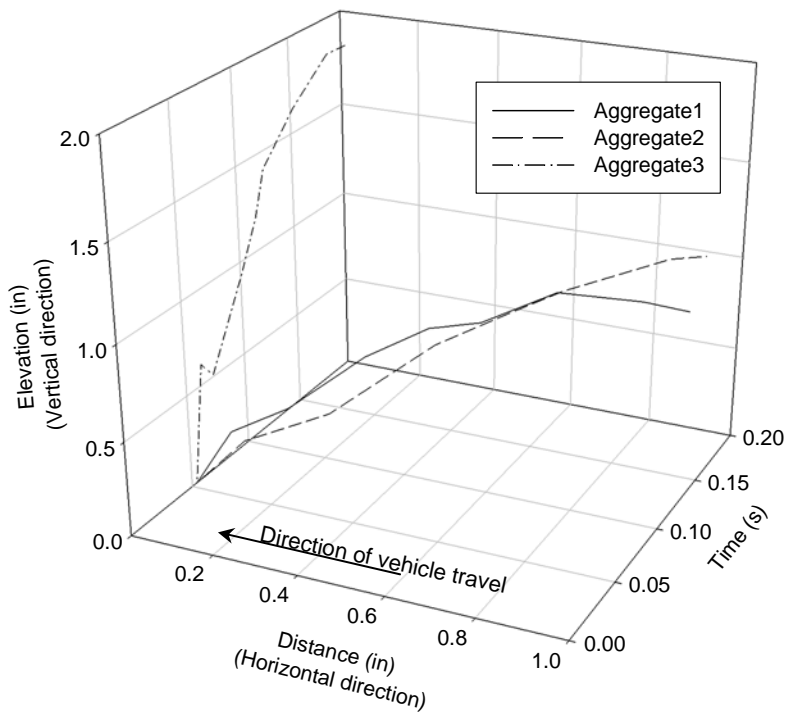


Figure 81. Aggregate trajectory relative to the direction of vehicle travel

SHOULDER TEST SECTIONS

Six granular shoulder sections were selected to test chemical and mechanical stabilization products. The test sections were either experiencing an edge drop-off or severe rutting due to a soft subgrade layer. The granular layers of four test sections were chemically stabilized using S.S. polymer (a polymer emulsion product), foamed asphalt, Feed Energy soybean oil, or portland cement. For two sections, a soft subgrade layer was stabilized using class C fly ash and three geogrid products.

The rest of this chapter summarizes the construction procedures for each test section and evaluates the sections' performance based on field and laboratory testing.

Test Section No. 1: S.S. Polymer, Highway 122, Clear Lake, IA

Site Description

The first test section was located along the westbound shoulder of Highway 122 near Clear Lake, IA. The outside shoulder test section was approximately 1,500 ft. long by 8 ft. wide. The 6 to 12 in. adjacent to the pavement were experiencing erosion due to wind induced by high-profile vehicles and vehicle off-tracking (Figure 82). Elevation profiles relative to the pavement edge were obtained at 50 and 300 ft. from the beginning of the test section. The profiles revealed an edge drop-off equal to 1.5 and 3 in. at 50 and 300 ft, respectively. Further, the slopes at 50 and 300 ft. were 8% and 10%, respectively, which are higher than the 4% slope specified by the Iowa DOT (Figure 83). A sample of the granular material was obtained for grain size distribution analysis (Figure 84). The soil sample is classified as GM (silty gravel; A-1-b). The in situ moisture content of the soil was about 4.9%. S.S. polymer was selected on a trial basis for this test section.



Figure 82. Erosion of the granular shoulder adjacent to the pavement edge on Hwy 122, April 18, 2005

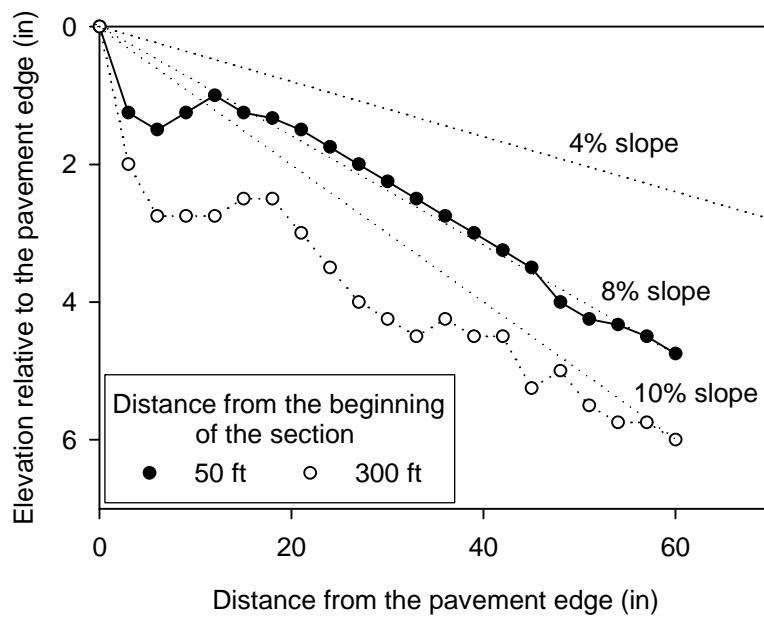


Figure 83. Elevation profiles relative to the pavement edge, Hwy 122

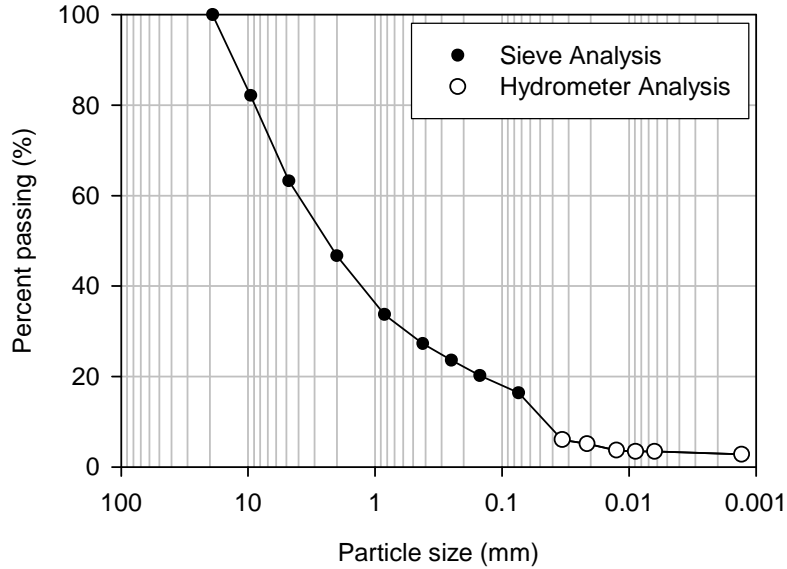


Figure 84. Grain size distribution analysis, Hwy 122

Shoulder Reconstruction

The S.S. polymer was topically applied on April 28, 2005. The polymer was diluted with water at a ratio of 3:1 by volume. The polymer was then sprayed on the surface using a special distributor across a distance of 3 ft. adjacent to the pavement (Figure 85). Three passes were performed, and in each pass about 233 gallons were topically applied. According to field personnel, a total of 700 gallons were applied. After the third pass, the shoulder was compacted using a pneumatic tire roller, as shown in Figure 86. It was observed that the time needed for the S.S polymer to seep through the shoulder material increased during the third pass, relative to the two previous passes.



Figure 85. S.S. polymer topically applied to the granular shoulder, April 28, 2005



Figure 86. Compacting the shoulder section after three topical applications, April 28, 2005

Field Monitoring

DCP tests were performed after applying the S.S. polymer, as shown in Figure 87. The tests were performed inside the stabilized area (14 in. from the pavement) and outside the stabilized area (45 in. from the pavement) to compare strength gain at both locations. The tests were performed immediately after applying and compacting the S.S. polymer (i.e., 0 hours) and were repeated at the same location after 2 hours, 3 hours, 6 days, and 30 days from the reconstruction date.

The results indicate no significant increase in the CBR value in the upper 8 in. At depths between 8 and 20 in., the strength is considerably reduced, as indicated by low CBR values. In addition, there is no significant difference between the CBR values inside and outside the stabilized area.

The shoulder section was inspected after the months from the repair date. It was observed that the 6 to 12 in. strip adjacent to the pavement was delaminated, resulting in a 0.5 in. edge drop-off (Figure 88a). The S.S. polymer penetrated a distance of approximately 0.5 in., forming a thin granular film over the shoulder granular material (Figure 88b). It is believed that under repeated traffic loads this film started to delaminate, exposing the untreated granular material.

Elevation profiles at 50 and 300 ft. were measured with time (Figure 89). The results reveal that topically stabilizing the granular layer with S.S. polymer did not mitigate further edge drop-off development. After one month, an edge drop-off of 1.5 and 1.2 in. at 50 and 300 ft, respectively, was observed. Additional vehicle off-tracking increased the edge drop-off to 2.2 in. at 300 ft. As shown in Figure 90, new crushed limestone material was added in areas where the edge drop-off exceeded 2 in.

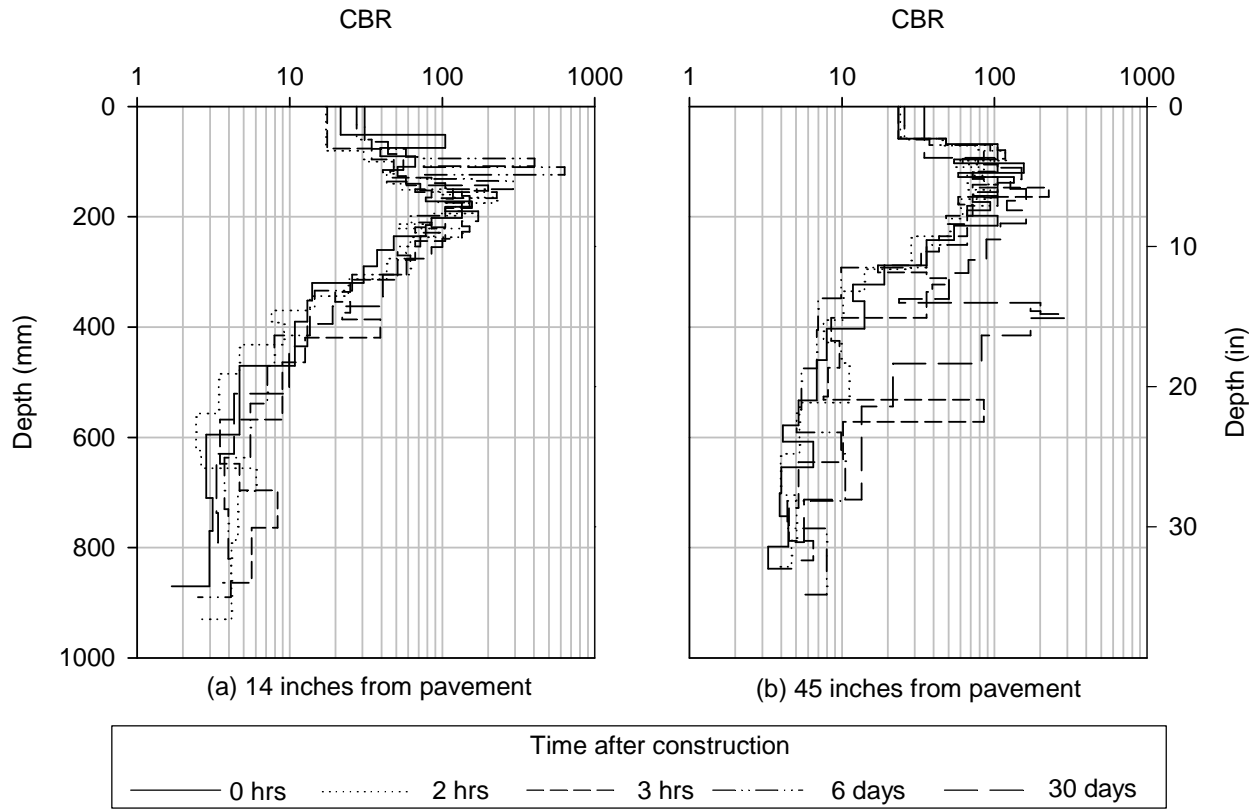


Figure 87. DCP test results, (a) inside the stabilized area and (b) outside the stabilized area

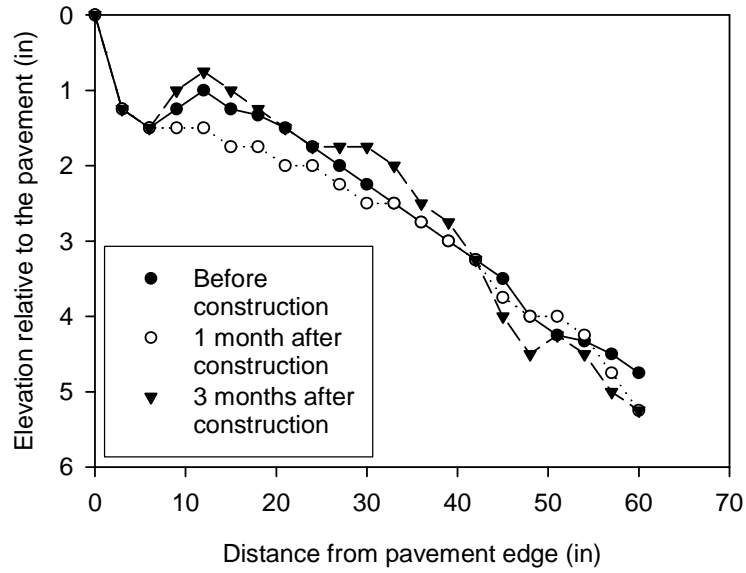


(a) Delaminated strip near pavement edge

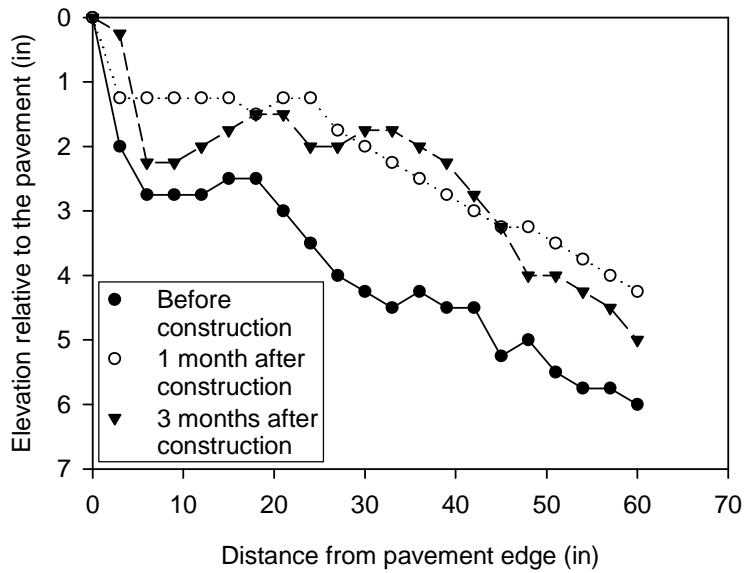


(b) Thin granular film forming on top of granular material

Figure 88. Delamination of the bonded granular material under the impact of traffic, June 11, 2005



(a)



(b)

Figure 89. Elevation profile relative to the pavement edge collected at (a) 50 ft. and (b) 300 ft. from the beginning of the section

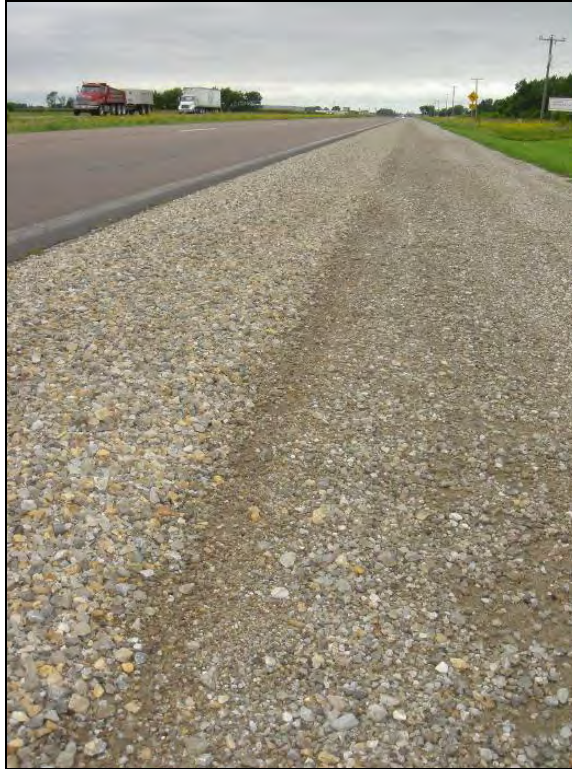


Figure 90. Crushed limestone added to areas with high edge drop-off on Hwy 122, July 26, 2005

Laboratory Testing

Due to the unsatisfactory performance of the S.S. polymer, a succinct laboratory study was conducted in an attempt to identify the reasons behind the inadequate performance. In addition, the laboratory study aimed to identify the most favorable procedure for applying S.S. polymer to the granular material used to construct shoulders in Iowa.

Constant Head Permeability Test

To measure the permeability of the granular material, constant head permeability tests were carried out. Two samples with different gradations were tested. Sample 1 was the material collected from the shoulder section to represent the upper bound of the Iowa DOT gradation requirement, while sample 2 was altered to represent the lower bound of the Iowa DOT gradation requirement (i.e., more permeable). The permeability measured for samples 1 and 2 were 0.001 and 0.002 cm³/sec, respectively. Changing the gradation of the granular material from the upper bound to the lower bound increased the permeability by 100%. This greatly influenced the depth of S.S. polymer penetration, as demonstrated in the seepage analysis test.

Seepage Analysis

The purpose of the seepage analysis was to measure the penetration depth of the S.S. polymer when applied at the surface of the granular material samples. Two Proctor-size samples were prepared with similar gradations to the samples prepared for the permeability tests (i.e., samples representing the upper and lower bound of the Iowa DOT gradation requirement). Similar to the documented field application, a 3:1 water to S.S. polymer mixture was applied at the surface of the Proctor-size samples and allowed to seep for four days. Approximately 29 ml of the S.S. polymer mixture was applied to simulate the amount used in the field. After four days, the samples were extracted and the depth of S.S. polymer penetration was measured.

On average, the depth of penetration of the S.S. polymer for sample one (upper bound gradation) was 1.3 in. As shown in Figure 91, the upper 1.3 in. of the extruded sample was cemented together, while the lower portion of the sample was loose. Unlike sample 1, the S.S. polymer penetrated the full depth of the second sample (lower bound gradation) due to its higher permeability.

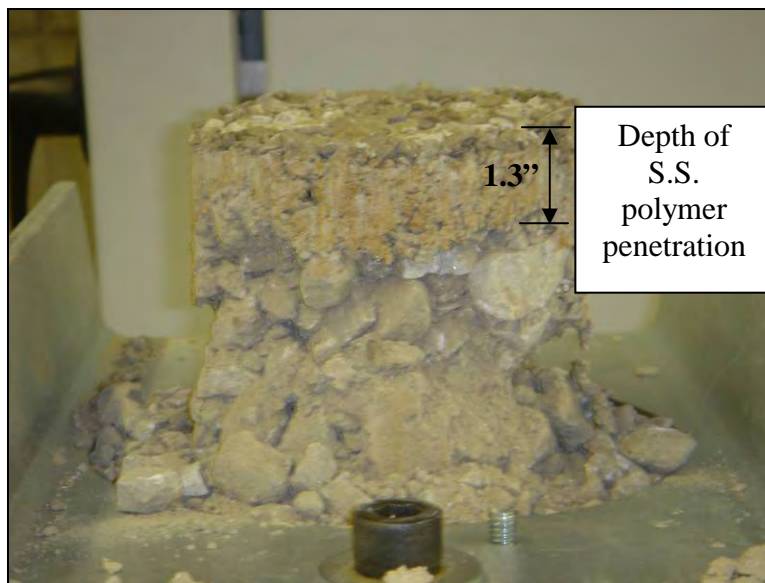


Figure 91. Measured penetration depth of S.S. polymer for upper bound gradation

Unconfined Compression Test

The purpose of this test was to determine whether there is an optimum binder content for the S.S. polymer when it is used to stabilize granular material. To achieve this objective, the granular material was mixed with varying percentages of the diluted 3:1 S.S. polymer. Four Proctor-size specimens were prepared with 3%, 5%, 8%, and 11% S.S. polymer by weight. Two additional specimens were prepared at 5% binder content and were soaked in water for four hours prior to testing. All samples were lab cured at 68° F for seven days. The unconfined compression tests revealed that the highest compressive strength (419 psi) was achieved at a binder content of 5%

(Figure 92 and Figure 93). The compressive strength did not increase with increasing binder content. The soaked samples disintegrated after four hours, and the unconfined compression test was not conducted (Figure 94). This indicates that granular material stabilized with S.S. polymer may not perform well if saturated and that at least durability testing is needed.



Figure 92. Unconfined compression test conducted on S.S. polymer-stabilized sample

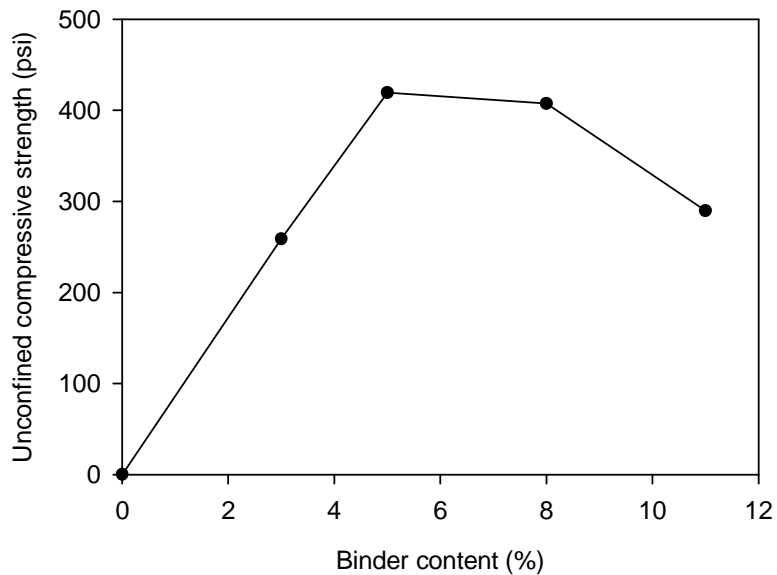


Figure 93. Unconfined compressive strength results for unsoaked samples



Figure 94. Disintegrated specimen after soaking for four hours

Summary and Conclusions for Test Section No. 1

- The granular shoulder section on the westbound of Highway 122 was experiencing 1.5 to 3 in. rut adjacent to the pavement.
- On a trial basis, the section was stabilized with S.S. polymer to prevent progression of the edge drop-off and erosion.
- The stabilization method performed inadequately, and the 6 to 12 in. strip adjacent to the pavement edge showed signs of delamination after 30 days.
- The S.S. polymer penetrated to a depth of approximately 0.5 in., forming a granular film that was delaminated.
- DCP tests revealed that strength did not increase with time within the upper 15 in. of the shoulder. In addition, the granular material is overlying a soft subgrade, as indicated by the low CBR values.
- The constant head permeability test showed that the lower bound gradation has a higher permeability value than the upper bound gradation, which results in higher S.S. polymer penetration depths. This observation was confirmed by performing seepage analysis tests.
- The optimum S.S. polymer content to be used with the shoulder granular material is 5%. This binder content may change with different S.S. polymer concentrations or soil types.
- Specimens stabilized with S.S. polymer disintegrated after soaking for four hours, indicating the potential for poor performance of the polymer under wet conditions.

Recommendations for Test Section No. 1

- To achieve better binding, the S.S. polymer should be mixed at optimum binder content with the granular layer.
- For topical applications, a more permeable granular material is to be used to increase the seepage depth. Additionally, it is recommended that other polymer concentrations (e.g., 7:1 and 9:1) be evaluated.
- Durability testing is recommended to determine performance of the S.S. polymer under wet-dry and freeze-thaw conditions.
- It is proposed to excavate and mix the granular material at the Highway 122 shoulder section with S.S. polymer at optimum binder content (5%). The material should then be placed and compacted. The depth of the stabilized layer should be about 6 in.

Test Section No. 2: Foamed Asphalt, I-35

Site Description

The paved shoulders on the northbound of I-35 (from milepost 147 to 155) were being reconstructed due to severe distress. The distresses observed included alligator cracking, shoulder drop-off, and longitudinal and transverse cracking. Stabilization of the granular layer using FA was selected as the repair process because of its previous good performance at a shoulder section placed in 2001 on Highway U.S. 30, west of Boone, IA. A section on the outside shoulder of the northbound lane near milepost 152.30+30 ft. was selected for monitoring during and after construction. The shoulder section was about 6 ft. wide and the edge line was 4.5 in. from the pavement edge.

Shoulder Reconstruction

The construction procedures included mixing about 3% to 4% class C fly ash with the granular material prior to placing the FA (Figure 95). Full-depth reclamation of existing shoulder materials with FA and fly ash was conducted to a depth of 10 in. using a reclaimer, as shown in Figure 96. The reclaiming drum was 8 ft. wide. Water was added to the reclaimed foamed asphalt via a water truck that followed the road reclaimer to achieve moisture content near the optimum for compaction. Compaction of the FA was accomplished using a vibratory pad foot followed by a smooth drum roller. Two days after construction, the FA surface was sealed using a seal coat (chip seal), as shown in Figure 97.



Figure 95. Fly ash added to the granular material on I-35 milepost 150 northbound, September 1, 2005



Figure 96. Full depth reclamation of FA on I-35 milepost 150 northbound, September 1, 2005



Figure 97. FA surface sealed using chip seal on I-35 milepost 150 northbound, September 1, 2005

Field Monitoring

A standard Proctor test was performed to determine the optimum moisture content and maximum dry density (Figure 98). The optimum moisture content and the maximum dry density were determined to be 14% and 116 lbs/ft³, respectively. Using a nuclear gauge device, the field moisture content and the field dry density were determined with depth at five locations (5 ft. apart) along the monitored shoulder section (Figure 99 and Figure 100). The field moisture

contents at locations 1 through 4 were on the dry side of optimum moisture content (1% to 2% below optimum), while at location 5 the field moisture contents was on the wet side (about 1.5% above optimum). When compared to the maximum dry density obtained by the standard Proctor test, the relative compaction in the field varied from 95% to 100% compaction. At two locations, the percent compaction exceeded 100%. DCP tests were conducted before and after compaction of the FA and at 6 and 40 days after reconstruction (Figure 101). The data collected at 40 days was excluded because the DCP could not penetrate beyond a depth of 3.9 in. The results show that immediately after compaction the CBR value increased from 0.4 to 14 for the upper 12 in. Additional strength gain was observed after 6 days, as the CBR value increased to 59. This shows that FA was successful in increasing the short-term strength of reclaimed material.

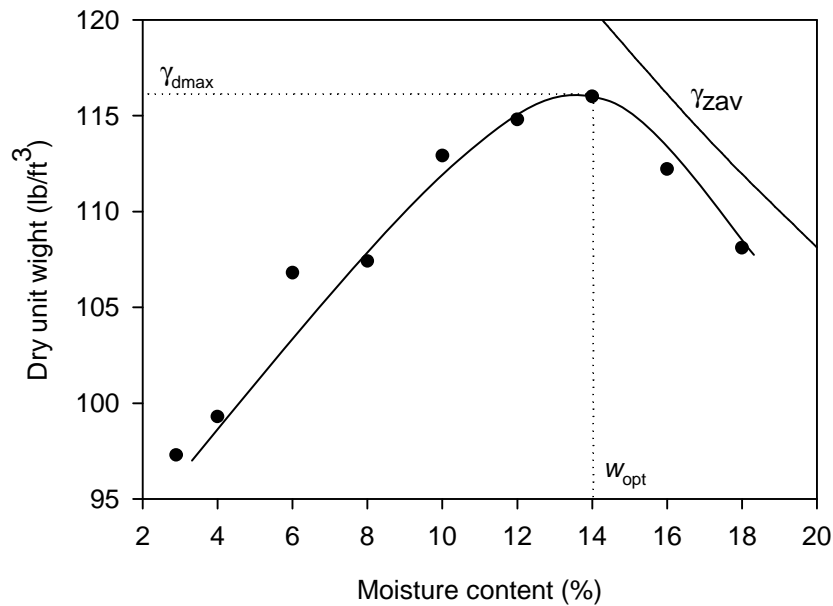


Figure 98. Optimum moisture content and maximum dry density determined by standard Proctor test, I-35 milepost 150 northbound

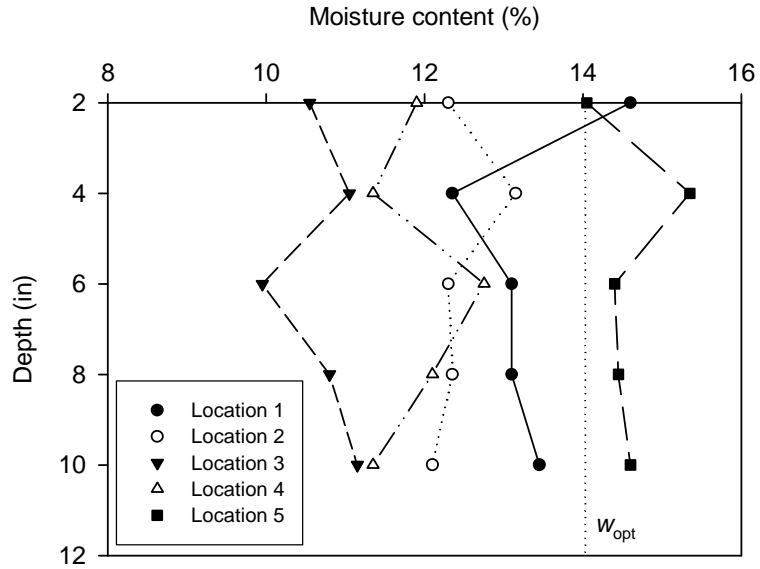


Figure 99. Variation of field moisture content with depth along the shoulder section, I-35 milepost 150 northbound

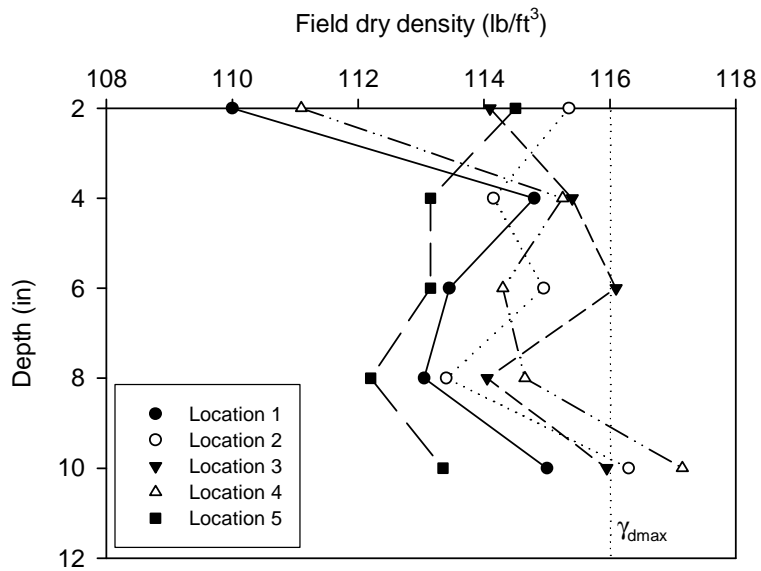


Figure 100. Variation of field dry density with depth along the shoulder section, I-35 milepost 150 northbound

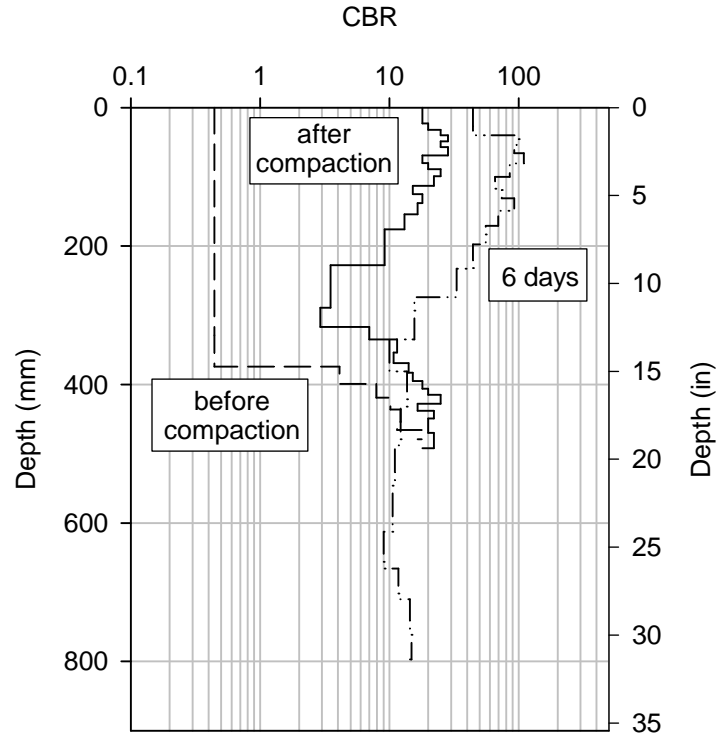


Figure 101. DCP test results showing strength gain with time, I-35 milepost 150 northbound

The test section was inspected after 10 months from the reconstruction date. It was observed that the test section failed along the pavement edges. Due to this failure, and as shown in Figure 102, edge drop-offs varying from 3 to 5 in. were formed. Along the horizontal curved road sections (in particular milepost 150, northbound lane), where vehicle off-tracking is likely, edge drop-offs had developed in a number of places. Thus, the area adjacent to the pavement edge was patched, as shown in Figure 103. Foamed asphalt was successful in improving the shoulder's short-term performance, as evidenced by the increase in CBR values. However, this stabilization technique failed to withstand loads imposed by off-tracking vehicles at the pavement edge. Inspection of the seal coat after 12 months from reconstruction did not result in any indications of seal coat failure, such as delaminating or substantial snow plow damage.



(a) Milepost 154 southbound



(b) Milepost 151 northbound

Figure 102. Edge drop-off caused by failure of foamed asphalt-stabilized section, July 25, 2006



Figure 103. Asphalt patch placed on the deteriorated shoulder adjacent to a horizontal curve, I-35 milepost 150 northbound, July 7, 2006

Laboratory Testing

Standard Proctor samples were prepared at the construction site for a laboratory durability study, which included unconfined compression testing, vacuum saturation, freeze-thaw and wet-dry testing. Table 13 presents the results of unconfined compressive strength for two control samples and six samples that were subjected to vacuum saturation testing (Figure 104), which was conducted in accordance with ASTM C 593-89 (Standard Specification for Fly Ash and Other Pozzolans for Use with Lime). On average, vacuum saturating the FA-stabilized samples resulted in a 21% decrease in compressive strength. Six samples were subjected to wet-dry condition testing that was conducted according to ASTM D559-96 (Standard Test Methods for Wetting and Drying Compacted Soil-Cement Mixtures). After the first drying cycle (oven drying the samples at 160° F for 42 hours) all six samples failed due to melting of the binding agent (Figure 105). In addition to the aforementioned tests, six samples were subjected to freeze-thaw conditions conducted according to ASTM D560-96 (Standard Test Methods for Freezing and Thawing Compacted Soil-Cement Mixtures). Figure 106 shows the percent volume change relative to the initial volume due to the freeze-thaw cycles for both brushed and non-brushed samples. On average, the volume increased by 12% and 18% for brushed and non-brushed samples, respectively. The maximum volume change observed was 26%. This indicates that under extreme conditions the FA-stabilized granular soil may noticeably expand, causing shoulder distresses. Figure 107 shows the percent mass loss for brushed samples relative to their original mass. The percent mass loss ranged from 1% to 6%, which is less than the 14% specified by NAVFAC (1999).

Table 13. Results of FA durability testing

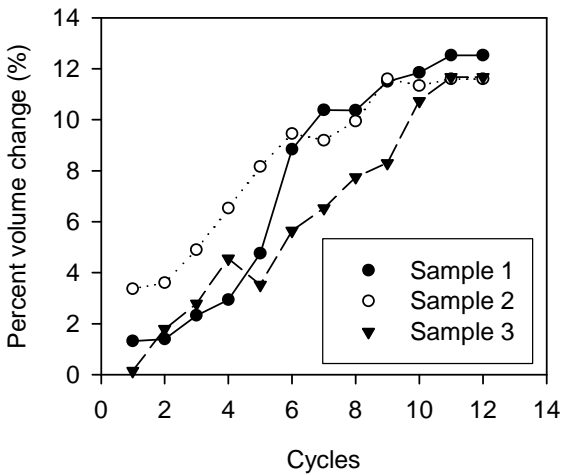
	Test	Sample No.	UCS (psi)	
Unconfined compressive test	Control	1	41	
		2	51	
	Vacuum saturation	1	41	
		2	17	
		3	50	
		4	39	
	5	35		
	6	36		
Durability testing	Freeze-thaw (brushed)	1	12	-
		2	11	-
		3	12	-
	Freeze-thaw (non-brushed)	1	15	1
		2	15	2
		3	26	6



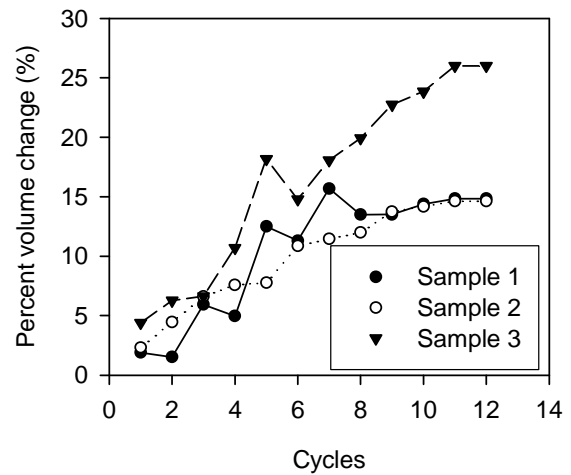
Figure 104. Vacuum saturation test conducted on granular material stabilized with foamed asphalt



Figure 105. Failure of foamed asphalt stabilized sample during wet-dry testing



(a) Non-brushed samples



(b) Brushed samples

Figure 106. Percent volume change caused by freeze-thaw cycles

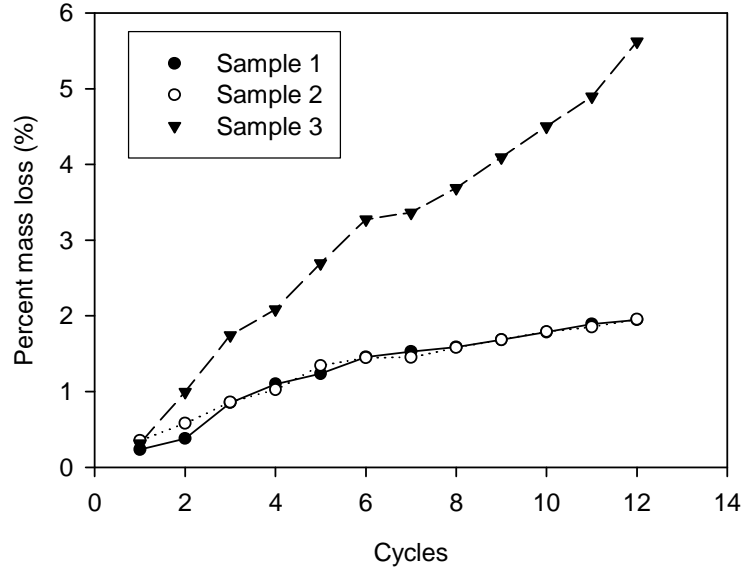


Figure 107. Percent mass loss during freeze-thaw cycles

Summary and Conclusions for Test Section No. 2

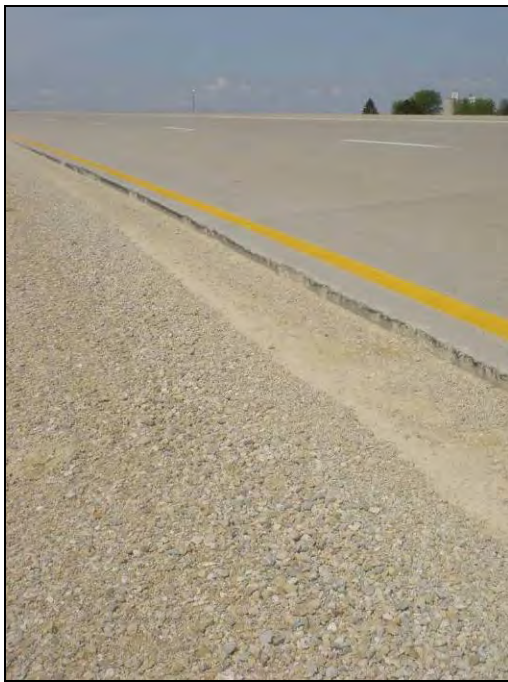
- Full depth reclamation to a depth of 12 in. using FA and 3% to 4% class C fly ash was utilized to stabilize shoulder sections on I-35.
- Field results show that compaction was performed at moisture contents ranging within 1% to 2% from optimum moisture content. The relative compaction achieved ranged from 95% to 100%.
- DCP tests demonstrated strength gain with time for the upper 10 in., as evidenced by the increase of CBR value from 0.4 to 59.
- Laboratory study revealed that vacuum saturation reduces the compressive strength by 21%, whereas freeze-thaw cycles showed that FA can expand by 18%, which would likely cause shoulder distresses. The percent mass loss due to freeze-thaw cycles is satisfactory.
- Foamed asphalt was successful in improving the properties of the shoulder section for a short duration. Further monitoring revealed considerable distress and strength loss at the pavement edge.

Test Section No. 3: Soybean Oil Soapstock, Highway 18, Rudd, IA

Site Description

The inside shoulder section on the westbound of Highway 18 milepost 202.50 near Rudd, IA, was experiencing edge drop-off, as shown in Figure 108. The drop-off is most likely caused by vehicles off-tracking and erosion from surface runoff, since the section is located on a super-elevated curve. The edge line is about 6 in. from the pavement edge.

Soil samples were obtained with distances from the pavement edge for laboratory grain size distribution analysis (Figure 109). The samples obtained at 0.5 and 3 ft. were collected from the eroded area and are classified as SW-SM (well-graded sand with silt; A-1-a) and GW (well-graded gravel; A-1-a), respectively. The samples collected at 4 and 6 ft. from the pavement edge were classified as SM (silty sand; A-1-b). The results show that the granular material closer to the pavement contains fewer fines. Loss of fine material, which is attributed to off-tracking and wind or water erosion, results in loose surface aggregate, which then migrates away from the pavement edge.



(a) Shoulder edge drop-off



(b) Tire marks along pavement edge

Figure 108. Shoulder on Hwy 18 milepost 202.50 near Rudd, IA, May 10 2006

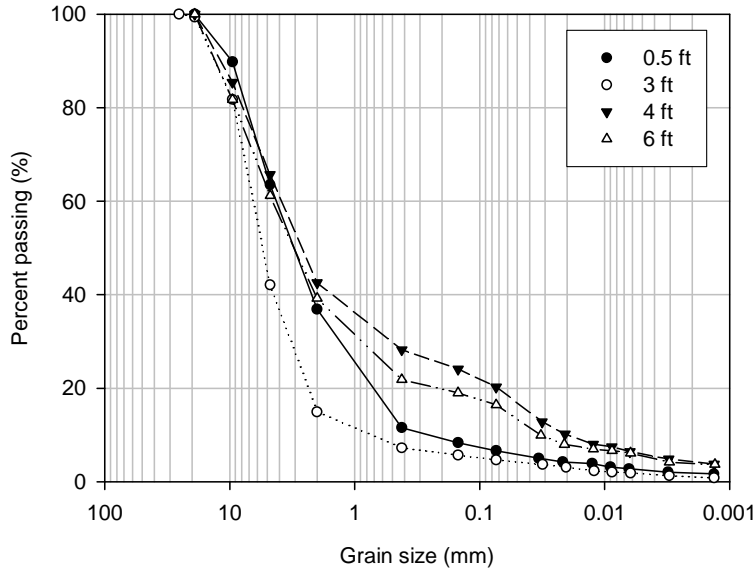


Figure 109. Grain size distribution analysis, Hwy 18 milepost 202.50 WB

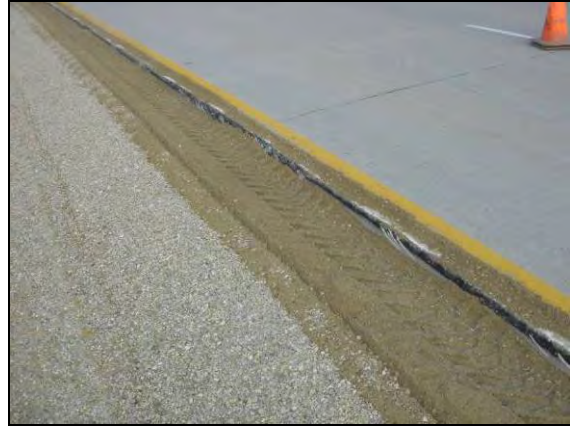
Shoulder Reconstruction

Feed Energy soybean oil was the selected stabilizer for this section due to the good performance observed at the granular shoulder section near Garner, IA (discussed in the Field Reconnaissance section of this report). The stabilized section was about 430 ft. (extending from milepost 202.50+70 ft. to milepost 202.45-100ft). The top 6 in. of a 3 ft. section adjacent to the pavement were tilled using a shoulder reclaimer, shown in Figure 110. Using an Iowa DOT distributor, two applications were carried out at a rate of about 0.7 gal/yd² (Figure 111). After each application, the oil was mixed with the granular material using the shoulder reclaimer, as shown in Figure 112. The granular material was then compacted by driving a loaded aggregate truck over the stabilized section, followed by one pass using a pneumatic roller (Figure 113).

Prior to applying a final topical application, the distributor became plugged with soybean oil, as shown in Figure 114. During transportation and application of the stabilizer, the Feed Energy soybean oil product was not continuously agitated, which resulted in separation of the soybean oil and emulsion. Therefore, the topical application was not carried out. It was decided to place and compact additional rock over the stabilized area. About 20 tons of new crushed limestone was added and compacted using a loaded aggregate truck and a pneumatic roller (Figure 115). Upon completion, the entire section was bladed.



(a) Shoulder reclaimer used



(b) Tilled granular layer to a depth of 6 in.

Figure 110. Tilling of a 3 ft. section adjacent to the pavement, August 22, 2006



Figure 111. Applying Feed Energy soybean oil to the shoulder section, August 22, 2006



Figure 112. Mixing Feed Energy soybean oil with shoulder granular material, August 22, 2006



Figure 113. Compacting the stabilized section using a pneumatic roller on Hwy 18 milepost 202.50 Rudd, IA, on August 22, 2006



Figure 114. Distributor plugging after separation of emulsion and soybean oil, August 22, 2006



Figure 115. Placing crushed limestone material over the stabilized area, August 22, 2006

Field Monitoring

The elevation profile relative to the pavement edge at milepost 202.50 was monitored before and after reconstruction, as shown in Figure 116. Before stabilization, an edge drop-off of about 3.25 in. was measured. Immediately after stabilization, the edge drop-off was eliminated and the shoulder slope was about 9%. Two months after the reconstruction date, an edge drop-off of about 2 in. was measured. Further, the maintenance office at District 2 placed asphalt millings at the shoulder test section (Figure 117).

Figure 118 shows the DCP test results measured after two months. DCP tests conducted at 0.5 and 3 ft. were inside the stabilized area, while the test at 6 ft. was outside the stabilized area. The results indicate that the Feed Energy soybean oil did not provide significant strength gain in the upper 8 in. Further, the CBR value for subgrade layer was about 10. The section was investigated after eight months from reconstruction. It was observed that the edge drop-off increased to about 3 in., as shown in Figure 119. The Feed Energy soybean oil applied at this test section did not mitigate edge drop-off formation.

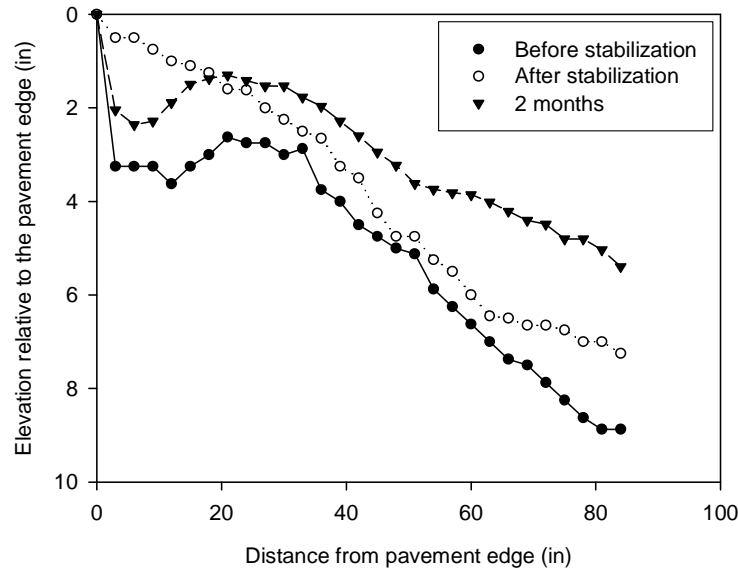


Figure 116. Elevation profile relative to the pavement edge, Hwy 18 milepost 202.50 W.B.



Figure 117. Asphalt millings placed at the shoulder test section and a 2 in. edge drop-off developed after two months, October 10, 2006

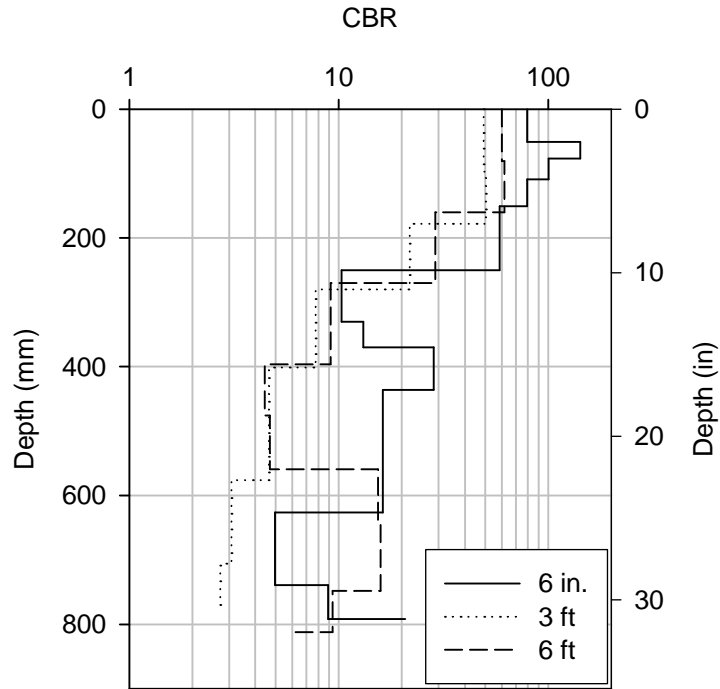


Figure 118. DCP test results, Hwy 18 milepost 202.50 W.B.



Figure 119. Three-inch edge drop-off after eight month on Hwy 18 milepost 202.50 near Rudd, IA, on June 23, 2006

Summary and Conclusions for Test Section No. 3

- The inside shoulder on the westbound lane of Highway 18 milepost 202.50 was experiencing significant edge drop-off.
- A 340 ft. long by 3 ft. wide by 6 in. deep section was stabilized using soybean oil.
- Two applications at a rate of 0.7 gal/yd² were placed and mixed with the granular material.
- Due to separation of the oil from the emulsion, the distributor became plugged and a topical application was not carried out.
- Additional rock was placed and compacted over the stabilized area.
- The elevation profiles show that the soybean oil did not succeed in mitigating the edge drop-off formation.
- DCP tests reveal that the soybean oil did not provide additional strength in the upper 8 in. of the stabilized test section. Further, the section was overlying a soft subgrade layer, indicated by the low CBR values at a depth greater than 20 in.
- Due to the success observed at the shoulder section stabilized with soybean oil near Garner, IA, it was concluded that the field performance of soybean oil as a stabilizer can vary significantly between products.

Test Section No. 4: Portland Cement, 16th St., Ames, IA

Site Description

The westbound shoulder section on 16th St. in Ames, IA, was about 12 ft. wide. The white line was offset 2 in. from the pavement edge. Edge drop-off and wash boarding had been ongoing problems at this section (Figure 120). The section undergoing the highest shoulder drop-off was on the westbound lane, opposite to Christensen St. (entrance to Iowa State University's College of Veterinary Medicine). The shoulder drop-off varied from 3 to 4 in.

A sample of the granular material was collected for laboratory grain size distribution analysis (Figure 121). The soil was classified as SW-SM (well-graded sand with silt; A-1-a). Based on the stabilizer selection chart provided by Chu et al. (1955), portland cement was the chemical stabilizer selected since the percent passing the No. 200 sieve was less than 25% and the PI was less than 10.

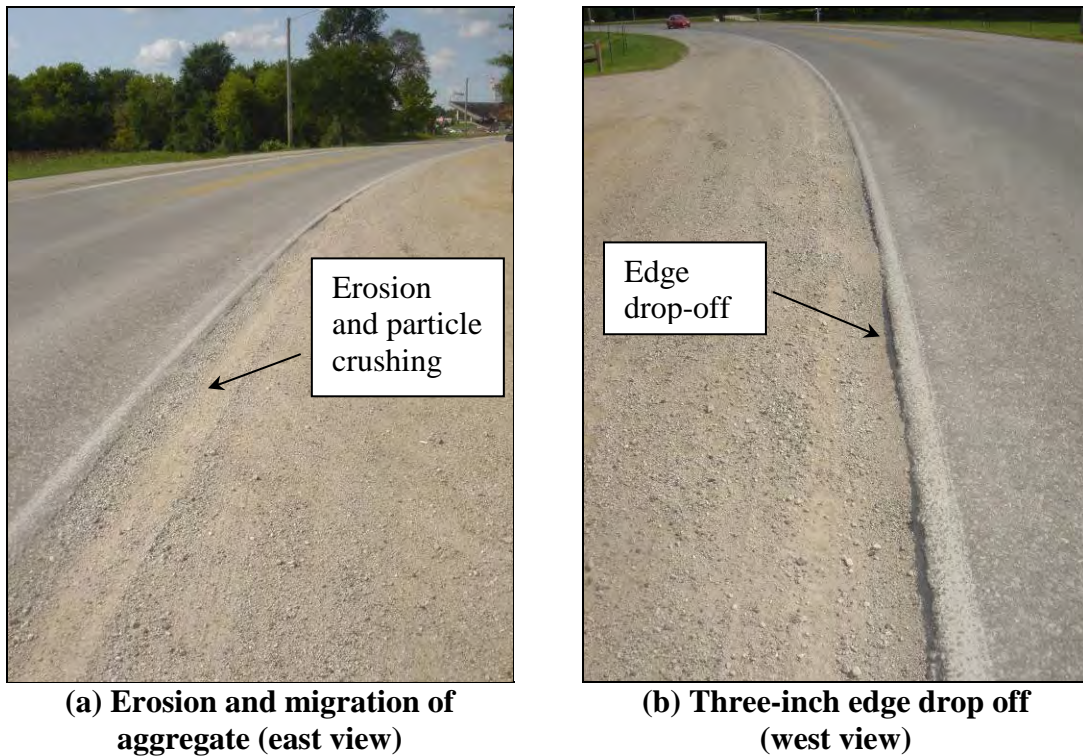


Figure 120. Edge drop-off and wash boarding along the pavement edge on 16th St. Ames, IA, on September 6, 2006

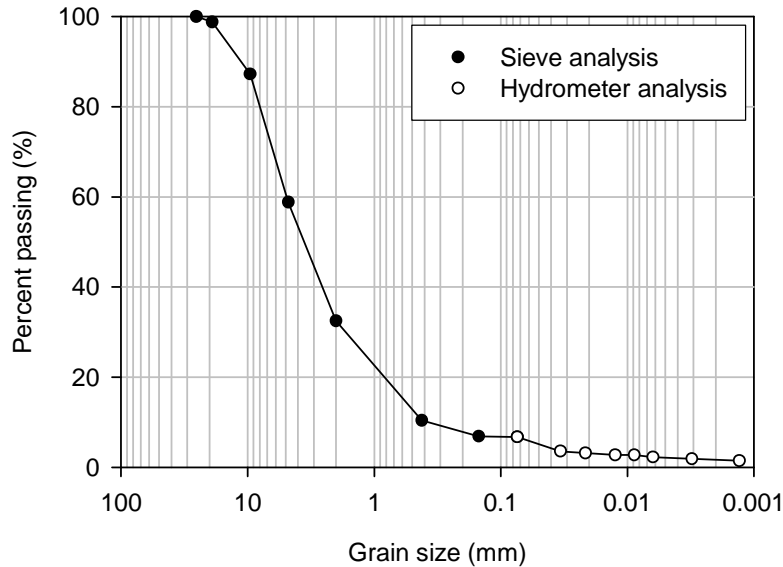




Figure 122. Blading of the shoulder section on 16th St. in Ames, IA, September 26, 2006



Figure 123. Truck carrying a water tank ahead of shoulder reclaimer, September 26, 2006



Figure 124. Spreading of cement over the reclaimed test section, September 26, 2006



(a) Before reclamation



(b) After reclamation

Figure 125. Mixing the cement with the granular material, September 26, 2006



Figure 126. Compaction of stabilized section using smooth drum roller, September 26, 2006

Field Monitoring

Several site inspections were performed to document the section performance. After 7 days, it was observed that a hard surface was formed along the first 100 ft. of the stabilized area (Figure 127). The width of the hard surface was about 8 in. As shown in Figure 128, wash boarding and minor erosion was observed towards the end of the section. The variation in section performance can be attributed to a nonuniform mixture and insufficient moisture, which was needed for cement hydration in the second 100 ft. section. CIV profiles were collected at 7, 14, and 28 days after construction to monitor strength gain throughout the stabilized area. Figure 129 shows the results of the Clegg impact tests conducted at the time. The results demonstrate a significant strength gain after 7 days. The average CIV increased from 40 before stabilization to 91 after stabilization. Additional strength gain was measured after 14 days. The average CIV after 14 days increased to 108. Clegg impact tests conducted after 28 days revealed no further strength gain.

The section was inspected after four months from reconstruction. Edge drop-off varying from 1 to 2 in. was noted along the edges of the pavement (Figure 130). The section was inspected again after eight months from reconstruction. The edge drop-off problem continued to progress, as shown in Figure 131. The measured edge-drop off was about 3 in. Even though the strength of the shoulder section increased after stabilization, the shoulder section continued to erode.

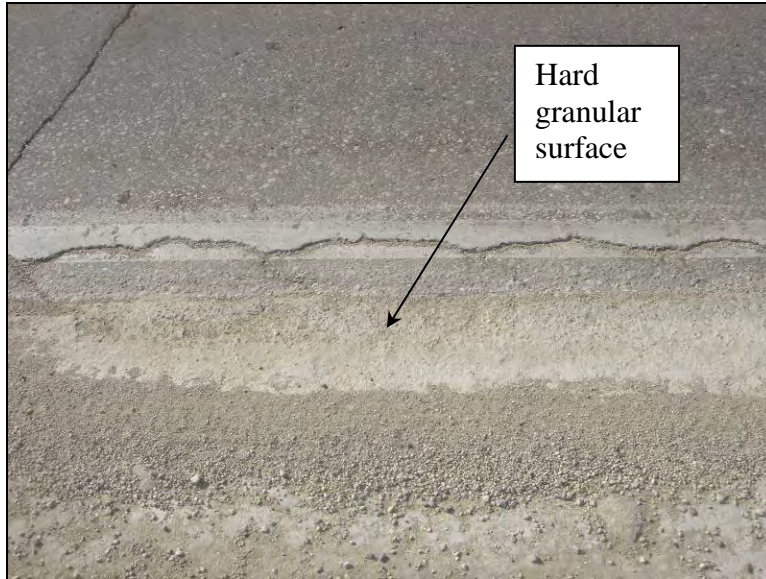


Figure 127. Hard granular surface formed seven days after construction, October 3, 2006



Figure 128. Development of wash boarding towards the end of the section (seven days after construction), October 3, 2006

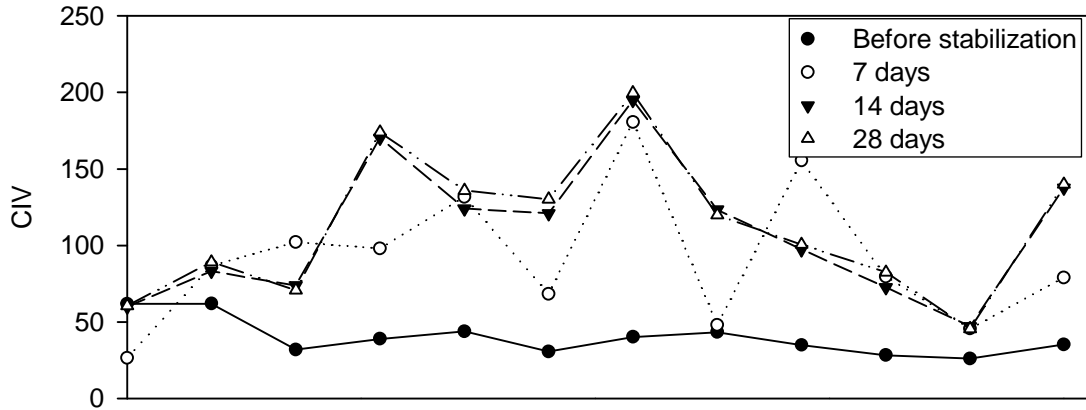


Figure 129. Variation of CIV profile with time, 16th St. Ames, IA



Figure 130. Significant edge drop-off observed after four months on 16th St. Ames, IA, December, 2007



Figure 131. Three-inch edge drop-off adjacent to pavement after eight months, May 18, 2007

Summary and Conclusions for Test Section No. 4

- The westbound shoulder on 16th St. in Ames, IA was undergoing edge drop-off and erosion.
- Portland cement was selected to stabilize the shoulder.
- A 200 ft. long by 1.5 ft. wide by 0.5 ft. deep test section was mixed and compacted with water and 10% portland cement.
- The first 100 ft. section performed adequately, and a hard cemented granular surface was observed. Wash boarding and erosion were observed along the second 100 ft.
- The difference in the performance of the test section can be attributed to a nonuniform mix or insufficient moisture for the hydration process in the second 100 ft.
- CIV profiles demonstrated significant improvement in the strength properties of the test section after 7 and 14 days. No additional strength was measured after 28 days.
- Edge drop-offs were observed along the stabilized area after four months from reconstruction.
- After eight months, the edge drop-off further progressed to a depth of about 3 in.
- Cement stabilization improved the strength properties of the shoulder section; however, edge drop-off development and erosion were not mitigated.

Recommendations for Test Section No. 4

- Laboratory testing should be performed to measure the durability of cement-stabilized granular material. Freeze-thaw, wet-dry, and vacuum saturation tests are the recommended laboratory tests.
- Increasing the depth of the stabilized layer as well as the cement and water contents are some simple methods that may further improve the shoulder section's performance.
- Improving the mixing procedure, increasing the moisture content, and allowing for curing time may enhance the shoulder's performance.

Test Section No. 5: Fly Ash, Highway 34, Batavia, IA

Site Description

The problem shoulder sections were located near Batavia, IA, on Highway 34. The shoulder section on the east side of Batavia had a crushed limestone granular layer, while on the west side the base course consisted of a blend of 50% recycled asphalt pavement and 50% recycled concrete. The granular layer thickness was a nominal 6 in.

The subgrade supporting the crushed limestone layer was a clay paleosol layer with high plasticity and high in situ moisture content, about 25% (Figure 132). The shoulder sections were experiencing severe rutting under traffic loadings, as shown in Figure 133 and Figure 134. At one location, the rut depth ranged from 5 to 7 in.

DCP tests were conducted at several locations along the shoulder section to determine the CBR values of both the shoulder limestone layer and underlying subgrade layer. The results are shown in Figure 135. The CBR values of the granular and subgrade layer are about 13 and 6, respectively.

Elevation profiles were obtained at two locations along the shoulder section. The elevations were determined using a rod placed at the edge of the pavement and leveled with the pavement elevation, as shown in Figure 136. Shoulder elevations were collected every 3 in. relative to the pavement. The results, which are shown in Figure 137, indicate that the slopes of both locations are similar to the 4% specified by Iowa DOT.



(a) Clay paleosol layer underlying granular layer



(b) Clay material rolled into thin thread

Figure 132. Subgrade material, September 22, 2005



Figure 133. Severe rutting at the shoulder section, Milepost 207.8-90' Westbound, September 22, 2005



Figure 134. Closer image of the shoulder rutting shown in Figure 133, September 22, 2005

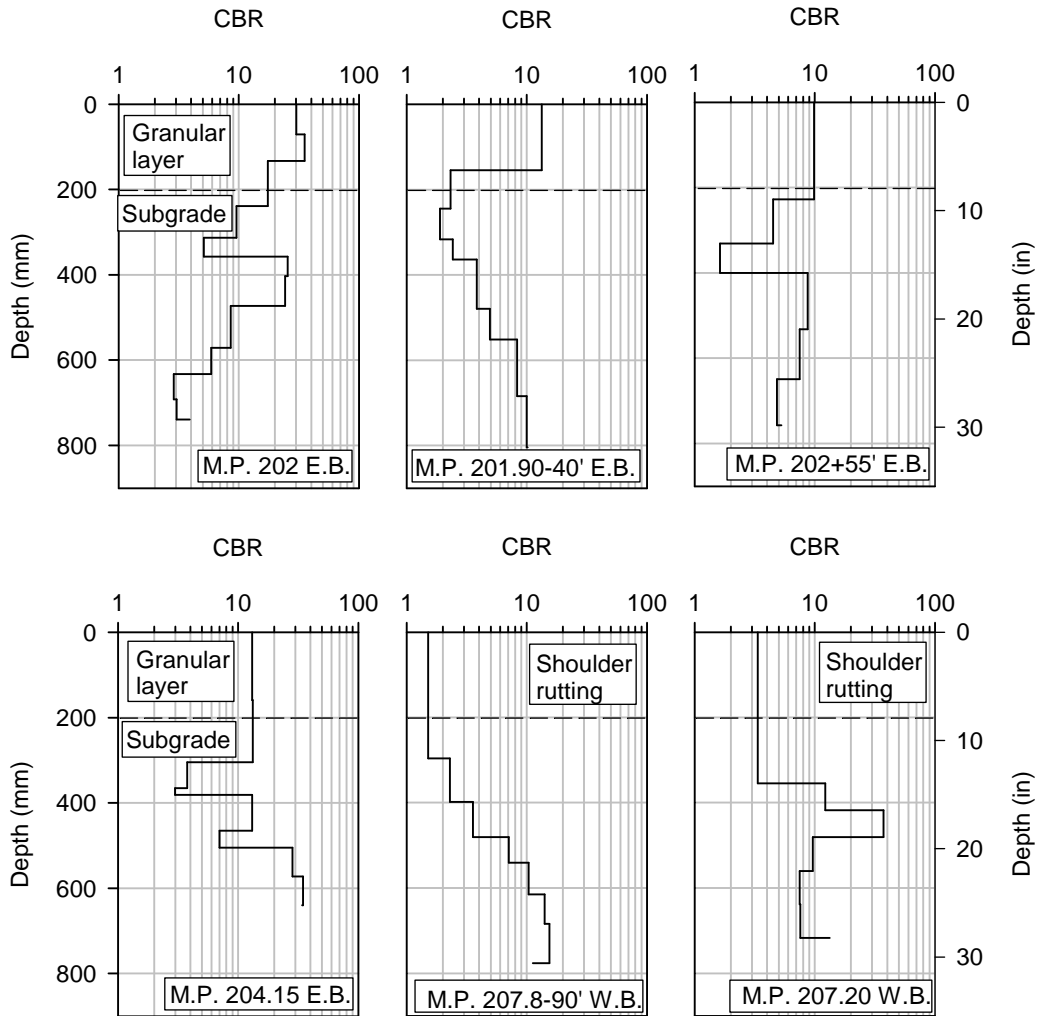


Figure 135. Summary of CBR values collected at Highway 34, September 22, 2005



Figure 136. Determining shoulder elevations relative to the pavement, September 22, 2005

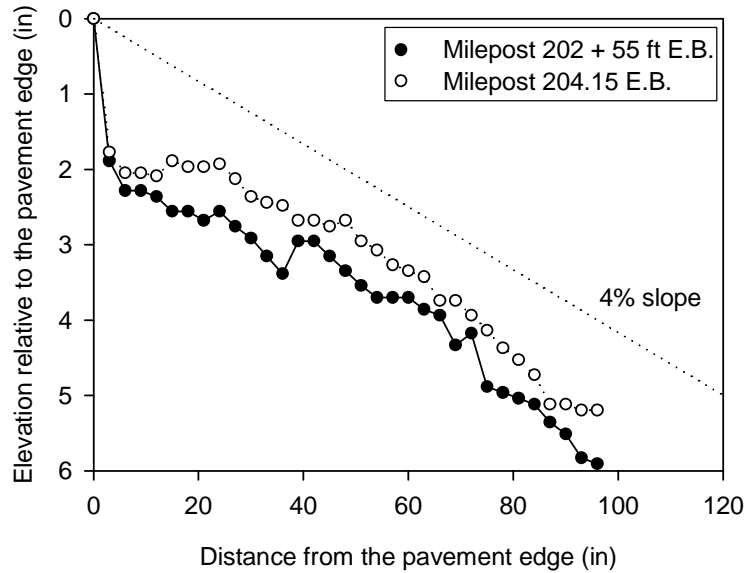


Figure 137. Elevation profiles relative to the pavement edge, September 22, 2005

Laboratory Study

A laboratory study was conducted to classify and stabilize the subgrade material. Class C fly ash from the Ottumwa Generating Station (OGS) was selected as the stabilization agent for the subgrade. This power plant is located near Chillicothe, IA, which is close to the project site. The objective was to develop a mix design with UCS 100 psi.

Chemical Analysis (X-Ray Diffraction and X-Ray Fluorescence)

A chemical analysis consisting of X-Ray diffraction (XRD) and X-Ray fluorescence (XRF) testing was first conducted. XRD was used to characterize the crystalline materials in the clay; XRF was conducted to quantify elements in both the clay and the fly ash. The results of XRD testing indicate that the clay material was composed mainly of kaolinite and traces of illite and quartz (Figure 138). The XRF results show that there was a high percentage of silica and alumina in both the clay and the fly ash. The clay material has small percentages of iron, calcium, and potassium oxides. The fly ash has high percentage of calcium oxide and relatively small percentages of magnesium, iron, and sodium oxides (Table 14).

Soil Analysis

A grain size distribution analysis was conducted on the subgrade and granular materials (Figure 139). The subgrade clay material was classified as CH (fat clay with sand; A-7-6). The granular material was classified as GW (well-graded gravel; A-1-a). The engineering properties of the soils are shown in Table 15.

pH Test

It is important to raise the pH of the clay-fly ash mixture to approximately 11.5 to form silicate/aluminate gel (Heebink and Hassett 2001). This gel reacts with calcium in the presence of water to form calcium-silicate/aluminate, which is a cementitious material that increases the soil strength. Therefore, a pH test was conducted using a pH meter instrument to determine the pH of the clay soil stabilized with varying percentages of fly ash (Figure 140). The tests were conducted at 2% fly ash increments. The results, which are shown in Figure 141, indicate that the pH peaked at 18% fly ash.

Fly Ash Set Time

Fly ash set time testing was conducted to determine the initial and final set time for the fly ash. The initial set time is the time at which the rate of strength gain starts to increase rapidly. Approximately 54g of water ($w=27\%$) was added to 200g of fly ash and mixed thoroughly to form a paste. The paste was next placed in a shallow brass dish, and strength gain with time was measured using a pocket penetrometer (Figure 142). When the pocket penetrometer read 4.5 tsf, the test was terminated, indicating that the fly ash reached the final set time. The test was carried out for three batches (Figure 143). The results show that the OGS fly ash has an initial and a final set time of approximately 15 and 20 minutes, respectively. This is considered a relatively fast-setting fly ash.

Unconfined Compressive Strength

To stabilize the subgrade material, fly ash was added and mixed with the clay material at 5%, 10%, 15%, and 20% (based on dry soil weight). Nine ISU 2x2 samples were prepared for the different fly ash contents (for a total of 36 samples) with a compaction delay of 30 minutes. For 5% and 10% fly ash, six total blows were used to compact the samples. The compaction energy was similar to that of a standard Proctor sample. For 15% and 20% fly ash, the soil-fly ash mixture was drier; therefore, 8 total blows were used to compact the samples. The samples were then divided into three groups. The first group was cured for 7 days at 100° F to simulate 28-day strength, while the second group was cured for 7 days at 100° F followed by vacuum saturation prior to testing. Figure 144 and Figure 145 show the vacuum saturation test. The third group of samples was cured for 7 days at 70° F.

UCS was measured to determine the optimum binder content to achieve 100 lb./in², which is believed to be sufficient strength for stabilizing the shoulder section (Figure 146). The results of the UCS tests are shown in Figure 147. The highest compressive strengths measured were for the samples cured at 100° F for 7 days. Vacuum saturating the samples prior to testing resulted in strength reduction of approximately 30%. The results also indicate that strength increases with increasing fly ash content. The addition of 20% fly ash resulted in an average compressive strength of 114 psi. Twenty percent fly ash was selected as the optimum binder content for stabilizing the subgrade material.

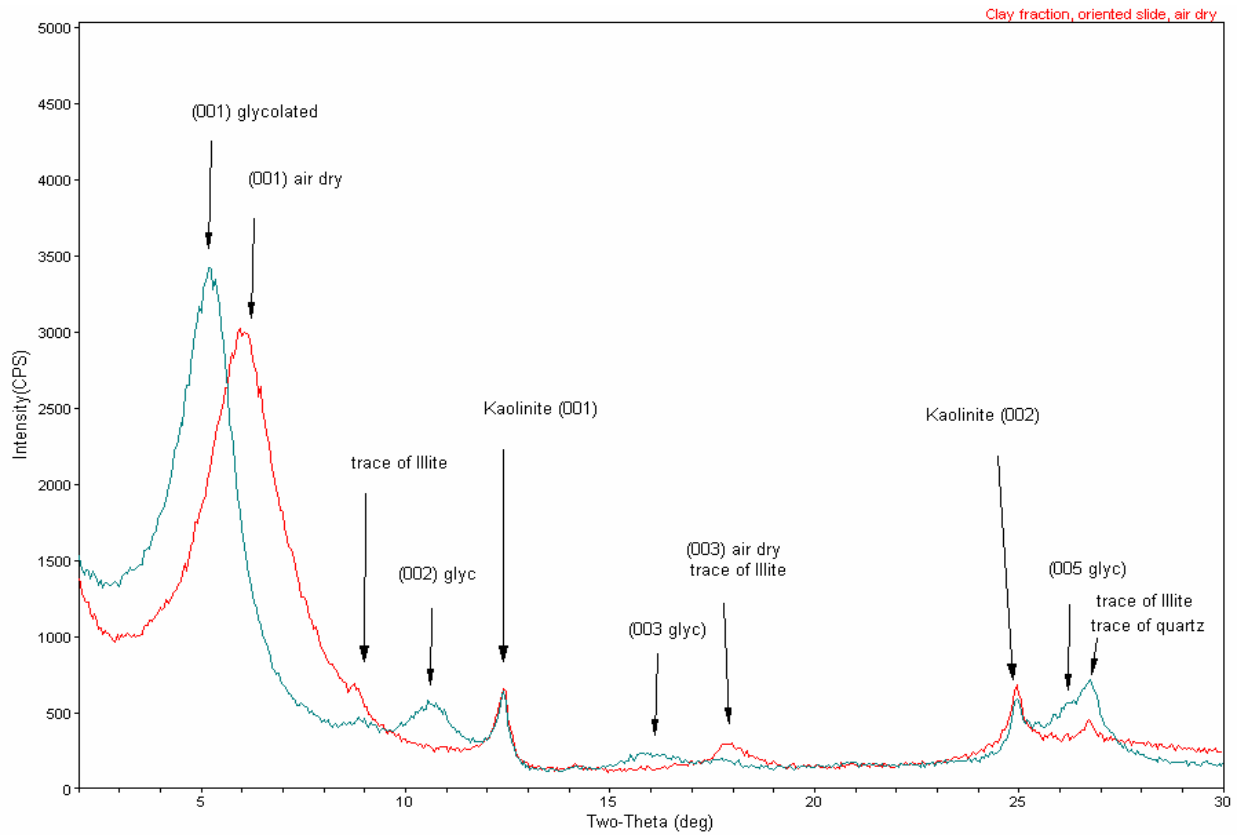


Figure 138. Results of XRD for the clay material

Table 14. Chemical composition of the clay and OGS fly ash materials

Sample description	Moisture (%)	Na ₂ O (%)	MgO (%)	Al ₂ O ₃ (%)	SiO ₂ (%)	SO ₃ (%)	K ₂ O (%)	CaO (%)	Fe ₂ O ₃ (%)
Clay	4.74	0.69	0.71	10.57	75.28	0.02	1.31	1.19	3.46
OGS Fly ash	0.06	2.50	5.51	18.61	34.48	2.35	0.43	25.98	5.44

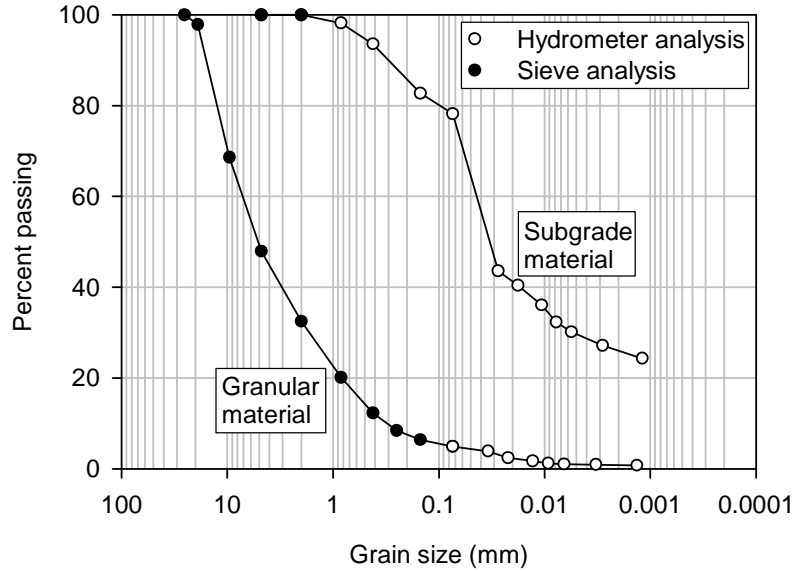


Figure 139. Grain size distribution of the clay subgrade material, Highway 34, Batavia, IA

Table 15. Engineering properties of the subgrade and granular materials

Material	D ₁₀	D ₃₀	D ₆₀	%P _{#4}	%P _{#200}	LL	PI	Classification		Field moisture content (%)
								USCS	AASHTO	
Clay subgrade	-	0.006	0.04	100	78	50	32	CH	A-7-6	20
Granular layer	0.3	1.7	7.2	48	5	-	-	GW	A-1-a	20

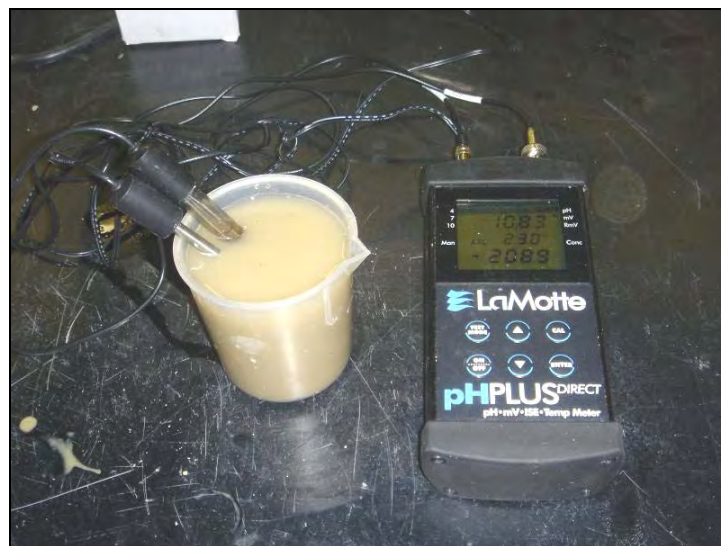


Figure 140. pH meter used to determine the pH of stabilized clay

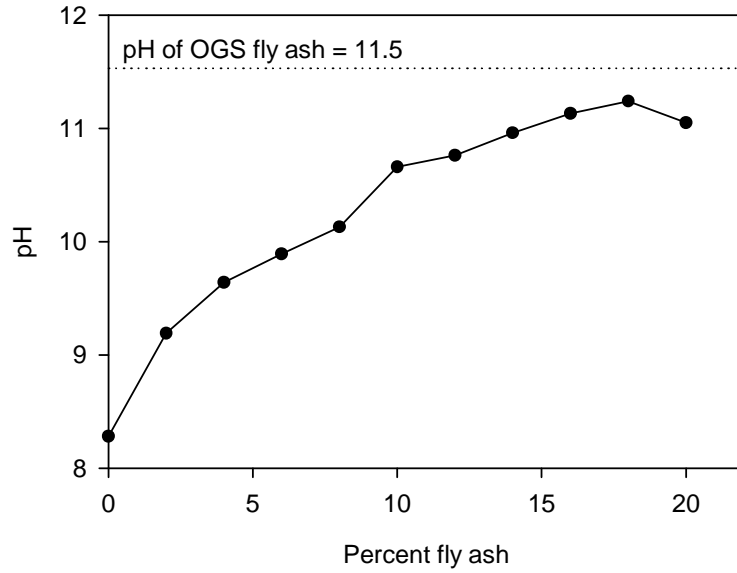


Figure 141. Results of the pH test conducted for the subgrade clay mixed with varying percentages of fly ash



Figure 142. Fly ash set time testing

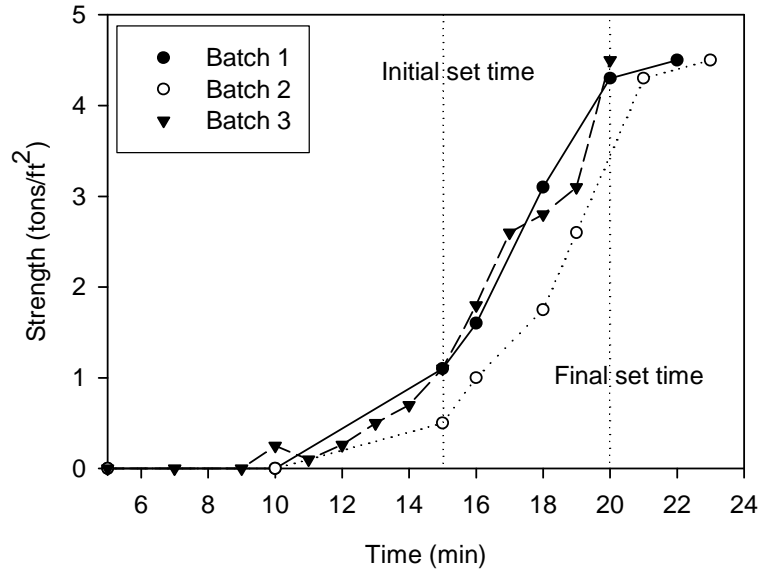


Figure 143. Results of fly ash set time for three batches



Figure 144. Vacuum saturation apparatus

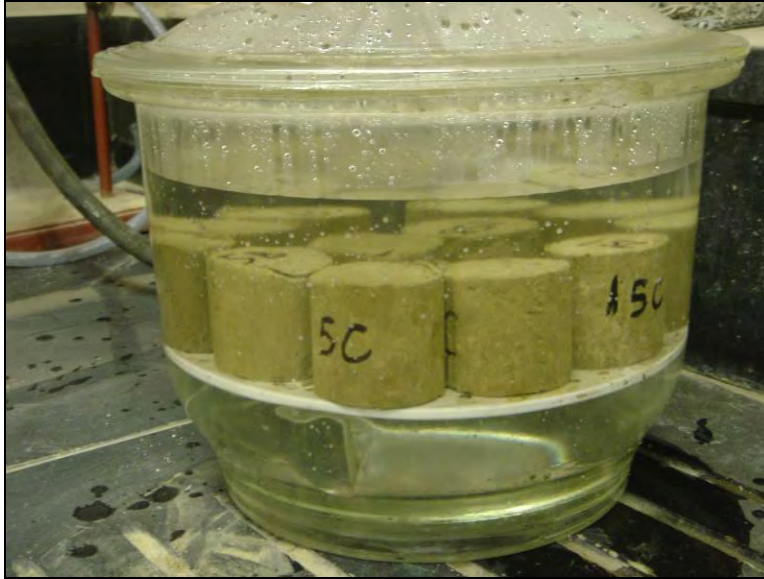


Figure 145. Stabilized samples under saturation for one hour



Figure 146. Unconfined compression test

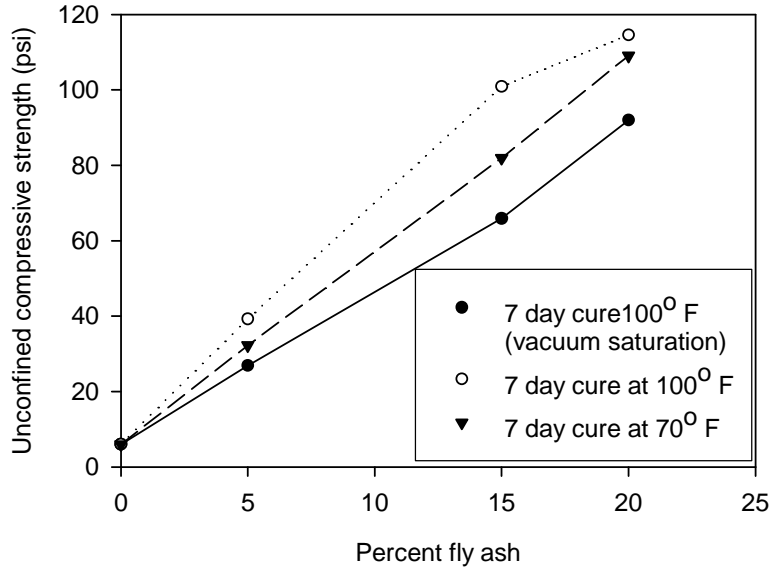


Figure 147. Unconfined compressive strength after seven-day cure

Shoulder Reconstruction

Reconstruction of the 8 ft. wide shoulder along the westbound lane of Highway 34 started on October 31, 2005. The upper 6 in. of crushed limestone were windrowed using a motor grader. Some of the limestone rock was contaminated by the subgrade clay. A semi trailer bottom dump truck spread the fly ash on top of the subgrade layer (approximately 15% to 20%) (Figure 148). The top 12 in. of the subgrade were mixed with fly ash using a full-depth road reclaimer, as shown in Figure 149. Water was added using a water truck, as shown in Figure 150, to increase the moisture content of the mix. Next, a pad foot roller was used to compact the stabilized mix. No time was allowed for the mixture to cure. The crushed limestone was recovered using a motor grader and compacted using a smooth wheel roller (Figure 151 and Figure 152). No additional limestone rock was added. Some locations along the shoulder section were left unstabilized for control groups.



Figure 148. Semi trailer bottom dump truck spreading fly ash on top of subgrade layer, October 31, 2005



Figure 149. Mixing fly ash with subgrade soil using a road reclaimer, October 31, 2005



Figure 150. Water truck used to increase moisture content of clay-fly ash mixture, October 31, 2005



Figure 151. Motor grader used to recover windrowed aggregate, October 31, 2005



Figure 152. Smooth wheel roller used to compact the crushed limestone layer, October 31, 2005

Field Monitoring

The shoulder section was continuously monitored to document strength gain and to detect signs of distress or rut development. The monitored section extended approximately 2.85 miles (from milepost 207.80 to 204.95).

DCP tests were conducted immediately after shoulder stabilization was completed and at 1, 7, and 12 months after reconstruction. The DCP test results, which are shown in Figure 153, were conducted at the stabilized sections at 3.0 and 6.0 ft. away from the pavement edge. Tests conducted within the stabilized area showed an increase of the CBR values in the upper 12 in. after 1 month. The CBR values increased after 7 months at only three locations (M.P. 207.80, M.P. 207.75, and M.P.207.10). The CBR value at one location (M.P. 205.05) did not increase with time at both 3 and 6 ft. from the pavement edge, which may be attributed to a nonuniform clay-fly ash mix along the monitored section. However, the value was still higher than the CBR measured at the same milepost in the unstabilized region (16 ft. from the pavement edge). After 19 months, CBR values determined from DCP tests increased in the upper 12 in. at all locations except milepost 207.20, where the CBR value was similar to the value measured after 12 months. The average CBR values for the upper 8 in. of the clay layer at 3 and 6 ft. from the pavement edge are summarized in Table 16. The results indicate an increase in average CBR with time except at one location (milepost 207.20), where the CBR value decreased after one year. At the other locations, small increases were measured from 7 to 12 months. The calculated CBR values continued to increase after 19 months. Most of these increases, however, occurred in the granular layer (upper 8 inches). Additionally, no considerable increase was noted at mileposts 207.10 and 207.20 at 6 ft. from the pavement edge.

DCP tests were also conducted outside the stabilized area at 16 ft. from the pavement edge. All CBR values were between 2 and 6, which were significantly lower than those measured within the stabilized area after 7 months (Figure 154). This indicates that the recommended stabilization procedure was successful in improving the strength of the soft shoulder section.

Plate load tests were performed at both the stabilized and control sections after 7 months to determine the elastic modulus (E) of the granular layer. The tests were performed by applying a load on a 12 in. steel plate and measuring plate deflection using three linear variable differential transducers. A total of eight tests were conducted: five tests at stabilized locations and three tests at control sections (Figure 155). The results show that the E values calculated for the first and second load cycles (E_{R2}) were higher for the stabilized sections than for the control sections (Table 17). On average, E was 319 and 98 psi for the stabilized and control sections, respectively, while E_{R2} was 951 and 291 psi for the stabilized and control sections, respectively. The results indicate that the stabilized sections have a stiffer response and therefore can withstand higher traffic loads with less shoulder deformation.

The plate load tests were repeated at the stabilized sections after one year from reconstruction. No tests were conducted at the control sections because they were undergoing fly ash stabilization during the time of inspection. The results, shown in Figure 156, indicate that the E and E_{R2} values increased at all test sections. For example, at milepost 207.75, E increased from 462 to 583 psi, whereas E_{R2} increased from 925 to 1,269 psi. After 19 months, the monitored sections continued to gain strength, as evidenced by the higher E values. On average, E measured after 19 months increased by about 20% over that measured at 12 months. Since the CBR values calculated from DCP tests after 19 months increased mainly in the upper 8 in., the increase in E can be attributed to the stiffening of the granular layer. Table 18 summarizes the E values measured at the stabilized sections after 7, 12, and 19 months.

Figure 158 shows the transition from a stabilized to a control section after one month from reconstruction. The rut depth for the stabilized section was significantly lower. Similarly, Figure 159 shows the rut depth after 7 months. The measured rut depth was about 0.2 and 6 in. for the stabilized and control sections, respectively. When subjected to heavy truck loading, the stabilized off-ramp on Highway 34 showed no rutting, demonstrating adequate performance (Figure 160). The monitored sections were performing adequately after 19 months from reconstruction (Figure 161).

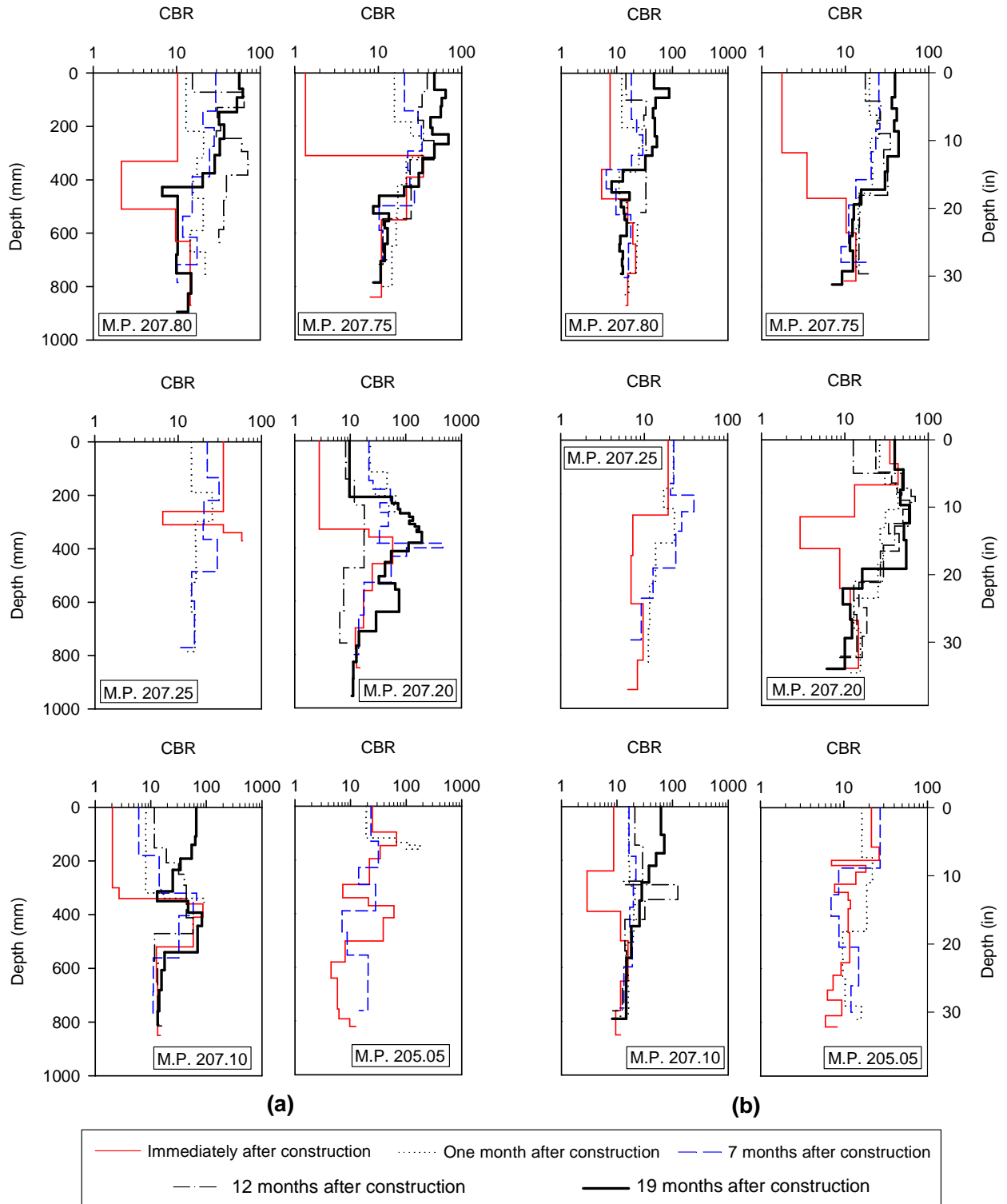


Figure 153. DCP test results with time at (a) 3.0 ft. and (b) 6.0 ft. from pavement edge

Table 16. Average CBR value with time in the upper 8 in.

		After	1	7	12	19
	Milepost	reconstruction	month	months	months	months
CBR (%)	207.80	10	13	27	35	30
(3.0 ft.	207.75	1	16	18	35	52
from	207.25	35	15	25	-	-
pavement	207.20	3	30	25	9	85
edge)	207.10	2	8	7	13	30
	205.05	38	19	26	-	-
	Average	15	17	21	23	49
CBR (%)	207.80	8	12	19	23	56
(6.0 ft.	207.75	2	21	22	21	37
from	207.25	16	21	22	-	-
pavement	207.20	35	29	30	27	28
edge)	207.10	9	16	17	23	28
	205.05	22	17	27	-	-
	Average	15	19	23	24	37

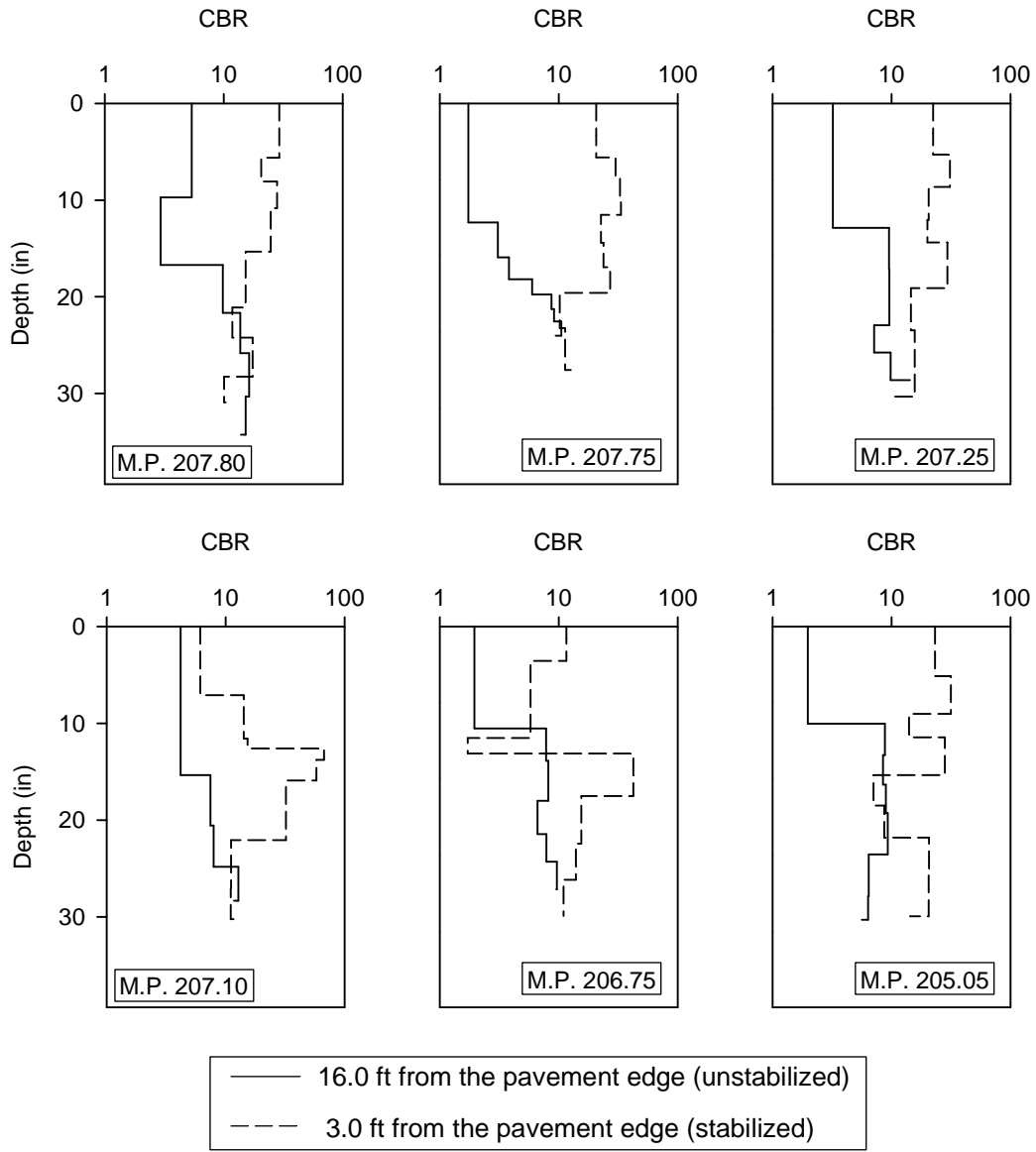


Figure 154. DCP test results after seven months, June 8, 2006

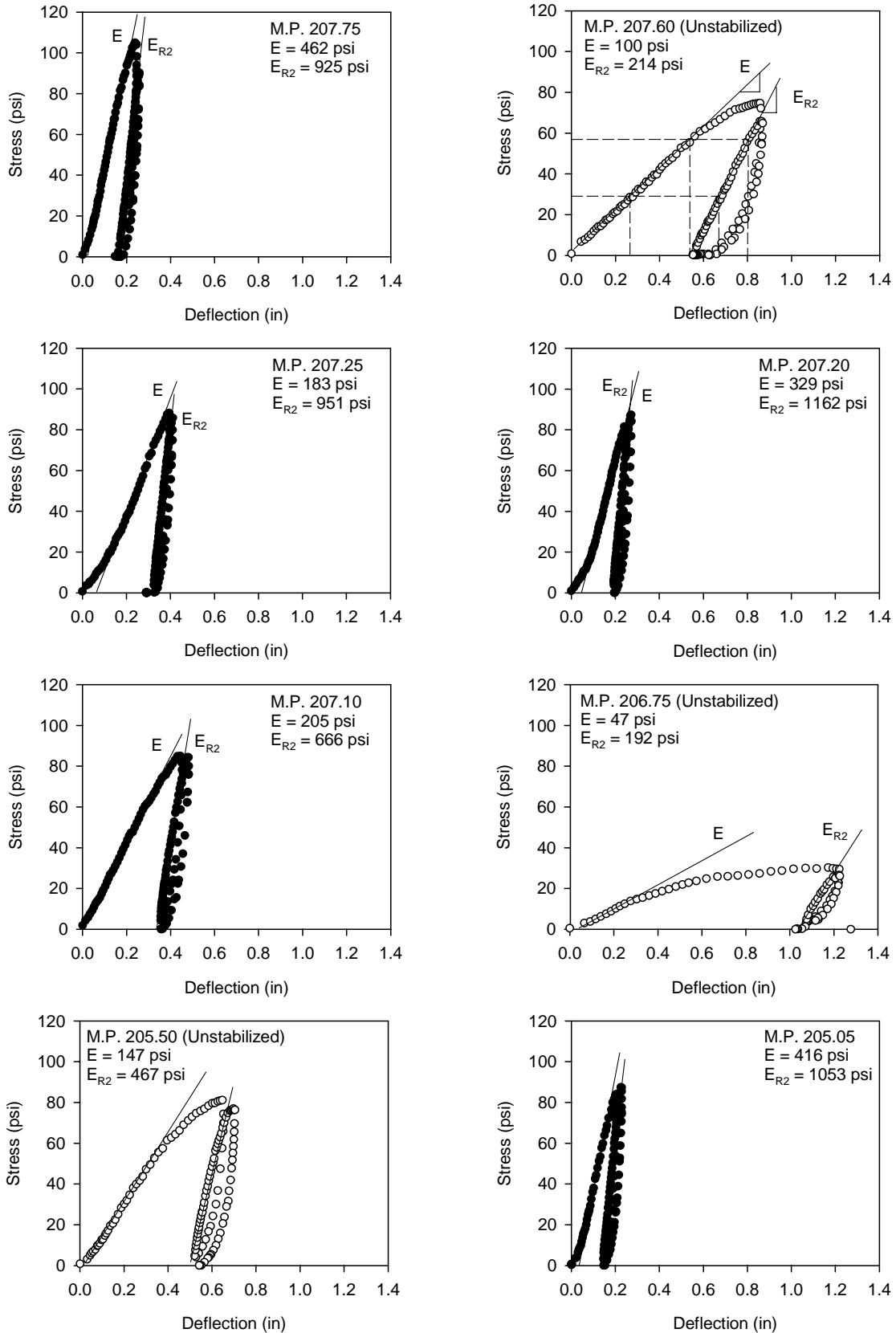


Figure 155. Plate load test results, June 8, 2006

Table 17. E values calculated for shoulder sections after seven months

Milepost	Description	E (psi)	E _{R2} (psi)
207.75	Stabilized	462	925
207.60	Control	100	214
207.25	Stabilized	183	951
207.20	Stabilized	329	1162
207.10	Stabilized	205	666
206.75	Control	47	192
205.50	Control	147	467
205.05	Stabilized	416	1053

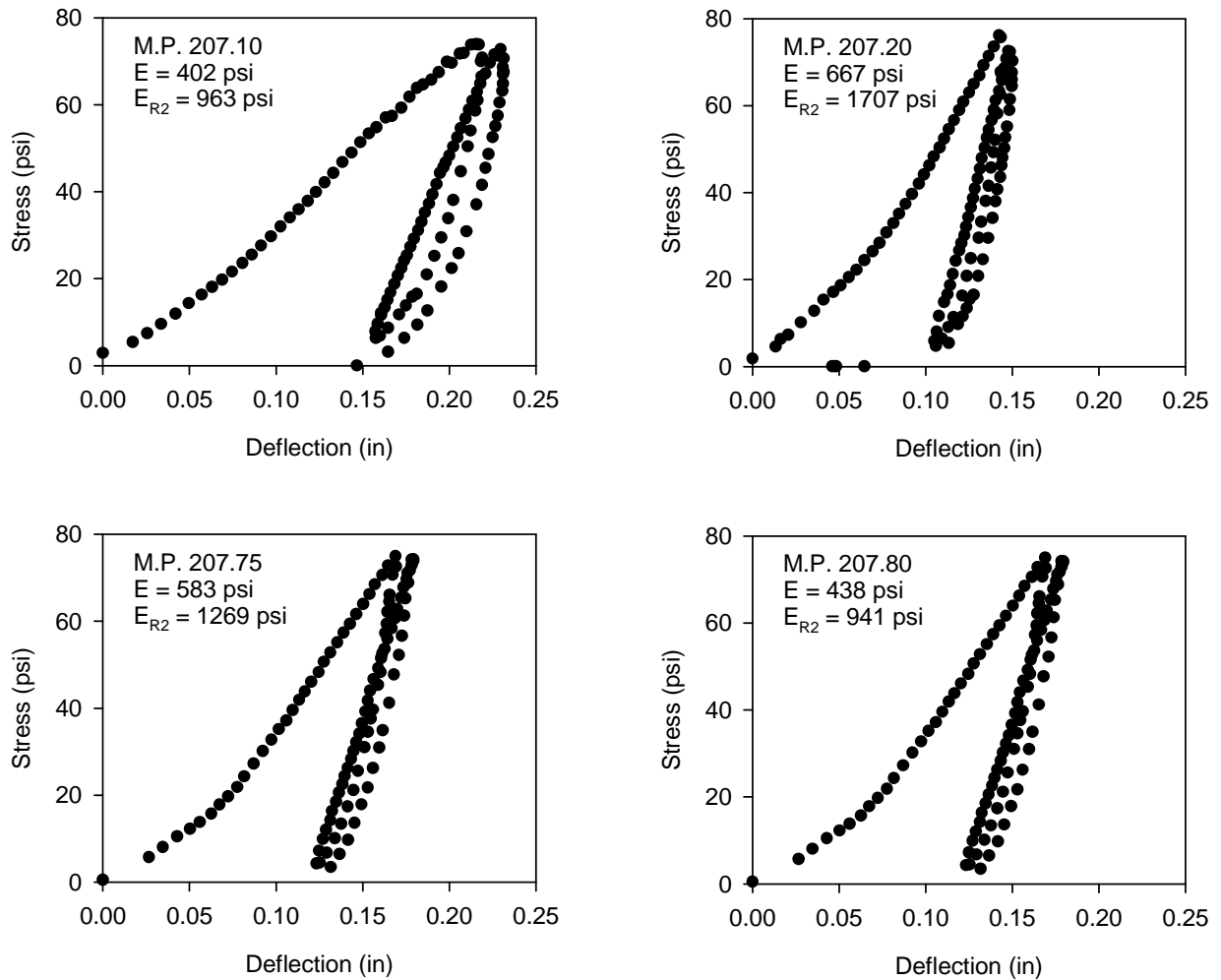


Figure 156. Plate load test results, October 10, 2006

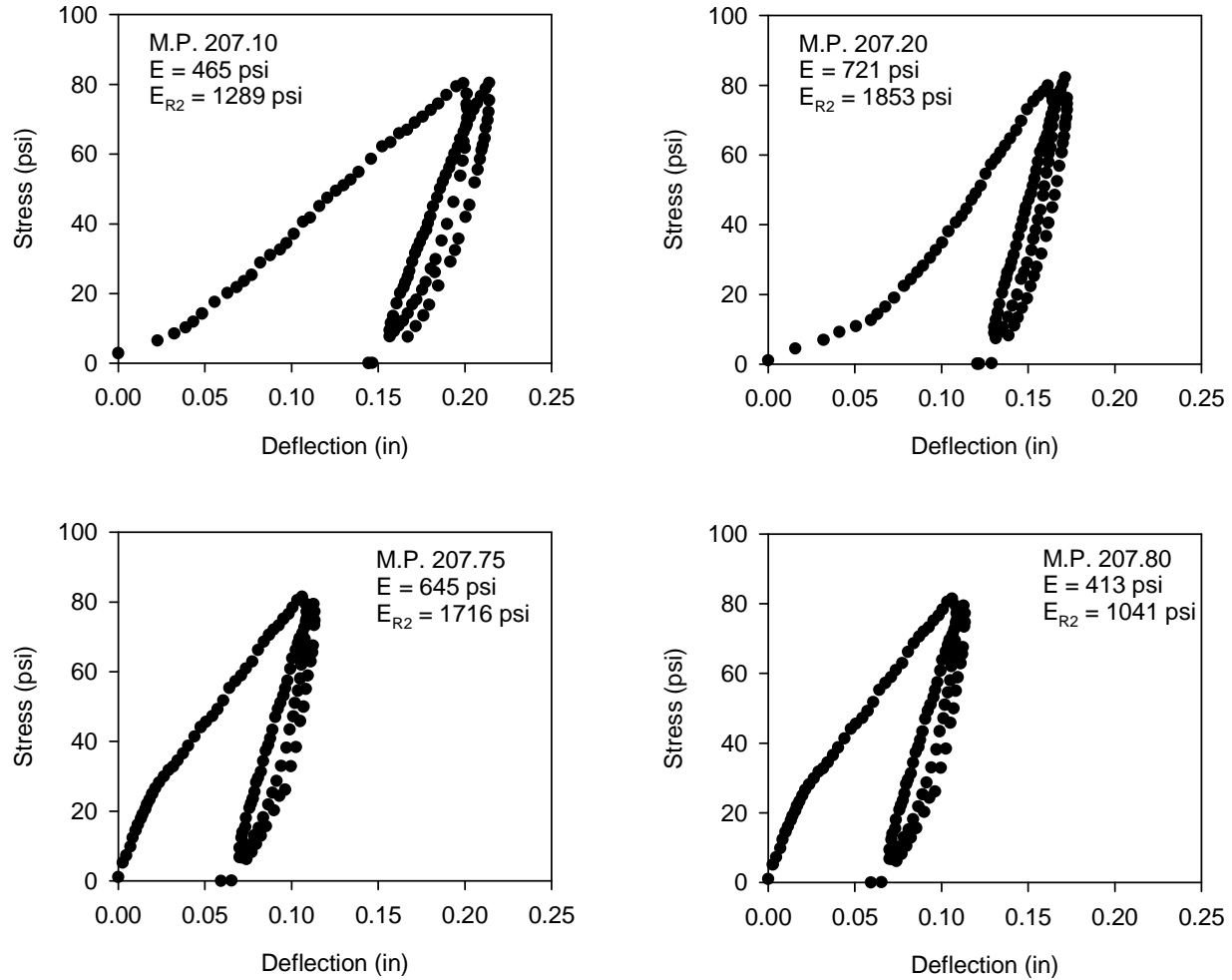


Figure 157. Plate load test results, May 4, 2007

Table 18. Summary of E values measured with time from shoulder reconstruction

Milepost	E (psi)					
	E			E _{R2}		
	7 months	12 months	19 months	7 months	12 months	19 months
207.75	462	583	645	925	1269	1716
207.20	329	667	721	1162	1707	1853
207.10	205	402	465	666	963	1289

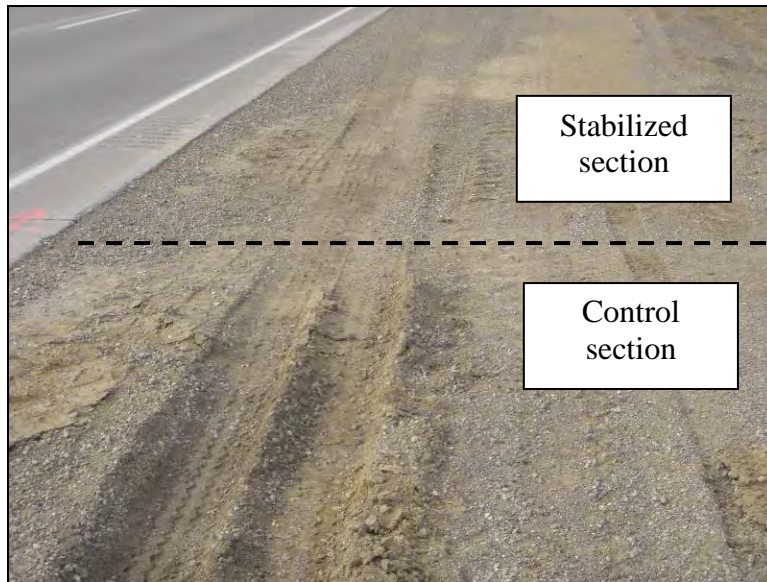
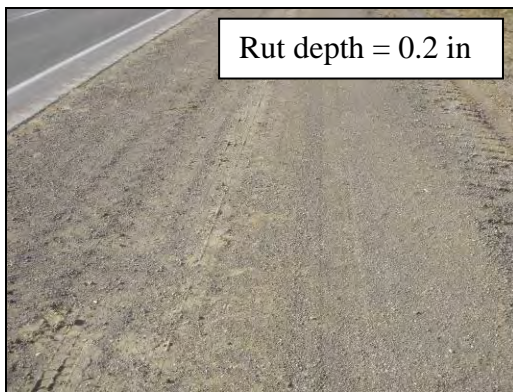
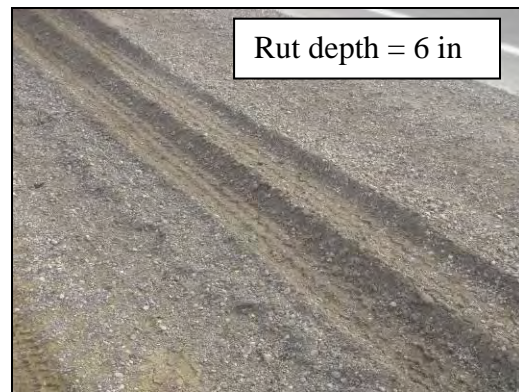


Figure 158. Higher rut depth observed along the control section after one month from shoulder reconstruction, November 23, 2005



(a) Stabilized



(b) Control

Figure 159. Performance of shoulder section after seven months, June 8 2006



Figure 160. Stabilized shoulder along the exit ramp showing no rut under heavy traffic load, June 8, 2006



(a) Milepost 207.80



(b) Milepost 207.20

Figure 161. No shoulder rutting observed after 19 months, May 14, 2007

New Shoulder at Highway 34 Bypass

The outside granular shoulder at station 410+50 ft. on the new Highway 34 bypass west of Batavia, IA, was inspected in October 2006. Visually, the section appeared to be in a suitable condition, as shown in Figure 162. No edge drop-off or shoulder rutting was observed. However, when the section was loaded using a Freightliner truck, pumping and rutting along the wheel paths was observed (Figure 163). Repetitive loading increased the rut depth. As shown in Figure 164, about 3 in. of rut developed along the wheel path after six truck passes.

Full-depth DCP tests were performed at 2, 6 and 12 ft. from the pavement edge (Figure 165). The results show that the CBR value in the upper 8 in. of crushed limestone varied from 6 to 12. The underlying earth shoulder fill layer had a CBR value of 4 to 10. The subgrade underlying the earth fill had a CBR value of 2 to 29. The section was inspected again in May 2007, and DCP tests were carried out at the same locations. The results demonstrate an improvement in the strength of the shoulder layer, as evidenced by the higher CBR values in the upper 8 in. However, the underlying earth shoulder fill and the subgrade layer continued to show low CBR values. Although this represents only one measurement location, if similar conditions exist at other locations, future maintenance problems from severe rutting may be a concern.



Figure 162. Newly constructed granular shoulder section, October 17, 2006

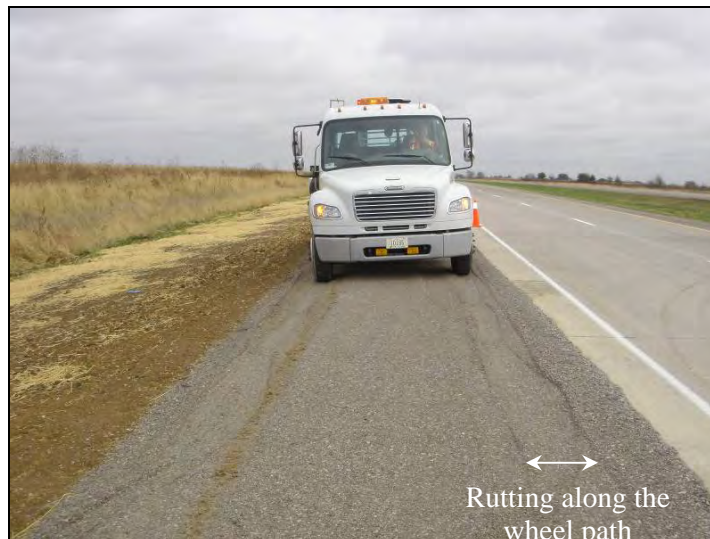


Figure 163. Shoulder rutting developed along wheel path with repetitive loading, October 17, 2006



Figure 164. About 3 in. of rut developed after six passes

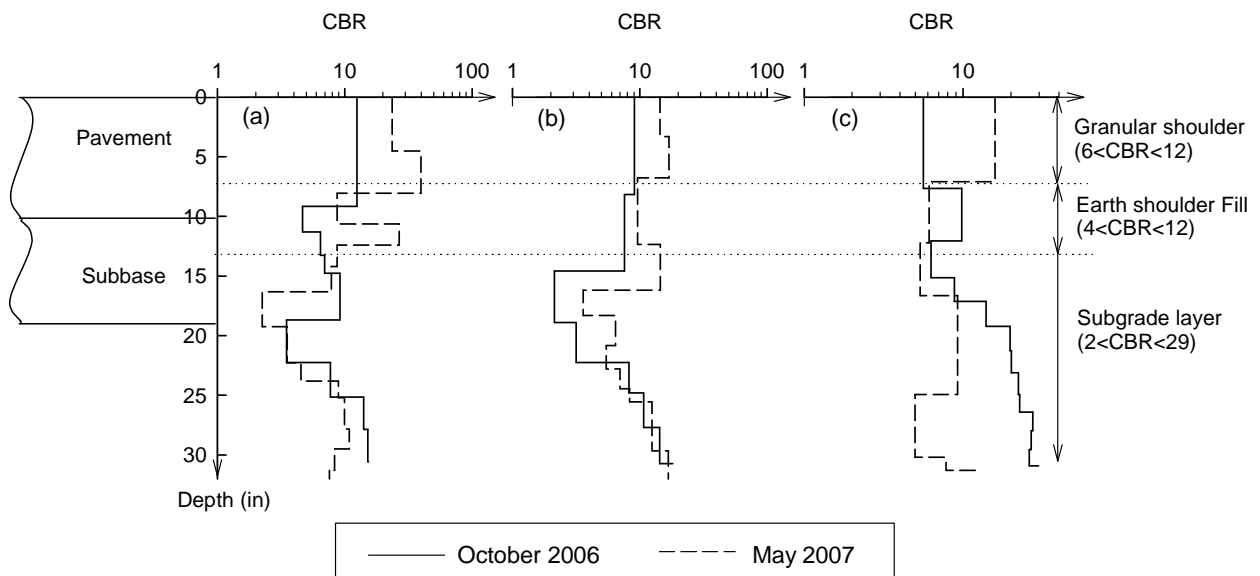


Figure 165. Results of DCP testing at (a) 3 ft., (b) 6 ft., and (c) 12 ft. from pavement edge

Summary and Conclusions for Test Section No. 5

- The shoulder section located on Highway 34 near Batavia, IA, was 8 miles long and 8 ft. wide. However, at most locations, the shoulder width exceeded 8 ft. The site was exhibiting severe rutting problems due to soft subgrade conditions.
- The subgrade material, which was classified as CH according to USCS and A-7-6 according to AASHTO classification, has a liquid limit of 50 and a plasticity index of 32, respectively. The material was clay Paleosol, typically encountered in the southeast region of Iowa.
- The CBR of the granular and subgrade layers was 10 and 2, respectively. Elevation profiles collected at two locations showed that the slopes are flatter than the Iowa DOT-specified 4%.
- The fly ash used was OGS class C fly ash from a power plant located near Chillicothe, IA. The fly ash has an initial and a final set time of 15 and 20 minutes, respectively.
- XRD results show that the clay material consists mainly of kaolinite and traces of illite and quartz. The XRF test shows a high percentage of silica and alumina in both the clay and the fly ash.
- According to pH test results, 16% to 20% fly ash was required to raise the pH of the soil-fly ash mixture to the desired pH value (11.5).
- Stabilizing the clay with 20% fly ash resulted in an unconfined compressive strength of 114 psi after seven-day curing at 100° F. Vacuum saturating the samples resulted in a strength reduction of 30%.
- The shoulder section was reconstructed by windrowing the upper 6 in. of crushed limestone and mixing 15% to 20% class C fly ash with the upper 12 in. of the subgrade clay. The mix was compacted using a pad foot roller, and the limestone was reclaimed and compacted using a smooth wheel roller.
- DCP tests demonstrated an increase in CBR values with time. All stabilized sections showed higher CBR values than the unstabilized sections.
- Plate load tests showed that the stabilized sections have much higher E value than the control sections. Further, E values measured after one year were significantly higher than those measured after 7 months. After 19 months, CBR and E values increased relative to the values measured after 12 months.
- Preliminary testing conducted at the new Highway 34 bypass revealed low CBR values for the underlying earth shoulder fill and subgrade layers.
- Fly ash stabilization was successful in improving both the short- and long-term performance of the shoulder section.

Recommendations for Test Section No. 5

- The shoulder section should continue to be monitored to document the effect of freeze-thaw cycles on section performance.
- Fly ash stabilization techniques can be implemented at other sites suffering from similar conditions (i.e., a weak subgrade layer). The percentage of fly ash and the repair procedure, however, may vary depending on the site characteristics.

Test Section No. 6: Geosynthetic Stabilization, Highway 218, Nashua, IA

Site Description

The inside granular shoulders on Highway 218 near Nashua, IA, were experiencing severe rutting due to soft subgrade conditions (Figure 166a). The problematic shoulder section extended a distance of about 6 miles (between mileposts 224 and 218). A field investigation was conducted to identify and isolate soft regions that needed repair. This was achieved by driving a fully loaded dump truck (47,040 lb.) over the shoulder section and then measuring the rut depth at pre-identified locations along the wheel path (Figure 166b), conducting CIV tests, and conducting DCP tests. Figure 167 shows profiles of rut depth and CIV with distance, starting from milepost 224. The figure shows that the region with highest rut depth and lowest CIV, indicating soft conditions, extends from milepost 220.85 to 219.60 (about 6,600 ft.). DCP tests conducted within this region show a weighted average CBR of 6 in the upper 8 in. and 5 at a depth between 8 and 20 in. (Figure 168).



(a) Rutting extending to the underlying clay layer



(b) Measuring rut depth inside the wheel path

Figure 166. Severe rutting along the inside shoulder, June 1, 2006

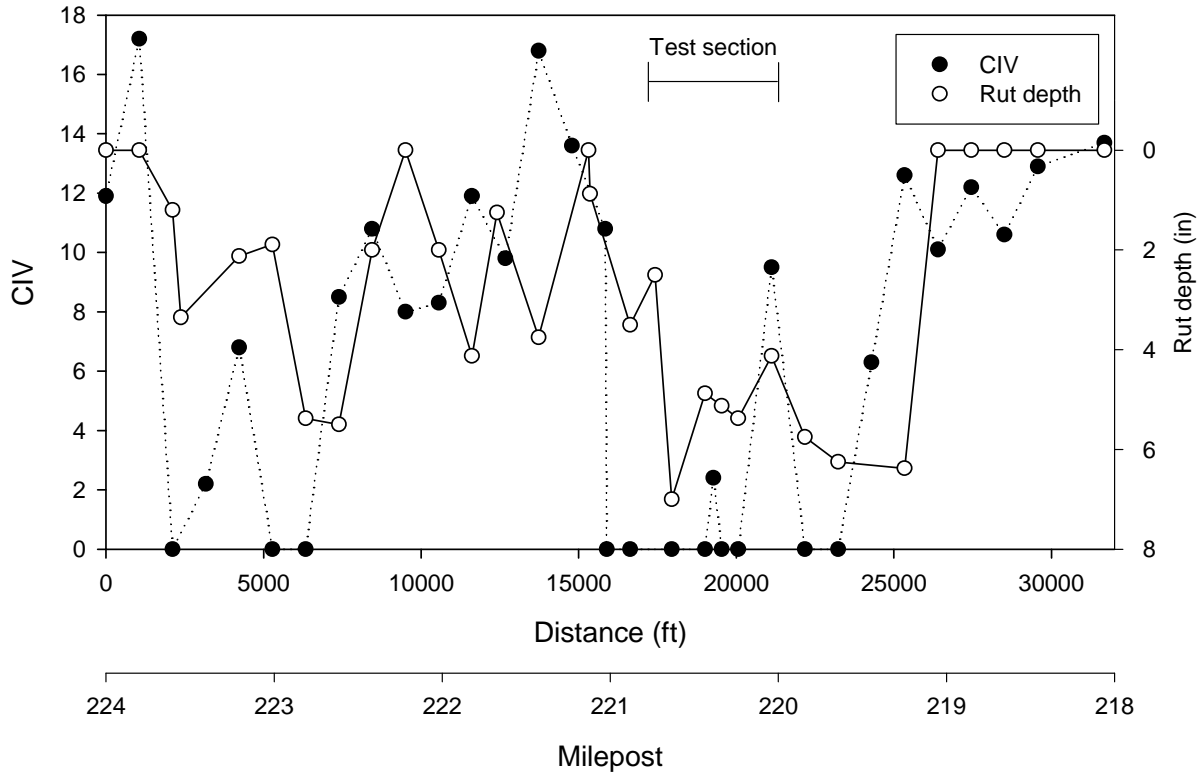


Figure 167. Profile of rut depth measured inside the wheel path and CIV measured at 2 ft. from pavement edge, June 1, 2006

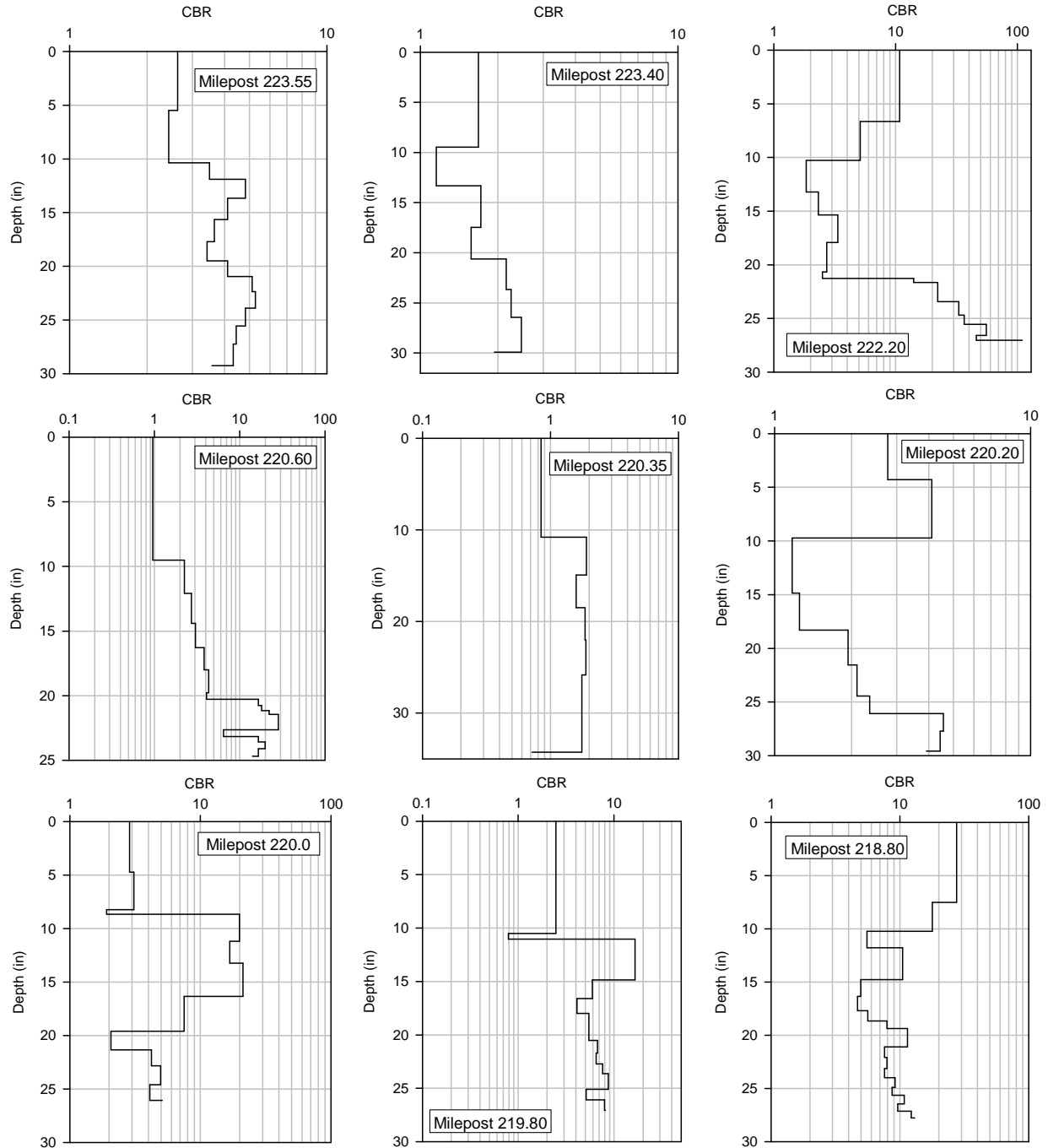


Figure 168. DCP results conducted at several locations along inside shoulder, June 1, 2006

Laboratory Study

A laboratory study was conducted to obtain the engineering properties of the subgrade and granular material (Table 19). The subgrade material was classified as SC (clayey sand; A-4). The granular material was classified as GW (well-graded gravel; A-1-a). The standard Proctor test showed that optimum moisture content and maximum dry density were 15% and 114 lb./ft³,

respectively. The in situ moisture contents and densities were determined at 14 locations along the section using driven cores, and these values were compared to the standard Proctor curve (Figure 169). The data show that in situ densities are lower than the standard Proctor curve, even in well performing sections. However, densities obtained between milepost 220.60 and 219.80 were significantly lower than the maximum dry density. Also, field moisture contents were significantly higher than the optimum moisture content.

Table 19. Engineering properties of subgrade and granular materials

Material	D ₁₀	D ₃₀	D ₆₀	C _u	C _c	%P ₂₀₀	%P _{#4}	LL	PI	USCS	AASHTO
Granular	0.75	2.9	6.1	8.12	1.8	4	52	-	-	GW	A-4
Subgrade	0.001	0.008	0.19	190	0.34	49	95	32	23	SC	A-1-a

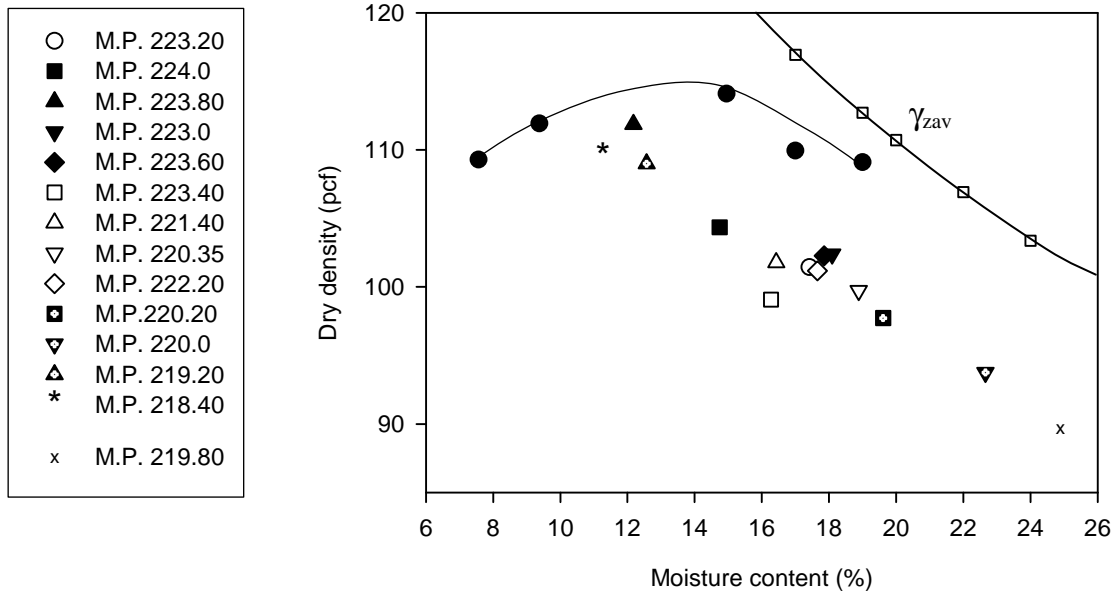


Figure 169. Moisture-density relationship for subgrade material

Field Reconstruction

Geogrid was selected to stabilize the shoulder section. Three geogrid types were selected: Tensar BX1200, BX1100, and BX4100. The purpose of using three geogrid types was to compare performance, as there are mechanical and cost differences between them (Table 20). For each test section, the geogrid was placed at the interface between the subgrade and a new 8 in. overlying crushed limestone layer. As shown in Figure 170, the test section was approximately 1,020 ft. long, extending from milepost 220.60 to 220.40, and was about 8 ft. wide. The first 200 ft. was a control section and was left unstabilized. Following the control section was a 328 ft. long section stabilized with BX1200 geogrid. Two sections, each 246 ft. long, followed the BX1200 section. These sections were stabilized with either BX1100 or BX4100.

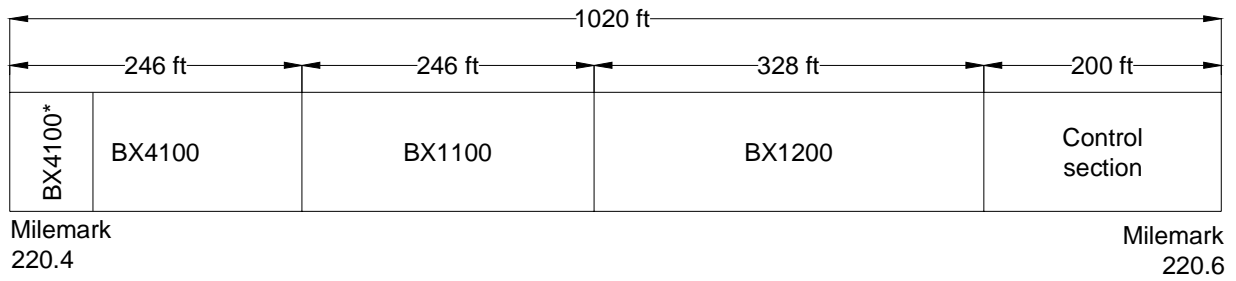
The existing granular layer was stripped and discarded because of its contamination with clay from the underlying subgrade layer. Figure 171 shows a motor grader removing the contaminated layer. About 500 tons of crushed limestone was delivered to the site and placed on the pavement adjacent to the test section (Figure 172). The subgrade was leveled using a skid loader and then compacted using a pneumatic roller (Figure 173 and Figure 174). Using a power saw, the geogrid pieces were cut to 8 ft. wide, as shown in Figure 175, to match the width of the stabilized area. The geogrids were rolled over the soft subgrade, starting with the BX1200 and then followed by the BX1100 and the BX4100. The geogrids were overlapped (about 2 ft. overlap) in the direction of spreading the aggregate. That is, 2 ft. of the BX1200 was placed over the BX1100, etc. (Figure 176 and Figure 177). Beyond approximately 1,000 ft, the BX1400 geogrid was damaged. The damage occurred during transportation of the geogrid to the site. The research group decided to install the defective grid without alteration to study the effect of improper geogrid installation. The damaged section is denoted by BX4100*. A motor grader and then a pneumatic roller were utilized to spread and compact the aggregate (Figure 178 and Figure 179). After placing the aggregate layer, it was observed that parts of the geogrids were not properly covered with aggregate (8 ft. away from pavement) and the edges of the BX1100 and BX4100 were exposed (Figure 180). The entire process of excavating the contaminated material, placing the geogrid, and placing and compacting the aggregate took approximately five hours, and upon construction completion the section was opened to traffic. Unlike some chemical stabilization, mechanical stabilization approaches using geogrid are fast to install and do not require curing time, which is a benefit for minimizing the disturbance to traffic.

Table 20. Mechanical properties and costs of the selected geogrids

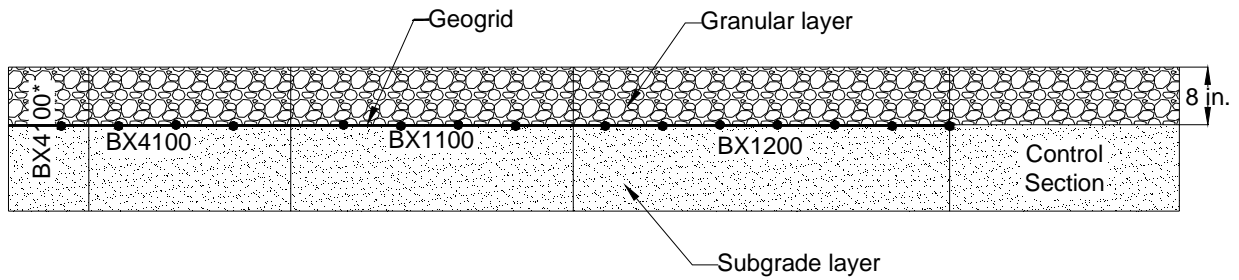
Geogrid	Aperture stability (Kg-cm/deg)	Aperture dimension (in.)		Cost per yd ² , installed (\$)
		MD ^a	XMD ^b	
BX 1200	6.5	1.0	1.3	3.50–3.75
BX 1100	3.2	1.0	1.3	2.50–2.75
BX 4100	2.8	1.3	1.3	1.50–1.75

^a MD: Machine direction

^b XMD: Cross machine direction



(a) Plan view



(b) Cross section

Figure 170. Proposed test sections



Figure 171. Motor grader removing the contaminated granular layer, June 23, 2006



Figure 172. Placing virgin aggregate next to the test section, June 23, 2006



Figure 173. Skid loader leveling the subgrade, June 23, 2006



Figure 174. Pneumatic roller used to compact the subgrade, June 23, 2006



Figure 175. Cutting the geogrids to 8 ft. wide sections, June 23, 2006



Figure 176. Rolling the BX 1200 geogrid over the soft subgrade layer, June 23, 2006



Figure 177. Overlapping geogrids in the direction of aggregate spreading, June 23, 2006



Figure 178. Spreading the new crushed limestone over the geogrid, June 23, 2006



Figure 179. Compacting the granular layer using a pneumatic roller, June 23, 2006



Figure 180. Exposed edges of the geogrid after construction was completed, June 23, 2006

Field Monitoring

An inspection was performed one month after the date of construction. About 5 in. deep ruts were observed in the control section, as shown in Figure 181. The stabilized sections showed no signs of rutting (Figure 182).

Plate load tests were conducted immediately after construction and then at 3 months and 10 months (Figure 183). Results measured immediately demonstrate that the highest E value for both the loading and reloading stages were measured at the section stabilized with the BX1200 geogrid. E was also slightly higher at the section stabilized with the BX1100 geogrid than at the section stabilized with the BX4100 geogrid (Figure 184). This may be attributed to the small difference in their aperture stability modulus (the aperture stability modulus of BX1100 and BX4100 are 3.2 and 2.8 kg-cm/degree, respectively). The lowest E and highest soil deflection values were measured at the control section. Plate load testing conducted after 3 months shows higher E values for all the geogrid sections, compared to the values measured immediately after construction (Figure 185). On average, E_{R2} increased by about 36%, 18%, and 42% for the BX1200, BX1100 and BX4100 sections, respectively. The increase in E with time can be caused by progressive lateral confinement of aggregate due to repetitive traffic loads. Further, as the section is loaded, the subgrade layer deforms, applying tension forces to the geogrid, which adds to the stability of the section. The E measured at the control section after 3 months (i.e., 50 ft. and 100 ft.) increased relative to the values measured immediately after construction. This is due

to the limestone rock that was added several weeks after construction to alleviate the rutting. Plate load test results obtained at 10 months show a reduced E for the control section and the BX1100 section (Figure 186). The average E was reduced by about 23% and 8% for the control and BX1100 sections, respectively. The reduction at the section stabilized with BX1100 geogrid may be attributed to partial exposure of the geogrid, reduction in the granular layer thickness, or the relative loosening of the granular layer after the freeze-thaw period. The sections stabilized with the BX1200 and the BX4100 geogrids continued to show an increase in E over time. At 10 months, the E values increased by 5% and 26% over the values measured at 3 months. Table 21 summarizes the plate load test results.

A comparison of plate load test results between Test Section Nos. 5 (fly ash stabilization) and 6 (geogrid) at stress levels between 30 and 50 psi reveals that fly ash stabilization resulted in a stiffer shoulder section, as evidenced by the higher E values and smaller deflections. Soil deflections measured at the stabilized area of Test Section No. 5 ranged from 0.1 to 0.7 in., while soil deflections measured at the stabilized areas of Test Section No. 6 ranged from 0.4 to 1.2 in., depending on the geogrid type.

For Test Section No. 6, CIV tests using a 44 lb. (20 kg) hammer were performed every 50 ft. to obtain a profile, as shown in Figure 187. The results show that the CIVs significantly increased immediately after installing the geogrids. CIV also increased at the control section as a result of compacting the subgrade during the geogrid installation procedure and adding virgin rock material. After 3 months, additional strength at the stabilized sections was observed, as indicated by the further increase in the CIVs. CIVs measured at the control section did not increase. There was no significant difference between the CIVs measured at the geogrid sections, even though the aperture stability modulus, and thus stiffness, varies for each geogrid type. It is possible that the CIVs for the 44 lb. Clegg hammer are influenced by a relatively shallow depth and thus are unable to detect degrees of confinement. At 10 months, CIVs were reduced in all the stabilized sections. Exposure of the geogrids and reduction in the granular layer thickness may be the reason behind this reduction.

CIV testing was also conducted using the 9.9 lb. (4.5 kg) hammer at 1, 3, and 8 ft. from the pavement edge (Figure 188). CIVs were performed every 50 ft. along the shoulder after 3 months. The highest CIVs were measured at 1 ft. from the pavement edge, where the granular layer was thickest. CIVs decreased with increasing distance from the pavement edge due to reduction in the granular layer thickness. The lowest CIVs were measured at 8 ft., which was just outside the stabilized area. Similarly to the CIVs measured using the 44 lb hammer, this lighter hammer did not differentiate between the geogrid types. Further, CIV tests conducted beyond 1,000 ft. revealed that the defective BX4100 geogrid did not improve the shoulder properties.

DCP tests were also conducted before stabilization and after 3 months (Figure 189). The results show an increase in the CBR values of the granular layer at all stabilized sections. For BX1200, the CBR increased from 3 to 18, while for the BX1100 and BX4100, the CBR values increased from 4 to 19 and from 3 to 15, respectively. There was no significant change in CBR values below the depth of the geogrid.

Parts of the defective BX4100 geogrid were exposed after 4 months from installation, as shown in Figure 190. The exposure was a result of severe rutting. As expected, improper installation of the geogrid reduced the effectiveness of the geogrid. At 10 months, additional geogrids were exposed. Figure 191 shows the exposed geogrids at the sections stabilized with BX1200 and BX1100. The exposed portions were about 8 ft. from the pavement edge, where the grids were overlaid by 1 to 2 in. of rock.



Figure 181. Development of shoulder rutting one month after shoulder construction, July 25, 2006



Figure 182. No rutting at the test section stabilized with BX1200, July 25, 2006

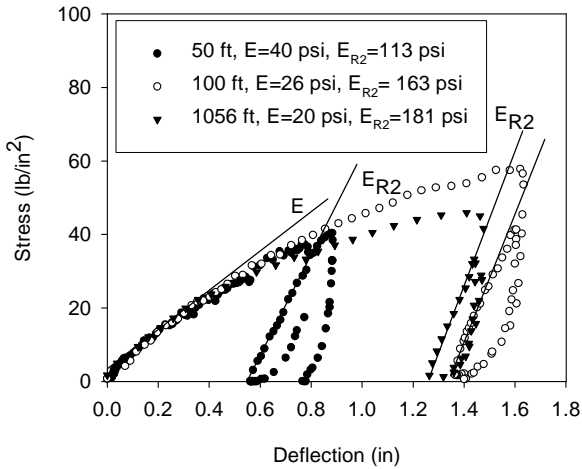


(a) Truck used as a reaction for performing the test

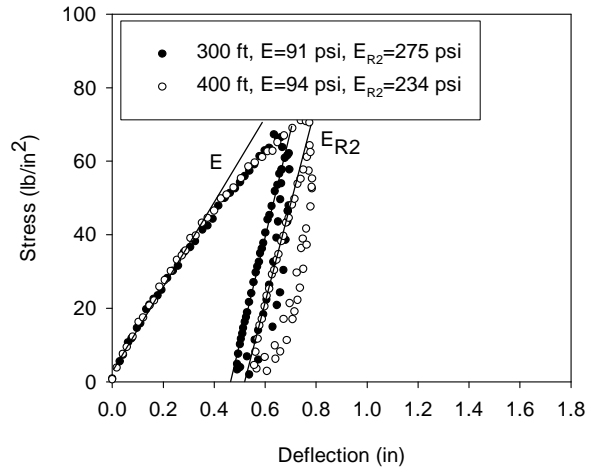


(b) Plate load test setup

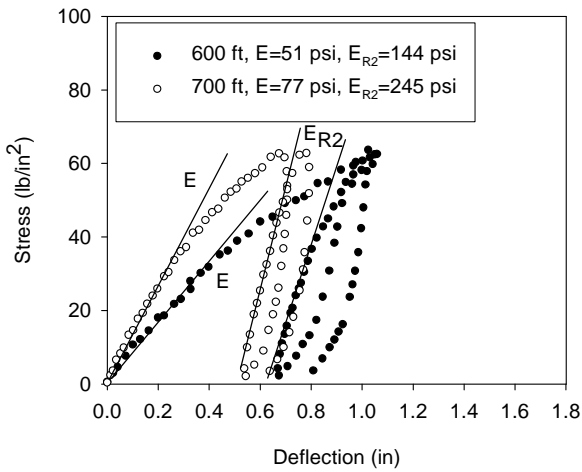
Figure 183. Plate load test conducted at the inside shoulder, July 25, 2006



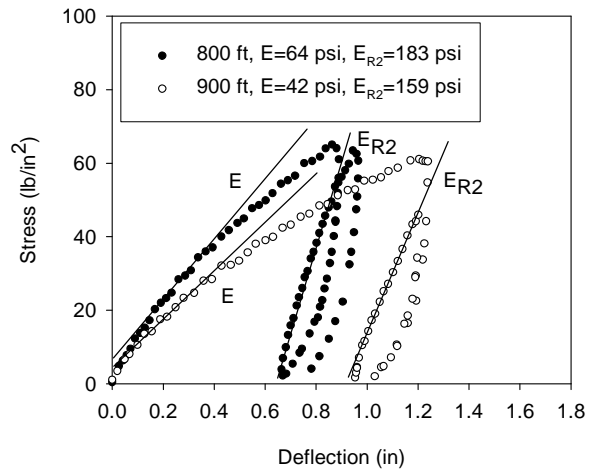
Control Section



BX1200

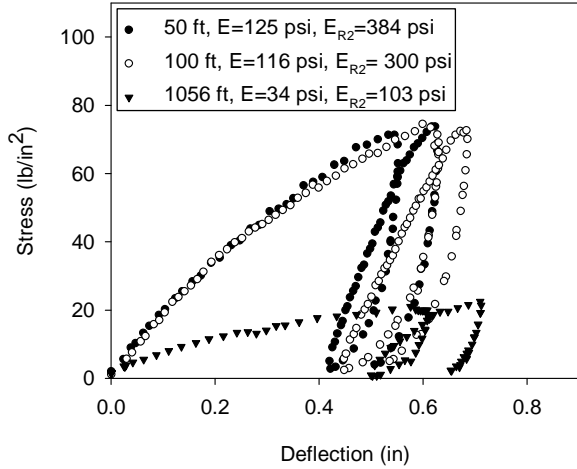


BX1100

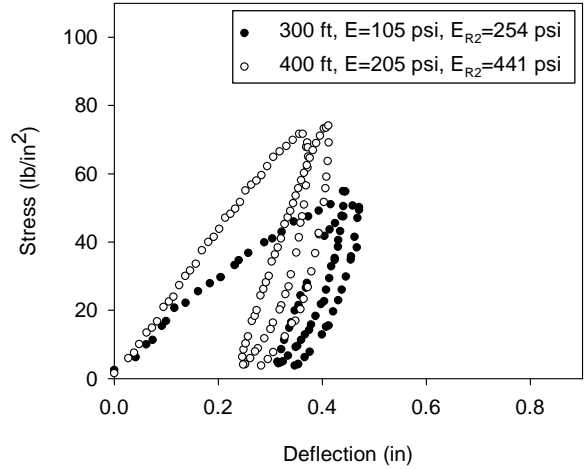


BX4100

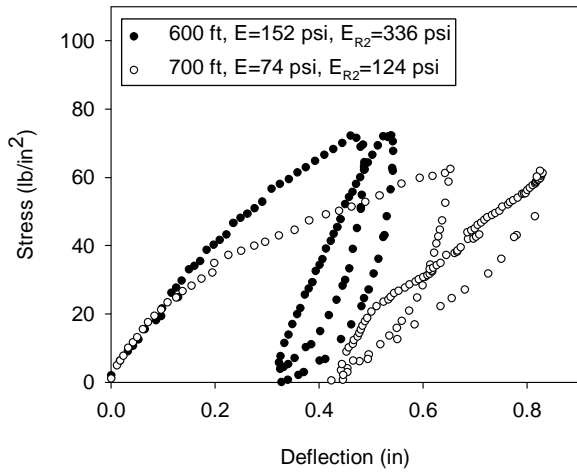
Figure 184. Plate load test results immediately after construction, June 23, 2006



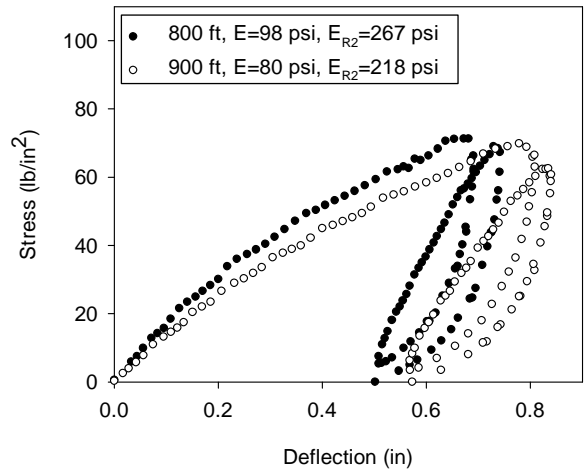
Control Section



BX1200

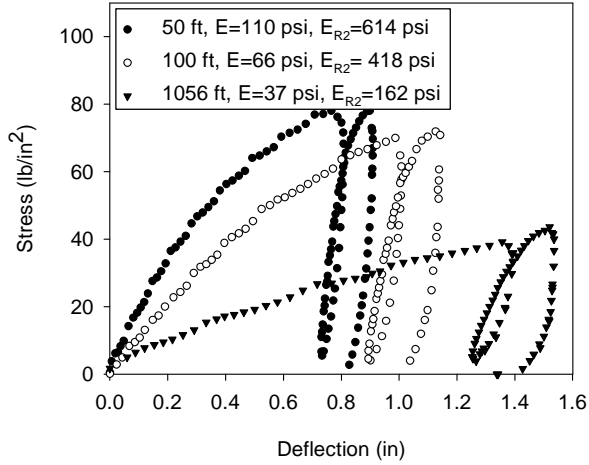


BX1100

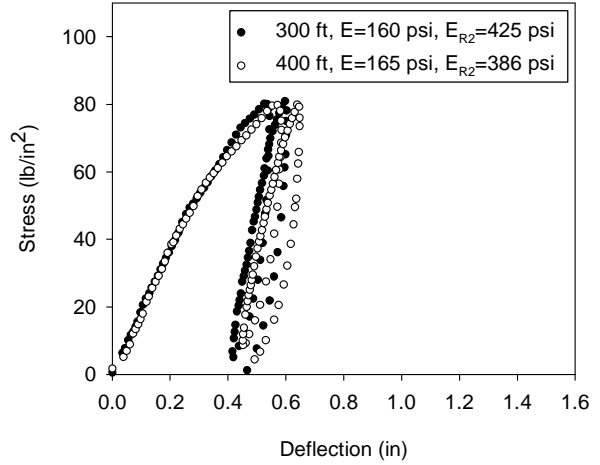


BX4100

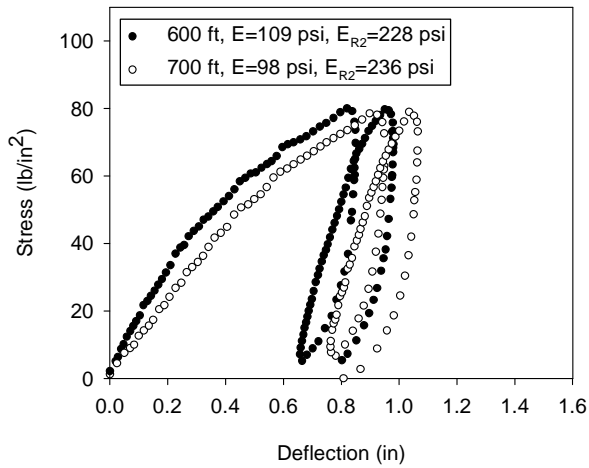
Figure 185. Plate load test results three months after construction, September 27, 2006



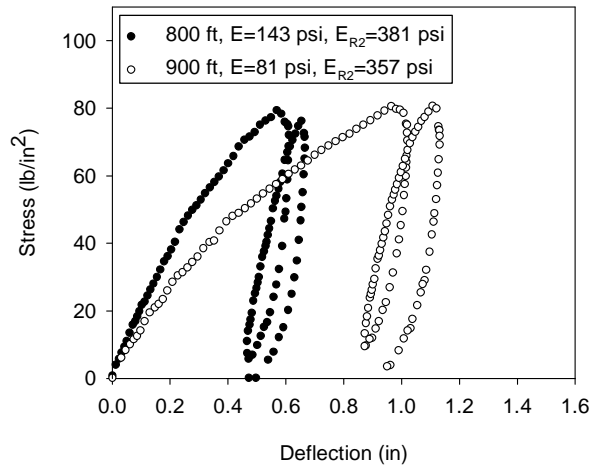
Control Section



BX1200



BX1100



BX4100

Figure 186. Plate load test results ten months after construction, April 17, 2007

Table 21. Summary of E values determined from plate load testing

Section	Distance (ft.)	After construction		3 months after construction		10 months after construction	
		E (psi)	E _{R2} (psi)	E (psi)	E _{R2} (psi)	E (psi)	E _{R2} (psi)
Control section	50	40	113	125	384	110	614
	100	26	163	116	300	66	418
	1,056	20	180	34	103	37	162
BX1200	300	91	275	105	254	160	425
	400	94	234	205	441	165	386
BX1100	600	51	144	152	336	109	228
	700	77	245	74	124	98	236
BX4100	800	64	183	98	267	143	381
	900	42	159	80	218	81	357

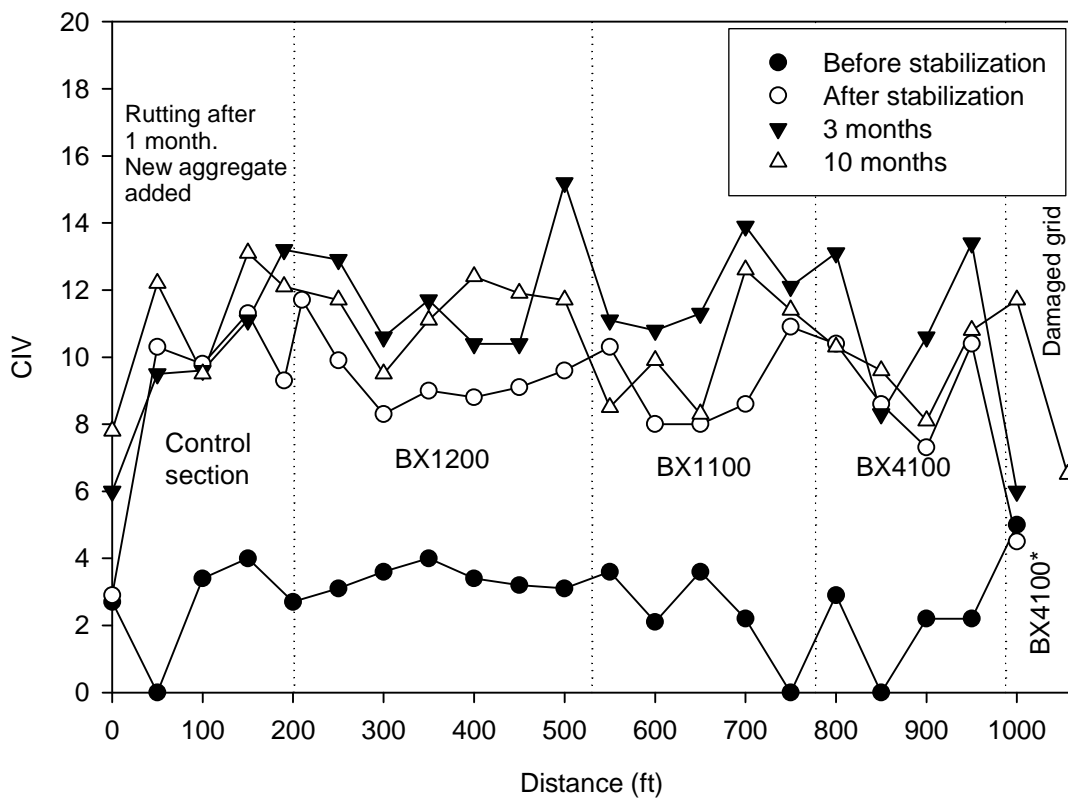


Figure 187. Profile of CIV with time

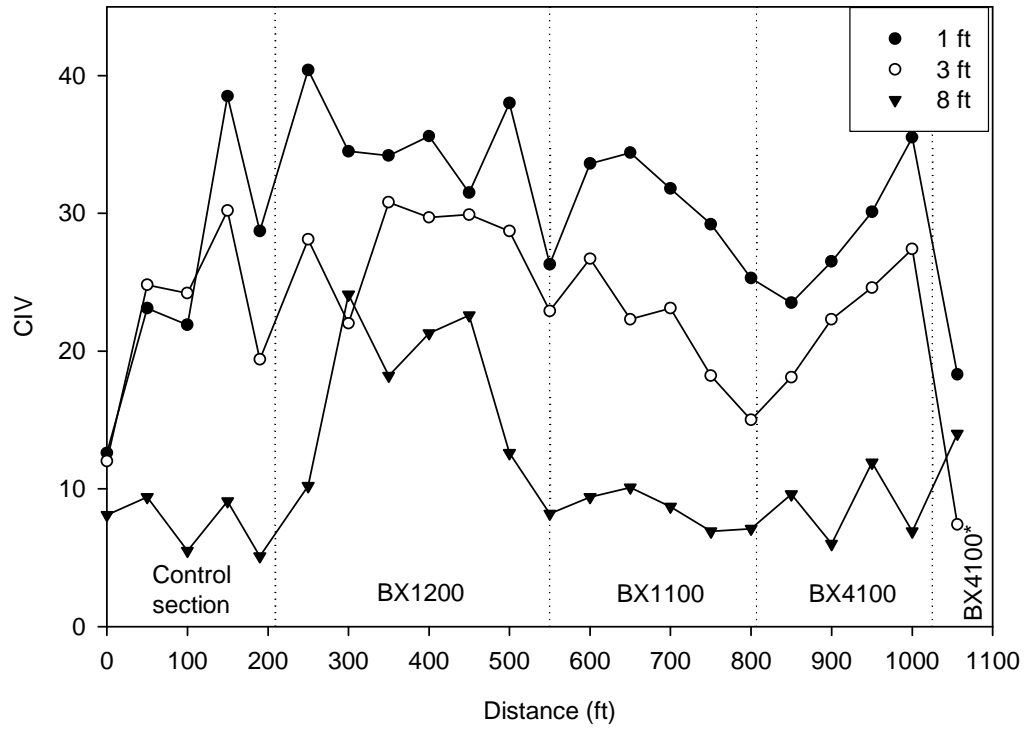


Figure 188. Profile of CIV with distance from the pavement edge

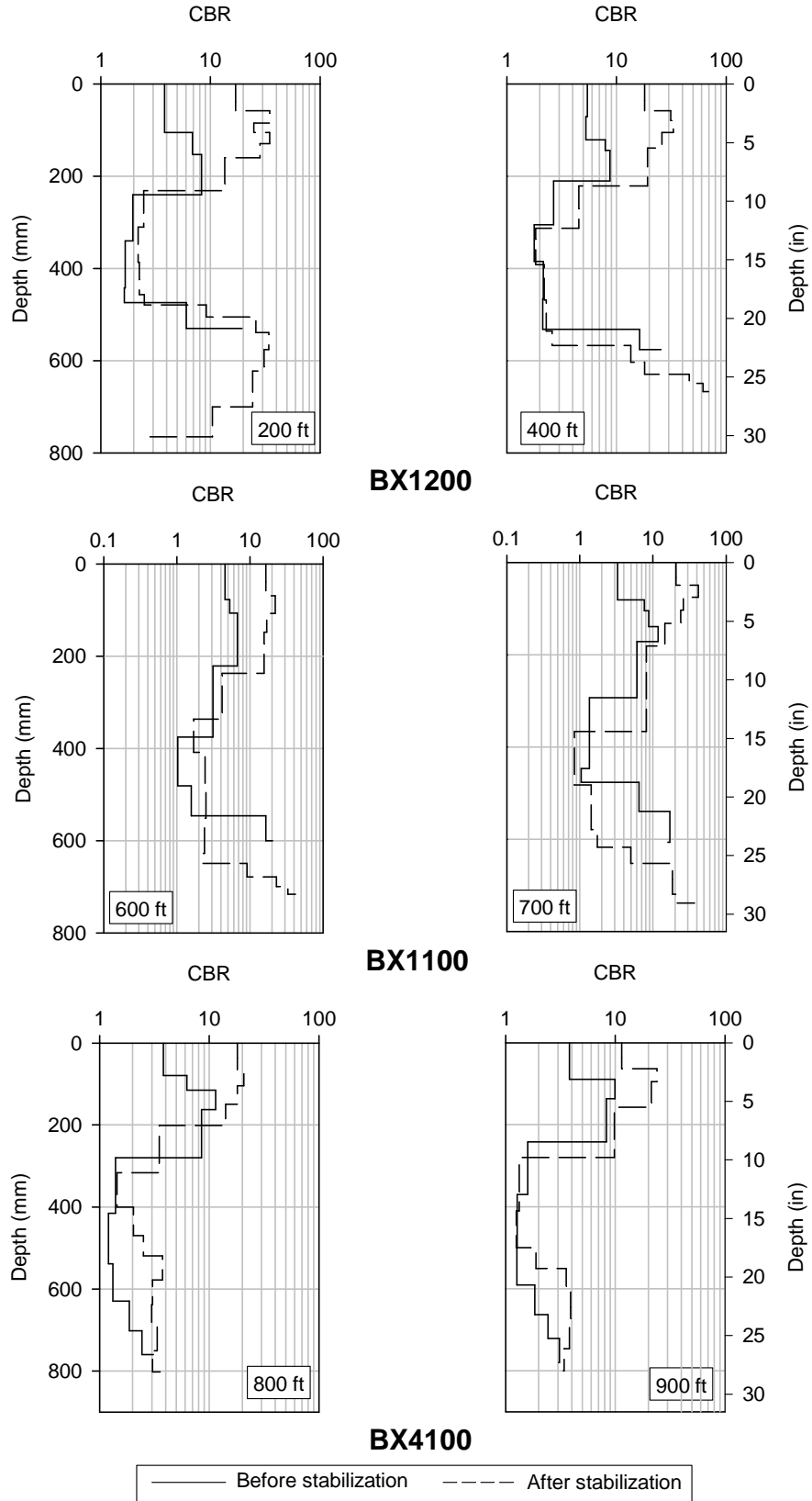


Figure 189. DCP results before and after stabilization, Highway 218, Nashua, IA

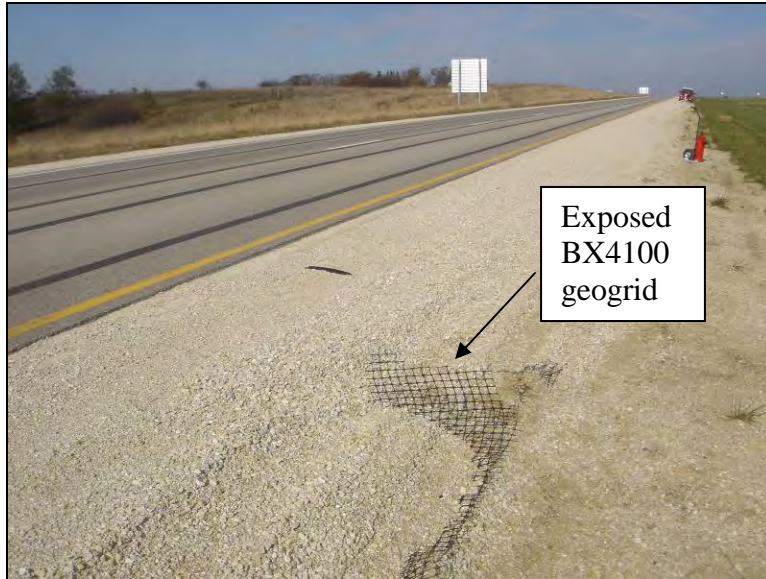


Figure 190. Exposed BX4100 geogrid, October 24, 2006



(a) BX1200 geogrid



(b) BX1100 geogrid

Figure 191. Exposed geogrid about 8 ft. from the pavement edge, April 17, 2007

Summary and Conclusions

- A test section about 1020 ft. long with a soft subgrade was stabilized using three Tensar geogrids. The geogrids were placed at the interface between the subgrade and the granular layer.
- The test section was constructed by stripping the contaminated rock, placing the geogrids at the interface of the two layers, and spreading and compacting new crushed limestone. The thickness of the new granular layer was about 8 in. near the pavement edge; however, the thickness decreased with increasing distance from the pavement edge. At about 8 ft. from the pavement edge, the geogrids were covered by 1 to 2 in. of rock.
- The control section started to develop rutting one month after construction. The stabilized sections showed no signs of shoulder rutting.
- Plate load tests showed a significant difference in the E values between the stabilized and the control section. Further, the E values increased with time. Some sections showed a reduction in E after 10 months due to exposure of the geogrids and reduction in granular layer thickness.
- The section stabilized with the BX1200 geogrid produced the lowest E value and soil deflection, whereas the BX4100 geogrid section produced the lowest E value and highest soil deflection. For this application, all three geogrids were adequate.
- Profiles measured over time revealed an increase in CIVs. After 10 months, CIVs were reduced as a result of geogrid exposure. CIVs were generally highest near the pavement edge, where the granular layer was thickest.
- CBR values, determined from DCP testing, significantly increased for the upper 8 in. after 3 months.
- After 4 months, parts of the defective BX4100 near the end of the section were exposed. Thus, the damaged geogrid does not improve the strength characteristics of the shoulder.
- At 10 months, more geogrids were exposed at about 8 ft. from the pavement edge, where the granular layer thickness was insufficient.
- All geogrids considerably improved the performance of the shoulder test section and eliminated shoulder rutting. However, the strength properties showed some reduction after one winter cycle due to the exposure of geogrids, a decrease in granular layer thickness, or loosening of the granular layer under freeze-thaw effects.
- When adequately overlaid by a uniform granular layer thickness, geogrids can be effective in improving the strength properties of shoulder sections overlying soft foundation soils.

Recommendations

- The test section should continue to be monitored to document its long-term performance.
- Future monitoring will also verify whether repetitive snow plowing will lead to further exposure of the geogrids.
- It is recommended that the geogrid be entirely covered with 6 to 8 in. of crushed limestone to prevent any damage to the grid from traffic or maintenance operations.

Key Findings from All Shoulder Test Sections

Test Section No. 1, S.S. Polymer

- The section stabilized with S.S. polymer performed inadequately, and the 6 to 12 in. strip adjacent to the pavement edge showed signs of delamination.
- The S.S. polymer penetrated a depth of approximately 0.5 in., forming a granular film that became detached under the impact of traffic.
- CBR values did not increase with time at the upper 15 in.
- Using granular material that complied with the lower bound of the gradation curve specified by the Iowa DOT resulted in a higher S.S. polymer penetration depth.
- Further durability testing and evaluation using diluted S.S. polymer (e.g., 7:1 or 9:1) are needed.

Test Section No. 2, Foamed Asphalt

- Full-depth reclamation using FA and class C fly ash was utilized to stabilize shoulder sections on I-35.
- CBR values increased with time for the upper 10 in.
- Laboratory vacuum saturation tests reduced the compressive strength by 20%.
- Freeze-thaw testing showed that FA can expand by 18%; however, the percent mass loss due to freeze-thaw cycles was satisfactory.
- Edge drop-off and shoulder distresses were observed at the test section after approximately one year.
- FA was successful in improving the properties of the shoulder section for a short duration. For longer durations, the stabilized section showed significant signs of distress near the pavement edge.

Test Section No. 3, Soybean Oil

- A 340 ft. long by 2 ft. wide by 6 in. deep section was stabilized using Feed Energy soybean oil.
- Two applications at a rate of 0.7 gal./yd² were placed and mixed with the granular material.
- Due to separation of the oil and emulsion, the distributor became plugged and a topical application was not carried out.
- Elevation profiles show that the Feed Energy soybean oil did not succeed in mitigating the formation of the edge drop-off.
- DCP tests revealed no CBR increase in the upper 8 in. of the stabilized test section.
- After 8 months, a 3 in. edge drop-off along the pavement edge was measured.

Test Section No. 4, Portland Cement

- A 200 ft. long by 1.5 ft. wide by 0.5 ft. deep test section was mixed and compacted with water and 10% portland cement.
- The first 100 ft. section performed adequately, and a hard cemented surface was observed. Wash boarding and erosion were observed along the second 100 ft.
- CIV profiles demonstrated significant improvement after 7 and 14 days. No additional strength was measured after 28 days. CIVs outside the stabilized area were lower than those measured near the pavement edge.
- Edge drop-offs and erosion were observed along the stabilized area after 4 months. After 8 months, the edge drop-off further progressed to a depth of about 3 in.

Test Section No. 5, Fly Ash

- The shoulder section located on Highway 34 near Batavia, IA, was 8 miles long and 8 ft. wide.
- Based on DCP test results, the CBR values for the granular and subgrade layers were 10 and 2, respectively.
- XRD results show that the clay material consists mainly of kaolinite and traces of illite and quartz. XRF results show that there was a high percentage of silica and alumina in both the clay and the fly ash.
- pH tests showed that 16% to 20% fly ash addition was required to raise the pH of the soil-fly ash mixture to the desired pH value (11.5).
- Stabilizing the clay with 20% fly ash resulted in an unconfined compressive strength of 114 psi after seven-day curing at 100°F. Vacuum saturating the samples resulted in a strength reduction of 30%.
- The shoulder section was reconstructed by windrowing the upper 6 in. of the crushed limestone and mixing 15% to 20% class C fly ash with the upper 12 in. of the subgrade clay. The mix was compacted using a pad foot roller, and the limestone was reclaimed and compacted using a smooth wheel roller.
- DCP tests demonstrated an increase in CBR values over time. All stabilized sections showed higher CBR values than the unstabilized sections.
- Plate load tests showed that the stabilized sections had much higher E values than the control sections. Further, E values measured after one year were significantly higher than those measured after 7 months. After 19 months, CBR and E values increased relative to the values measured after 12 months.
- Preliminary testing conducted at the new Highway 34 bypass revealed low CBR values for the underlying earth shoulder fill and subgrade layers.
- Fly ash stabilization was successful in improving both the short- and long-term performance of the shoulder section.

Test Section No. 6, Geosynthetics

- A test section about 1,020 ft. long with soft subgrade was stabilized using three Tensar geogrids. The geogrids were placed at the interface between the subgrade and the granular layer.
- The control section started to develop rutting after one month. The stabilized sections showed no signs of shoulder rutting.
- Plate load tests showed a significant difference in E values between the stabilized and control sections. Further, the E values increased with time.
- CIVs were highest near the pavement, since the thickness of the rock layer was highest there. CIVs measured outside the stabilized area were low, indicating soft shoulder conditions.
- CBR values, determined from DCP testing, increased after 3 months for the upper 8 in.
- All geogrids considerably improved the performance of the shoulder test section and eliminated rutting.
- The E values and CIVs showed some reduction after 10 months, possibly due to the exposure of geogrids or a decrease in granular layer thickness.

LABORATORY EVALUATION OF STABILIZERS

Introduction

The stabilized test sections discussed above produced varying results for mitigating distress, erosion, or edge drop-off. Poor performance for some sections was attributed to difficulties in construction methods (such as the separation of oil and emulsion in Test Section No. 3) or inadequate stabilization procedures (such as topical application and compaction of S.S. polymer in Test Section No. 1) and not necessarily the effectiveness of the stabilizer. Therefore, a laboratory study was carried out to evaluate the effectiveness of selected products in stabilizing granular soil.

The stabilizers selected for the laboratory investigation were S.S. polymer, Soiltac polymer, portland cement, and dustlock soybean oil. In review, S.S. polymer and Soiltac polymer are commercially available polymer emulsion products with a milky white appearance and are generally used as a dust suppressant. They stabilize the soil by bonding soil and aggregate particles. Dustlock soybean oil is a dust suppressant product that stabilizes the soil by keeping the dust particles bound together. Dustlock soybean oil is the same soybean oil product that was used to stabilize the granular shoulder section on Highway 18 near Garner, IA (discussed in the Field Reconnaissance section of this report).

Test Procedures

For each stabilizer, six standard Proctor samples were prepared using compaction method B (material passing 3/8 in. sieve). The nominal moisture content for all samples was about 4%. Samples were prepared by mixing the granular material with the stabilizer, compacting in split molds, and curing for 24 hours at a temperature of about 70°F. The samples were then extracted and placed in an oven for 7 days at 100°F.

The selected addition and dilution rates for each stabilizer are shown in Table 22. The addition rates used for S.S. polymer and Soiltac polymer were based on an assumed penetration depth of 0.5 in., which was the approximate penetration depth observed in the field when S.S. polymer was applied topically. Therefore, the addition rate was multiplied by nine to determine the amount of stabilizer needed for the entire Proctor sample. The S.S. polymer addition rate was 5% by weight, which was determined in an earlier laboratory study to be the optimum amount (discussed in this report under Laboratory Testing of Test Section No. 1). The addition rate of Soiltac polymer was based on the rate recommended by the manufacturer for stabilizing base material. The dilution rate was determined by calculating the difference between the optimum moisture (6%) and the sample moisture content (4%). The addition rate of portland cement was about 7% by dry weight to coincide with the cement percentage used at Test Section No. 4. The addition rate of the dustlock soapstock was determined by calculating the amount of stabilizer needed to achieve 60% saturation of the volume of air in a sample. Three samples were tested in axial compression, while the other three were subjected to vacuum saturation followed by compression testing.

Table 22. Summary of laboratory test procedures

Stabilizer	No. of samples	Addition rate	Dilution rate	Curing method
S.S. polymer	6	5% by dry weight	1:5 by volume	seven-day oven cure at 100° F
Soiltac polymer	6	0.36 gal/yd ²	2%	
Portland cement	6	7% by dry weight	-	
Dustlock soybean oil	6	1.0 gal/yd ²	-	

Test Results

The results of the compression tests conducted on the stabilized granular samples are shown in Table 23. Figure 192 shows the compression tests conducted on the Soiltac polymer-stabilized and soapstock-stabilized samples. Granular material stabilized with Soiltac polymer showed the highest compressive strength, which was about 1,118 psi.

Compressive strength, however, decreased by about 75% when the samples were subjected to vacuum saturation. The average compressive strengths of samples stabilized with S.S. polymer and portland cement were 445 psi and 694 psi, respectively. After vacuum saturation, the average strengths of S.S. polymer and portland cement samples were reduced to 76 psi and 254 psi, respectively. The average strength of samples stabilized with dustlock polymer was about 706 psi. Compared to other stabilizers, dustlock polymer-stabilized samples demonstrated minimal strength reduction after vacuum saturation. The compressive strength after vacuum saturation was about 623 psi. The small reduction in strength after vacuum saturation is attributed to the presence of soybean oil in the sample, which acted as a water repellent. Figure 193 shows the granular samples stabilized with dustlock polymer after the vacuum saturation test was conducted. It was noted that the samples were almost dry with, minor water infiltration. This indicates that dustlock polymer may provide higher resistance to erosion and edge drop-off formation, and thus durations between subsequent applications can be extended. Figure 194 is a bar chart summarizing the unconfined compressive strength achieved for each stabilizer.

Summary and Conclusions

- A laboratory study was conducted to evaluate the effectiveness of two polymer emulsion products, portland cement, and a soybean oil product in stabilizing the shoulder granular layer.
- Six standard Proctor samples were prepared for each stabilizer. Three samples were tested in compression, while the other three were subjected to vacuum saturation followed by compression test.
- The average strength of S.S. polymer-stabilized samples was about 445 psi, which decreased to 76 psi after vacuum saturation.

- The average strength of Soiltac polymer-stabilized samples was about 1,118 psi, which was the highest compressive strength recorded among the stabilizers. Vacuum saturating the samples resulted in an average compressive strength of about 252 psi.
- The average strength of portland cement-stabilized samples was about 694 psi, which decreased to 254 psi after vacuum saturation.
- Dustlock polymer-stabilized samples demonstrated an average compressive strength of about 706 psi, which decreased to 623 psi after vacuum saturation. The stabilized samples showed the smallest strength reduction after vacuum saturation, since dustlock soybean oil is a water repellent product.

Table 23. Summary of laboratory test results

Sample	Test	Weight (lb.)	Load (lb.)	Stress (psi)	
S.S. polymer	1	Vacuum saturation	3.71	878	70
	2	followed by	3.70	1,095	87
	3	compression	3.63	894	71
	4		3.71	6,250	497
	5	Compression	3.72	5,370	427
	6		3.79	5,162	411
Soiltac polymer	1	Vacuum saturation	3.74	2,610	208
	2	followed by	3.49	2,710	216
	3	compression	3.98	4,160	331
	4		3.87	18,330	1,459
	5	Compression	3.57	13,270	1,056
	6		3.89	10,530	838
Portland cement	1	Vacuum saturation	3.72	5,670	451
	2	followed by	3.86	2,180	173
	3	compression	3.98	1,750	139
	4		3.74	9,800	780
	5	Compression	3.83	8,120	646
	6		3.78	8,250	657
Dustlock soybean oil	1	Vacuum saturation	4.39	9,230	735
	2	followed by	4.07	6,640	528
	3	compression	4.54	7,610	606
	4		4.23	6,450	513
	5	Compression	4.36	10,040	799
	6		4.31	10,140	807



(a) Soiltac-stabilized sample



(b) Soapstock-stabilized sample

Figure 192. Axial compression test



Figure 193. Soapstock-stabilized samples after vacuum saturation test

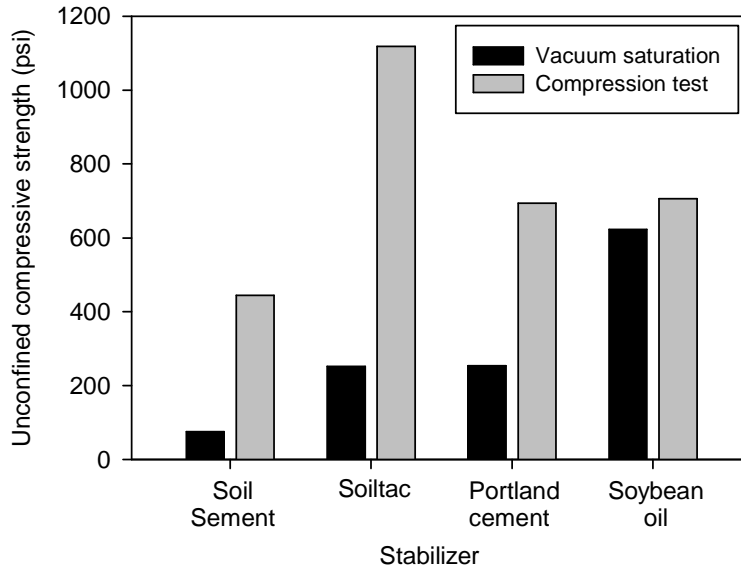


Figure 194. Summary of compressive strength results

Recommendations

- All four products showed potential to be used as a stabilizer for the shoulder granular layer.
- For maintenance applications, S.S. polymer and Soiltac polymer may require topical applications, in contrast to dustlock soybean oil, due to their lower resistance when subjected to vacuum saturation.
- For optimum stabilization results, it is recommended that the products be uniformly mixed and compacted with the granular layer.

LABORATORY BOX STUDY

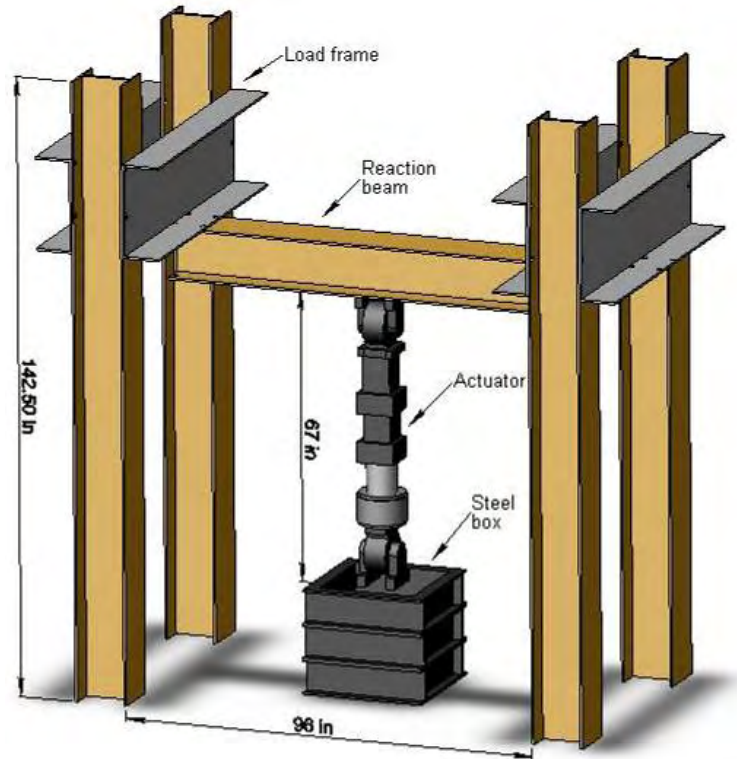
Introduction

As demonstrated in previous sections, field tests showed that subgrade layers with CBR values less than 10 were encountered at approximately 50% of the inspected sections. When subjected to traffic loads, these shoulders may develop considerable rutting. To explore the effects of these low CBR values, a laboratory study was conducted to simulate a shoulder section overlying a soft subgrade. Cyclic loading with three loading stages was used to study the performance of the laboratory model for selected mechanical and chemical stabilization techniques. This section describes the model setup, descriptions of each test, and the test results.

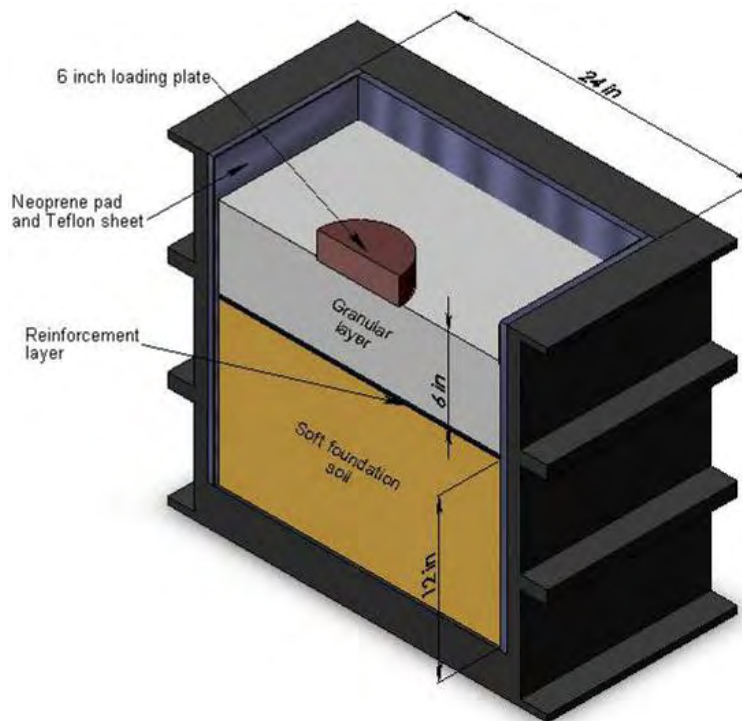
Test Setup

The laboratory apparatus consisted of a loading frame, reaction beam, and a hydraulic actuator. The actuator has a maximum force of 55 kips (250 kN) and a dynamic stroke of 6 in. (Figure 195a). As shown in Figure 195b, an 8 ft³ steel box was used to contain the soil, which was loaded using a 6 in. diameter loading plate. The steel box consisted of twelve 8 in. c-channels assembled together to form a 2 ft. x 2 ft. x 2 ft. box. To minimize friction and stress concentrations, a compressible 0.5 in. thick neoprene pad and a Teflon sheet were placed at the interface between the soil and the steel box (Figure 196). The subgrade soil was placed at the bottom of the box and compacted in 3 in. lifts by applying a static load to reach a final depth of 12 in. The reinforcement layer was placed at the interface between the subgrade and the overlying granular layer. As with the foundation layer, the granular layer was compacted by applying a static load to reach a final thickness of about 6 in. (Figure 197). To ensure soft foundation conditions for all tests, the target range of CBR values for the subgrade layer was selected to vary between 3 and 5. The target range of CBR values for the granular layer was 4 to 7.

The hydraulic actuator was used to apply a sinusoidal load pulse to the 6 in. diameter loading plate (Figure 198). Three incremental cyclic loads were applied to the soil, each sustained for 5,000 cycles (total of 15,000 cycles) at a frequency of 1 Hz. The initial cyclic pressure was 40 lb./in², which was then increased to 80 lb./in² and then to 120 lb./in². The applied pressures were selected to simulate the stress applied by 0.5, 1.0, and 1.5 units of the American-British standard axle load (17,984 lb.), with a tire inflation pressure of 80 lb./in² (550 kPa) and 6 in. of tire contact area (Giroud and Han 2004b). The frequency of one cycle per second was sufficient for sustaining the applied load, despite the large deflections observed for some tests. The hydraulic actuator control system was used to collect displacement data at predetermined load cycles. Further, the DCP and Clegg hammer were used to calculate a CBR value for each soil layer before and after the test, while a light weight deflectometer (LWD) test with an 8 in. (200 mm) diameter loading plate was conducted to document changes in the E values of the granular and subgrade layers. E values measured with LWD testing are denoted E_{LWD}.

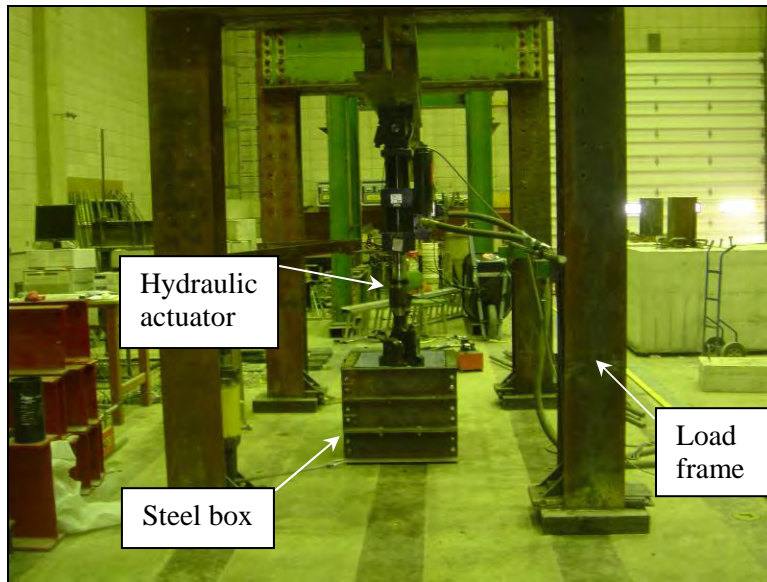


(a) Steel frame and hydraulic actuator used for loading the stabilized soil

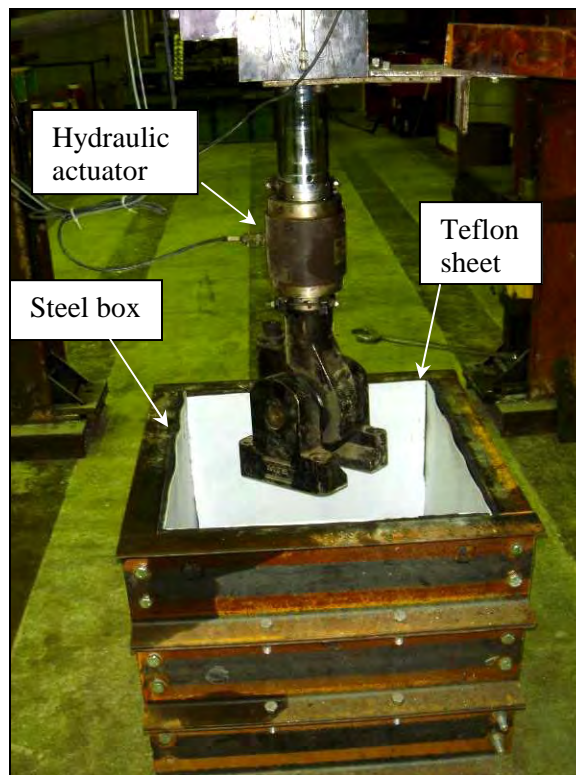


(b) Steel box used to contain the soil

Figure 195. Schematic of the laboratory apparatus setup



(a) Overall view of the testing equipment



(b) Closer view of the actuator and the steel box

Figure 196. Photographs of the laboratory test setup

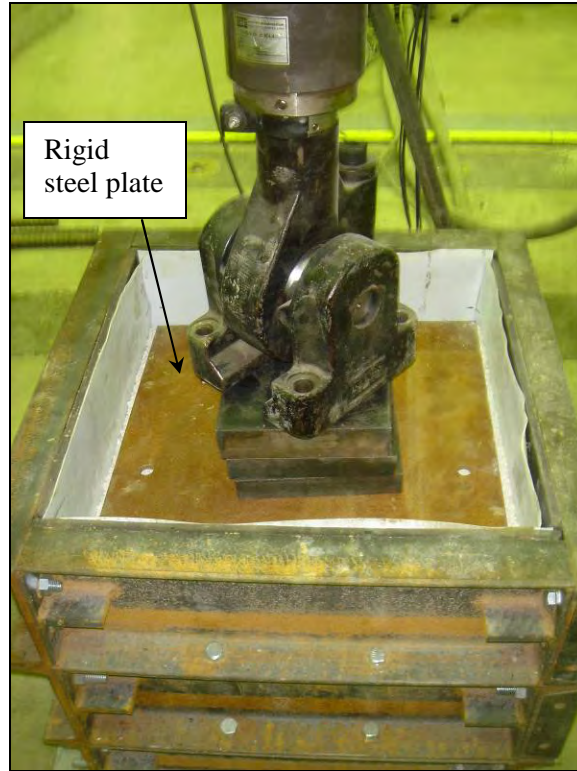


Figure 197. Applying a static load to compact the soil

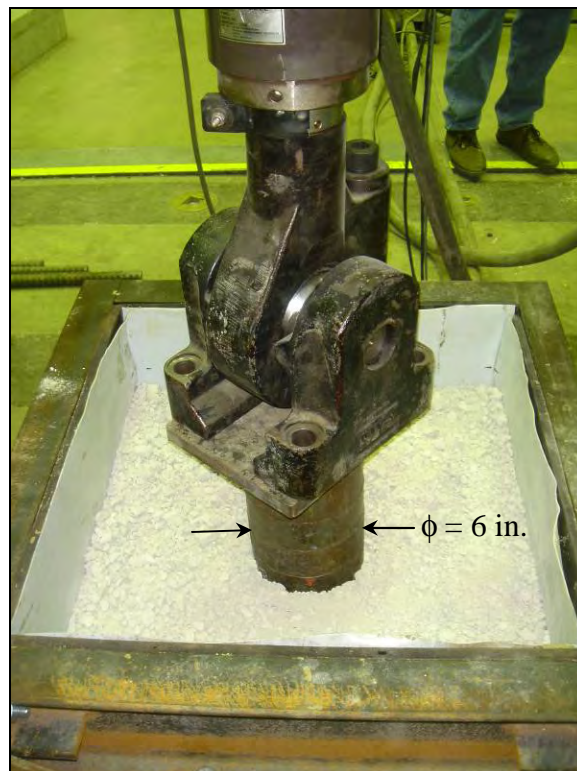


Figure 198. Applying cyclic loading to the soil using a 6 in. plate

During the test, and at each loading stage, the deflection of the reaction beam was measured using a dial gauge, as shown in Figure 199. A linear relationship was observed between the load applied and the beam deflection (Figure 200). The measured deflection was taken into account when calculating the corresponding soil displacement.

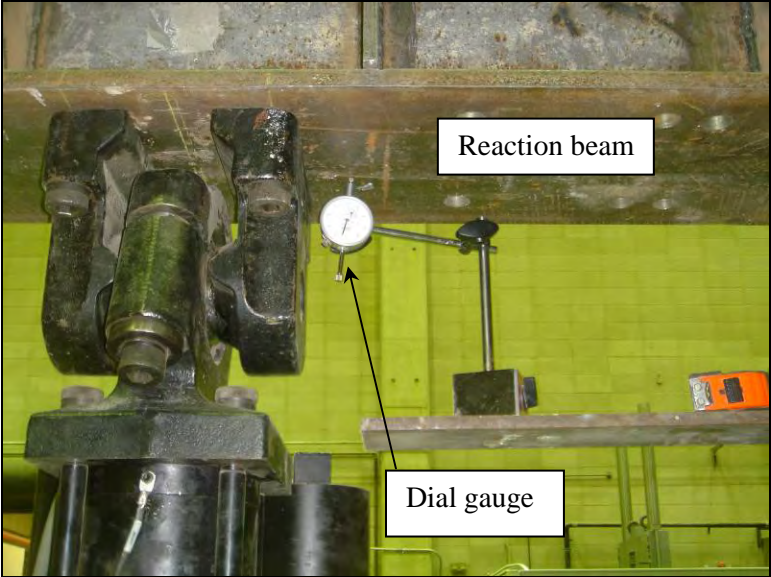


Figure 199. Measuring the reaction beam deflection

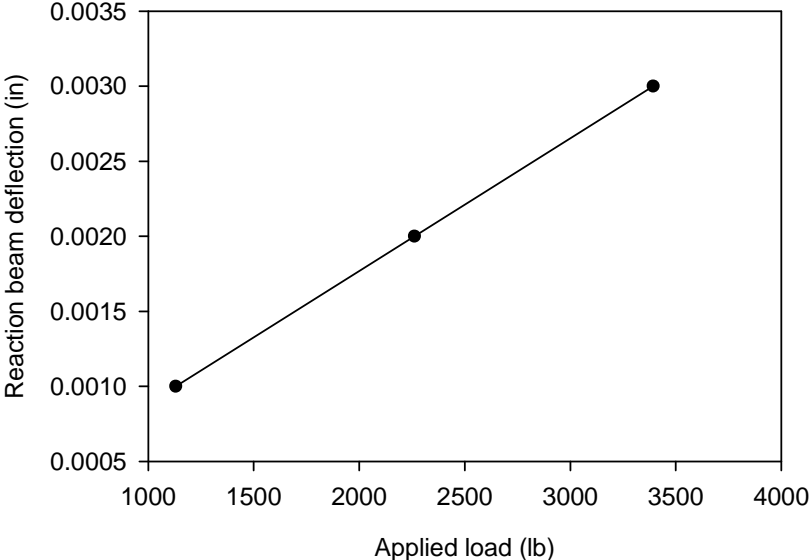


Figure 200. Magnitude of beam deflection with applied loads

Finite Element Analysis

An analytical model of the laboratory box study was developed using finite element analysis to evaluate the boundary conditions of the laboratory experiments (i.e., the addition of a compressible neoprene layer at the interface between the soil and the steel box). Axisymmetric elastic-plastic analyses were carried out using SLOPE/W software. The details of this analysis are shown in Appendix C.

Three models were developed and evaluated in this study. The first model represents the rigid steel walls of the box directly interacting with the soil. The second model represents the addition of a compressible neoprene layer at the interface between the steel box and the soil. The third model represents field conditions where no boundaries exist.

The results indicate that adding a compressible layer at the interface between the laboratory box and the soil mobilizes more vertical soil displacement than if the soil were interacting directly with the rigid steel wall. Adding a compressible soil layer will therefore result in soil displacement values closer to those encountered in the field.

Materials

Subgrade Soil

The soil used as a subgrade material was obtained from a test pit near Batavia, IA, and thus was identical to the subgrade material stabilized using class C fly ash (discussed in this report under Test Section No. 5). The material was classified as CH (fat clay; A-7-6) and has a liquid limit and a plasticity index of 50 and 32, respectively.

Granular Materials

The materials used for the granular layer in this study are Class A crushed limestone and RAP. The crushed limestone was classified as SP-SM (poorly graded sand with silt; A-1-a). The grain size distribution analysis is shown in Figure 201. Standard Proctor test results show that the optimum moisture content and maximum dry density are 6% and 122.60 lb./ft³, respectively (Figure 202). A grain size distribution analysis was performed on the RAP material, as shown in Figure 203. The material was classified as GP (well graded gravel; A-1-a). The fines content was about 0.5%, compared to 10% for the crushed limestone.

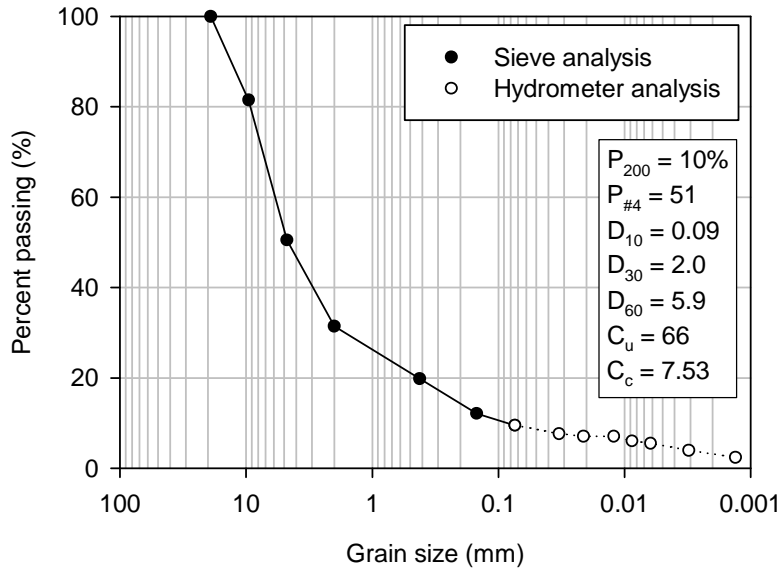


Figure 201. Grain size distribution analysis for the granular material used in the laboratory box testing

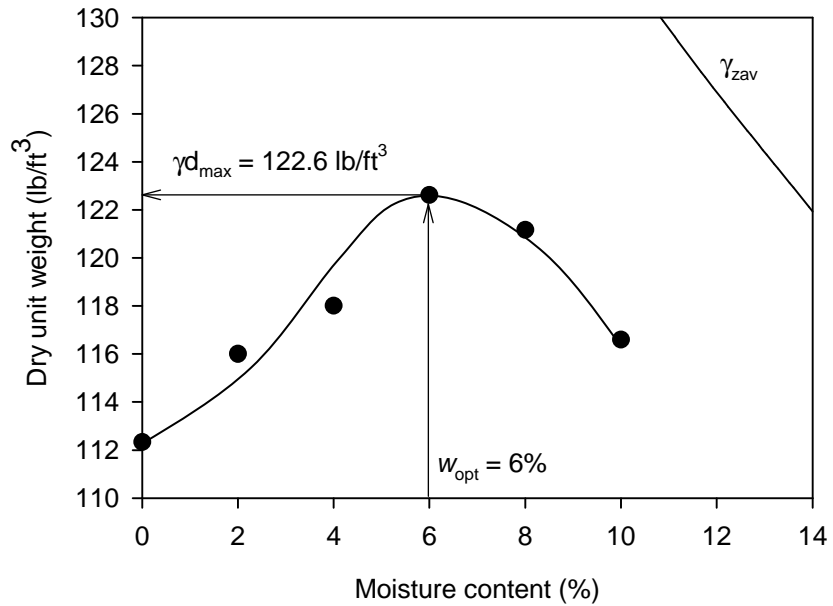


Figure 202. Relationship between moisture content and dry unit weight for the granular material used in the laboratory box testing

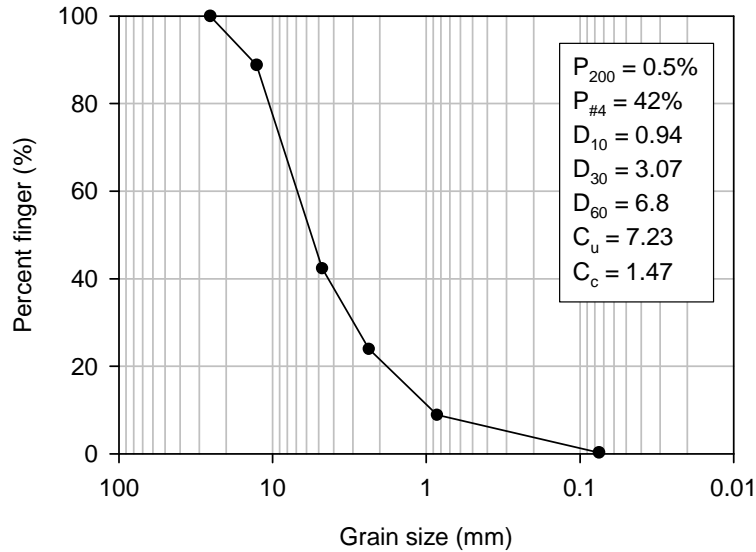


Figure 203. Grain size distribution for the RAP material

Reinforcement

The laboratory study investigated the performance of three biaxial geogrid types, one woven geotextile, and one nonwoven geotextile in alleviating the shoulder rutting developed under repeated traffic loads. The geogrids selected were the same as the ones used in Test Section No. 6 on Highway 218 (i.e., Tensar BX1200, BX1100, and BX4100). The geotextiles used in this study included GEOTEX 315ST, which is a woven geotextile film used mainly for soil separation and stabilization, and GEOTEX 601, which is a needle-punched nonwoven geotextile fiber. The properties of the selected geosynthetics are summarized in Table 24.

Table 24. Engineering properties of the selected geosynthetics

Property	Test method	Geosynthetic				
		BX 1200	BX 1100	BX 4100	GEOTEX 315ST	GEOTEX 601
Grab tensile strength (lb.)	ASTM D4632	-	-	-	315	160
Tensile strength ¹ (5% strain) (lb./ft.)	ASTM D6637	810	580	550	-	-
Elongation (%)	ASTM D4632	-	-	-	15	50
Aperture stability ² (kg-cm/deg.)	-	6.5	3.2	2.8	-	-
Aperture dimension ³ (in.)/ Apparent opening size	ASTM D4751	1.0	1.0	1.3	40 US Std. sieve (0.425 mm)	70 US Std. sieve (0.212 mm)

1. Tensile strength values are measured in the machine direction

2. Measured in accordance with U.S. Army Corps of Engineers methodology for measurement of torsional rigidity

3. Reported aperture dimension are measured in machine direction

Test Results

Test No. 1, Control Test

The control test was conducted to simulate the observed field condition where a granular shoulder overlies a soft subgrade layer. The moisture content of the subgrade material during placement was about 25%, which was similar to the field moisture contents measured at Test Section Nos. 5 and 6. The dry densities for the subgrade and granular layers were 121 lb./ft³ and 85 lb./ft³, respectively. Table 25 summarizes the soil properties obtained before and after the test. The CBR value of the subgrade layer, calculated from DCP tests, increased from 3 to 9 after the test was completed. CBR values were also calculated from CIV data using a correlation developed by Al-Amoudi et al. (2002), as shown in Table 25. Almost no change in the properties of the granular material was noted from before to after the test. The displacement recorded by the hydraulic actuator control system is shown in Figure 204. The maximum soil displacement measured after 15,000 cycles was 11.2 in. The measured values are comparable to the values derived from the semi-empirical design method developed by Giroud and Han (2004) at the end of each loading stage (i.e., 5,000, 10,000, and 15,000 cycles). It was noted that at a low number of cycles (5,000 cycles) the difference between the measured and predicted displacement was not significant. However, with an increasing number of cycles, the design method was observed to overpredict the measured soil displacement. Visual inspection of the subgrade layer after the test revealed considerable aggregate punching into the subgrade, to a depth of approximately 2 in.

Table 25. Soil properties before and after the test, control test

	Soil property	Initial value	Final value
Subgrade layer	CBR ¹ (%)	4	9
	CBR ¹ (%)	5	6
Granular layer	CBR ² (%)	4	10
	CIV	2.9	7.1
	E _{LWD} (lb./in. ²)	725	580

¹ CBR values calculated from DCP tests

² CBR values calculated from Clegg impact test (Al-Amoudi et al. 2002)

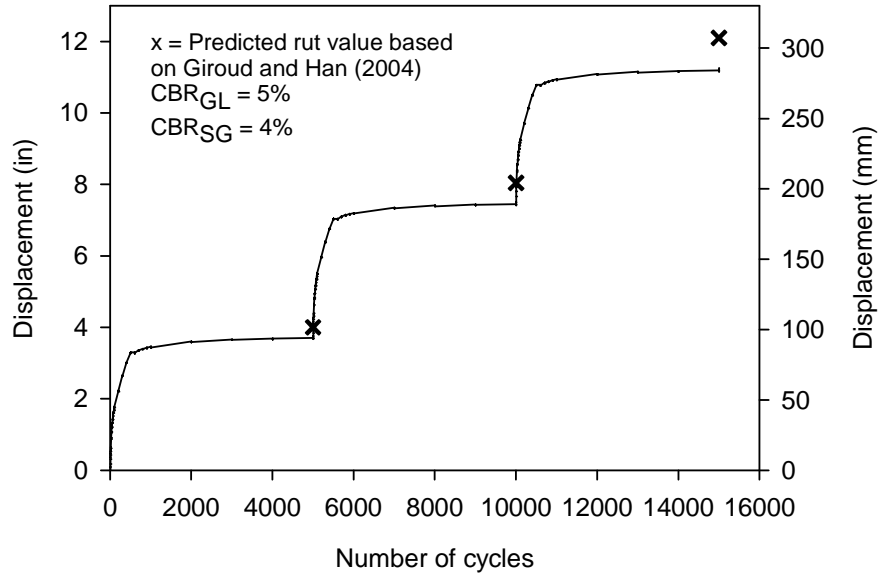


Figure 204. Soil displacement with increasing number of cycles, control test

Test No. 2, BX1200 (Not Anchored)

In this test, a BX1200 geogrid was placed at the interface between the subgrade and the granular layers. The dimensions of the grid were designed to be about 0.25 in. shorter than the dimensions of the box to eliminate any interaction between the grid and the box. The moisture content of the subgrade material during placement was about 25%. The dry densities of the subgrade and granular layers were 118 lb./ft³ and 89 lb./ft³, respectively. The soil properties before and after the test are shown in Table 26. The CBR value of the subgrade layer increased from 5 to 7 after the test, indicating less soil densification than was observed during Test No. 1. Further, the subgrade modulus (E_{LWD}) increased from 1,015 to 1,740 lb./in². No significant change in the properties of the granular layer was measured. The measured soil displacement over an increasing number of cycles is shown in Figure 205. The maximum measured soil displacement at 15,000 cycles was 4.95 in., which was about 40% less than that measured for the control test. The calculated rut depth was similar to the soil displacement measured at the end of the first load stage (i.e., 5,000 cycles). However, the calculated soil displacement was significantly lower than that measured at the end of the second and third loading stages. Examining the unanchored geogrid after the test revealed that the geogrid was pulled to the center of the box (a phenomenon that would not occur in the field) under the effect of repetitive cyclic loading (Figure 206). This observation may explain the difference between the measured and predicted soil displacement. Similar to the control test, most of the soil displacement occurred during the first 500 cycles of each load increment. The amount of aggregate punching through the subgrade layer was less than in Test No. 1, but it was not eliminated. Visual inspection revealed an aggregate punching depth of about 1 in.

Table 26. Soil properties before and after the test, BX1200 Geogrid (not anchored)

	Soil property	Initial value	Final value
Subgrade layer	CBR ¹ (%)	4	7
	CBR ² (%)	4	9
	CIV	3.2	6.2
	E _{LWD} (lb./in ²)	1015	1740
Granular layer	CBR ¹ (%)	5	5
	CBR ² (%)	5	7
	CIV	3.7	5.4
	E _{LWD} (lb./in ²)	435	435

¹ CBR values calculated from DCP tests

² CBR values calculated from Clegg impact test (Al-Amoudi et al. 2002)

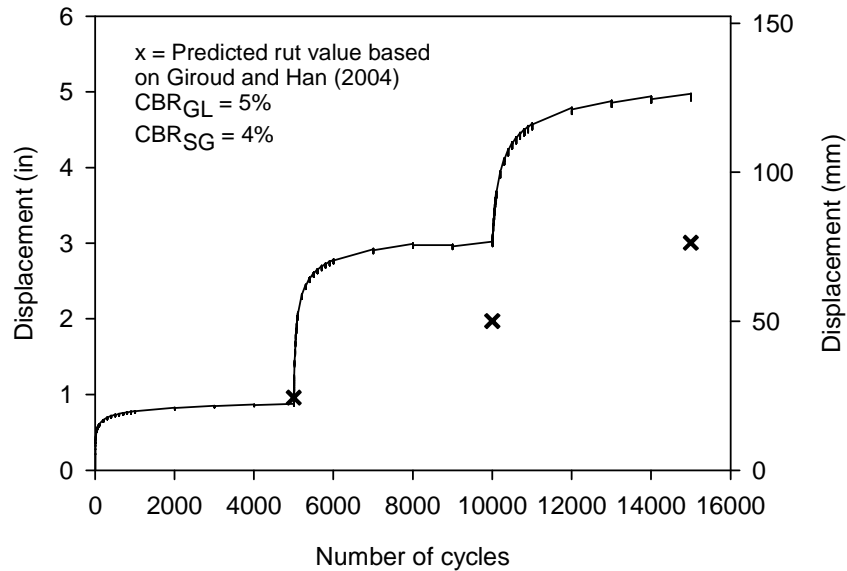


Figure 205. Soil displacement with increasing number of cycles, BX1200 (not anchored)

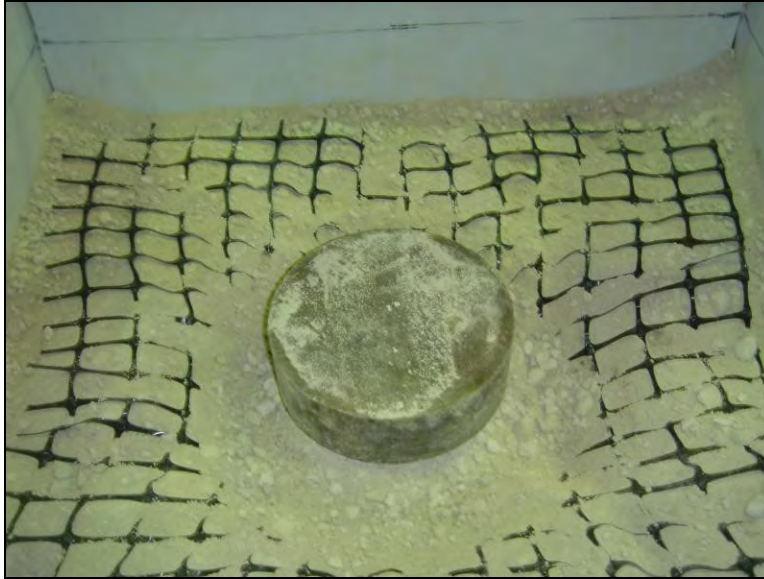


Figure 206. Unanchored geogrid pulled to the center of the box under the impact of cyclic loading

Test No. 3, BX1200 (Partially Anchored)

The BX1200 geogrid was placed at the interface between the subgrade and granular layers and was anchored to the soil at the four corners of the geogrid using steel rods driven to the bottom of the subgrade layer. The moisture content of the subgrade during placement was about 25%. The dry densities of the subgrade and granular layers were 122 lb./ft³ and 90 lb./ft³, respectively. Table 27 presents the soil properties measured for both layers before and after the test. As a result of soil displacement, the CBR value of the subgrade layer increased from 5 to 8, and the E_{LWD} increased from 1,160 lb./in² to 1,595 lb./in². The results showed no change in the properties of the granular layer before and after the test. Figure 207 demonstrates the measured and predicted soil displacement over an increasing number of cycles. It was noted that partially anchoring the geogrid resulted in decreasing the soil displacement relative to Test No. 2 (in which the geogrid was not anchored). For example, at 10,000 cycles the soil displacements measured were 3.06 and 2.69 in. for Tests No. 2 and 3, respectively. On average, partially anchoring the geogrid reduced the soil displacement by 10%. Similar to Test No. 2, there was no significant difference between the measured and predicted soil displacement at the end of the first loading stage. The difference, however, increased over an increasing number of cycles. At 15,000 cycles, the difference between the measured and predicted soil displacement was 1.87 in. for Test No. 2 and 1.36 in. for Test No. 3. Visual inspection showed punching of aggregate through the subgrade soil to a depth of about 1 in.

Table 27. Soil properties before and after the test, BX1200 Geogrid (partially anchored)

	Soil property	Initial value	Final value
Subgrade layer	CBR ¹ (%)	5	8
	CBR ² (%)	6	11
	CIV	4.2	8.1
	E _{LWD} (lb./in ²)	1160	1595
Granular layer	CBR ¹ (%)	6	6
	CBR ² (%)	7	6
	CIV	4.8	4.4
	E _{LWD} (lb./in ²)	580	580

¹ CBR values calculated from DCP tests

² CBR values calculated from Clegg impact test (Al-Amoudi et al. 2002)

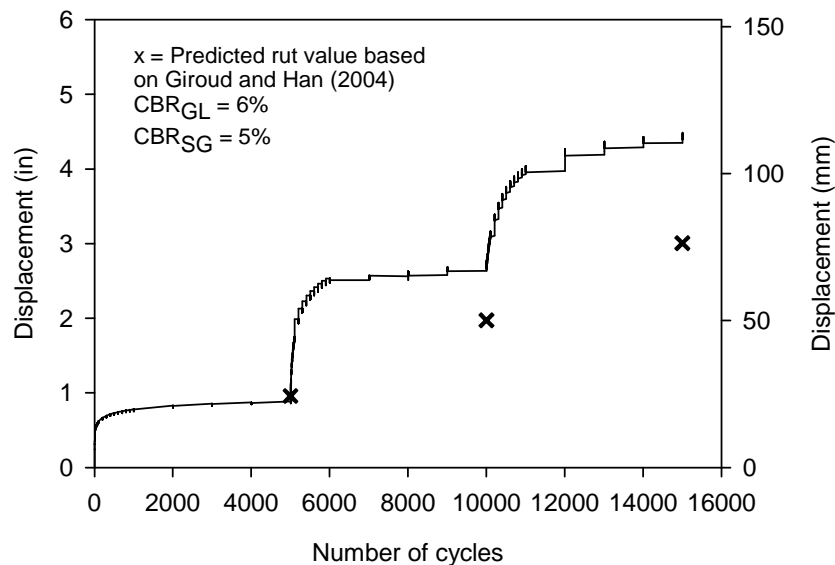


Figure 207. Soil displacement with increasing number of cycles, BX1200 (partially anchored)

Test No. 4, BX1200

The setup of this test was similar to that of the previous two tests, except that the entire perimeter of the BX1200 geogrid was fixed in order to eliminate any geogrid movement. This was accomplished by locking the geogrid between the c-channels, which were used to assemble the sides of the steel box. The moisture content of the subgrade during placement was about 25%. The dry densities of the subgrade and granular layers were 119 lb./ft³ and 96 lb./ft³, respectively. Table 28 presents the soil properties measured for both layers before and after the test. The CBR value of the subgrade, calculated from the DCP test, increased from 4 to 7. The subgrade E_{LWD} also increased from 1,160 lb./in² to 1,450 lb./in². The CBR and E_{LWD} values of the granular layer did not change considerably before and after the test. Figure 208 shows the measured and predicted soil displacement over an increasing number of cycles. As a result of locking the entire

geogrid perimeter, the measured soil displacement was further reduced relative to Test Nos. 2 and 3. At 15,000 cycles, the soil displacement was 40% lower than that measured in Test No. 3. Further, minimizing the movement of the geogrid reduced the differences between the measured and predicted soil displacement at all three loading stages (Table 29). Therefore, other mechanical reinforcements used later in this laboratory study were fixed to the steel box in a similar manner.

Table 28. Soil properties before and after the test, BX1200 Geogrid

	Soil property	Initial value	Final value
Subgrade layer	CBR ¹ (%)	4	7
	CBR ² (%)	6	11
	CIV	4.1	7.8
	E _{LWD} (lb./in ²)	1160	1450
Granular layer	CBR ¹ (%)	5	6
	CBR ² (%)	6	7
	CIV	4.3	5.3
	E _{LWD} (lb./in ²)	580	725

¹ CBR values calculated from DCP tests

² CBR values calculated from Clegg impact test (Al-Amoudi et al. 2002)

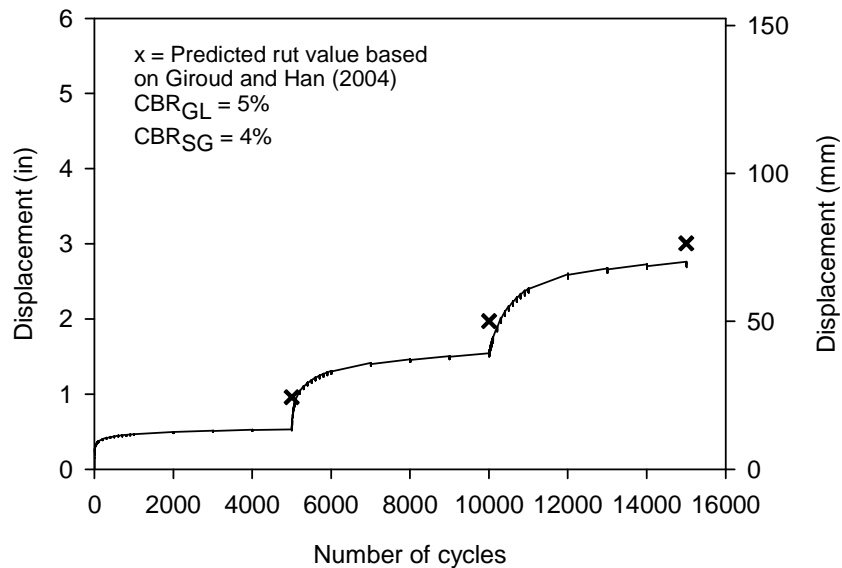


Figure 208. Soil displacement with increasing number of cycles, BX1200

Table 29. Summary of predicted and measured soil displacement for the BX1200 geogrid reinforced tests

Load cycle	Predicted soil displacement (in.)	Measured soil displacement (in.)		
	(based on Giroud and Han 2004)	Test 2	Test 3	Test 4
5,000	0.96	0.91	0.94	0.53
10,000	1.97	3.06	2.69	1.51
15,000	3.01	4.95	4.39	2.69

Test No. 5, BX1100

In this test, the subgrade layer was stabilized by placing the Tensar BX1100 geogrid at the interface between the granular and subgrade layers. This geogrid has an aperture stability modulus of 3.2 kg-cm/deg., so it is relatively weaker than the BX1200 geogrid. The moisture content of the subgrade during placement was about 25%, and the dry densities of the subgrade and granular layers were 119 lb./ft³ and 86 lb./ft³, respectively. Table 30 presents the soil properties measured for both layers before and after the test. The CBR value of the subgrade increased from 5 to 8, and E_{LWD} increased from 1,305 lb./in² to 1,740 lb./in². No significant change was measured in the properties of the granular layer. Figure 209 shows the measured and predicted soil displacement over an increasing number of cycles. The soil displacement measured at 15,000 cycles was about 12% higher than that measured in Test No. 4. Further, the predicted soil displacement was higher than the measured one by about 17%.

Table 30. Soil properties before and after the test, BX1100 Geogrid

	Soil property	Initial value	Final value
Subgrade layer	CBR ¹ (%)	5	8
	CBR ² (%)	5	9
	CIV	4	6.6
	E _{LWD} (lb./in ²)	1305	1740
Granular layer	CBR ¹ (%)	4	5
	CBR ² (%)	6	5
	CIV	4.7	3.6
	E _{LWD} (lb./in ²)	435	435

¹ CBR values calculated from DCP tests

² CBR values calculated from Clegg impact test (Al-Amoudi et al. 2002)

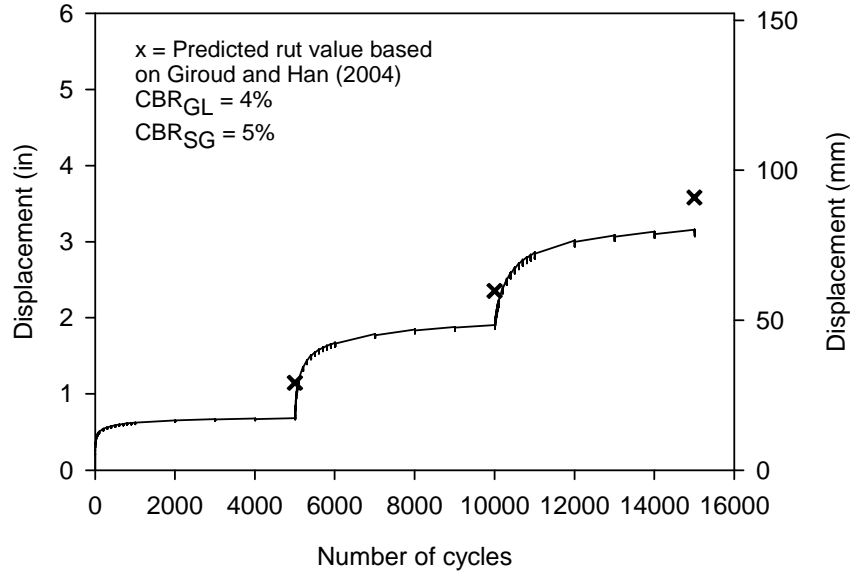


Figure 209. Soil displacement with increasing number of cycles, BX1100

Test No. 6, BX4100

The subgrade layer in this test was stabilized using the BX4100 geogrid, which has an aperture stability modulus of 2.8 kg-cm/deg. The moisture content of the subgrade during placement was about 25%, and the dry densities of the subgrade and granular layers were 122 lb./ft³ and 90 lb./ft³, respectively. Table 31 presents the soil properties measured for both layers before and after the test. The CBR value of the subgrade increased from 5 to 9, and E_{LWD} increased from 1,305 lb./in² to 2,321 lb./in². Similar to previous tests, no change was observed in the properties of the granular layer. Figure 210 shows the measured and predicted soil displacement over an increasing number of cycles. There was no significant difference between the soil displacements measured using the BX4100 and the BX1100 geogrids. This may be attributed to the similar strength properties of both geogrids. Further, the predicted soil displacement was about 16% higher than the measured one. Table 32 compares the results obtained for the three biaxial geogrids. It is apparent that the BX1200 showed better performance; nonetheless, the other geogrid types significantly reduced the soil displacement when compared to the control test.

Table 31. Soil properties before and after the test, BX4100 Geogrid

	Soil property	Initial value	Final value
Subgrade layer	CBR ¹ (%)	5	9
	CBR ² (%)	5	11
	CIV	3.8	8
	E _{LWD} (lb./in ²)	1305	2321
Granular layer	CBR ¹ (%)	4	5
	CBR ² (%)	5	6
	CIV	3.7	4.1
	E _{LWD} (lb./in ²)	435	870

¹ CBR values calculated from DCP tests

² CBR values calculated from Clegg impact test (Al-Amoudi et al. 2002)

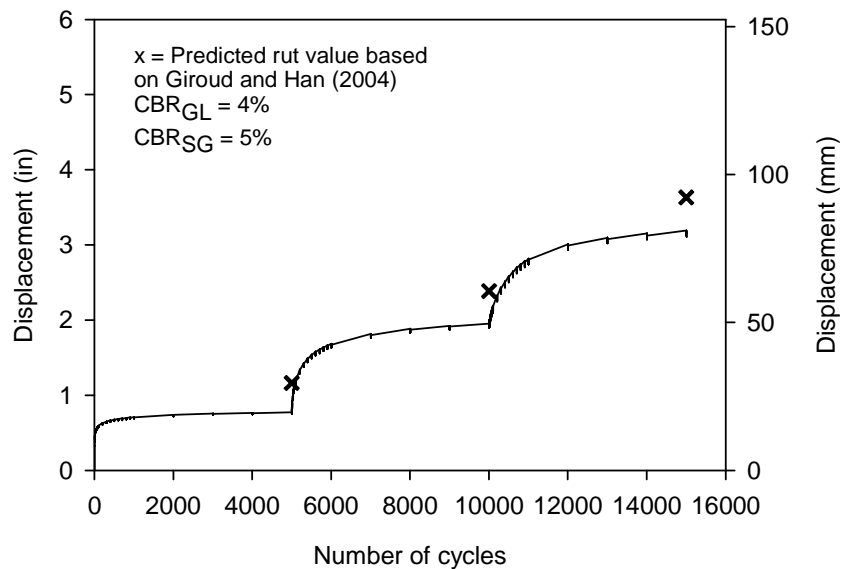


Figure 210. Soil displacement with increasing number of cycles, BX4100

Table 32. Comparison among measured soil displacements for the three biaxial geogrid types

Load cycles	Measured soil displacement (in)		
	BX1200	BX1100	BX4100
5,000	0.53	0.68	0.77
10,000	1.51	1.90	1.95
15,000	2.69	3.06	3.01

Test No. 7, Woven Geotextile

In this test, a woven geotextile layer (GEOTEX 315ST) was placed at the interface between the subgrade and granular layers. The moisture content of the subgrade soil was about 25% during placement. The dry densities of the granular and subgrade soils were 85 lb./ft³ and 121 lb./ft³, respectively. Table 33 shows the soil properties before and after the test for both soil layers. The CBR value of the subgrade layer, calculated from DCP tests, increased from 4 to 10, and E_{LWD} increased from 1,305 lb./in² to 2,031 lb./in². The CBR and E_{LWD} values of the granular layer did not change. Figure 211 presents the measured and predicted soil displacement over an increasing number of cycles. When compared to Test Nos. 5 and 6 (BX1100 and BX4100), the measured soil displacement was lower by about 28% for the first and second loading stages. For the third loading stage, the soil displacement exceeded the displacements measured during Test Nos. 5 and 6 by 11%. Comparing the measured to the predicted soil displacement demonstrates that the design method overpredicted the soil displacement by about 70%. Additionally, one advantage of using a woven geotextile is the complete separation of the granular and subgrade material, which eliminated aggregate punching into the subgrade layer.

Table 33. Soil properties before and after the test, woven geotextile

	Soil property	Initial value	Final value
Subgrade layer	CBR ¹ (%)	4	10
	CBR ² (%)	6	9
	CIV	4.1	6.3
	E _{LWD} (lb./in ²)	1305	2031
Granular layer	CBR ¹ (%)	5	6
	CBR ² (%)	5	8
	CIV	3.4	6.1
	E _{LWD} (lb./in ²)	435	435

¹ CBR values calculated from DCP tests

² CBR values calculated from Clegg impact test (Al-Amoudi et al. 2002)

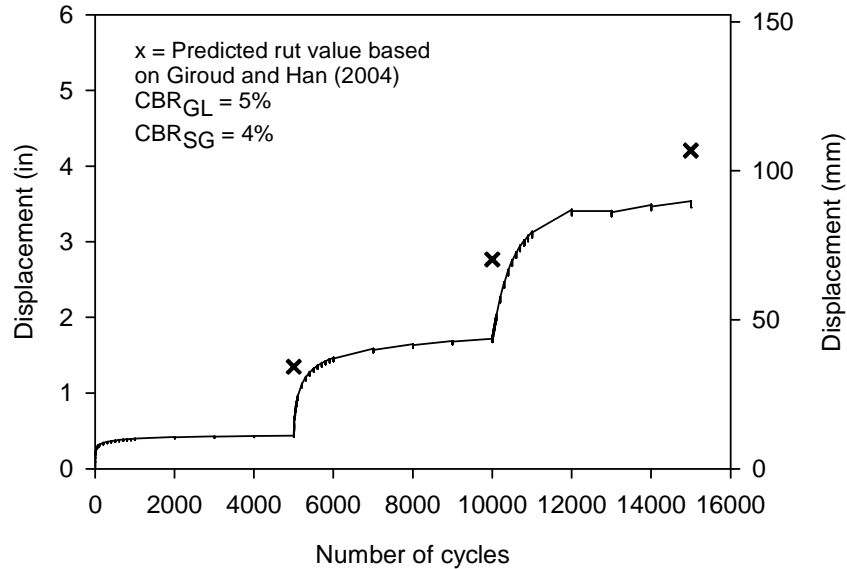


Figure 211. Soil displacement with increasing number of cycles, Woven geotextile

Test No. 8, Nonwoven Geotextile

In this test, a nonwoven geotextile (GEOTEX 601) was selected to stabilize the soft subgrade soil. The dry densities of the granular and subgrade soils before the test were 89 lb./ft³ and 120 lb./ft³, respectively. Table 34 shows the soil properties before and after the test for both soil layers. The CBR value of the subgrade layer increased from 4 to 9, and E_{LWD} increased from 1,015 lb./in² to 2,321 lb./in². No significant change was observed in the properties of the granular layer. Figure 212 presents the measured and predicted soil displacement over an increasing number of cycles. For the first 5,000 cycles, both the woven and nonwoven geotextiles showed similar performances. As the number of cycles increased, however, the nonwoven geotextile managed to reduce soil displacement by up to 14% relative to the woven geotextile. Further, for the first two loading stages, the nonwoven geotextile showed better performance than the geogrids. However, at the third loading stage, the soil displacement increased rapidly to exceed that measured with the geogrids (i.e., Test Nos. 4, 5, and 6). The predicted soil displacement at the three loading stages was about 70% higher than the measured one. The Giroud and Han (2004) method appears to overpredict rut values for soil stabilized with geotextiles. Visual inspection revealed that the geotextile also eliminated aggregate punching through the subgrade.

Table 34. Soil properties before and after the test, nonwoven geotextile

	Soil property	Initial value	Final value
Subgrade layer	CBR ¹ (%)	4	9
	CBR ² (%)	5	9
	CIV	3.6	6.5
	E _{LWD} (lb./in ²)	1015	2321
Granular layer	CBR ¹ (%)	6	7
	CBR ² (%)	7	8
	CIV	4.9	5.8
	E _{LWD} (lb./in ²)	580	580

¹ CBR values calculated from DCP tests

² CBR values calculated from Clegg impact test (Al-Amoudi et al. 2002)

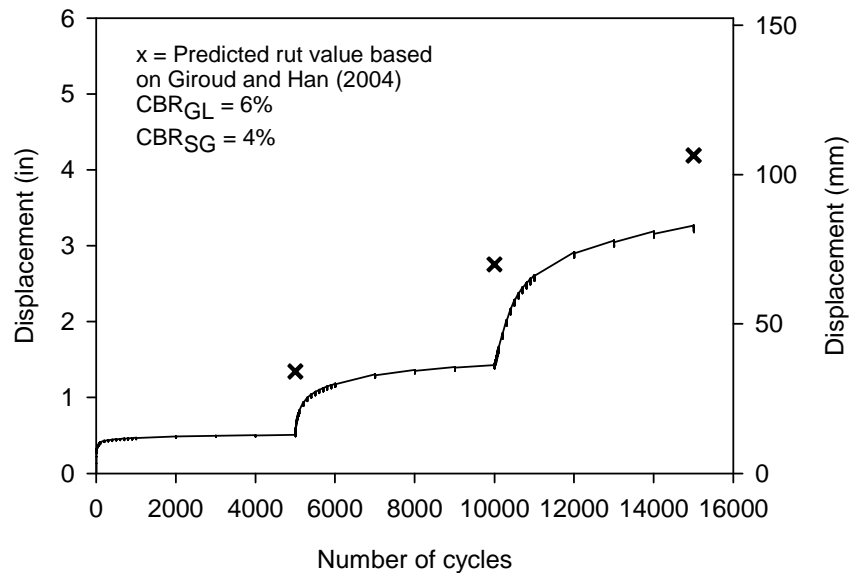


Figure 212. Soil displacement with increasing number of cycles, nonwoven geotextile

Test No. 9, BX1200 with Recycled Asphalt Pavement

Due to the increasing use of recycled material in shoulder applications, this test aimed to document the performance of a granular layer consisting of RAP material (Figure 213). Similar to the setup for Test No. 4, the underlying subgrade was stabilized by placing a BX1200 geogrid at the interface between the two layers. The dry densities of the granular and subgrade soils before the tests were 89 lb./ft³ and 122 lb./ft³, respectively. Table 35 shows the soil properties before and after the test for both soil layers. The CBR value of the subgrade layer increased from 4 to 8, and E_{LWD} increased from 1,160 lb./in² to 1,740 lb./in². There was no significant change in the properties of the granular layer before and after the test. Figure 214 shows the cumulative soil displacement over an increasing number of cycles. The figure also shows the predicted soil

displacement at 5,000, 10,000, and 15,000 cycles. On average, the measured soil displacement was about 20% higher than the predicted value. Compared to Test No. 4 (which used granular layer comprised of crushed limestone), the soil displacement was about 50% higher when the RAP material was used.



Figure 213. RAP material overlying soft subgrade soil

Table 35. Soil properties before and after the test, BX1200 with RAP

	Soil property	Initial value	Final value
Subgrade layer	CBR ¹ (%)	4	8
	CBR ² (%)	5	10
	CIV	4	7
	E _{LWD} (lb./in ²)	1160	1740
Granular layer	CBR ¹ (%)	5	5
	CBR ² (%)	6	6
	CIV	4.0	4.2
	E _{LWD} (lb./in ²)	580	580

¹ CBR values calculated from DCP tests

² CBR values calculated from Clegg impact test (Al-Amoudi et al. 2002)

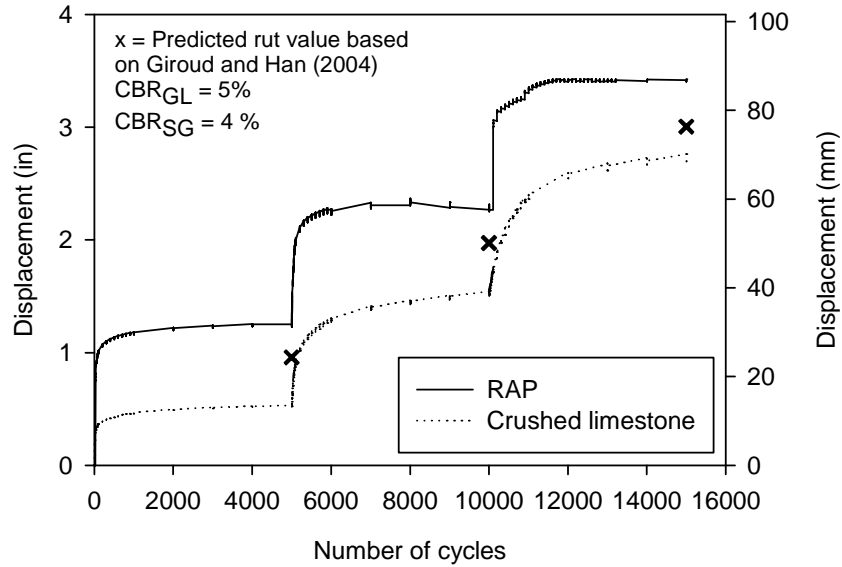


Figure 214. Soil displacement with increasing number of cycles, BX1200 with RAP

Test No. 10, Fly Ash Stabilization

This test evaluated the performance of unpaved shoulder systems that include chemical stabilization of the subgrade soil. Similar to Test Section No. 5 in the field evaluations, the subgrade soil in this laboratory study was stabilized using about 20% OGS class C fly ash. The moisture content of the subgrade material prior to mixing the fly ash was about 21%. The fly ash was mixed with the subgrade material, compacted in 3 in. lifts to a depth of 12 in., and allowed to cure for seven days at approximately 70° F. The granular material used in this test consisted of crushed limestone. To carry out the laboratory test with a CBR value comparable to that measured for Test Section No. 5, the strength of the subgrade layer was periodically measured using DCP testing. After seven days, the CBR value of the subgrade layer was equal to 21. The dry densities of the granular and subgrade soils before the tests were 88 lb./ft³ and 125 lb./ft³, respectively. Table 36 shows the soil properties before and after the test for both soil layers. The CBR value of the subgrade layer increased from 21 to 24 after the test was completed. Further, the E_{LWD} value increased from 4,061 lb./in² to 4,496 lb./in². There was no considerable change in the properties of the granular layer. Figure 215 shows the cumulative soil displacement over an increasing number of cycles, as well as the predicted soil displacements at 5,000, 10,000, and 15,000 cycles. On average, the predicted soil displacement was about 45% higher than the measured one. At 15,000 cycles, the measured soil displacement was 1.9 in., which was the lowest soil displacement out of all laboratory test samples. Stabilizing the subgrade material using fly ash reduced the soil displacement by 42%, 62%, and 61% relative to the tests using BX1200, BX1100, and BX4100 geogrids, respectively. Compared to the control test, fly ash stabilization reduced soil displacement by about six times.

Table 36. Soil properties before and after the test, OGS class C fly ash

	Soil property	Initial value	Final value
Subgrade layer	CBR ¹ (%)	21	24
	CBR ² (%)	23	25
	CIV	16.4	18.1
	E _{LWD} (lb./in ²)	4061	4496
Granular layer	CBR ¹ (%)	4	5
	CBR ² (%)	5	6
	CIV	4.1	4.4
	E _{LWD} (lb./in ²)	435	580

¹ CBR values calculated from DCP tests

² CBR values calculated from Clegg impact test (Al-Amoudi et al. 2002)

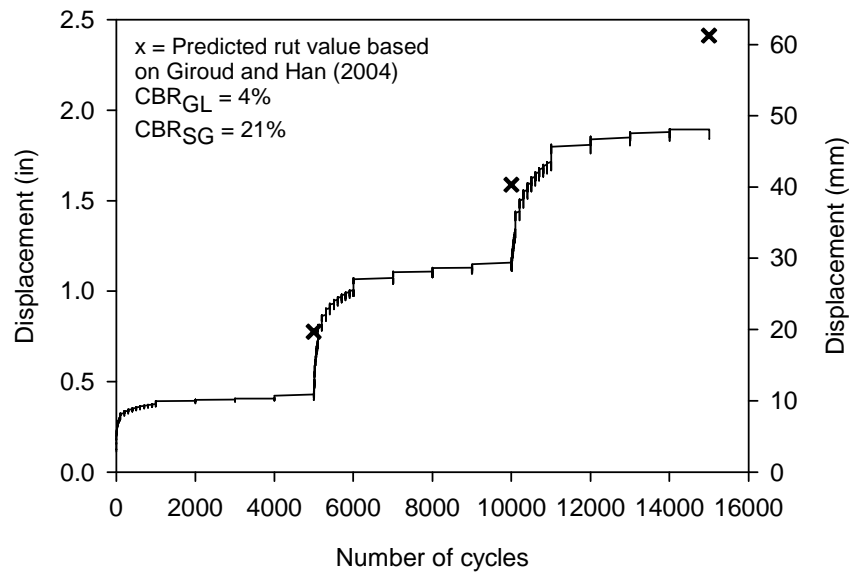


Figure 215. Soil displacement with increasing number of cycles, OGS class C fly ash

Summary and Conclusions

A laboratory study was conducted to simulate a shoulder section overlying a subgrade with a low CBR value. Cyclic loading in three loading stages was used to study the performance of the laboratory shoulder model stabilized with selected mechanical and chemical techniques. At each loading stage, one of three pressures was applied and sustained for 5,000 cycles at a frequency of 1 Hz. These pressures were 40, 80, and 120 psi. The soil properties before and after each test, as well as the cumulative soil displacement over the increasing number of cycles, were recorded. A summary of the soil properties measured during each test is shown in Table 37. Figure 216 compares the soil displacements measured during each test, while Figure 217 illustrates the measured versus predicted soil displacements. The highest deviation between the predicted and measured soil displacements was observed for the unanchored BX1200 geogrid.

The following conclusions were drawn from the laboratory study:

- The control test showed the highest soil displacement. The cumulative soil displacement after 15,000 cycles was 11.2 in.
- Locking the mechanical reinforcement between the box's c-channels to simulate field conditions by preventing the geogrid movement resulted in lower soil displacement values. Locking the mechanical reinforcements also resulted in smaller differences between measured and predicted soil displacements.
- The CBR and E_{LWD} values of the subgrade layer always increased after the test as a result of soil densification. The soil properties of the granular layer did not change significantly.
- The BX1200 geogrid reduces soil displacement by about 75% relative to the control test, while the BX1100 and BX4100 geogrids alleviated soil displacement by about 70% relative to the control test.
- All geogrids tested did not prevent aggregate punching through the subgrade layer. The approximate punching depth was 1 in.
- The woven and nonwoven geotextiles reduced the soil displacement by about 70% relative to the control test. The performance of the nonwoven geotextile, however, started to diminish at the third loading stage while soil displacement increased rapidly.
- Both woven and nonwoven geotextiles were successful in separating the granular and subgrade layers.
- Using RAP material and the BX1200 geogrid reduced the soil displacement by three times as much as the control test did. The soil displacement was 50% higher with RAP than with crushed limestone.
- Stabilizing the subgrade soil with 20% fly ash resulted in the lowest soil displacement. Fly ash stabilization reduced the soil displacement by 40% relative to Test No. 4 (BX1200 with crushed limestone). The recorded soil displacement was also six times lower than that of the control test.
- For all tests where the reinforcements were fixed to the steel box and for the fly ash stabilization test, the Giroud and Han (2004) semi-empirical method overpredicted the soil displacements at the end of each loading stage.
- In tests where the reinforcements were not fixed, the measured soil displacement was considerably higher than the predicted values.

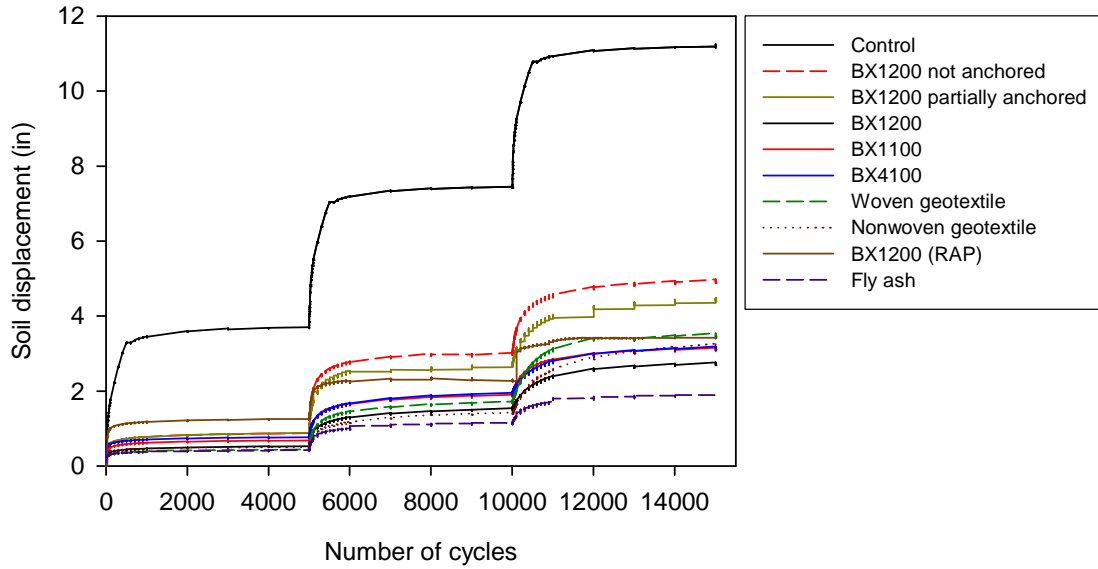


Figure 216. Summary of cumulative measured soil displacement for all tests

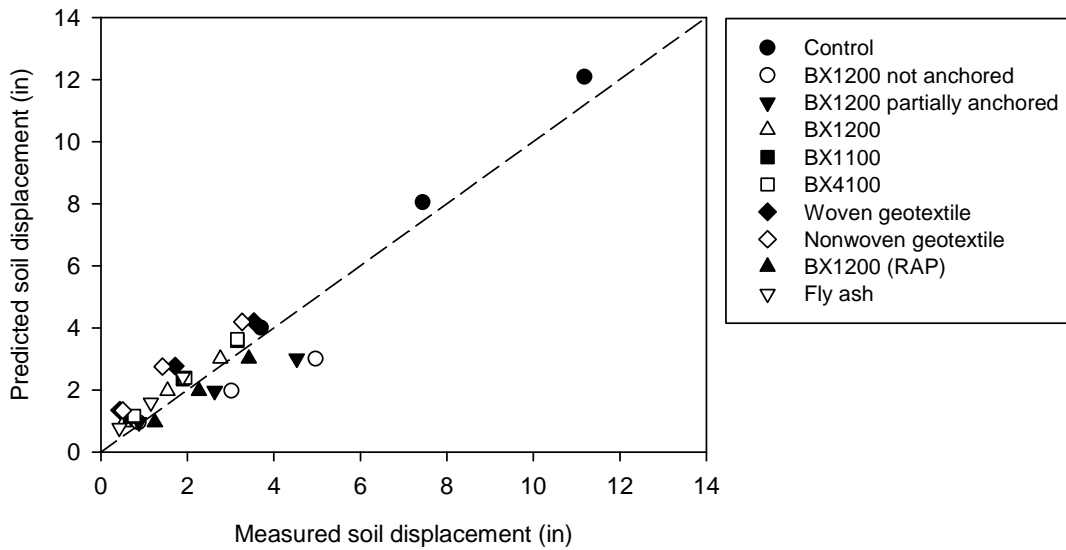


Figure 217. Comparison of measured and predicted soil displacement

Table 37. Summary of soil properties measured before and after each test

Test no.	Test description	Dry density of granular layer (pcf)	Dry density of subgrade layer (pcf)	CBR of granular layer (%)		CBR of subgrade layer (%)		CIV of granular layer		CIV of subgrade layer		E _{Granular} (lb./in ²)		E _{Subgrade} (lb./in ²)	
				Before test	After test	Before test	After test	Before test	After test	Before test	After test	Before test	After test	Before test	After test
1	Control	85	121	5	6	4	9	2.9	7.1	-	-	580	-	-	-
2	BX1200 ^a	89	118	5	5	4	7	3.7	5.4	3.2	6.2 ₇₂₅	435	435	1015	1740
3	BX1200 ^b	90	122	6	6	5	8	4.8	4.4	4.2	8.1	580	725	1160	1595
4	BX1200	88	119	5	6	4	7	4.3	5.3	4.1	7.8	580	725	1160	1450
5	BX1100	86	119	4	5	5	8	4.7	3.6	4.0	6.6	435	435	1305	1740
6	BX4100	90	122	4	5	5	9	3.7	4.1	3.8	8	435	870	1305	2321
7	Woven geotextile	85	121	5	6	4	10	3.4	6.1	4.1	6.3	435	435	1305	2031
8	Nonwoven geotextile	89	120	6	7	4	9	4.9	5.8	3.6	6.5	580	580	1015	2321
9	BX1200 with RAP	89	122	5	5	4	8	4.0	4.2	4.0	7.0	580	580	1160	1740
10	Fly ash	88	125	4	5	21	24	4.1	4.4	16.4	18.1	435	580	4061	4496

- a. Not anchored
- b. Partially anchored

SHOULDER DESIGN CHARTS

During the field reconnaissance phase, several granular shoulders were overlying a subgrade layer with a weighted average CBR less than 10. The research team, therefore, developed shoulder design charts to help mitigate the shoulder rutting that occurs due to the bearing capacity failure of the subgrade layer. The design charts can be a quick tool for designing new granular shoulders, provide a basis for QA/QC specifications, and predict the behavior of existing shoulders. The charts were developed from both the semi-empirical method proposed by Giroud and Han (2004), which was outlined in the Literature Review section of this report, and an equation developed by the U.S. Army Corps of Engineers in 1989 that predicts surface rutting for low-volume roads (Bolander et al. 1995). The equation is shown below:

$$RD = 0.1741 \frac{P_k^{0.4704} t_p^{0.5695} R^{0.2476}}{(\log t)^{2.002} C_1^{0.9335} C_2^{0.2848}} \quad (3)$$

Where, RD = rut depth, inches; P_k = equivalent single wheel load in kips; t_p = tire pressure, psi; t = thickness of top layer, inches; R = repetition of load or passes; C_1 = CBR of granular layer; C_2 = CBR of subgrade layer.

Using a standard axle load of 18 kips, a tire pressure of 80 psi, and a granular layer thickness of 6 in., Equation (3) can be simplified to the following:

$$RD = 9.6213 \frac{R^{0.2476}}{C_1^{0.9335} C_2^{0.2848}} \quad (4)$$

Figure 218 illustrates the first design chart for which the rut depth is plotted versus the subgrade CBR value for different load cycles. The chart was developed for a 6 in. thick granular layer, an 18 kips axle load, an 80 psi tire pressure, and a CBR value of 6 for the granular layer. To use this chart, the weighted average of the subgrade CBR must be calculated, as demonstrated in Appendix A. Field and laboratory rut depth measurements were used to validate this developed chart. The measured rut depths are in relatively good agreement with the charts developed using the Giroud and Han (2004) method, indicating that this chart is applicable for designing granular shoulders. The method proposed by the U.S. Army Corps of Engineers, however, appears to overestimate rut depth.

Several other charts were developed to help describe the influence of other factors, such as the CBR value of the granular layer, the number of cycles, and the axle load, on the magnitude of rut depth. According to the Giroud and Han (2004) method, the CBR value of the granular layer does not considerably affect the rut depth value. The effect of the granular layer CBR on rut depth is more noticeable when the equation proposed by the U.S. Army Corps of Engineers is used (Figure 219).

The effect of granular layer thickness on rut depth is demonstrated in Figure 220. The figure shows that increasing the thickness of the granular layer will result in a slight reduction in the expected rut depth value using the Giroud and Han (2004) design method. This emphasizes the fact that the CBR of the subgrade layer is still the governing factor controlling rut depth. The reduction in the rut depth value is more substantial, however, if the U.S. Army Corps of Engineers' design method is used.

Another plot was developed to demonstrate the effect of loads on rut development (Figure 221). The plot, which was developed for a 6 in. thick granular layer, a granular layer CBR value of 6, and 10,000 load cycles, shows that rut depth increases considerably with increasing axel loads for both the Giroud and Han (2004) and U.S. Army Corps of Engineers design methods. The traffic level and loads are therefore an important factor in rut depth development.

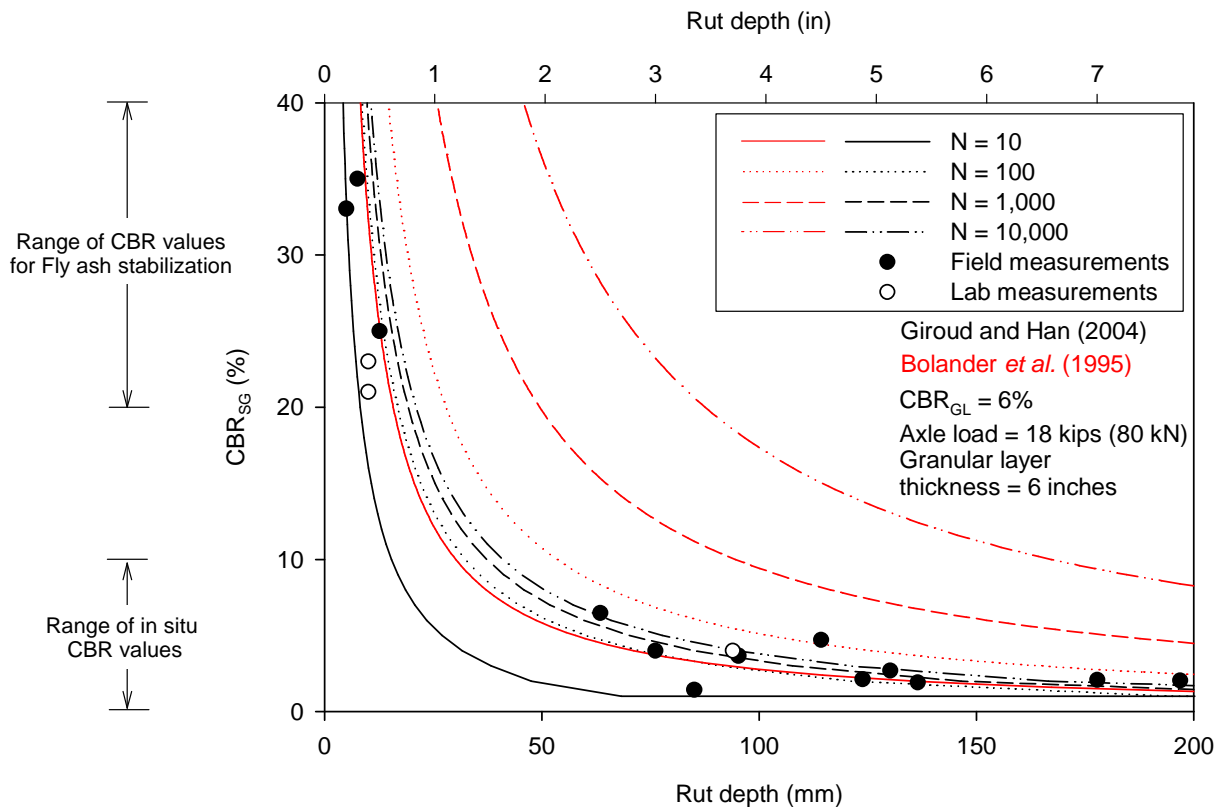


Figure 218. Relationship between subgrade CBR and expected granular shoulder rut depth

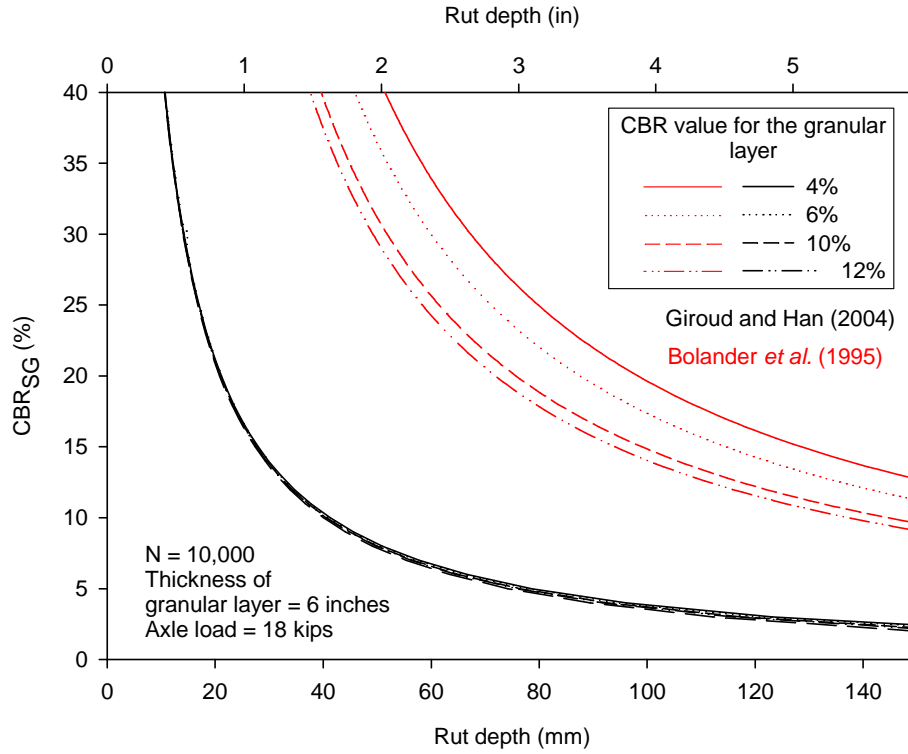


Figure 219. Influence of the granular layer CBR value on the magnitude of rut depth

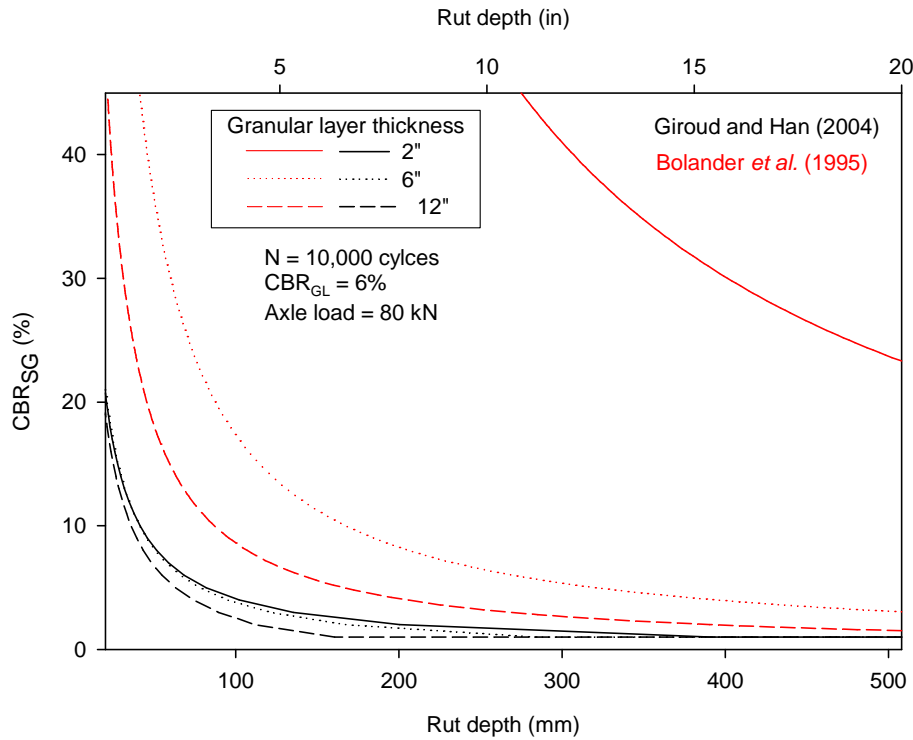


Figure 220. Influence of granular layer thickness on the magnitude of rut depth

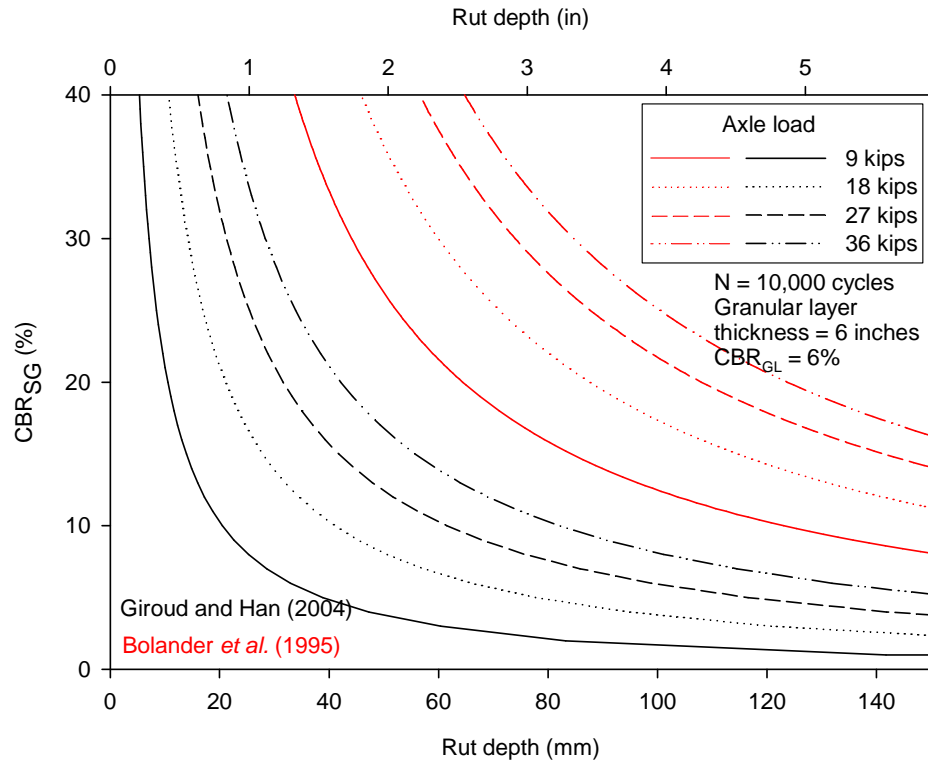


Figure 221. Influence of axle load on the magnitude of rut depth

ECONOMIC EVALUATIONS OF SHOULDER MAINTENANCE AND CONSTRUCTION

This investigation of economic considerations examined both possible improvements and possible repairs for aggregate shoulders. The analysis of each of these procedures should be considered separately.

On the one hand, improvements increase the level of service and reduce maintenance effort. That is, it is desirable to reduce the exposure of road users to edge ruts near the travel lanes, but it is also desirable to reduce the amount of maintenance activities that groom aggregate shoulders and fill edge ruts. Therefore, before an improvement is undertaken, road users have shoulders that function at some level, but an improvement of the shoulder conditions is desired. The following improvements were investigated in this section: (1) partially paved shoulders (both 2 ft. and 4 ft. widths), (2) foamed AC stabilization with HMA overlay, and (3) fully paved shoulders (both HMA and PC).

On the other hand, the repairs investigated in this section address problems with soft aggregate shoulders. Before a repair is undertaken, the affected roads are observed to have shoulders that have very limited functionality, especially for heavy vehicles. After the repair is undertaken, the result is a full-width aggregate shoulder that provides the standard level of service for a typical aggregate shoulder. As such, the post-repair maintenance costs that will be used in this analysis will be those found to be appropriate for a typical aggregate shoulder. The following repairs were investigated: (1) geogrid and (2) fly ash.

The following analysis is divided into three parts: maintenance costs, construction (investment) costs and life-cycle costs. Each of these parts addresses both the improvements and repairs investigated.

Sources of Cost Information

The cost estimating information for the economic evaluations of various shoulder alternatives come from a variety of sources, including interviews with Iowa DOT maintenance personnel, Iowa DOT standard costs, historical information on maintenance costs, an analysis of a particular bid letting, and historical information on construction costs. To allow for simple comparison, all costs have been calculated in costs per shoulder or lane-mile (for one side of the road).

Interviews

The researchers interviewed maintenance personnel in several locations to obtain information about current maintenance practices, productivity, and costs. Information was provided regarding equipment and personnel assignments and the number of miles of shoulder that can be maintained in a typical day. Material costs, such as aggregate, varied considerably by location. In some cases, for example, a maintenance garage will stockpile aggregate at a handy

location to allow for more convenient distribution. However, this approach incurs additional costs for stockpile handling and losses.

Standard Costs

During interviews, it was determined that the Iowa DOT has a standard cost system for accounting and record keeping. In 2006, Iowa DOT maintenance personnel were charged to projects at \$15.00 per hour, and a list was provided showing the hourly costs of various pieces of equipment.

Historical Maintenance Costs

The Iowa DOT accounting system allows managers to collect all costs from broad categories of activities and present them on an annual basis. Two of these categories included *maintenance of aggregate shoulders* and *maintenance of paved shoulders*. Average annual costs per mile were computed for these two categories.

Bid Letting Analysis

For unique items that have been constructed only once, the analysis of a particular bid letting that covers that process proved to be helpful.

Historical Construction Costs

The document entitled *Summary of Awarded Contract Prices for English & Metric Items*, published by the Iowa DOT Office of Contracts is an excellent source of historical construction cost information in Iowa. This document is published annually and summarizes the Iowa DOT's entire statewide experience in soliciting bids from contractors for Iowa DOT and selected local systems projects. Costs are listed according to an items code. The first four digits indicate the applicable Iowa DOT specification number and the last seven digits indicate the part of the specification to which the bid item applies. The item numbers are the same from year to year; this allows users to track prices from one year to the next. A twelve-month running average of the same information is also available at www.bidx.com. Under "Production States," select "Iowa," and then select the tab "Lettings." Look at the navigation bar at the right edge of the screen and select "Awarded Contract Prices (English Projects)."

The results of the cost analysis are summarized in Table 38, with the cost estimate and the source of each cost estimate given. For the purposes of this analysis, it is assumed that the transportation agency is maintaining a full-width aggregate shoulder and is contemplating various improvements, including partially paved shoulders, FA stabilization, or full-width paving. In addition, cost information is provided for situations where a transportation agency is maintaining a soft shoulder and wishes to execute a repair. In the following sections, a more detailed description of the cost calculations is provided, first for the maintenance costs and then for the construction costs. Graphs are provided that allow a visual comparison between

maintenance and construction costs. Finally, sample life-cycle cost analysis calculations are provided to serve as a guide for decision makers who wish to develop their own customized calculations.

Table 38. Summary of maintenance and construction costs

Objective of construction	Type of construction	Maintenance estimate		Construction estimate	
		Source	\$/Lane-mi.	Source	\$/Lane-mi.
Improvement	Partially paved shoulder	Interviews and standard costs	275*	Historical construction costs	30K—2 ft 47K—4 ft
Improvement	Foamed AC stabilization with HMA overlay	Historical maintenance costs	35*	Historical construction costs	81K
Improvement	Full paved shoulder	Historical maintenance costs	35*	Historical construction costs	159K—HMA 231K—PCC
Repair	Polymer Grid	Interviews and standard costs	550 **	Historical construction costs	37K
Repair	Fly Ash	Interviews and standard costs	550 **	Bid letting analysis	54K

* Maintenance cost estimate for full width aggregate shoulders is \$550 per lane mile per year based on interviews and standard costs

** Maintenance cost estimate for soft aggregate shoulders is \$1220 per lane mile per year based on interviews and standard costs

Maintenance Costs

Maintenance Costs for Typical Aggregate Shoulders

Interviews with Iowa DOT maintenance personnel indicate that there is considerable variability in maintenance requirements for aggregate shoulders, depending on traffic levels, road geometry, shoulder material, and weather. However, interview results indicated that it is typical to groom the shoulders twice per year and add aggregate to fill developing edge ruts every other year. The equipment and personnel used to accomplish this varies from one location to another and depends on the equipment available and the creativity of the garage personnel in developing homemade devices for specific tasks. However a typical grooming crew includes the following equipment train:

- Motor grader to blade material up against the edge rut
- Tractor (agricultural) with a blade for blading material off the pavement
- Pneumatic roller for compaction
- Sweeper for cleaning the pavement
- Truck with traffic control signs
- One worker for each vehicle

If aggregate is added to the edge rut, a fleet of trucks delivers the aggregate ahead of the equipment train, usually distributing the aggregate from a narrowed opening through the end gate to concentrate aggregate flow to the edge rut area.

Iowa DOT maintenance personnel provided standard costs for each piece of equipment and all personnel. Based on the procedure established in the interviews and the standards costs, a cost estimate was developed, as shown in Table 39.

Table 39. Maintenance costs for typical aggregate shoulders

I. Assumptions	
1. Shoulders maintained twice a year	
2. Operation rate is 4 mph including the efficiency of workers	
3. If new aggregate is added, area covered is 3 inches high and 6 inch wide (material added per mile 33.0 ton)	33
4. Three 45 minute round trips per mile are required for trucks to deliver edge rut aggregate	
II. Equipment	
	\$/hr.
Motor Grader	20.15
MD Tractor (A23)	14.40
Penumatic Roller (A57)	0.00
Truck for aggregate	7.18
Truck for traffic control (LD Truck)	7.18
Sweeper	0.00
III. Operators	
	\$/hr
Motor Grader	15.00
MD Tractor	15.00
Penumatic Roller	15.00
Truck for aggregate	15.00
Truck for traffic control	15.00
Sweeper	15.00
IV. Material	
	\$/ton
Aggregate	12.25

2121-742520 Type B Granular Shoulder in place
 Summary of Awarded Contract Prices, 2005, Iowa DOT
 Assume that stockpile expense is equivalent to placement expense

Table 39. Maintenance costs for typical aggregate shoulders (continued)

V. Maintenance operations

1. Groom-- Blade the aggregate from from the outer edge of the shoulder up to the pavement edge to cover the edge rut (without adding any new aggregate)

Equipment cost	\$/hr	hr/mi	\$/mi
Motor Grader	20.15	0.25	5.04
MD Tractor (A23)	14.40	0.25	3.60
Penumatic Roller (A57)	0.00	0.25	0.00
Truck for traffic control (LD Truck)	7.18	0.25	1.80
Sweeper	0.00	0.25	0.00
Total per mile =			10.43

Operator cost	\$/hr	hr/mi	\$/mi
Motor Grader	15.00	0.25	3.75
MD Tractor	15.00	0.25	3.75
Penumatic Roller	15.00	0.25	3.75
Truck for traffic control	15.00	0.25	3.75
Sweeper	15.00	0.25	3.75
Total per mile =			18.75

No. of maintenance times /year	2
Total cost of mile of road per year =	58.365

2. Add new aggregate to cover the edge rut

Equipment cost	\$/hr	hr/mi	\$/mi
Motor Grader	20.15	0.25	5.04
MD Tractor (A23)	14.40	0.25	3.60
Penumatic Roller (A57)	0.00	0.25	0.00
Truck for aggregate	7.18	2.25	16.16
Truck for traffic control (LD Truck)	7.18	0.25	1.80
Sweeper	0.00	0.25	0.00
Total per mile =			38.96

Operator cost	\$/hr	hr/mi	\$/mi
Motor Grader	15.00	0.25	3.75
MD Tractor	15.00	0.25	3.75
Penumatic Roller	15.00	0.25	3.75
Truck for aggregate	15.00	2.25	33.75
Truck for traffic control	15.00	0.25	3.75
Sweeper	15.00	0.25	3.75
Total per mile =			52.50

Material Cost /ton	\$/ton	tons/mi	\$/mi
Aggregate	\$ 12.25	33.00	\$ 404.25
Total per mile = \$			404.25

No. of maintenance times /year	1
Total cost of mile of road per year =	495.71

TOTAL ANNUAL COSTS

If edge of shoulder is within 1 ft from edge line	
Groom 2 X / yr and add aggregate 1 X / yr	554.07
Round to	550.00

If edge of shoulder is 2 ft or more from edge line	
Groom 1 X / yr and add aggregate every other yr.	277.04
Round to	275.00

The Iowa DOT captures the costs of maintenance activities using a series of function codes. The Iowa DOT provided the research team with the shoulder maintenance function codes associated with shoulder maintenance. The costs from 2002–2006, along with the five-year average, are shown below in Table 40. The costs are the total costs reported, and they were converted to lane-mile costs using 10,900 lane miles of granular shoulders.

For aggregate shoulders, function codes 634 (Repair with Aggregates) and 640 (Blade Shoulders) were reviewed, and estimates were made for granular shoulder maintenance activities. The historical data indicates that the maintenance cost for granular shoulders is approximately \$550 per lane-mile.

Table 40. Shoulder maintenance costs from 2002 to 2006

	Function	5 yr. avg.	2002	2003	2004	2005	2006
628	Repair Shoulder with Bituminous Mix	57,114	65,528	29,849	58,393	84,123	47,679
629	Seal Edge Ruts & Bituminous Shoulders	26,737	79,231	11,615	3,985	25,088	13,767
632	Shoulder Joint & Crack Filling/Sealing	17,130	18,504	18,267	406	11,383	37,089
633	Paved Shoulder Repair	12,303	4,494	6,115	13,819	30,549	6,538
634	Repair with Aggregates	2,675,873	4,282,869	1,859,514	1,599,800	3,583,381	2,053,800
636	Mow Shoulders	799,384	905,672	746,500	697,346	837,890	809,511
638	Hand Mowing	266,596	398,516	251,482	227,339	244,041	211,605
640	Blade Shoulders	1,869,264	1,751,425	1,660,393	1,776,391	1,908,611	2,249,499
641	Rebuilding Shoulders with Earth	43,049	74,101	50,069	23,464	53,992	13,620
643	Other Shoulder Maintenance Activities	346,456	335,833	262,282	405,448	422,049	306,670
	Totals	6,113,907	7,916,172	4,896,086	4,806,390	7,201,107	5,749,778

Figure 222 and Figure 223 show a cross section of a typical aggregate shoulder and provide a graph of the cumulative cost of maintenance over a number of years.

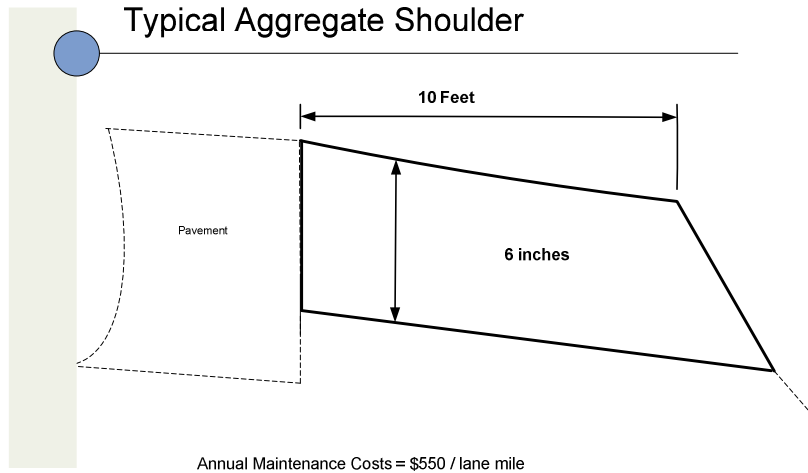


Figure 222. Typical aggregate shoulder

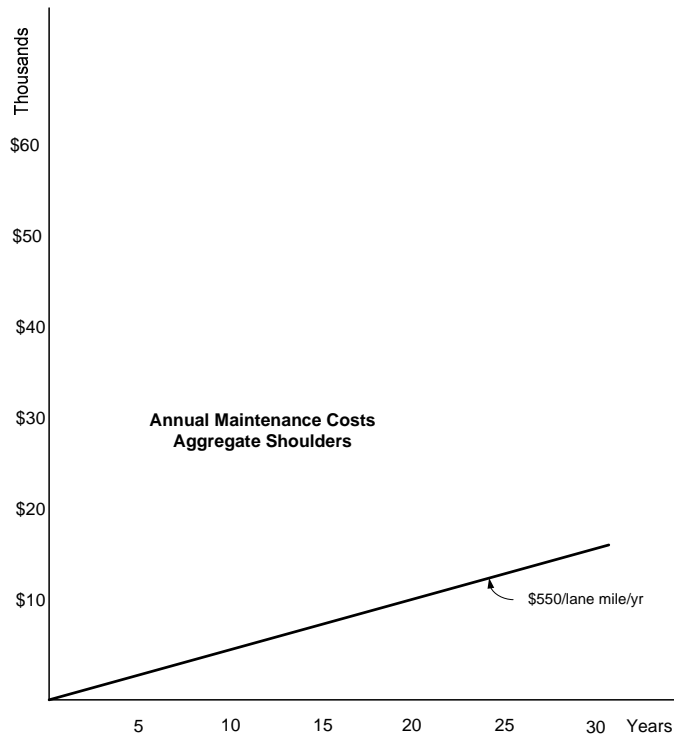


Figure 223. Annual maintenance cost for a typical aggregate shoulder

Maintenance Costs for Partially Paved Shoulders

Interviews with maintenance personnel indicated that the maintenance requirements for aggregate shoulders adjacent to 2 ft. and 4 ft. widening units are less than those for aggregate shoulders immediately adjacent to the driving lanes. However, insufficient information was available for a calculated estimate. Therefore, an assumption was made that maintenance

activity for aggregate shoulders adjacent to widening units would be half that for aggregate shoulders adjacent to active traffic lanes. Maintenance costs for all paved shoulders are based on historical costs that were collected from the Iowa DOT's maintenance cost accounting system and converted into an average cost per mile.

Maintenance Costs for Fully Paved Shoulders (Including Foamed AC Stabilization with HMA Overlay)

The maintenance costs for all shoulder types from 2002 to 2006, along with the five-year average, are shown in Table 41. The costs are the total costs reported, but these were converted to lane-miles using 4,600 lane-miles of paved shoulders. For paved shoulders, function codes 628 (Repair shoulder with bituminous mix), 629 (Seal edge ruts and bituminous shoulders), 632 (Shoulder joint and crack filling/sealing), and 633 (Paved shoulder repair) were reviewed, and estimates were made for paved shoulder maintenance activities. The historical data indicates that the maintenance cost for granular shoulders is approximately \$35 per lane mile.

Maintenance Costs for Soft Shoulders

Recently, the Iowa DOT has experienced a number of challenges with extremely soft shoulders on newly constructed roads. The problem usually becomes evident when trucks pull off the roadway and onto the shoulders and sink into the surface, producing deep ruts, and in some cases getting mired up to the axels, requiring a tow truck to extract them. The site is then left with deep ruts and mud from underneath the surface mixed with the granular surfacing. Additionally, granular surfacing and mud are often dragged onto the main trafficway during the extraction process. For instance, the Charles City maintenance garages often respond to such incidents and have developed procedures to deal with these problems that carry additional maintenance costs. When comparisons are made between the cost of maintaining shoulders in the soft condition and the cost of making improvements, it should be understood that the comparison is between having a functional shoulder and having a nonfunctional shoulder that in some cases is dangerous because it gives the false appearance of being a functional shoulder.

Soft Shoulder Incident Costs

The research team interviewed John Mixdorf, Charles City Maintenance Garage Supervisor, to obtain information to estimate the cost of responding to such incidents.

When an incident occurs, there are usually two parts to the response. The first part is to send a maintenance truck out to the site immediately after the incident occurs to sweep material off the roads. This usually requires one worker and a pickup truck and an hour of time. The second part of the response can occur several days later, if necessary. Generally, four workers are sent out with three trucks and a tractor that carries a blade. Since the area is soft, the Iowa DOT's experience is that a smaller tractor is more effective than a large road grader. One worker drives the tractor, another shovels, and two act as flaggers. Recently, the Iowa DOT has not had funding to provide new granular material, so the crew works the existing material to

improve conditions as much as possible. An estimate is provided based on hourly costs provided by Iowa DOT maintenance personnel.

If funding were available to replace aggregate, additional costs would be incurred. Based on their understanding of these incidents, researchers estimate that 3 in. of aggregate would have to be spread over an area 10 ft. wide and 300 ft. long. The requirement would be approximately 48 tons or four truckloads of aggregate.

It should be noted that, when the repairs are complete, the soft shoulder condition that caused the original incident would still exist. The repairs described here are only cosmetic. In some cases, maintenance workers hesitate to make the repairs, because if the repairs are not made, the problem is more obvious and would give large vehicles a visual indication not to pull off the paved portion of the road.

The Charles City Maintenance Garage is responsible for 40 miles of US 218 (Avenue of the Saints, AADT = 7,700), approximately 30% of which has soft shoulders. Incidents occur in the months of April through November at a rate of approximately three every month. During the winter months the ground is frozen and therefore not soft, and no incidents occur. A cost estimate based on the previous information is provided in Table 41.

Table 41. Cost estimate for soft shoulder maintenance

Description	QTY Units	Unit Price	Amount	Unit Price Reference
Initial Response (one hour)				
Worker	1.00 HR	15.00	15.00	Cost provided by Ames Maintenance Garage
Truck	1.00 HR	7.18	7.18	Cost provided by Ames Maintenance Garage
Total			22.18	
Cosmetic Clean Up (2.5 hours)				
Workers (Crew of 4)	10.00 HR	15.00	150.00	Cost provided by Ames Maintenance Garage
Tractor with Blade	2.50 HR	14.40	36.00	Cost provided by Ames Maintenance Garage
Trucks (3 each)	7.50 HR	7.18	53.85	Cost provided by Ames Maintenance Garage
Total			239.85	
Replace aggregate				
Granular Shoulder, Type A	48.75 TONS	12.88	627.90	2005 Iowa DOT Unit Prices Item 2121-7425010

Notes on Aggregate Replacement:

Cost for Iowa DOT crews to place aggregate is assumed to be similar to that for state wide average for contractors in referenced document
 Replace aggregate 3 in deep, 10 ft wide and 300 ft long (half the standard depth for a shoulder)
 In place density is 135 lb/cu ft.

Grand Total per incident	889.93
Incidents per year (3 per month for 9 months)	27.00
Cost per year	24,028.11
Miles affected (30% of 120 lane miles)	36.00
Cost per mile per year	667.45

Construction (Investment) Costs

Improvements for Aggregate Shoulders

The Iowa DOT has two standards for upgrading from granular shoulders to paved shoulders: one for non-NHS routes (generally under 3,000 AADT) and one for NHS routes (generally over 3,000 AADT). When a granular shoulder is upgraded to a paved shoulder, it is often done as part of a rehabilitation project that involves an HMA overlay of the traffic lanes. Under these circumstances, the total required minimum thickness includes the thickness of the overlay, since the overlay will be carried onto the shoulders.

Non-NHS highways receive 2 ft. widening units that are at least 8 in. thick. NHS highways receive 4 to 6 ft. widening units that are at least 6 in. thick.

The risk of structural failure is greatest immediately after the first lift of hot mix is placed next to the pavement. For example, if a 4 in. overlay is planned and a shoulder is intended to be 6 in. thick (NSH Standards), a 2 in. base course would need to be placed next to the pavement across the width of the widening unit. This 2 in. base course may not be able to withstand the loads of truck traffic before the total thickness of 6 in. is provided. For this reason, a minimum thickness of 3 in. for the hot mix base course is required. When this is done, a shoulder that is slightly thicker than the minimum requirements will result, because the overlay must be maintained at the specified overlay thickness. In this example, the resulting shoulder will be 7 in. thick.

Additional thickness will be provided in areas of known structural problems. Few structural failures have been reported, and the ones that have been reported have occurred in the base course before the overlay has been placed.

Funding

Safety funding is often used to finance shoulder construction projects. When safety funding is sought, the shoulder projects compete against all other safety projects, such as grade separations at high-incident crash locations. Despite this competition, several shoulder projects have been funded in this way.

Another source of funding is 3R funding. This funding is distributed according to the needs of the system, especially with regard to distress and facility condition.

One possible strategy for providing more paved shoulders would be to build paved shoulders in as many places as can be justified using safety funding, then fill in the gaps using 3R funding.

Construction Costs for Partially Paved HMA Shoulders

The cost estimate for partially paved shoulders is based on the following construction procedure:

1. Excavate and salvage existing aggregate shoulder material to stockpile
2. Place special backfill base
3. Place HMA widening unit base hot mix asphalt and tack coat
4. Blade salvaged aggregate shoulder material from stockpile and shape

Based on the bid tabulation calculations from Project HES-030-4 (72)-2H-8 (HMA Paved Shoulder–New, Boone County, bid order 151, letting date 12/20/05), the cost of mobilization, preparation, traffic control, and clean up are 15% of the costs for the other costs described in the previous sections, so that amount was added to the estimate. This project involved placing 4 ft. partially paved shoulders on a four-lane portion of US 30 from I-35 west to IA 17 in Story and Boone Counties. The cost estimate for both 2 ft. and 4 ft. partially paved shoulders is provided in Table 42. Figure 224 shows a cross section of the partially paved shoulders. Figure 225 and Figure 226 illustrate cumulative maintenance and capital costs associated with partially paving shoulders.

Table 42. Construction costs for partially paved shoulders

Description	QTY Units	Unit Price	Amount	Unit Price Reference
Partially Paved HMA Shoulder-- 2' non NHS				
Base Widening HMA Mix	510.58 TONS	21.51	10,982.49	2005 Awarded Contract Prices Iowa DOT Item: 2213-8200000
Binder PG 58-28	30.63 TONS	194.98	5,973.13	2005 Awarded Contract Prices Iowa DOT Item: 2303-0245828
CRS-2 Tack	117.22 GAL	1.12	131.28	2005 Awarded Contract Prices Iowa DOT Item: 2307-0600454
Excavation Class 13	260.83 CY	10.29	2,683.96	2005 Awarded Contract Prices Iowa DOT Item: 2213-2713300
Special Backfill	369.60 TONS	12.64	4,671.74	2005 Awarded Contract Prices Iowa DOT Item: 2102-0425070
Blading and Shaping Shoulder Material	52.80 STA	29.77	1,571.86	2005 Awarded Contract Prices Iowa DOT Item: 2214-7450050
Subtotal			26,014.46	
Allowance for mob., prep. traffic control, and clean up.		15%	3,902.17	
Total			29,916.63	

Notes:

Per Iowa DOT standard road plan RG-8 rev. 10/17/06
 Width = 2 ft. Thickness = 8 in.

Partially Paved HMA Shoulder -- 4', NHS				
Base Widening HMA Mix	765.60 TONS	21.51	16,468.06	2005 Awarded Contract Prices Iowa DOT Item: 2213-8200000
Binder PG 58-28	45.94 TONS	194.98	8,956.60	2005 Awarded Contract Prices Iowa DOT Item: 2303-0245828
CRS-2 Tack	234.43 GAL	1.12	262.56	2005 Awarded Contract Prices Iowa DOT Item: 2307-0600454
Excavation Class 13	391.25 CY	10.29	4,025.94	2005 Awarded Contract Prices Iowa DOT Item: 2213-2713300
Special Backfill	739.20 TONS	12.64	9,343.49	2005 Awarded Contract Prices Iowa DOT Item: 2102-0425070
Blading and Shaping Shoulder Material	52.80 STA	29.77	1,571.86	2005 Awarded Contract Prices Iowa DOT Item: 2214-7450050
Subtotal			40,628.51	
Allowance for mob., prep. traffic control, and clean up.		15%	6,094.28	
Total			46,722.78	

Note:

Per Iowa DOT standard road plan RG-8 rev. 10/17/06

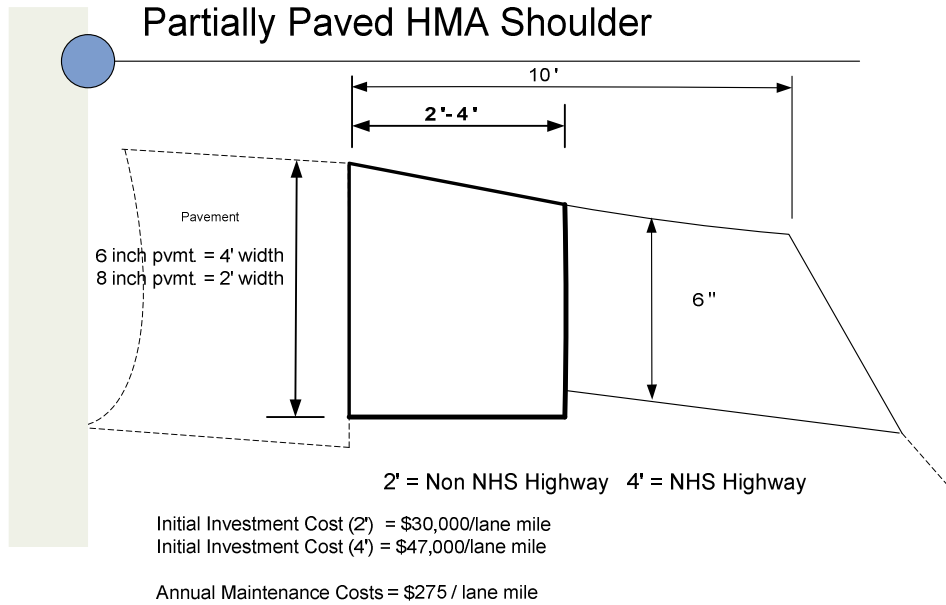


Figure 224. Partially paved HMA shoulder

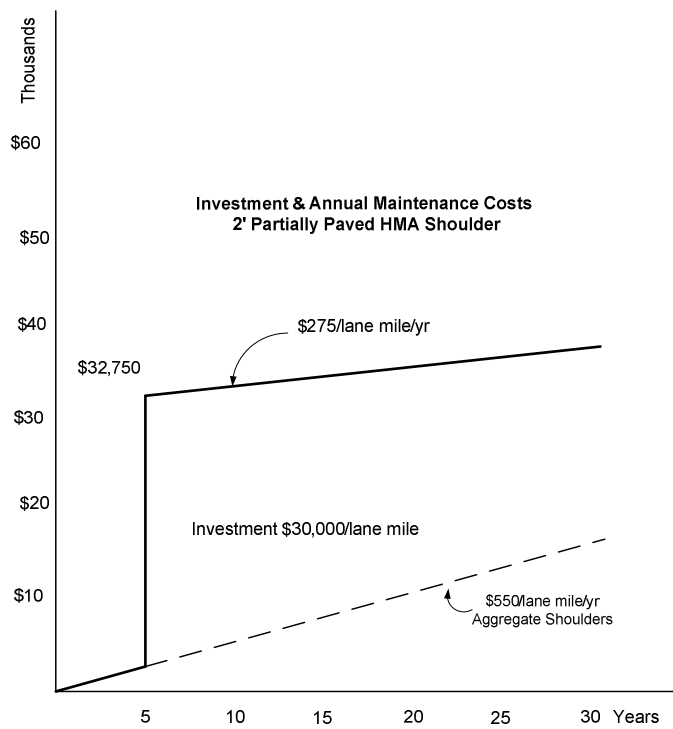


Figure 225. Construction costs for two ft. partially paved HMA shoulder

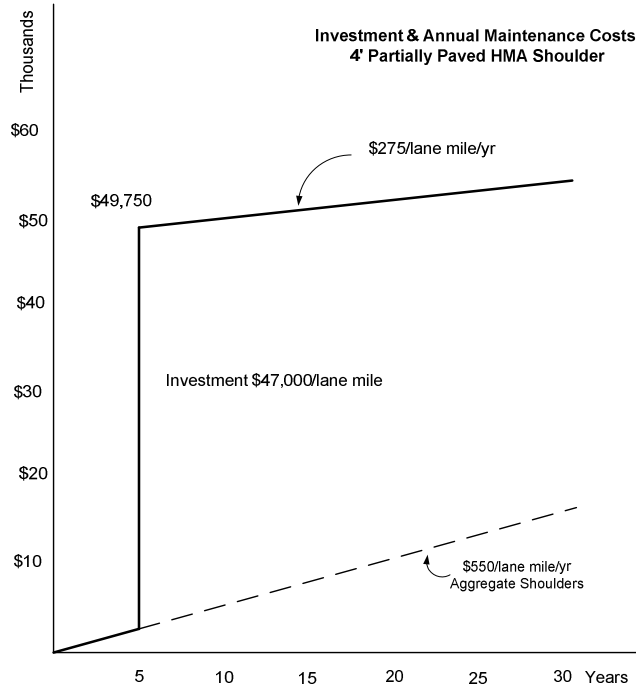


Figure 226. Construction costs for four ft. partially paved HMA shoulder

Construction Costs for Foamed AC with HMA Overlay

In some cases, stabilizing the existing shoulder materials with FA and providing an overlay may be a viable alternative that should be considered. This process could possibly be applied to highly deteriorated existing asphalt shoulders or to aggregate shoulders. The cost estimate is based on the following construction procedure:

1. Conduct full-depth pulverization, add FA binder, and immediately compact the material.
2. Place HMA overlay on shoulders in conjunction with mainline overlay construction.

An allowance of \$5,000 per mile of shoulder was provided for mobilization, preparation, traffic control, and clean up. The cost of maintaining the resulting shoulder was assumed to be the same as other paved shoulders and was based on historical information from the Iowa DOT’s maintenance cost accounting system. The cost estimate for foamed AC stabilization with HMA overlay is provided in Table 43. Figure 227 shows a cross section of the construction, while Figure 228 illustrates cumulative maintenance and capital costs associated with this improvement.

Table 43. Cost estimate for foamed AC with HMA overlay

Description	QTY	Units	Unit Price	Amount	Unit Price Reference
Foamed AC with HMA Overlay					
Full Depth Reclamation	4,693.00	SY	2.40	11,263.20	2005 Awarded Contract Prices Iowa DOT Item: 2318-1001210
Asphalt Stabilizing Agent (Foamed Asphalt)	61.24	TONS	251.00	15,371.24	2005 Awarded Contract Prices Iowa DOT Item: 2318-1001220
HMA, Intermed or Suf, No Spl Friction Req, 1.2 in., 300K ESAL (Should	1,531.20	TONS	20.29	31,068.05	2005 Awarded Contract Prices Iowa DOT Item: 2303-0023500
Binder PG 58-28	91.87	TONS	194.98	17,913.20	2005 Awarded Contract Prices Iowa DOT Item: 2303-0245828
Subtotal				75,615.69	
Allowance for mob., prep. traffic control, and clean up.			\$5K per mile max	5,000.00	
Total				80,615.69	

Notes:

Density of shoulder before recycling is 145 lb/ft³

Density of HMA overlay is 145 lb/ft³

Added foamed asphalt is 4% by weight

Added hot mix binder is 6% by weight

Reclamation and overlay width 8 ft.

Reclamation and overlay and overlay depth 6 in.

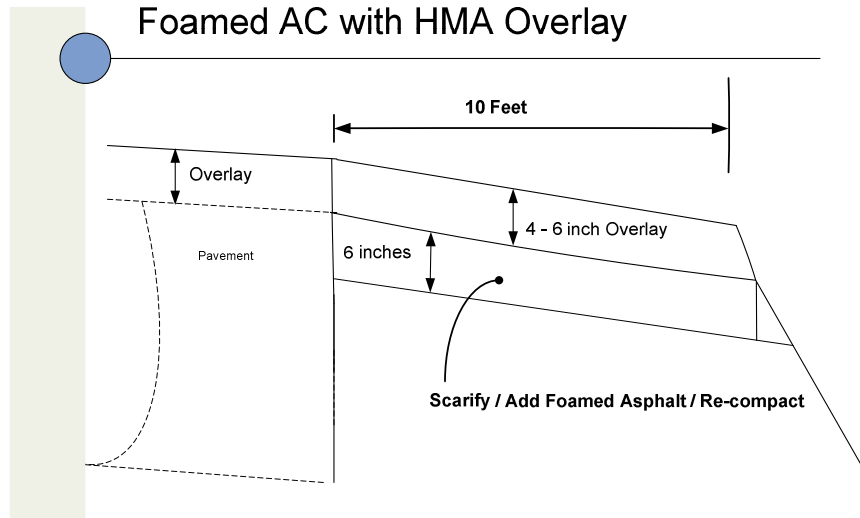


Figure 227. Shoulder repair using foamed asphalt with HMA overlay

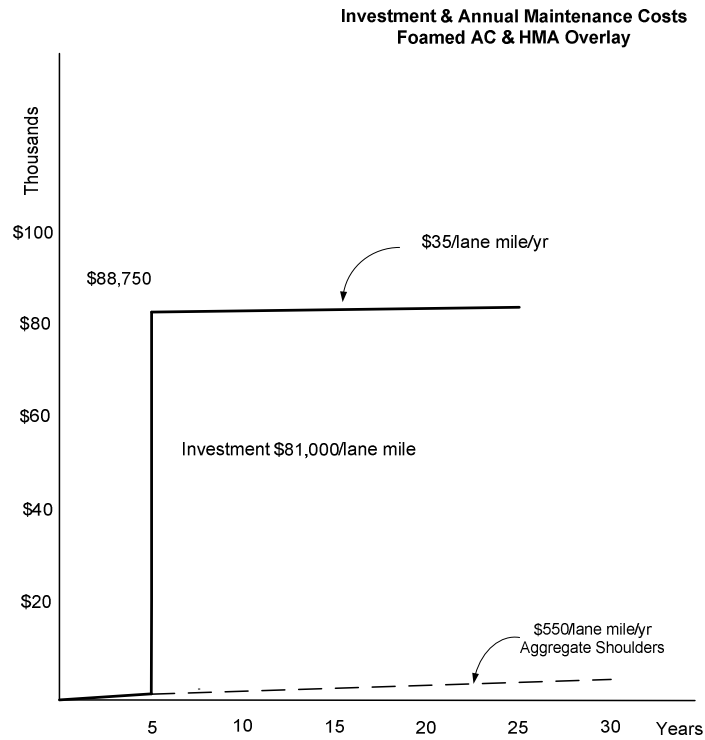


Figure 228. Annual maintenance cost for foamed asphalt with HMA overlay

Construction Costs for Full-Width Paved Shoulders

Upgrades are sometimes made to full-width paved shoulders. When they are made, alternative bids are usually solicited for 8 in. HMA and 7 in. PCC shoulders. Cost estimates were developed for fully paved shoulders (HMA and concrete) that are constructed according to standard plans. An allowance of \$5,000 per mile is provided for incidentals other than paving and base construction, and an item was included to cover the cost of excavating the existing aggregate shoulders. If the paved shoulders are added to a newly constructed pavement in an area that is not under traffic, it is likely that this allowance could be reduced considerably. The cost estimates for both full-width PCC pavement and HMA shoulders are provided in Table 44. Figure 229 shows a cross section of these shoulders, while Figure 230 and Figure 231 illustrate cumulative maintenance and capital costs associated with the PCC and HMA full-width shoulders, respectively.

Table 44. Cost Estimate for full-width paved shoulder construction

Description	QTY	Units	Unit Price	Amount	Unit Price Reference
Full Width Paved Shoulder (HMA)					
Excavation Class 13	587.50	CY	10.29	6,045.38	2005 Awarded Contract Prices Iowa DOT Item: 2213-2713300
Paved Shoulder HMA Mixture, 8 in	5,866.67	SY	20.70	121,440.00	2005 Awarded Contract Prices Iowa DOT Item: 2122-5500080
Special Backfill, 6 in thick	2,079.00	TONS	12.64	26,278.56	2005 Awarded Contract Prices Iowa DOT Item: 2102-0425220
Subtotal				153,763.94	
Allowance for mob., prep. traffic control, and clean up.			\$5K per mile max	5,000.00	
Total				158,763.94	

Note:

Shoulder is 10 ft. wide

Full Width Paved Shoulder (PCCP)					
Excavation Class 13	587.50	CY	10.29	6,045.38	2005 Awarded Contract Prices Iowa DOT Item: 2213-2713300
Paved Shoulder P. C. Concrete, 7 in.	5,866.67	SY	32.95	193,306.67	2005 Awarded Contract Prices Iowa DOT Item: 2122-5500080
Special Backfill, 6 in thick	2,079.00	TONS	12.64	26,278.56	2005 Awarded Contract Prices Iowa DOT Item: 2102-0425220
Subtotal				225,630.60	
Allowance for mob., prep. traffic control, and clean up.			\$5K per mile max	5,000.00	
Total				230,630.60	

Note:

Shoulder is 10 ft. wide

Full Width Paved Shoulders

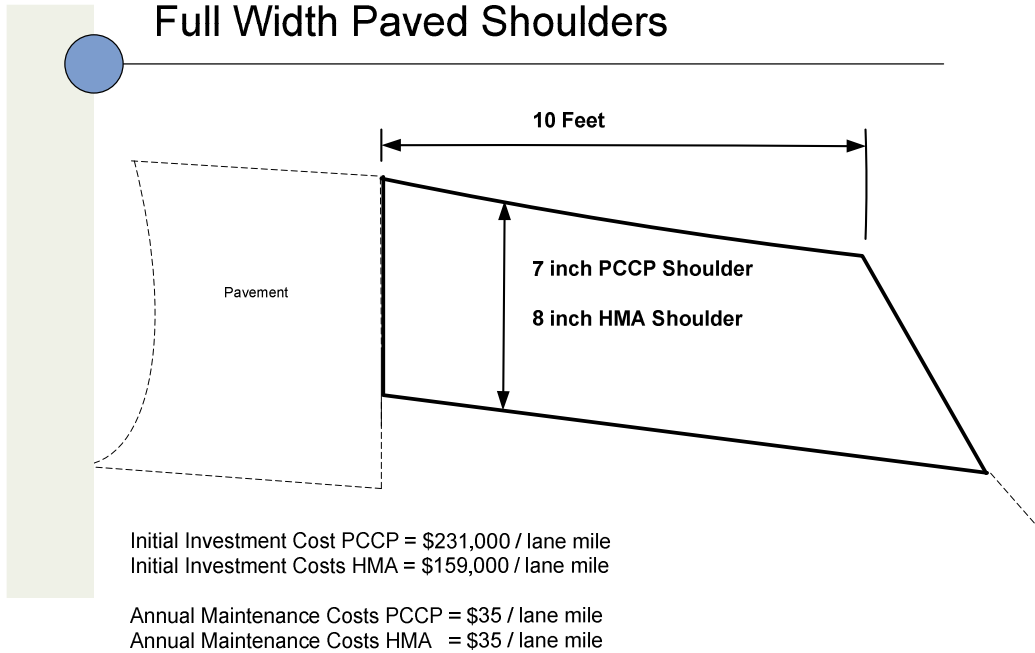


Figure 229. Full-width paved shoulders

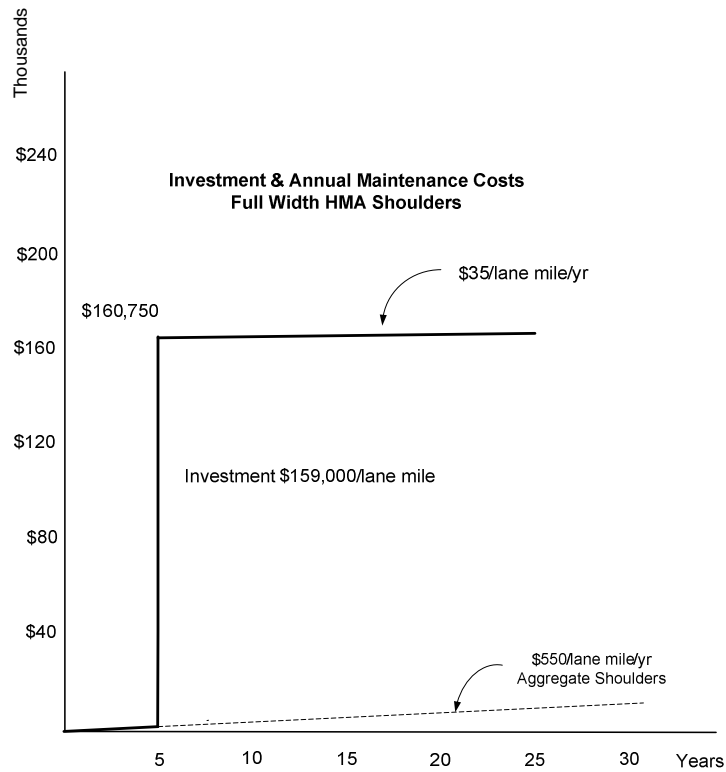


Figure 230. Annual maintenance costs for full-width HMA shoulders

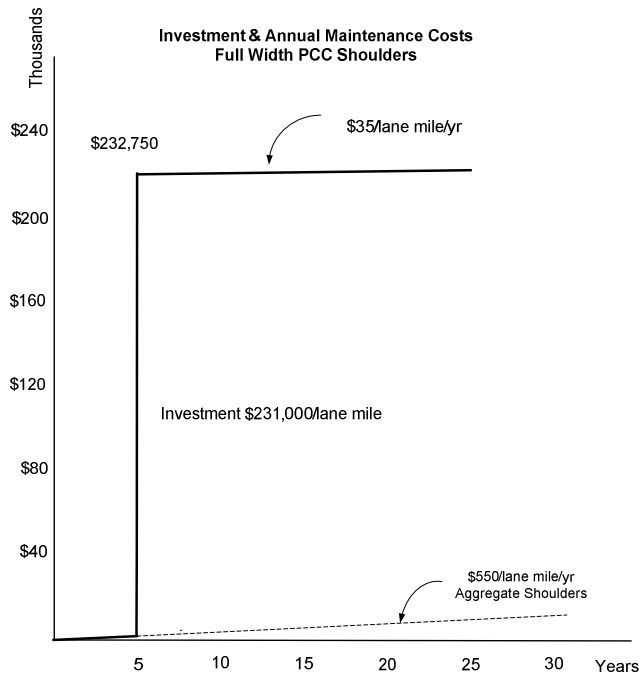


Figure 231. Annual maintenance costs for full-width PCC shoulders

Construction Costs for Soft Shoulder Repairs

To address the challenges of soft shoulders, two construction methods have been demonstrated within this project: geogrid reinforcement and fly ash stabilization. The procedure for geogrid reinforcement is as follows:

1. Blade and stockpile existing shoulder aggregate.
2. Place geogrid rolls.
3. Salvage as much existing aggregate as possible and return it to cover the geogrid (assume 50% loss).
4. Top off the shoulder with virgin aggregate.
5. Compact and clean up.

The cost for this repair was estimated by analyzing historical construction costs. The construction procedure for fly ash stabilization is as follows:

1. Blade and stockpile existing shoulder aggregate.
2. Stabilize subgrade with fly ash using full-depth reclamation equipment.
3. Salvage as much existing aggregate as possible and return it to cover the geogrid (assume 50% loss).
4. Top off the shoulder with virgin aggregate.
5. Compact and clean up.

The cost for this repair was estimated by analyzing the letting results for Contract ID 90-0347-133 (Wapello County, bid order 305, letting date 09/19/06). The costs selected for analysis were the average of three bids rather than the low bid, because Iowa DOT personnel suggested that this average would be more representative of future costs. They speculated that the low bidder underbid the actual costs to some extent. The cost estimates for both geogrid and fly ash shoulder repairs are provided in Table 45. Figure 232 and Figure 233 show a cross section of the geogrid and fly ash repairs, respectively. Figure 234 and Figure 235 illustrate cumulative maintenance and capital costs associated with the geogrid and fly ash repairs, respectively.

An allowance of 15% of the costs for mobilization, preparation, traffic control, and clean up was provided. An upper limit of \$5,000 per mile was imposed based on input from the technical advisory committee. This upper limit was applied to the fly ash repair, but not to the geogrid repair. After soft shoulder issues have been addressed with these procedures, it is assumed that normal granular shoulder maintenance costs resume.

Table 45. Cost estimate for geogrid and fly ash shoulder repairs

Description	QTY	Units	Unit Price	Amount	Unit Price Reference
Polymer Geogrid Repair for Soft Shoulders					
Reclaim and Stockpile Present Surfacing Material	1,267.20	CY	3.50	4,435.20	2005 Awarded Contract Prices Iowa DOT Item: 2126-8300200
Subgrade Stabilization Material, Polymer Grid	4,694.00	SY	2.93	13,753.42	2005 Awarded Contract Prices Iowa DOT Item: 2113-0001100
Replace reclaimed aggregate (use place only item)	739.20	TONS	3.66	2,705.47	2005 Awarded Contract Prices Iowa DOT Item: 2121-7425011
Purchase new aggregate	739.20	TONS	12.64	9,343.49	See note below
Blading and Shaping Shoulder Material	52.80	STA	29.77	1,571.86	2005 Awarded Contract Prices Iowa DOT Item: 2214-7450050
Subtotal				31,809.44	
Allowance for mob., prep. traffic control, and clean up.			15%	4,771.42	
Total				36,580.85	

Notes:

Placement of reclaimed materail based on "Granular Shoulder Type A, Place Only 2121-7425011"

Purchase of new aggregate based on:

"Granular Shoulders, Type B 2121-7425050" minus "Granular Shoulder Type A, Place Only 2121-7425011"

Type B placement is the more likely senario, however the quantities of "Type A place only" were small in 2005, so the "Type B Place Only" was judged by the authors to be the better selection for pricing

223

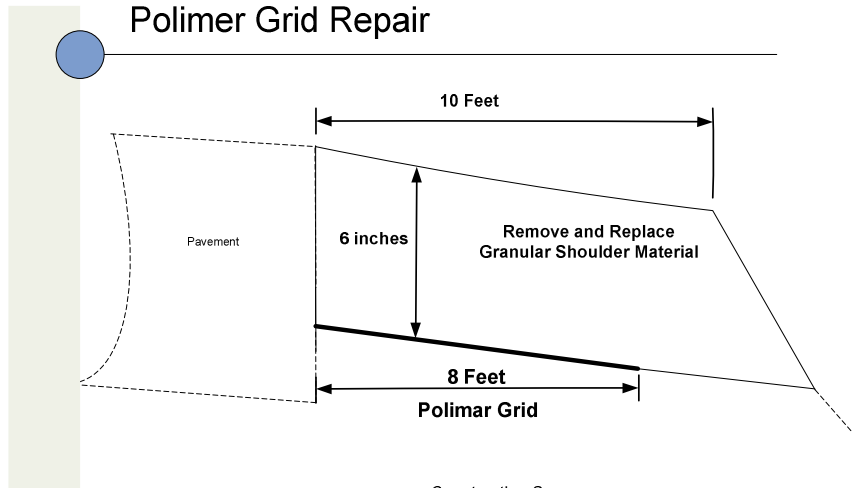
Fly Ash Stabilization for Soft Shoulders					
Reclaim and Stockpile Present Surfacing Material	405.00	CY	14.19	5,746.95	See note below, Iowa DOT Item: 2102-130300
Granular Shoulders, Type A	991.00	TONS	12.70	12,585.70	See note below, Iowa DOT Item: 2214-102100
Blading and Shaping Shoulder Material	52.80	STA	109.76	5,795.33	See note below, Iowa DOT Item: 2528-101000
('Square Meter' Item) Stabilized Soil	4,693.00	SY	2.36	11,075.48	See note below, Iowa DOT Item: 2599-999911
('Megagram' Item) Fly Ash, Class C	339.00	TONS	40.38	13,688.82	See note below, Iowa DOT Item: 2601-103000
Subtotal				48,892.28	
Allowance for mob., prep. traffic control, and clean up.			\$5K/mile maximum	5,000.00	
Total				53,892.28	

Notes:

Based on the average of 3 contractor bids for Constract ID: 90-0347-133, Wapello County, Bid Order 305, Letting Date: 09/19/06

The original bid was in metric units and has been converted to English Units.

Iowa DOT Project Personnel Suggested using the average of 3 bids because they did not believe that the low bid could be repeated in the future.



- Construction Sequence
1. Remove & store existing aggregate
 2. Place polimer grid
 3. Replace / re-compact aggregate
 4. Add aggregate & bring to grade

Initial Investment Cost = \$37,000 / lane mile

Annual Maintenance Costs = \$550 / lane mile

Figure 232. Polymer grid repair

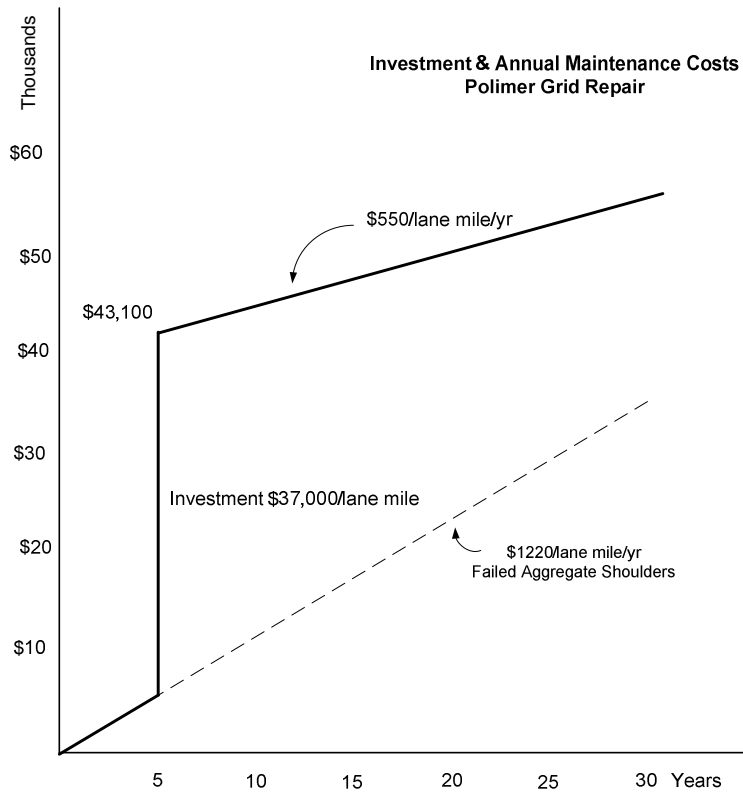
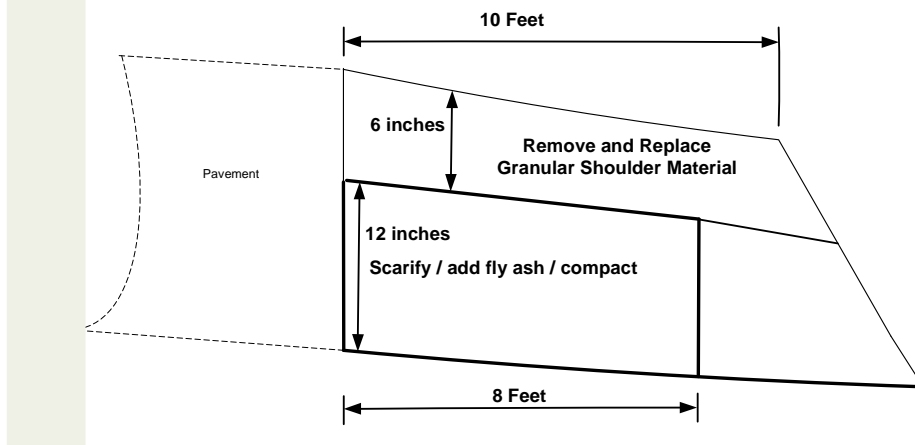


Figure 233. Annual maintenance costs for geogrid repair

Fly Ash



- Construction Sequence
1. Remove & store existing aggregate
 2. Scarify one foot deep with fly ash and compact
 3. Replace / re-compact shoulder aggregate
 4. Add aggregate & bring to grade

Initial Investment Cost = \$54,000 / lane mile

Annual Maintenance Costs = \$550 / lane mile

Figure 234. Maintenance of shoulder sections using fly ash

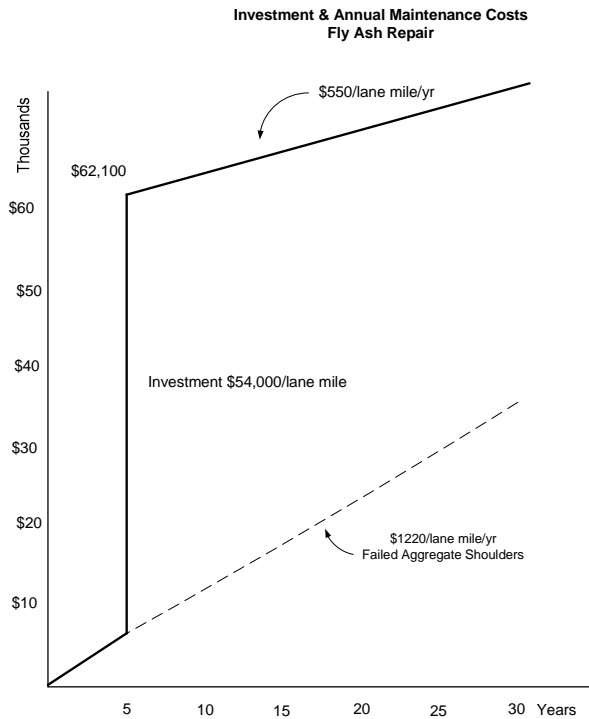


Figure 235. Annual maintenance costs for fly ash shoulder repair

Economic Evaluation (Life-Cycle Costs)

An economic evaluation is frequently conducted when comparing competing infrastructure improvements. Since the maintenance costs for these improvements are accrued over several years, it is helpful to evaluate the costs and benefits for the alternatives at the same point in time. This is referred to as evaluating using equivalent single payments (present worth) or equivalent uniform series of payments.

The following section will look at the benefits/costs and present worth calculations for ongoing gravel shoulder maintenance and shoulder improvements that include partial paving along the roadway edge, fly ash applications, foamed asphalt application with an HMA overlay, and paving shoulders to full width. An analysis will also be conducted of the polymer grid and fly ash soft shoulder repair techniques.

Benefits and Costs

In many engineering projects, benefits and costs are developed and then either the ratio of benefits to costs is calculated or the net value of benefits and costs is calculated. In this study, the benefits identified for each of the options are the savings in maintenance costs when shoulder improvements or repairs are completed, and the costs are the expenditures for the improvement or repair investment (construction) and the ongoing maintenance expenses. For example, when the calculations for 2 ft. partially paved HMA shoulders are reviewed, the benefits include the reduction in maintenance costs from \$550/lane-mile/year to \$275/lane-mile/year, and costs include the maintenance costs for the first five years (\$550/lane-mile/year), the investment cost of \$30,000/lane-mile/year, and the ongoing maintenance cost of \$275/lane-mile/year.

Table 46 tabulates the net value of the benefits and costs for this example, which is -\$26,194 (i.e., the costs are greater than the benefits). Note that benefits that are considered are only the easily quantifiable savings in maintenance efforts. Other benefits, such as the higher level of service provided by paved shoulders, greater safety by not exposing traffic to possible edge ruts, and avoidance of conflicts between traffic and granular shoulder maintenance operations, are not considered in this analysis. It is recommended that decision makers carefully consider these benefits separately before a final decision is made regarding possible shoulder improvements.

Table 46. Cost-benefit analysis

Description	QTY	Units	Unit Price	Amount	Unit Price Reference
Partially Paved HMA Shoulder-- 2' non NHS					
Base Widening HMA Mix	510.58	TONS	21.51	10,982.49	2005 Awarded Contract Prices Iowa DOT Item: 2213-8200000
Binder PG 58-28	30.63	TONS	194.98	5,973.13	2005 Awarded Contract Prices Iowa DOT Item: 2303-0245828
CRS-2 Tack	117.22	GAL	1.12	131.28	2005 Awarded Contract Prices Iowa DOT Item: 2307-0600454
Excavation Class 13	260.83	CY	10.29	2,683.96	2005 Awarded Contract Prices Iowa DOT Item: 2213-2713300
Special Backfill	369.60	TONS	12.64	4,671.74	2005 Awarded Contract Prices Iowa DOT Item: 2102-0425070
Blading and Shaping Shoulder Material	52.80	STA	29.77	1,571.86	2005 Awarded Contract Prices Iowa DOT Item: 2214-7450050
Subtotal				26,014.46	
Allowance for mob., prep. traffic control, and clean up.			15%	3,902.17	
Total				29,916.63	

Notes:

Per Iowa DOT standard road plan RG-8 rev. 10/17/06

Width = 2 ft. Thickness = 8 in.

Partially Paved HMA Shoulder -- 4', NHS					
Base Widening HMA Mix	765.60	TONS	21.51	16,468.06	2005 Awarded Contract Prices Iowa DOT Item: 2213-8200000
Binder PG 58-28	45.94	TONS	194.98	8,956.60	2005 Awarded Contract Prices Iowa DOT Item: 2303-0245828
CRS-2 Tack	234.43	GAL	1.12	262.56	2005 Awarded Contract Prices Iowa DOT Item: 2307-0600454
Excavation Class 13	391.25	CY	10.29	4,025.94	2005 Awarded Contract Prices Iowa DOT Item: 2213-2713300
Special Backfill	739.20	TONS	12.64	9,343.49	2005 Awarded Contract Prices Iowa DOT Item: 2102-0425070
Blading and Shaping Shoulder Material	52.80	STA	29.77	1,571.86	2005 Awarded Contract Prices Iowa DOT Item: 2214-7450050
Subtotal				40,628.51	
Allowance for mob., prep. traffic control, and clean up.			15%	6,094.28	
Total				46,722.78	

Note:

Per Iowa DOT standard road plan RG-8 rev. 10/17/06

Figures 236, 238, 240, 242, 244, 246, 248 and 250 are cash flow diagrams that illustrate the expenditures and benefits and the years in which they occur. An upward pointing arrow indicates a positive value, normally the value of a benefit, and a downward pointing arrow indicates a negative value, which is normally an expenditure. The arrow lengths are not to scale but are relative to the value of the activity. The linear scale lists the years and allows the costs/benefits to be viewed over a given period of time. In these figures, the time period illustrated is 30 years.

Present Worth Calculations

Whenever an infrastructure investment is considered that is on the magnitude of maintaining or upgrading roadway shoulders, an economic evaluation is a prudent activity to pursue. Since the costs for the alternatives and the ongoing maintenance events are accrued over several years, it is helpful to evaluate the costs and benefits for each alternative at the same point in time. This is often referred to as evaluating using equivalent single payments (present worth) or an equivalent uniform series of payments, depending on whether a single cost/benefit is being evaluated or a uniform series of costs/benefits.

For such an analysis in this report, the year 2007 will be the reference point in time. The present worth of the costs/benefits method combines all investments and costs and all annual expenses into a single present worth sum that represents the sum necessary at time zero (2007) to finance the total disbursements over the analysis period. Of the alternatives compared, the one with the lowest present worth is considered the most economical. For the present analysis, the interest rate used is 4% and is compatible with government bonds and other government financing plans. The planning horizon was selected at 30 years, so this is also the length of the analysis. In each case, it is assumed that the improvement or repair occurs five years after it is first planned; that is why the major investment is shown in year five.

Figures 237, 239, 241, 243, 245, 247, 249, and 251 illustrate the present worth calculations for the scenarios illustrated above. The details of the cost calculations have been discussed in previous sections of this report.

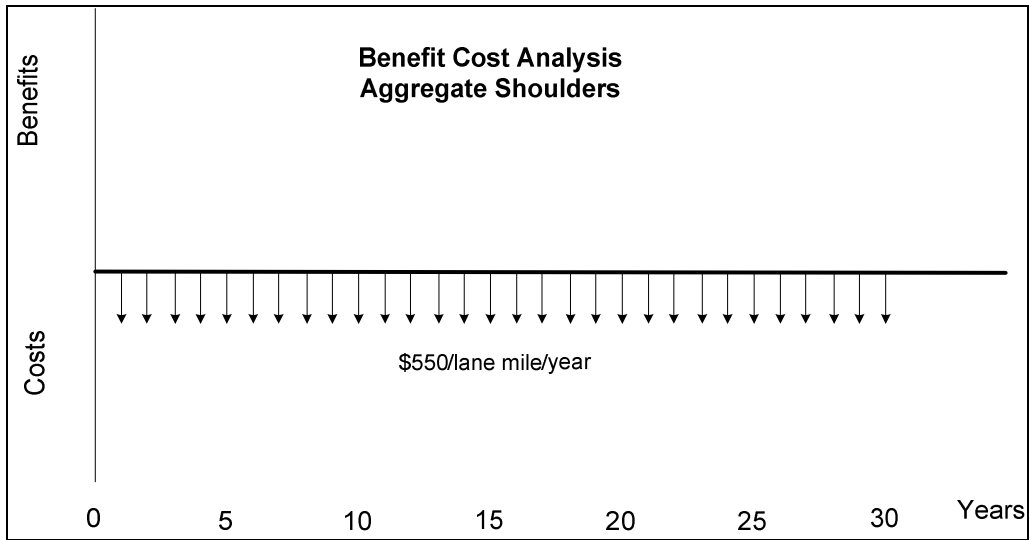


Figure 236. Benefit-cost analysis for aggregate shoulders

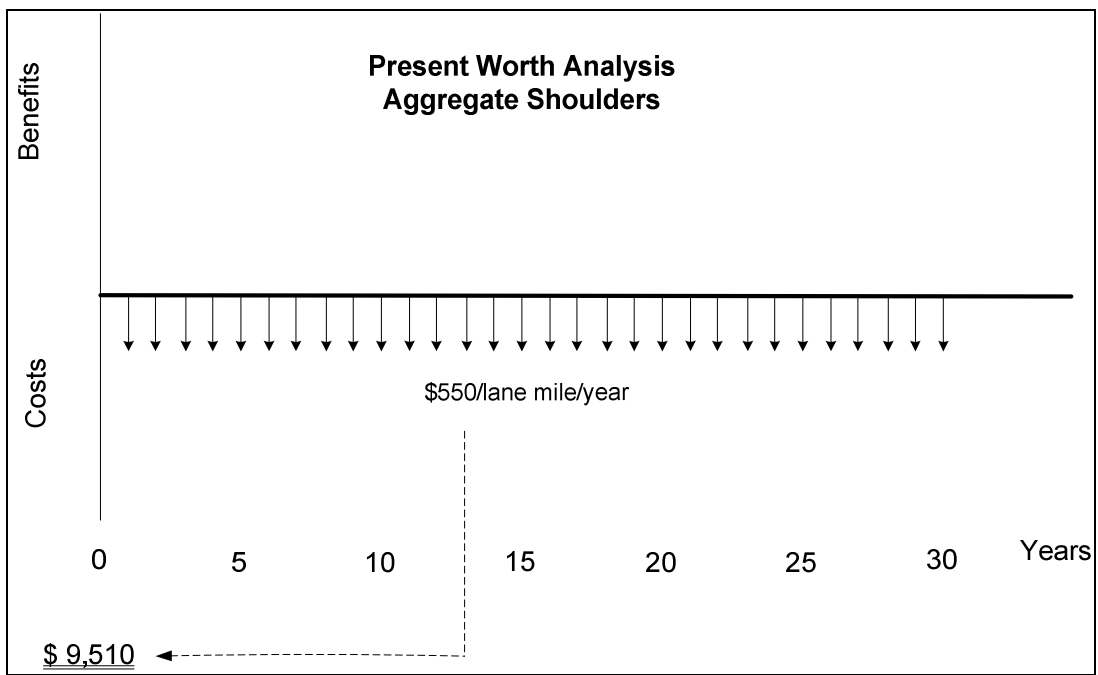


Figure 237. Present worth analysis for aggregate shoulders

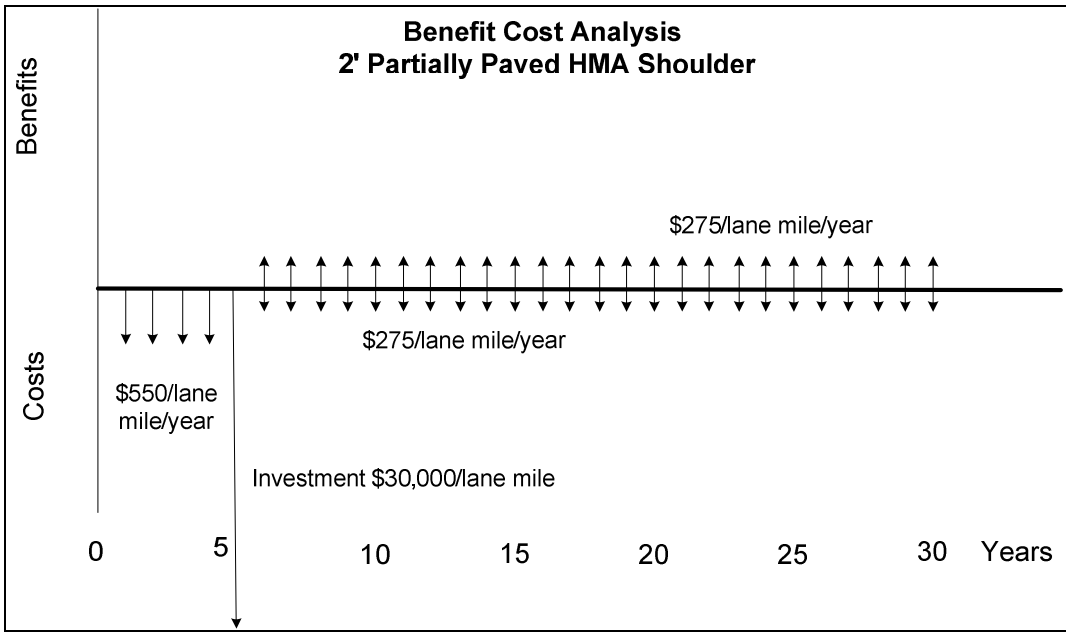


Figure 238. Benefit-cost analysis for 2 ft. partially paved HMA shoulder

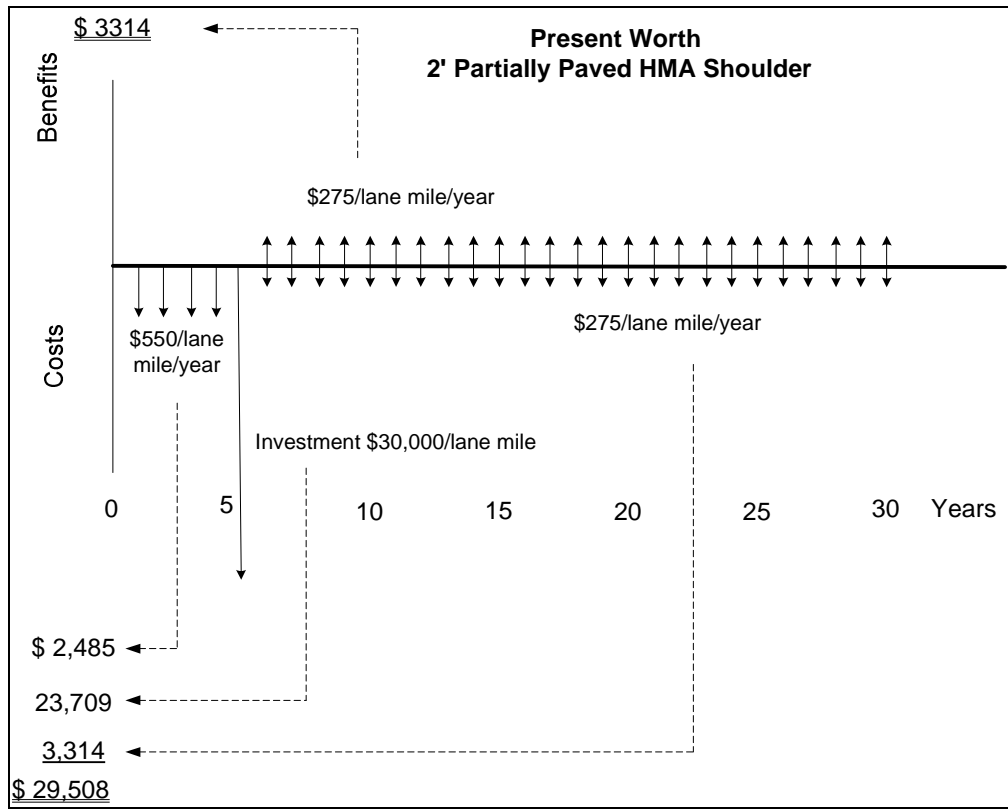


Figure 239. Present worth analysis for 2 ft. partially paved HMA shoulder

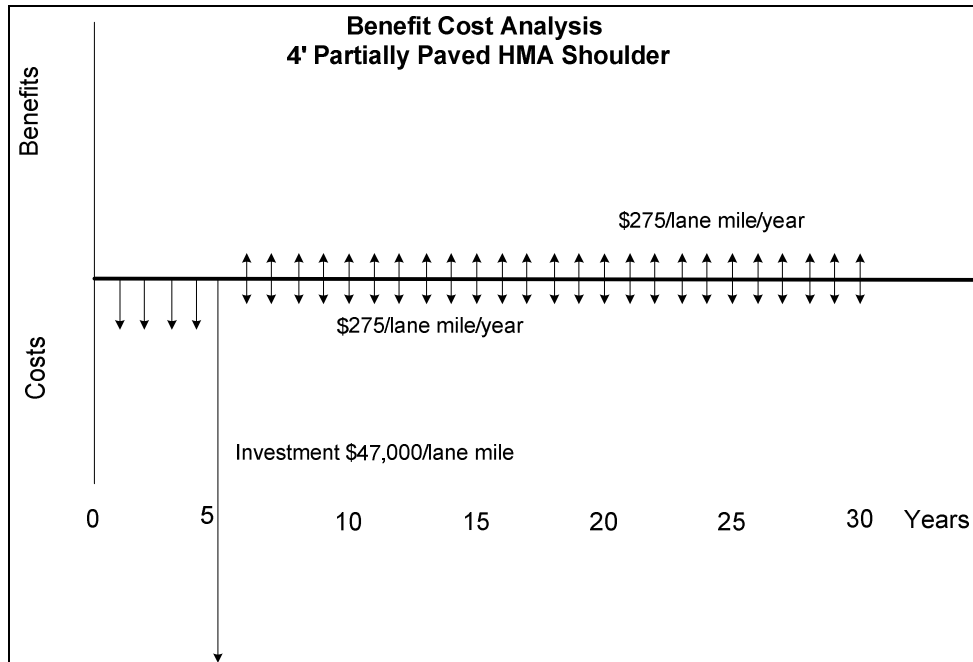


Figure 240. Benefit-cost analysis for 4 ft. partially paved HMA shoulder

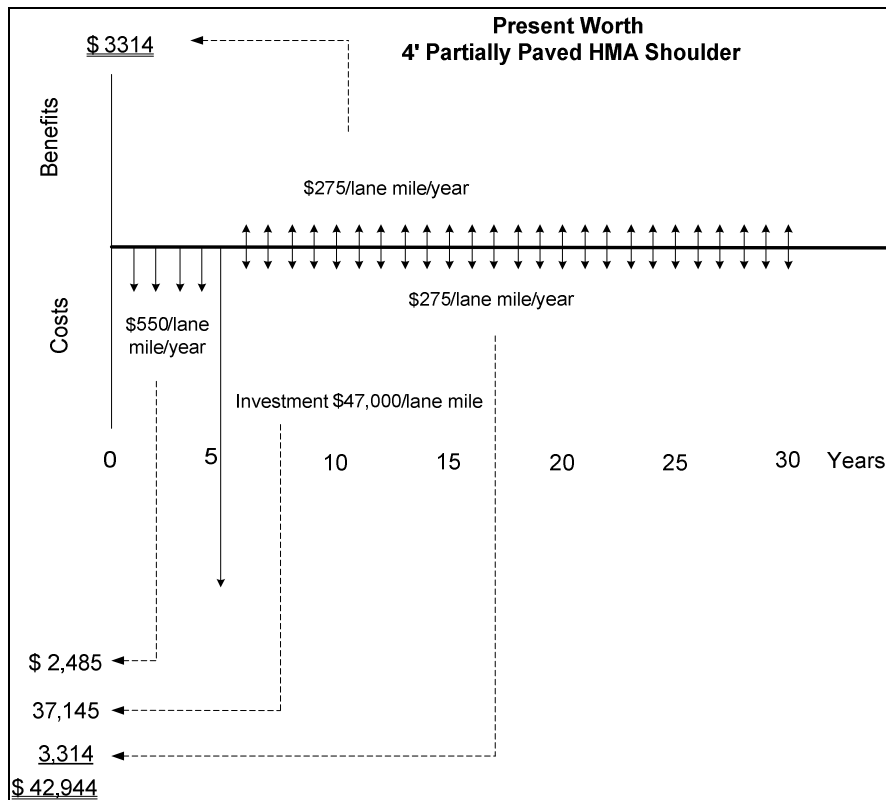


Figure 241. Present worth analysis for 4 ft. partially paved HMA shoulder

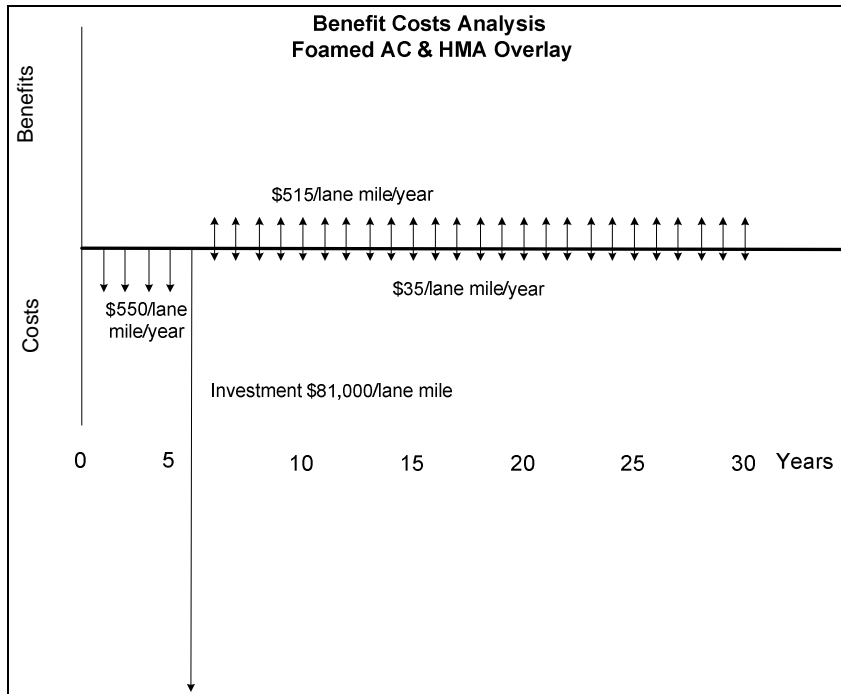


Figure 242. Benefit-cost analysis for foamed asphalt and HMA overlay

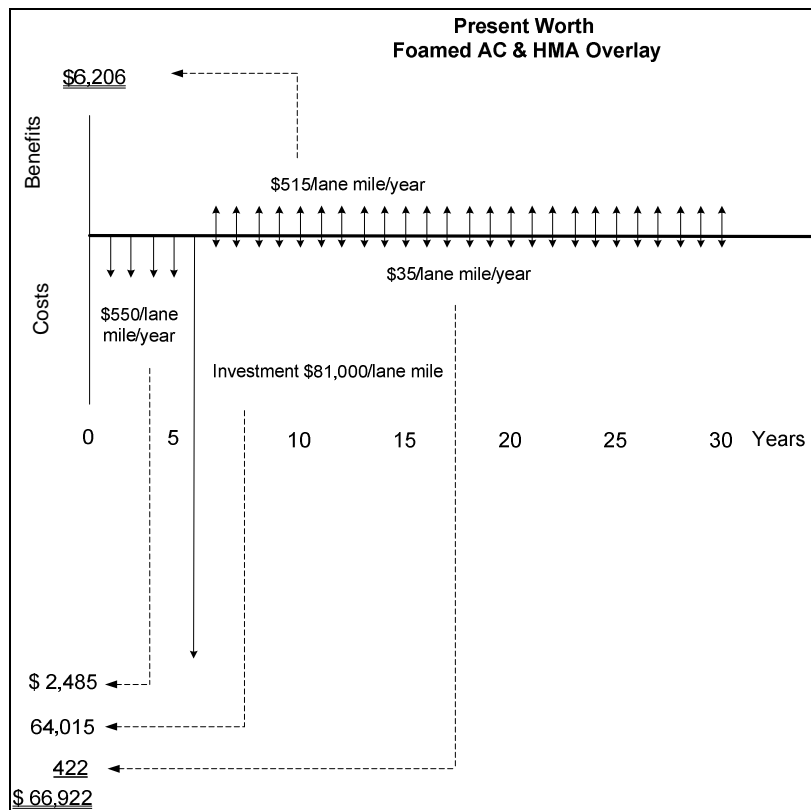


Figure 243. Present worth analysis for foamed asphalt and HMA overlay

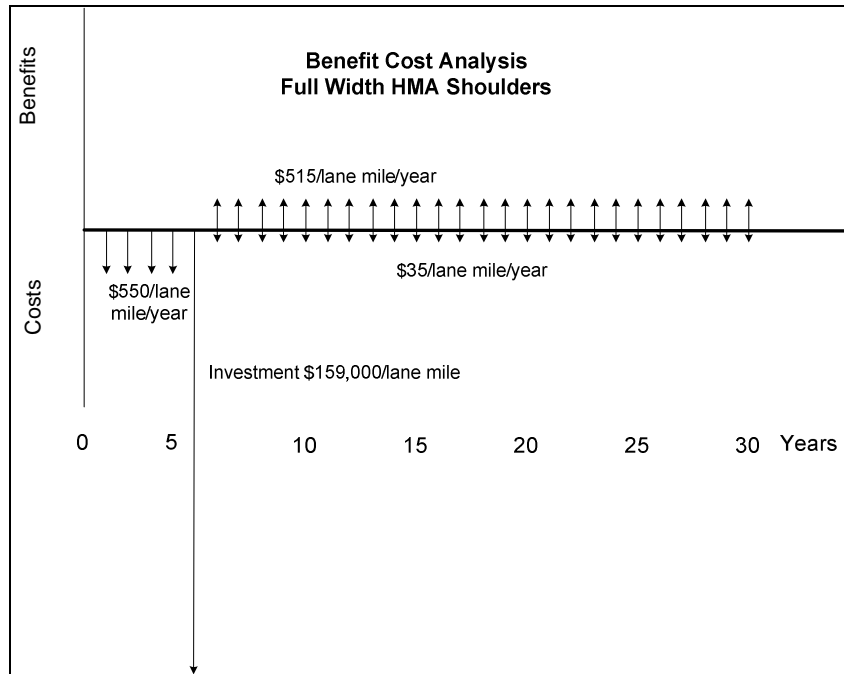


Figure 244. Benefit-cost analysis for full-width HMA shoulders

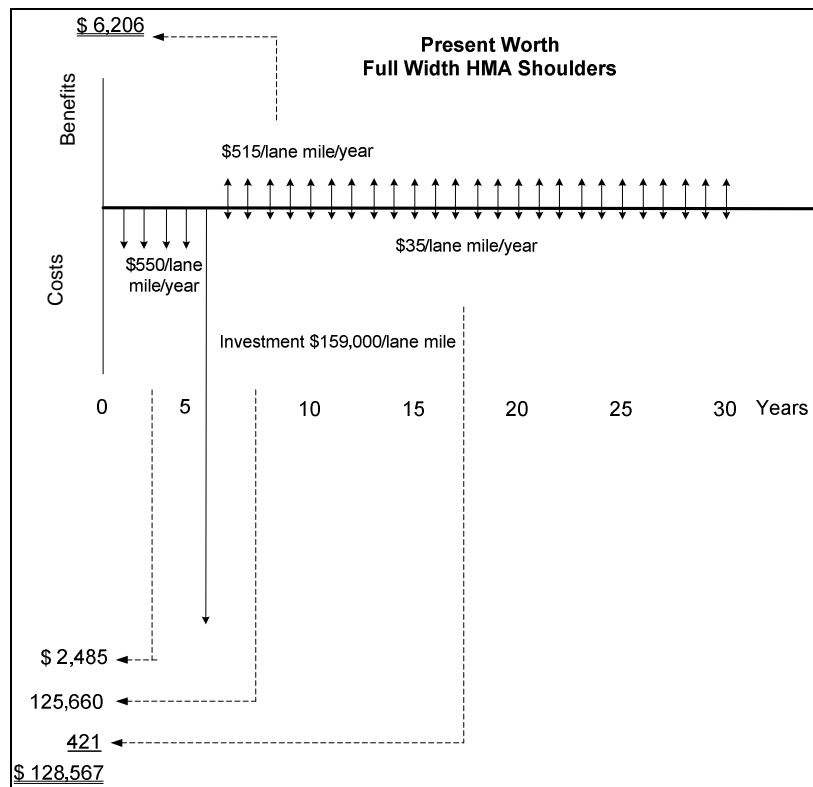


Figure 245. Present worth analysis for full-width HMA shoulders

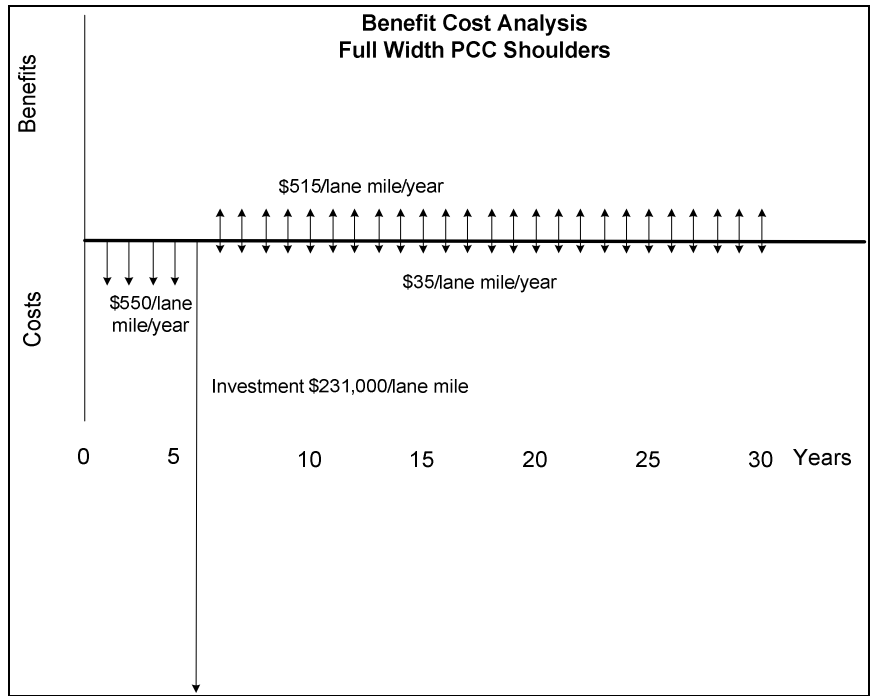


Figure 246. Benefit-cost analysis for full-width PCC shoulders

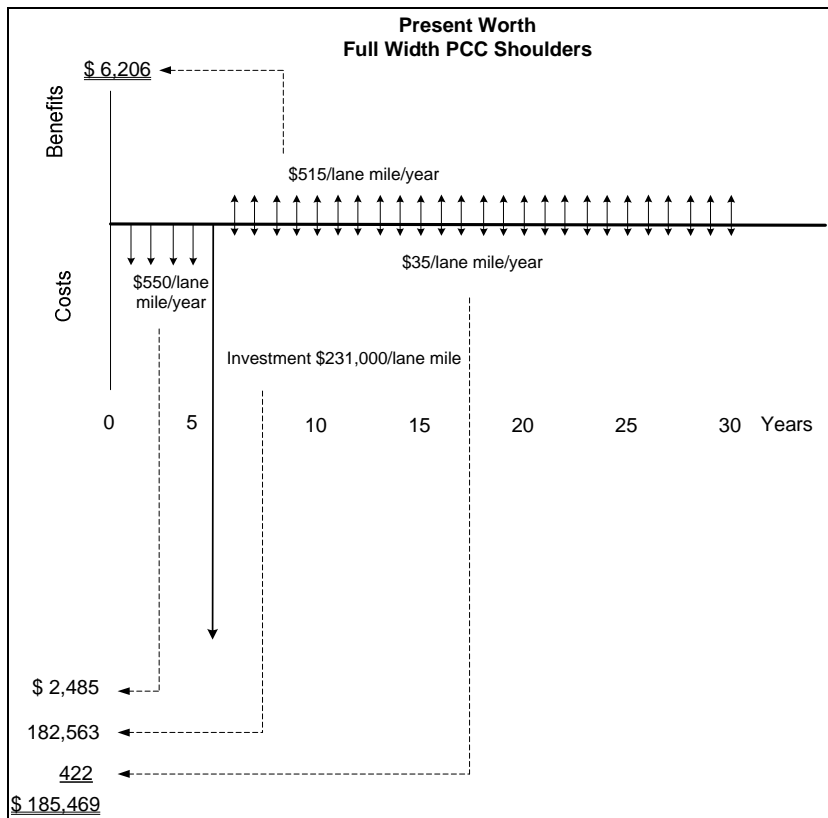


Figure 247. Present worth analysis for full-width PCC shoulders

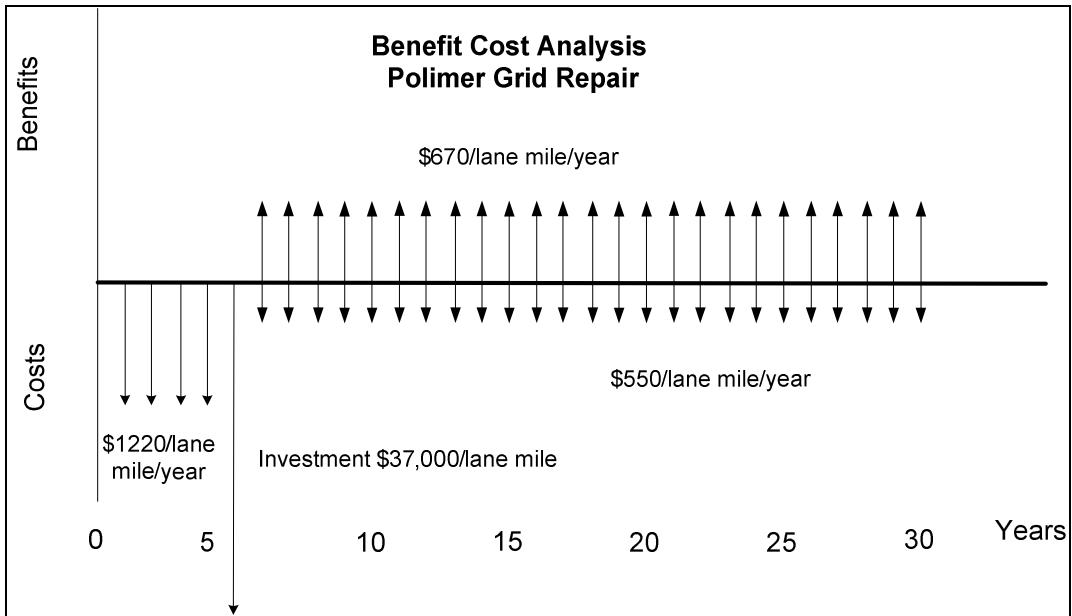


Figure 248. Benefit-cost analysis for polymer grid repair

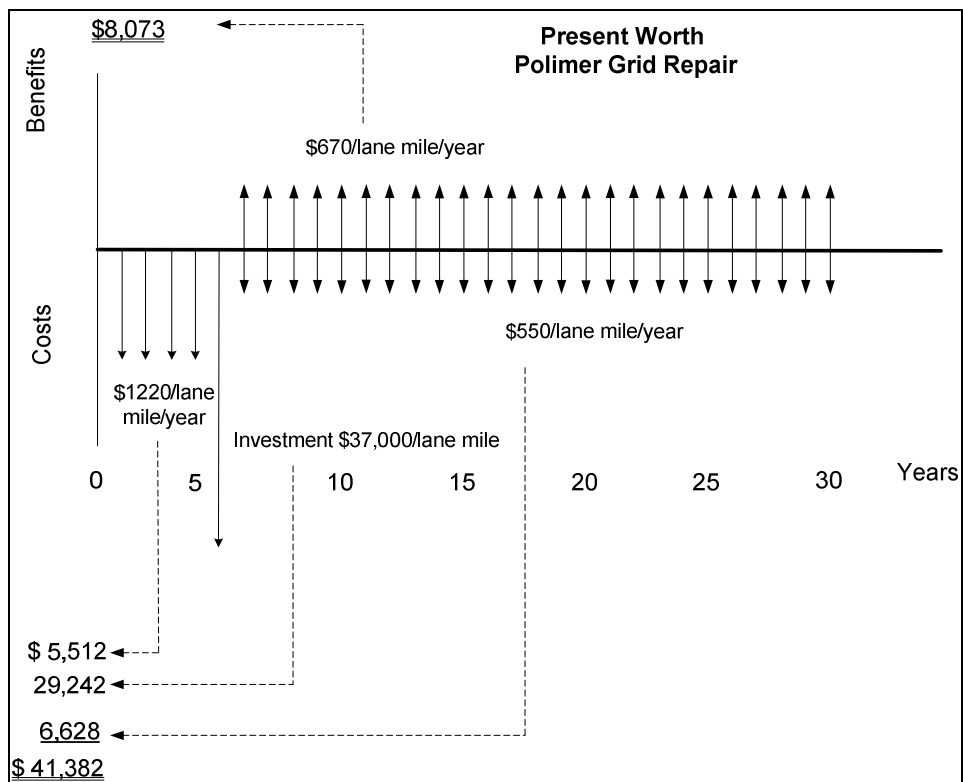


Figure 249. Present worth analysis for polymer grid repair

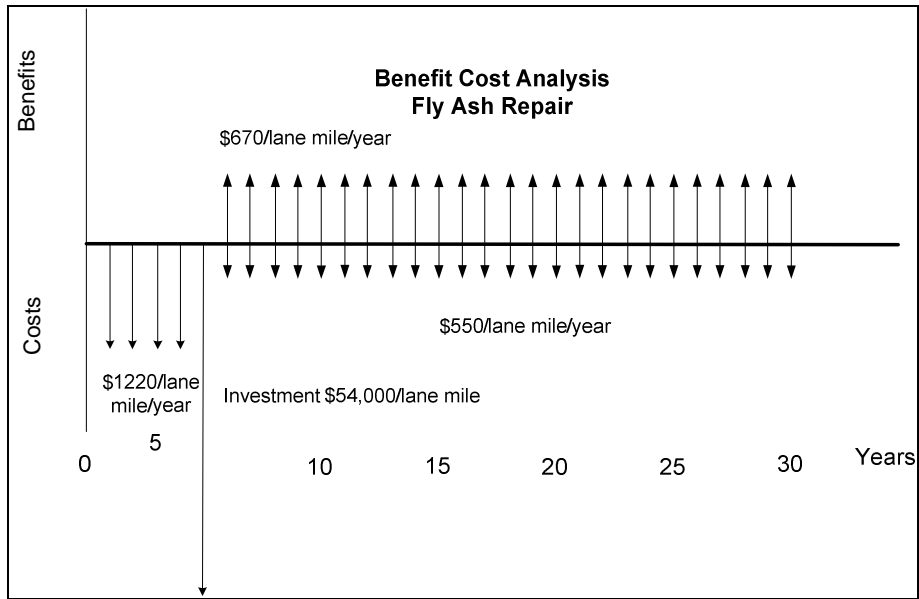


Figure 250. Benefit-cost analysis for fly ash repair

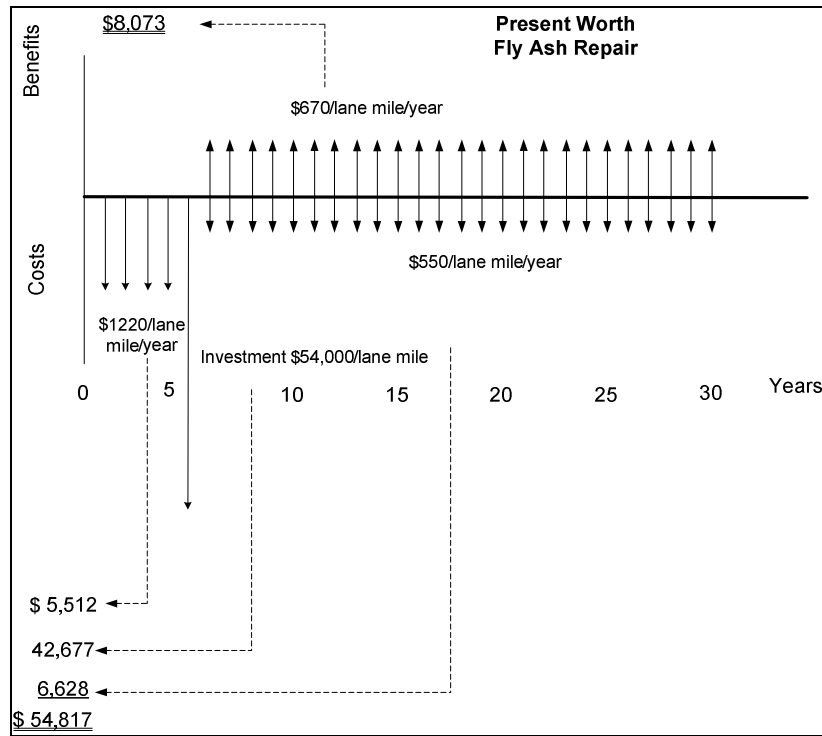


Figure 251. Present worth analysis for fly ash repair

Formulas for Calculating Present Worth

The terms used in present worth calculations include the following: F = future amount of money, P = present amount of money, r = interest rate (4 % is used in the calculations), N = number of years, and A = uniform series of payments. These terms are then used in the following formulas:

$$(1) \text{ Single Payment: } P = \frac{F}{(1+i)^N} \text{ or } P = F(\text{pwf}')$$

Where, pwf' is the present worth factor for a single payment, as found in interest tables.

$$(2) \text{ Uniform Annual Series: } P = [A] \left[\frac{(1+i)^N - 1}{i(1+i)} \right] \text{ or } P = A(\text{pwf})$$

Where, pwf is the present worth factor for uniform annual payment, as found in interest tables.

Mathematical Expressions

The mathematical expressions used in the present worth calculation include the monetary amount, the factor being used, the interest rate, and the number of years used. There are two expressions, one for a single payment and one for an annual series. An example calculation for each expression is shown below. These examples are unrelated to the subsequent calculations.

Example 1. What is the present value of a \$40,000 payment received at the end of the fifth year in the future?

\$40,000 is multiplied by the present worth factor for a single payment (pwf') at 4% interest for five years, which is found in compound interest tables.

Single Payment:

$$P = (\$40,000)(\text{pwf}' - 4\% - 5) (3)$$

$$= (\$40,000)(0.8219) = \$32,876$$

Example 2. What is the present value of five annual payments of \$40,000 each, made at the end of each year?

\$40,000 is multiplied by the present worth factor for a uniform series (pwf) at 4% interest for five years, which is found in compound interest tables.

$$\begin{aligned} \text{Annual Series:} \\ P &= (\$40,000)(\text{pwf} - 4\% - 5) (4) \\ &= (\$40,000)(4.452) = \$178,080 \end{aligned}$$

Present Worth Conclusions for Shoulder Maintenance Expenditures

The present worth calculations for the types of expenditures examined in this report are shown in Table 47.

Table 47. Calculations for present worth of the expenditures

Benefit Cost Present Worth Values				
Category	Activity	Benefit	Costs	Net Value
Maintenance	Granular Shoulders	\$0.00	-\$9,510.00	-\$9,510.00
Improvements	Partial Paved			
	2 foot	\$3,314.00	-\$29,508.00	-\$26,194.00
	4 foot	\$3,314.00	-\$42,944.00	-\$39,630.00
	Foamed AC	\$6,206.00	-\$66,922.00	-\$60,716.00
	Full Width Paving			
	HMA	\$6,206.00	-\$128,567.00	-\$122,361.00
	PCCP	\$6,206.00	-\$185,469.00	-\$179,263.00
Repair				
	Polimer Grid	\$8,073.00	-\$41,382.00	-\$33,309.00
	Fly Ash	\$8,073.00	-\$54,817.00	-\$46,744.00

Observations from Economic Analysis

Summary

The forgoing cost analysis provides a structure that transportation officials can modify and use in the future to aid in decision making. The analysis is structured so that costs can easily be updated by referencing the latest edition of *Awarded Contract Prices*, published by the Iowa DOT Office of Contracts, and the Iowa DOT standard costs for maintenance labor and equipment. The cost estimates were developed for five possible improvements and two possible soft shoulder repairs:

Improvements

1. Partially paved shoulders, 2 ft. width
2. Partially paved shoulders, 4 ft. width
3. Foamed AC stabilization with HMA Overlay
4. Full-width paving ACC
5. Pull-width paving PCC

Soft Shoulder Repairs

1. Polymer grid
2. Fly ash

The construction (investment) costs ranged from \$30,000 to \$231,000 per lane-mile for improvements. After an appropriate reduction for the present worth of future maintenance savings is considered, the present worth of each alternative ranged from approximately \$26,000 to \$122,000 (both cash outflows) per lane-mile; this was based on a 30-year planning horizon and an assumption that the improvement is made five years after the construction. The cost of repairs ranged from \$37,000 to \$54,000 per lane-mile, with the corresponding present worth ranging from \$33,000 to \$47,000 per lane-mile (both cash outflows).

The investment in shoulder improvements is made to garner an improved level of service, greater safety, and other benefits that are difficult to quantify. These may include elimination or mitigation of edge rut problems, provision of a stable and dust-free surface, improved shared use possibilities for bicycles and other non-motorized vehicles, reduction of conflict between traffic and shoulder maintenance operations, and release of maintenance personnel and equipment to perform other tasks. In making decisions about which shoulders to improve or repair, transportation officials should consider the cost of construction, traffic volume, crash history, and maintenance work force and equipment availability. Although the easily quantified monetary benefits of reduced shoulder maintenance associated with improvements are small in comparison to the required investment (construction costs), they do result in a small reduction in the present value of the necessary cash outflow.

Recommendations

The cost analysis process may be refined in the future by noting specific road segments that are being maintained and charging the costs to those road segments. The decision making process of

selecting the best investment may be refined by comparing construction (investment) costs to traffic volume on various road segments. By estimating the predicted traffic volume that will pass a mile of a proposed improvement during its lifetime, it may be possible to develop guidelines for allowable shoulder investments per vehicle-mile.

Cost of Granular Layer Stabilizers

An estimate was developed for the predicted construction costs of each of the stabilizers investigated in the laboratory. Based on the experience that the research team has had during field observations and in the laboratory, it is recommended that all of these stabilizing agents be incorporated by pulverizing with stabilizing equipment that is similar to the equipment that was used for the fly ash stabilization on US 34 near Batavia, IA. Therefore, the cost estimate for using these stabilizing agents is based on the estimate for fly ash stabilization with appropriate modifications.

The typical construction sequence is as follows:

- Set up traffic control.
- Blade the shoulder, removing vegetation and bringing it to proper cross section.
- Pulverize the shoulder and add the stabilizing agent using stabilizing equipment.
- Compact the shoulder.
- Blade, finish, sweep, and remove traffic control.

Since excavation of the existing shoulder material is not required, the time spent on the project and the amount of required equipment will be less than that of the other improvements analyzed for this project. Therefore, the allowance for mobilization, preparation, and traffic control will be approximately half the amount used for 2 ft. partially paved shoulders, or \$2,000 per mile. The cost for operating the stabilizing equipment and blading is assumed to be the same as it was for the fly ash soft shoulder repair. The cost estimate for these items was \$18,870.81 per mile, rounded to \$19,000 per mile (Table 48). Some of this expense (possibly up to \$7,000 per mile) may be reduced if maintenance forces from the road agency perform traffic control, cleanup, and blading.

Table 48. Cost per mile for stabilized construction without the cost of the stabilizing agent

Description	QTY	Units	Unit Price	Amount	Unit Price Reference
Stabilizing Granular Shoulders (doesnot include cost of stabilizing agent)					
Blading and Shaping Shoulder Material	52.80	STA	109.76	5,795.33	See note below, Iowa DOT Item: 2528-101000
('Square Meter' Item) Stabilized Soil	4,693.00	SY	2.36	11,075.48	See note below, Iowa DOT Item: 2599-999911
Subtotal				16,870.81	
Allowance for mob., prep. traffic control, and clean up.		\$2K/mile maximum		2,000.00	
Total				18,870.81	

Notes:

Based on the average of 3 contractor bids for Construct ID: 90-0347-133, Wapello County, Bid Order 305, Letting Date: 09/19/06

The original bid was in metric units and has been converted to English Units.

Iowa DOT Project Personnel Suggested using the average of 3 bids because they did not believe that the low bid could be repeated in the future.

The cost of the stabilizing agent is then added to this estimate (Table 49). The amount used is calculated by considering the application rate, dilution, and area to be covered. It is assumed that the width of shoulder to be stabilized will be 8 ft. wide and 6 in. deep, since that is the width of a typical drum for a stabilization machine and a standard depth for stabilization and aggregate shoulder depth. The following is a brief explanation of calculations and assumptions for each stabilizing agent:

- *S.S. polymer*. The dilution rate was assumed to be 7:1 (middle of the range). Note that the application rate is for diluted material.
- *Soiltac polymer*. The given application rate is for undiluted material. The dilution rate is adjusted to provide optimum moisture content for compaction. Therefore, the dilution rate does not affect cost calculations.
- *Dustlock soybean oil*. The stabilizing agent should fill 60 % of the voids after application. According to the research team’s field and laboratory experience, a typical void percentage for aggregate shoulder material is 10% to 15%. For the purposes of cost calculations, a void percentage of 12% was assumed.

The total estimated cost for each stabilizing agent is provided in Table 50. The costs range from \$24, 000 to 30,000 per lane-mile. In comparison, current aggregate shoulder maintenance costs are estimated at \$550 per lane-mile per year, and various improvement construction projects range from in cost from \$30,000 to \$231 per mile.

Table 49. Cost per gallon for products used in laboratory study of granular material stabilization

Product	Manufacturer	Description	Cost	Application rate	Dilution rate
S.S. polymer	Midwest Industrial Supply, Inc.	Polymer emulsion	\$8/gal.	0.7 gal./yd ²	5:1 to 9:1
Soiltac polymer	Soilworks, LLC	Polymer emulsion	\$5/gal.	0.36 gal./yd ²	$\gamma_{opt} - \gamma_{in situ}$
Dustlock soybean oil	Environmental Dust Control, Inc.	Soybean oil	\$2/gal.	1.0 gal./yd ²	-

Table 50. Estimated cost per mile for stabilized construction including stabilizing agent

Product	Construction cost per mile, Table 48	Cost per mile for stabilizing agent	Total cost per mile
S.S. polymer	\$18,900	\$8,500	\$8/gal.
Soiltac polymer	\$18,900	\$3,800	\$5/gal.
Dustlock soybean oil	\$18,900	\$22,700	\$2/gal.

Observation about Stabilizing Agents

Construction using stabilizing agents would result in improvement costs that are generally lower than those that have been analyzed elsewhere. Since excavation and disposal of existing shoulder material is not necessary, the time and cost of construction and conflicts with road users are reduced. However, the resulting improvement is not a fully paved surface, and the level of service provided by the resulting improvement may be less than that of a partially or fully paved shoulder. Consideration may be given to seal coating or otherwise lightly paving over the stabilized shoulder material. However, any light paving scheme carries with it risks of failure if heavy loads are imposed by truck traffic.

SUMMARY AND CONCLUSIONS

The main conclusions drawn from this research study are summarized below.

Relevant Research

The types of shoulders are as follows:

1. Earth shoulders
2. Granular shoulders
3. Blotter shoulders
4. Cold recycled asphalt
5. Asphalt concrete
6. Portland cement

The following are observations specific to granular shoulders:

- The most serious types of granular shoulder deterioration include rutting and edge drop-off. These most often occur within the first 2 ft. from the pavement edge. The factors that contribute to rutting and edge drop-off include the following:
 - Settlement of the shoulder
 - Degradation of the granular material
 - Erosion caused by surface drainage
 - High traffic volumes
 - Off-tracking by wide vehicles
- The initial construction costs for granular shoulders can be about 70% of the construction costs for paved shoulders. However, maintenance costs for granular shoulders are much higher than those of paved shoulders, and granular shoulder maintenance costs generally do not exceed the initial savings in construction costs.
- Expressway shoulders are granular unless the design year ADT exceeds 10,000, at which point paved shoulders are to be constructed.
- The painted edge line for NHS roadways are offset 2 ft. from the pavement edge to provide a 2 ft. paved and 8 ft. granular shoulder.
- According to a survey conducted by NCHRP Synthesis No. 63, the predominant slope for shoulders is 4%, or 1/2 in./ft.

Field Reconnaissance

- The two major problems observed during field reconnaissance are edge drop-off and subgrade layers with CBR values less than 10. Approximately 60% of the inspected sites had an edge drop-off greater than 1.5 in., 40% had a shoulder slope greater than 4%, and 50% had a subgrade CBR value less than 10.

- Changes in fines content and granular material gradation occur due to wind or water erosion and/or vehicle off-tracking. A high-speed video camera demonstration showed that vehicle off-tracking elevates and displaces aggregate in the opposite direction of vehicle travel.

Test Sections

Test Section No. 1, S.S. Polymer

- The section stabilized with S.S. polymer performed inadequately, and the 6 to 12 in. strip adjacent to the pavement edge showed signs of delamination.
- The S.S. polymer penetrated to a depth of approximately 0.5 in., forming a granular film that was detached under the impact of traffic.
- CBR values did not increase with time at the upper 15 in.
- Using granular material that complies with the lower bound of the gradation curve specified by the Iowa DOT resulted in a higher S.S. polymer penetration depth.
- Further durability testing and evaluation using diluted S.S. polymer (e.g., 7:1 or 9:1) is needed.

Test Section No. 2, Foamed Asphalt

- Full-depth reclamation using FA and class C fly ash was utilized to stabilize shoulder sections on I-35.
- CBR values increased with time for the upper 10 in.
- Laboratory vacuum saturation testing reduced the compressive strength by 20%.
- Freeze-thaw testing showed that FA can expand by 18%; however, the percent mass loss due to freeze-thaw cycles was satisfactory.
- Edge drop-off and shoulder distresses were observed at the test section after approximately one year.
- FA was successful in improving the properties of the shoulder section for a short duration. For longer durations, the stabilized section showed significant signs of distress near the pavement edge.

Test Section No. 3, Soybean Oil

- A 340 ft. long by 2 ft. wide by 6 in. deep section was stabilized using Feed Energy soybean oil.
- Two applications at a rate of 0.7 gal/yd² were placed and mixed with the granular material.
- Due to separation of the oil and emulsion, the distributor became plugged and a topical application was not carried out.
- Elevation profiles show that the Feed Energy soybean oil did not succeed in mitigating the formation of the edge drop-off.
- DCP tests reveal no CBR increase in the upper 8 in. of the stabilized test section.

- After eight months, a 3 in. edge drop-off along the pavement edge was measured.

Test Section No. 4, Portland Cement

- A 200 ft. long by 1.5 ft. wide by 0.5 ft. deep test section was mixed and compacted with water and 10% portland cement.
- The first 100 ft. section performed adequately, and a hard cemented surface was observed. Wash boarding and erosion were observed along the second 100 ft.
- CIV profiles demonstrated significant improvement after 7 and 14 days. No additional strength was measured after 28 days. CIV values outside the stabilized area were lower than those measured near the pavement edge.
- Edge drop-offs and erosion were observed along the stabilized area after four months. After eight months, the edge drop-off further progressed to a depth of about 3 in.

Test Section No. 5, Fly Ash

- The shoulder section located on Highway 34 near Batavia, IA, is 8 miles long and 8 ft. wide.
- Based on DCP results, the CBR values for the granular and subgrade layers were 10 and 2, respectively.
- XRD results show that the clay material consists mainly of kaolinite and traces of illite and quartz. XRF results show that there is a high percentage of silica and alumina in both the clay and the fly ash.
- pH tests showed that 16% to 20% fly ash addition is required to raise the pH of the soil-fly ash mixture to the desired pH value (11.5).
- Stabilizing the clay with 20% fly ash resulted in an unconfined compressive strength of 114 psi after seven days of curing at 100° F. Vacuum saturating the samples resulted in a strength reduction of 30%.
- The shoulder section was reconstructed by windrowing the upper 6 in. of crushed limestone and mixing 15% to 20% class C fly ash with the upper 12 in. of the subgrade clay. The mix was compacted using a pad foot roller, and the limestone was reclaimed and compacted using a smooth wheel roller.
- DCP tests demonstrated the increase of CBR values with time. All stabilized sections showed higher CBR values than the unstabilized sections.
- Plate load tests showed that the stabilized sections have a much higher E values than the control sections. Further, E values measured after one year were significantly higher than those measured after 7 months. After 19 months, CBR and E values increased relative to values measured after 12 months.
- Preliminary testing conducted at the new Highway 34 bypass reveal low CBR values for the underlying earth shoulder fill and subgrade layers.
- Fly ash stabilization was successful in improving both the short- and long-term performance of the shoulder section.

Test Section No. 6, Geosynthetics

- A test section, about 1020 ft. long with soft subgrade, was stabilized with three Tensar geogrids. The geogrids were placed at the interface between the subgrade and the granular layer.
- The control section started to develop rutting after one month. The stabilized sections showed no signs of shoulder rutting.
- Plate load tests showed a significant difference in E between the stabilized and the control sections. Further, the E value increased with time.
- CIVs were highest near the pavement, since the thickness of the rock layer was highest. CIVs measured outside the stabilized area were low, indicating soft shoulder conditions.
- CBR values, determined from DCP testing, increased for the upper 8 in. after three months.
- All geogrids considerably improved the performance of the shoulder test section and eliminated rutting.
- The E values and CIVs showed some reduction after 10 months, possibly due to the exposure of geogrids or a decrease in granular layer thickness.

Laboratory Evaluation of Stabilizers

- A laboratory study was conducted to evaluate the use of two polymer emulsion products, portland cement, and a soybean oil product in stabilizing the shoulder granular layer.
- Six standard Proctor samples were prepared for each stabilizer. Three samples were tested in compression, while the other three were subjected to vacuum saturation followed by compression testing.
- The average strength of S.S. polymer-stabilized samples was about 445 psi, which decreased to 76 psi after vacuum saturation.
- The average strength of Soiltac polymer-stabilized samples was about 1118 psi, which is the highest compressive strength recorded among all the tested stabilizers. Vacuum saturating the samples resulted in an average compressive strength of about 252 psi.
- The average strength of portland cement-stabilized samples was about 694 psi, which decreased to 254 psi after vacuum saturation.
- Dustlock soybean oil stabilized-samples demonstrated an average compressive strength of about 706 psi, which decreased to 623 psi when subjected to vacuum saturation.
- Dustlock stabilized-samples showed the smallest strength reduction when subjected to vacuum saturation, since soybean oil is a water repellent product.
- All four products showed potential in successfully stabilizing the granular layer.
- From a maintenance perspective, S.S. polymer and Soiltac polymer require more frequent topical applications than Dustlock soybean oil due to their lower resistance when subjected to vacuum saturation.
- For optimum stabilization results, it is recommended that the products are uniformly mixed, using the recommended application rates, and compacted with the granular layer.

Laboratory Box Study

- A laboratory box study was conducted to simulate a shoulder section overlying a subgrade with CBR values between 3 and 5.
- The laboratory apparatus consisted of a loading frame, reaction beam, and a hydraulic actuator. A steel box (2 ft. x 2 ft. x 2 ft.) was used to contain the soil and was loaded using a 6 in. diameter loading plate.
- Cyclic loading with three loading stages was used to study the performance of the laboratory model under selected mechanical and chemical stabilization techniques. At each stage, one of three pressures was applied and sustained for 5,000 cycles at a frequency of 1 Hz. These pressures were 40, 80, and 120 psi.
- The control test showed the highest soil displacement. The cumulative soil displacement after 15,000 cycles was 11.2 in.
- The CBR and E_{LWD} values of the subgrade soil typically increased after each test due to soil densification. No considerable change was noted in the strength properties of the granular layer.
- The BX1200 geogrid reduces soil displacement by about 75% relative to the control test, while the BX1100 and BX4100 geogrids alleviated soil displacement by about 70% relative to the control test. All geogrids tested did not prevent aggregate punching through the subgrade layer. The approximate punching depth was 1 in.
- The woven and nonwoven geotextiles reduced the soil displacement by about 70% relative to the control test. The performance of the nonwoven geotextile, however, started to decrease at the third loading stage, and soil displacement increased rapidly.
- Both woven and nonwoven geotextiles were successful in separating the granular and subgrade layers.
- Using RAP material and BX1200 geogrid resulted in reducing the soil displacement three times more than the control test did. The soil displacement was 50% higher than with crushed limestone.
- Stabilizing the subgrade soil with 20% fly ash resulted in the lowest soil displacement. Fly ash stabilization reduced the soil displacement by 40% percent relative to Test No. 4 (BX1200 with crushed limestone). The recorded soil displacement was also six times lower than that of the control test.
- For all tests where the reinforcements were fixed to the steel box and for the fly ash stabilization test, the Giroud and Han (2004) semi-empirical method overpredicted the soil displacements at the end of each loading stage.
- In tests where the reinforcements where not fixed, the measured soil displacement was considerably higher than the predicted values.

Shoulder Design Charts

- A shoulder design chart was developed to help mitigate shoulder rutting that arises from the bearing capacity failure of the subgrade layer.
- The chart, which is based on the CBR value of the subgrade layer and rut depth, was developed from the semi-empirical method proposed by Giroud and Han (2004) and from

an equation for calculating rut depth proposed by the U.S. Army Corps of Engineers in 1989.

- The developed design chart can be a rapid tool for designing new granular shoulders, providing a basis for QA/QC, and predicting the behavior of existing shoulders.
- Field and laboratory rut depth measurements were used to validate the developed chart. The measured rut depths are in a relatively good agreement with the predicted chart values.
- Several other charts were developed to help understand the influence of other factors, such as the CBR value of the granular layer, number of load cycles, and axle loads, on the magnitude of rut depth.

RECOMMENDATIONS

As a result of the research described in this report, the following are proposed on a pilot study basis:

- At edge drop-off shoulder sections, it is recommended that the effectiveness of mixing polymer emulsion products such as S.S. polymer or Soiltac polymer with the granular layer be evaluated.
- Other soybean oil products similar to dustlock soybean oil should be investigated, due to dustlock's previous success in stabilizing the shoulder section near Garner, IA, and due to its good performance in the laboratory study.

Shoulder Construction

- A minimum weighted average CBR value of the earth shoulder fill and the subgrade layers up to a depth of 20 in. should be about 12. The weighted average CBR value for the granular layer should not be less than 10.
- The DCP test and Clegg impact test are rapid tools that can be used in the field to verify the CBR values during shoulder construction.
- The provided design charts can be used as a design guide for the construction of new shoulders. By selecting an appropriate CBR value for each layer, and at the expected traffic level and loads, the allowable rut depth can be controlled. The design charts can also be used for QA/QC.

Shoulder Reconstruction

- In cases of shoulder rutting due to bearing capacity failure of the subgrade, it is proposed that fly ash or geogrid stabilization be used. The percentage of fly ash and moisture content added should be determined from laboratory testing. The geogrid should be placed at the interface of the subgrade and granular layer. The overlying granular layer should have a uniform thickness of about 6 to 8 in.

Edge Drop-Off

- To effectively use stabilizers such as portland cement, polymer emulsions, and soybean oil, improved mixing/compaction methods and equipment are needed. Such improvements may result in better short-term performance relative to the test sections.

REFERENCES

- AASHTO. 2001. *Guidelines for Geometric Design of Very Low-Volume Roads*. Washington, DC: American Association of State and Highway Transportation Officials.
- Asi, I.M. 2001. Stabilization of Sebkha soil using foamed asphalt. *Journal of Materials in Civil Engineering*, 13(5), 325–331.
- Al-Amoudi O.S., I.M. Asi, H.I. Al-Abdul Wahhab, and Z.A. Khan. 2002. Clegg hammer-California bearing ratio correlations. *Journal of Materials in Civil Engineering*, 14(6), 512–523.
- ASTM. 1989. ASTM C593, Standard specification for fly ash and other pozzolans for use with lime. *Annual Book of ASTM Standards, Vol. 04.01*. Philadelphia, PA: ASTM.
- ASTM. 1991. ASTM D698, Standard test methods for laboratory compaction characteristics of soil using standard effort (12,400 ft-lbf/ft³ (600 kN-m/m³)). *Annual Book of ASTM Standards, Vol. 04.08*. Philadelphia, PA: ASTM.
- ASTM. 1996. ASTM D559, Standard test methods for wetting and drying compacted soil-cement mixtures. *Annual Book of ASTM Standards, Vol. 04.08*. Philadelphia, PA: ASTM.
- ASTM. 1996. ASTM D560, Standard test methods for freezing and thawing compacted soil-cement mixtures. *Annual Book of ASTM Standards, Vol. 04.08*. Philadelphia, PA: ASTM.
- ASTM. 2000. ASTM D2487, Standard test method for classification of soils for engineering purposes. *Annual Book of ASTM Standards, Vol. 04.01*. Philadelphia, PA: ASTM.
- ASTM. 2005. ASTM D4318, Standard Test Method for Liquid Limit and Plasticity Index of Soils. *Annual Book of ASTM Standards, Vol. 04.08*. Philadelphia, PA: ASTM.
- Berg, R.R., B.R. Christopher, and S. Perkins. 2000. *Geosynthetic reinforcement of the aggregate base/subbase courses of pavement structures*. Roseville, MN: Geosynthetics Materials Association.
- Bergeson, K.L., M.J. Kane, and D.O. Callen. 1990. *Crushed stone granular surfacing materials*. ISU-ERI-AMES 90-411. Ames, IA: Iowa State University.
- Bergeson, K.L. and S.G. Brocka. 1996. Bentonite treatment for fugitive dust control. *Semisecular Transportation Conference Proceedings*. Ames, IA: Iowa State University.
- Bergmann, R. 2000. *Soil stabilizers on universally accessible trails*. Washington, DC: Forest Service, United States Department of Agriculture.

- Berthelot, C. and A. Carpentier. 2003. Gravel loss characterization and innovative preservation treatments of gravel roads. *Transportation Research Record*, 1819(2), 180–184.
- Bolander, P. 1999. Laboratory testing of nontraditional additives for stabilization of roads and trail surfaces. *Transportation Research Record*, 1652, 24–31.
- Bolander, P., D. Marocco, and R. Kennedy. 1995. *Earth and Aggregate Surfacing Design Guide for Low Volume Roads*. Report No. FHWA-FLP-96-001. Washington, DC: Forest Service, United States Department of Agriculture.
- Bowering, R. H. and C.L. Martin. 1976. Performance of newly constructed full-depth foamed bitumen pavements. Proceedings of the Eighth Australian Road Research Board Conference, Perth, Australia.
- Burnham, T. and D. Johnson. 1993. *In situ foundation characterization using the dynamic cone penetrometer*. Report No. 93-05. Maplewood, MN: Minnesota Department of Transportation.
- Bushman, W.H., T.E. Freeman, and E.J. Hoppe. 2004. *Stabilization techniques for unpaved roads*. Charlottesville, VA: Virginia Transportation Research Council, Virginia Department of Transportation.
- Butt, A.A., S.H. Carpenter, A.A. Selim, and K.A. Zimmerman. 1997. *Evaluation of South Dakota department of transportation's shoulder surfacing in new construction*. Pierre, SD: South Dakota Department of Transportation.
- Chu, T.Y., D.T. Davidson, W.L. Geocker, and C. Moh. 1955. Soil stabilization with lime-fly ash mixtures: Studies with silty and clayey soils. *Highway Research Board*, 108, 102–112.
- Collings, D., R. Lindsay, and R. Shunmugam. 2004. LTPP exercise on foamed bitumen treated base-evaluation of almost 10 years of heavy trafficking on MR 504 in Kwazulu-Natal. Proceedings of the 8th Conference on Asphalt Pavements for South Africa, Sun City, South Africa.
- Cook, D. 2002. Tree sap helps hold roadside shoulder together. *Road Management*, 72(5), 30–31.
- Das, B.M. 2006. *Principles of Geotechnical Engineering*. 6th Ed. Toronto, Canada: Thompson.
- Department of the Army, the Navy, and the Air Force. 1994. *Soil stabilization for pavements*. Army technical manual 5-822-14, Air Force manual 32-1019. Washington, DC: Department of the Army, the Navy, and the Air Force.
- Fang, H.Y. 1991. *Foundation engineering handbook*. 2nd Ed. New York, NY: VanNostrans Reinhold.
- Fannin, R.J. and O. Sigurdsson. 1996. Field observations on stabilization of unpaved roads with geosynthetics. *Journal of Geotechnical Engineering*, 544–553.

- Ferguson, G. 1993. Use of self-cementing fly ashes as a soil stabilization agent. *ASCE Geotechnical Special Publication No. 36*. New York, NY: ASCE.
- Ferguson, G., and S.M. Levenson. 1999. *Soil and Pavement Base Stabilization with Self-Cementing Coal Fly Ash*. Alexandria, VA: American Coal Ash Association.
- Ferguson, G., and J. Zey. 1990. Stabilization of pavement subgrade with class C fly ash. Ninth International Coal Ash Utilization Symposium, Orlando, FL.
- Folts, R.B. 1996. *Traffic and no-traffic on an aggregate surfaced road: Sediment production differences*. Washington, DC: USDA Forest Service.
- Giroud, J.P. and J. Han. 2004a. Design method for geogrid-reinforced unpaved roads. I. Development of design method. *Journal of Geotechnical and Geoenvironmental Engineering*, 130(8), 775–786.
- Giroud, J.P. and J. Han. 2004b. Design method for geogrid-reinforced unpaved roads. II. Calibration and applications” *Journal of Geotechnical and Geoenvironmental Engineering*, 130(8), 787–797.
- Giroud, J. P. and L. Noiray. 1981. Geotextile-reinforced unpaved road design. *Journal of the Geotechnical Engineering Division, Proceedings of the American Society of Civil Engineers*, 107(GT9), 1233–1254.
- Glogowski, P.E., J.M. Kelly, R.J. McLaren, and D.L. Burns. 1992. *Fly ash design manual for road and site applications, Volume 1: Dry or conditioned placement*. Research Project 2422-2. Moroeville, PA: GAI Consultants, Inc.
- Guthrie, W.S., S. Sebesta, T. Scullion. 2001. *Selection optimum cement content for stabilizing aggregate base materials*. College Station, TX: Texas Transportation Institute, Texas A&M University.
- Hallmark, S.L., D. Veneziano, T. McDonald, J. Graham, K.M. Bauer, R. Patel, and F.M. Council. 2006. *Safety Impacts of Pavement Edge Drop-offs*. Washington, DC: AAA Foundation for Traffic Safety.
- Heebink, L.V. and D.J. Hassett. 2001. Coal fly ash trace element mobility in soil stabilization. International Ash Utilization Symposium, Center for Applied Energy Research, University of Kentucky, Lexington, KY.
- Holts, R.D. and N. Sivakugan. 1987. Design charts for roads with geotextiles. *Geotextiles and Geomembranes*, 5, 191–199.
- Humphreys, J.B. and J.A. Parham. 1994. *The elimination or mitigation of hazards associated with pavement edge dropoffs during roadway resurfacing*. Knoxville, TN: University of Tennessee Transportation Center, University of Tennessee.

- Iowa Department of Transportation, Standard Road Plans. 2004. Standard Road Plan RH-370. Ames, IA: Iowa Department of Transportation.
- Jones, D., E. Sadzik, and I. Wolmarans. 2001. The incorporation of dust palliatives as a maintenance option in unsealed road management systems. *Australian Road Research Board (ARRB) Conference*, 1–12.
- Jones, T.E., R. Robinson, and M.S. Snaith. 1984. A field study on the deterioration of unpaved roads and the effect of different maintenance strategies. *Proceedings of the Eighth Regional Conference for Africa on Soil Mechanics and Foundation Engineering*, 293–303.
- Kendall, M., B. Baker, P. Evans, and J. Ramanujan. 2001. Foamed bitumen stabilization- The Queensland experience. *20th Australian Road Research Board (ARRB) Conference*, 1–32.
- Kirchner, H. and J.A. Gall. 1991. Liquid calcium chloride for dust control and base stabilization of unpaved road systems. *Transportation Research Record*, 1291, 173–178.
- Lee, H.D., and Y.J. Kim. 2003. *Development of a mix design process for cold-in-place rehabilitation using foamed asphalt, Phase I*. Final Report. Iowa Highway Research Board Project TR-474. Iowa City, IA: University of Iowa.
- Lones, R.A. and B.J. Coree. 2002. *Determination and Evaluation of Alternate Methods for Managing and Controlling Highway Related Dust*. Final Report. Iowa Highway Research Board Project TR-449. Ames, IA: Iowa Department of Transportation and Iowa State University Engineering Research Institute.
- Martins, G. 2006. *Personal Communication*. Iowa Department of Transportation, Ames, Iowa.
- Milligan, G.W.E., R.A. Jewell, G.T. Houlby, and H.J. Burd. 1989. A new approach to the design of unpaved roads-part I. *Ground Engineering*, 25–29.
- Monlux, S. 2003. Stabilizing unpaved roads with calcium chloride. *Transportation Research Record*, 1819(2), 52–56.
- Moosmuller, H. J.A. Gillies, C.F. Roger, D.W. DuBois, J.C. Chow, J.G. Watson, and R. Langston. 1998. Particulate emission rates for unpaved shoulders along a paved road. *Journal of the Air & Waste Management Association*, 48, 398–407.
- Morgan, R.J., V.R. Schaefer, and R.S. Sharma. 2005. *Determination and Evaluation of Alternative Methods and Controlling Highway-Related Dust, Phase II: Demonstration Project*. Iowa Highway Research Board Project No. TR-506. Ames, IA: Iowa Department of Transportation.

- Muthen, K.M. 1998. *Foamed asphalt-mix design procedure*. Report CR-98/077. Pretoria, South Africa: SABITA Ltd. and CSIR Transportek.
- National Cooperative Highway Research Program (NCHRP). 1979. *Design and use of highway shoulders, Synthesis of highway practice No. 63*. Washington, DC: Transportation Research Board, National Research Council.
- NAVFAC. 1998. *Demonstration of a polymer coating on contaminated soil piles*. Technical Data Sheet TDS-2057-ENV. Port Hueneme, CA: Naval Facilities Engineering Service Center.
- Nordlin, E.F., D.M. Parks, R.L. Stoughton, and J.R. Stoker. 1976. *The effect of longitudinal edge of paved surface drop-off on vehicle stability*. Sacramento, CA: Office of Transportation Laboratory, California Department of Transportation.
- Poole, D. 2005. *Personal Communication*. Midwest Industrial Supply, Inc., Canton, Ohio.
- Portland Cement Association (PCA). 1995. *Soil-cement construction handbook*. Skokie, IL: Portland Cement Association.
- Powell, W., G.R. Keller, and B. Brunette. 1999. Application for geosynthetics on forest service low-volume roads. *Transportation Research Record*, 1652, 113–120.
- Price, D.A. 1990. *Experimental gravel shoulders*. Final Report. Report No. CDOH-DTD-R-90-2. Denver, CO: Colorado Department of Transportation.
- Public Works Journal Corporation. 1980. Calcium chloride: Key to unpaved road conditions. *Public Works*, 111(4), 94–95.
- Ruckel, P.J., L.L. Kole, F. Abel, R.E. Zator, J.W. Button, and J.A. Epps. 1982. Foamix asphalt advances. *Asphalt Pavement Construction: New Materials and Techniques*. ASTM STP, 724, 93–109.
- Santoni, R.S., J.S. Tingle, and S.L. Webster. 2001. *Nontraditional stabilization of silty-sand*. Alexandria, VA: U.S. Army Engineer Research and Development Center.
- Souleyrette, R., T. McDonald, Z. Hans, A. Kamyab, T. Welch, and B. Storm. 2001. *Paved shoulders on primary highways in Iowa: An analysis of shoulder surfacing criteria, costs, and benefits*. Ames, IA: Center for Transportation Research and Education, Iowa State University.
- Steward, J., R. Williamson, and J. Mohney. 1977. *Guidelines for use of fabrics in construction and maintenance of low-volume roads*. Washington, DC: Forest Service, United States Department of Agriculture.
- Tensar Earth Technologies, Inc. 1996. *Design guideline for flexible pavements with Tensar geogrid base layers*. Tensar Technical Note, TTN:BR96. Atlanta, GA: Tensar Earth Technologies, Inc.

- Thenoux, G., and S. Vera. 2003. Evaluation of hexahydrated magnesium chloride performance as chemical stabilizer of granular road surfaces. *Transportation Research Record*, 1819, 44–51.
- U.S. Army Corps of Engineers. 2003. *Use of geogrids in pavement construction*, Technical Letter No. 1110-1-189. Washington, DC: U.S. Army Corps of Engineers.
- U.S. Navy. 1999. Materials testing. *Naval Facilities Engineering Command Publication NAVFAC MO 330*. Fort Leonard Wood, MO: U.S. Navy.
- Wagner, C. and Y. S. Kim. 2004. Construction of a safe pavement edge: Minimizing the effects of shoulder dropoff. *Annual Meeting of the Transportation Research Board*. Washington, DC. CD-ROM.
- White, D.J., and K.L. Bergeson. 2000. US highway 151 ash stabilization research project. *Progress Report ERI Project 400-60-85-00-3009*. Ames, IA: Engineering Research Institute, Iowa State University.
- White, D.J., D. Harrington, and Z. Thomas. 2005a. *Fly ash soil stabilization for nonuniform subgrade soils, Volume I: Engineering properties and construction guidelines*. CTRE Project 01-90. Ames, IA: Center for Transportation Research and Education, Iowa State University.
- White, D.J., V.R. Schaefer, and T.D. Rupnow. 2005b. *A pilot study to investigate the use of limestone aggregate screenings in road construction*. Ames, IA: Center for Transportation Research and Education, Iowa State University.

APPENDIX A. SAMPLE CALCULATION OF WEIGHTED AVERAGE CBR VALUES FOR THE GRANULAR AND SUBGRADE LAYERS

Below is a sample calculation of the weighted average CBR value for the granular and subgrade layers (Figure A.1). This calculation method was implemented throughout this report. The values were used to make inferences about the strength of each layer and were used in the shoulder design charts.

Granular Layer

$$CBR = \frac{(20 \times z_1) + (30 \times z_2)}{200}$$

Subgrade Layer

$$CBR = \frac{(10 \times z_3) + (2 \times z_4)}{(500 - 200)}$$

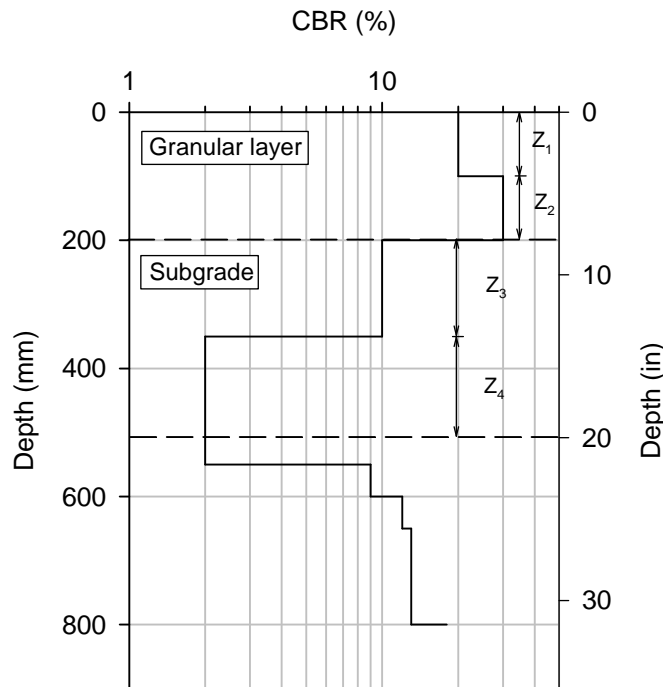


Figure A.1. Sample calculation of weighted average CBR values for the granular and subgrade layers

APPENDIX B. PROJECT MEETINGS

Throughout the course of this research, several district meetings were conducted to document the shoulders problems from the point of view of maintenance engineers. Meetings with engineers from Districts 1 and 3 and the Minnesota Department of Transportation (Mn/DOT) were conducted. A summary of these meetings is presented in this section.

District 1

The following information regarding shoulder problems and maintenance were noted during the meeting with District 1 maintenance engineers.

- Most shoulders in Iowa use aggregate shoulders.
- The guidelines for initiating maintenance is 1–1½ in. edge drop-off. Blading is the typical maintenance practice.
- Due to budget constraints, displaced rock adjacent to the shoulder is reclaimed without addition of new material.
- A four-vehicle operation is required to maintain the edge drop-off for a four-lane road:
 1. Reclaimer with “Right lane closed” sign mounted on it
 2. Truck with an arrow directing traffic to the left lane
 3. Tractor with a blade
 4. Last truck is a roller compactor with a “road work ahead” mounted on it.
- About 32 miles of repair can be covered in one day (about 4 miles/hr. of maintenance), though this varies depending on weather.
- In the cases of adding rock, a hopper dispenses 3 in. of rock on a skid mounted on the back of a truck. The rock is dropped by lifting the skid. The rock dropped follows the shoulder original slope.
- Most shoulders are maintained two times in the summer and once in the fall before the ground freezes (this practice depends on the availability of a motor grader). Sometimes personnel only repair edge rut spots.
- Maintenance of soft subgrade typically involves adding a 2 in. bituminous fillet adjacent to the pavement.
- Off-tracking mainly occurs because of skews on the road.
- Snow removal trucks can pull the rock away from the aggregate shoulder during plowing.
- Asphalt millings are added to steep slopes to bring the base up. They contain some oil, which improves the shoulder stability.
- Crushed concrete is used as a filler. It does not have the fines found in crushed limestone.
- Maintainers are usually shared between maintenance shops.
- Cost of aggregate is about \$20/ton.
- Operator hourly wage is \$15/hr.
- Trucks parking on ramps cause settlement. Shoulders adjacent to ramps are not as wide; therefore, the two outside wheels are on areas that should not be carrying any load.

- Chronic edge rut problems are encountered on hills. The severity of the problems increases if a pre-existing edge rut is present. The washed out material resides at the bottom of the hill.
- Liquid CaCl₂ has been used on gravel roads but not on shoulders.
- Previously, bituminous oil has been used to stabilize shoulders, but this practice was terminated due to machine availability and reduction in manpower.

District 3

The following information regarding shoulder problems and maintenance were noted during the meeting with District 3 maintenance engineers:

- The main concern in District 3 is maintenance of earth shoulders, which is the most common shoulder type in District 3.
- At the east and south parts of the district, the earth shoulders are maintained by adding 3 in. of crushed limestone. At the north and west parts, the shoulders are maintained by adding quartzite. Shoulders can also be maintained using a blend of virgin aggregate and recycled material.
- It is difficult to compact quartzite material due to its hydrophobic nature.
- More edge drop-offs were observed at quartzite shoulder sections because quartzite contains fewer fines.
- Some shoulder sites use seal coats to alleviate chronic edge drop-off problems.
- Three in. of granular material are added to the shoulders during resurfacing projects. The added material is not sufficient to withstand traffic loads. The maintenance costs would significantly increase if the shoulders were to be patched.

Minnesota Department of Transportation

- The Mn/DOT shoulder stabilization project is sponsored by Mn/DOT's New Technology, Research, and Equipment Committee and Mn/DOT's Maintenance Operation Research.
- The project involves monitoring shoulder field performance for two years. Edge drop-off, slope, and erosion of aggregates due to traffic and environment are monitored.
- Five shoulder sites are currently being evaluated. The aggregate materials used are listed below:
 - Class 1 Gravel
 - Class 2 Limestone
 - Class 5 Granite
 - 3/4 Mesabi select
 - Class 7 RCA/RAP/Gravel mix 1
 - Class 7 RCA/RAP/Gravel mix 2
- Changes in gradation are due to winter sanding, which can add thousands of pounds of sand per mile each year, and grinding aggregate to sand-size particles.
- Some districts are experimenting with the following materials:

- Crushed granite versus Class 1 gravel
 - Recycled aggregate blends
 - Liquid asphalts (CSS or CRS)
 - Rumble strips
 - Penetrating emulsion prime (PEP)
-
- Shoulder sections stabilized with liquid asphalt started to break down after five years.
 - PEP is originally used as a dust palliative and has a diesel odor.
 - Typical application rates for PEP vary from 0.3 to 0.9 g/yd² (single or double applications).
 - PEP is used with materials such as crushed limestone and pit gravel.
 - In dry conditions, the penetration depth of PEP increases.
 - Light rolling is the recommended method of compaction for materials stabilized with PEP.
 - In 2005, PEP was used to stabilize three shoulder sections. The application rate varied from 0.3 to 0.5 g/yd². PEP was absorbed by limestone fines. The penetration depth at one site was approximately 3/8 in. after two hours.
 - During the winter season, snow plows broke and displaced the stabilized surface away from the pavement.

APPENDIX C. FINITE ELEMENT ANALYSIS FOR LABORATORY BOX STUDY

Introduction

An analytical model of the laboratory box study was developed using finite element analysis to evaluate the boundary conditions of the laboratory experiments. Axisymmetric elastic-plastic analyses were carried out using SLOPE/W software.

Model Formulation

The shoulder section geometry, which consisted of a granular layer overlying a soft subgrade layer, was defined in SLOPE/W as shown in Figure C.1. A structured mesh was selected to define the granular and subgrade regions. The mesh was denser under the loading plate to better capture the soil response.

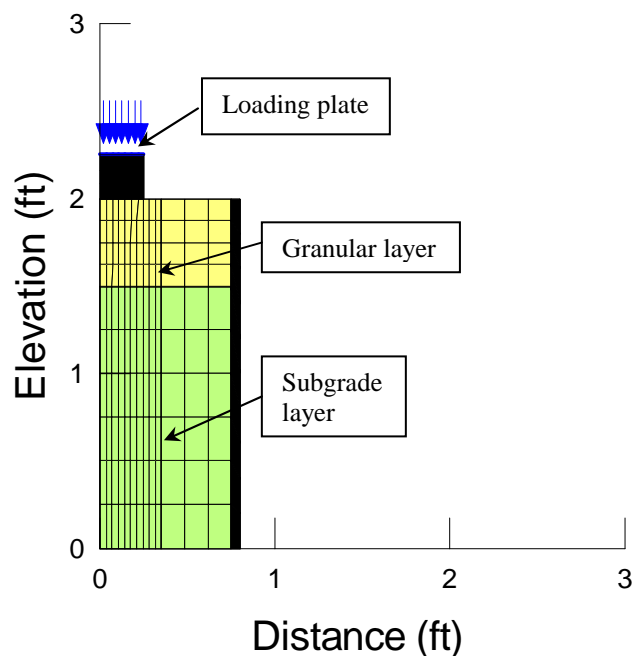


Figure C.1. Finite element model of the laboratory box

Boundary Conditions

The boundary conditions of the finite element model are shown in Figure C.2. The sides of the box were restrained in the x-direction, while the bottom of the box was restrained in both the x- and y-directions. The region representing the loading plate was restrained in the x-direction to allow for vertical movement only.

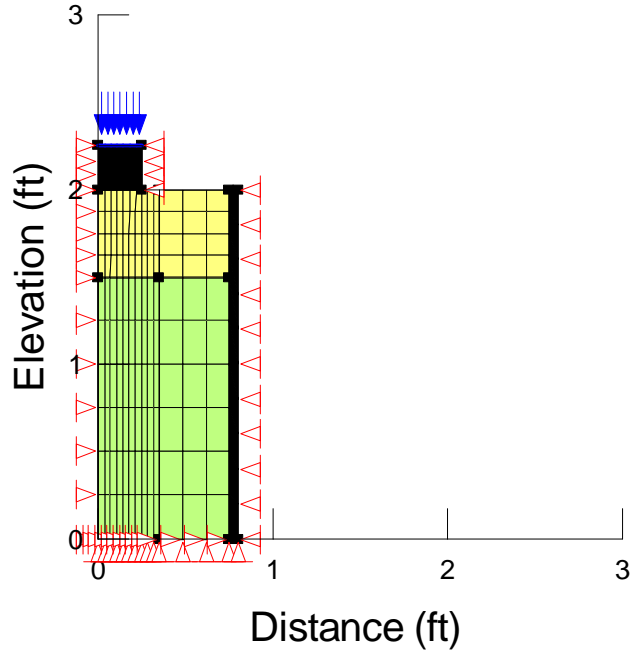


Figure C.2. Boundary conditions of the finite element model

Material Properties

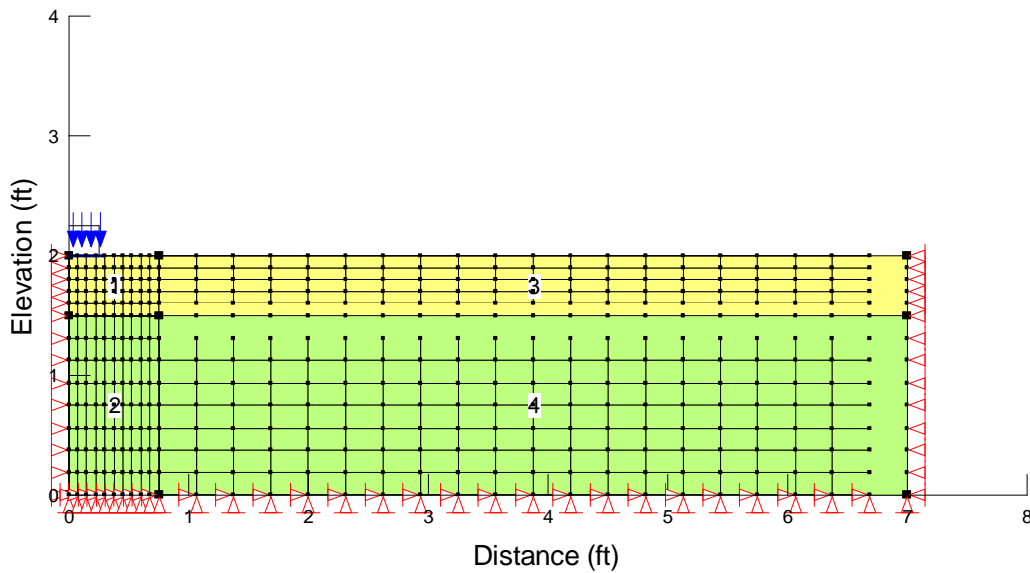
Table C.1 summarizes the materials' constitutive parameter values. E values for the granular and subgrade soils were selected based on the results of the LWD tests presented in this report under Laboratory Evaluation of Stabilizers. The Poisson's ratio for the neoprene pad was determined from the manufacturer, whereas E was measured.

Table C.1. Summary of material properties

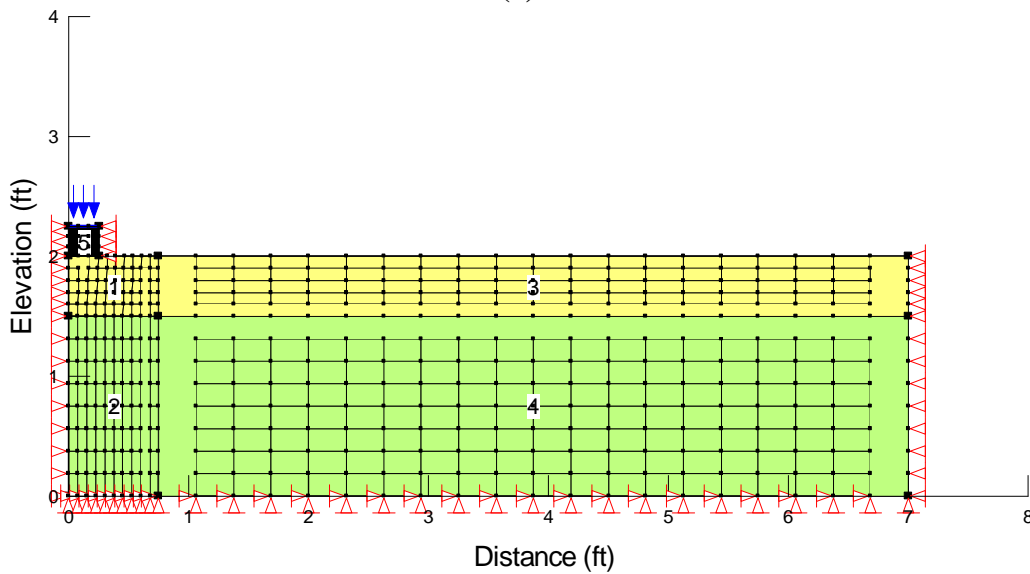
Material	Model	E (psi)	Cohesion (psi)	Friction angle	Poisson's ratio
Granular layer	Elastic-plastic	580	1	36	0.3
Subgrade layer	Elastic-plastic	1305	2	24	0.35
Steel wall/rigid loading plate	Elastic	30×10^6	-	-	0.2
Compressible neoprene wall	Elastic	19	-	-	0.4

Rigid and Flexible Loading Plate

The finite element analysis compares soil displacement and pressure distribution under a flexible and a rigid loading plate. A flexible loading plate is modeled by applying an edge boundary condition of 11,520 psf (80 psi), as shown in Figure C.3a. This value represents the American-British standard axle load (at a tire inflation pressure of 80 lb./in²). A rigid loading plate was modeled by defining a region 3 in. wide above the granular layer with E equal to 30 x 10⁶ psi (Figure C.3b). The defined region is restrained in the x-direction to allow for vertical displacement of the plate.



(a)



(b)

Figure C.3. Modeling (a) flexible and (b) rigid loading plate

Modeling

Three models were developed and evaluated in this study. The first model represents the rigid steel walls of the box directly interacting with the soil (Figure C.4). The second model represents the addition of a compressible neoprene layer at the interface between the steel box and the soil (Figure C.5). The third model represents field conditions where no boundaries exist. This was modeled by increasing the dimensions of the model to reduce the effect of boundary conditions (Figure C.6). In each model, a static load of 80 psi was applied.

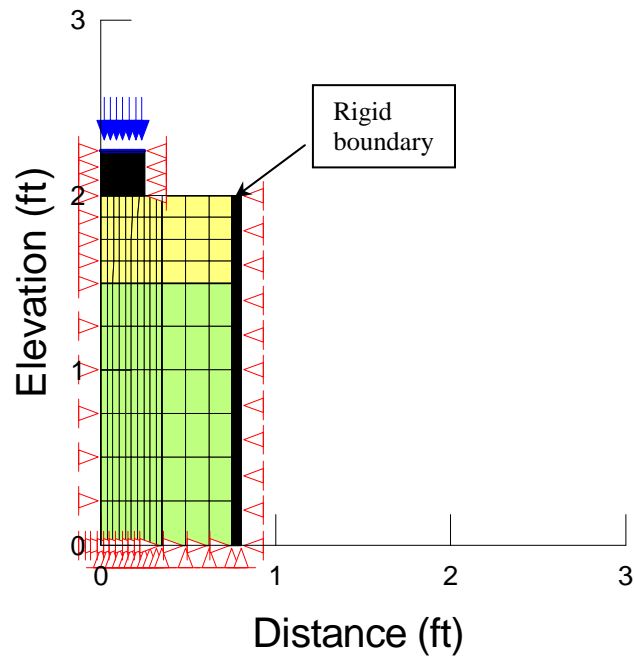


Figure C.4. Finite element model with a rigid wall

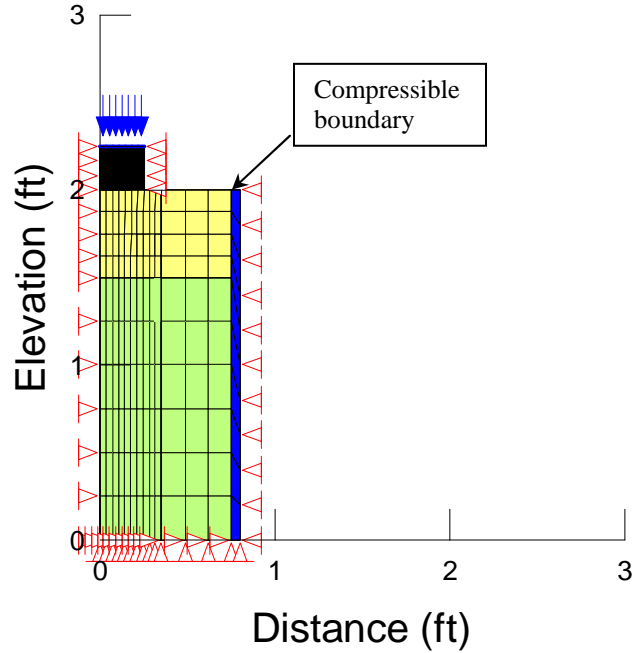


Figure C.5. Finite element model with compressible layer

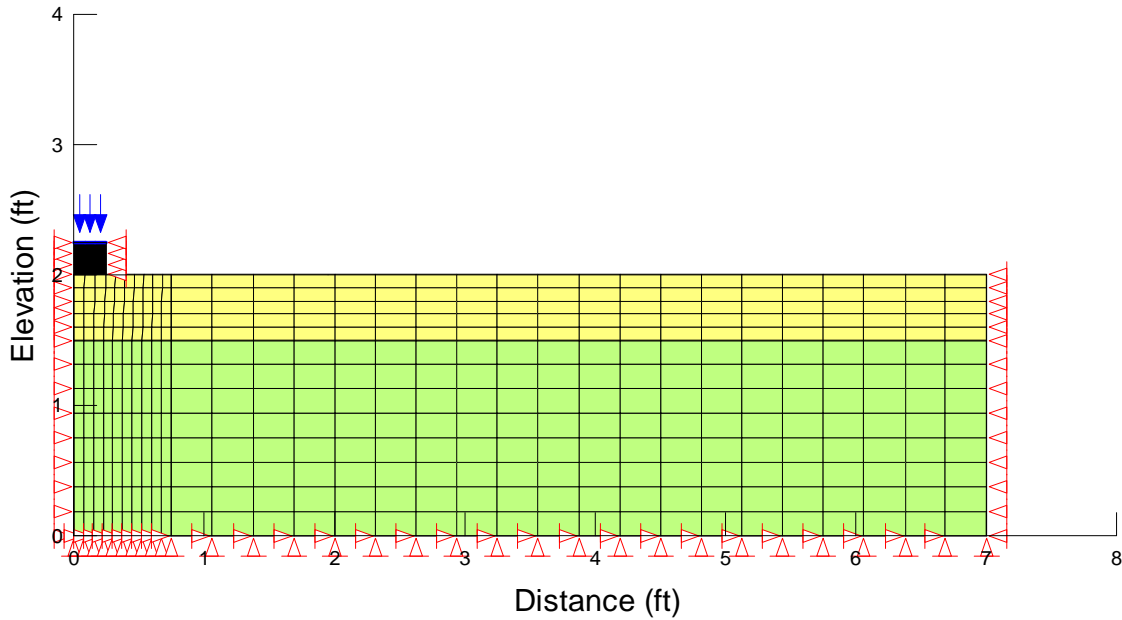


Figure C.6. Enlarged finite element model representing field conditions

Results

The effective stress and soil displacement under a rigid and a flexible plate are shown in Figure C.7 and Figure C.8, respectively. The results show that if a load is applied on a flexible plate the effective stress distribution is uniform, whereas the soil displacement takes the form of a

deflection basin. If the load is applied on a rigid plate the stress distribution under the plate is nonuniform, whereas the soil displacement is equal at all points. Based on visual observations, the behavior of the loading plate used in the laboratory box study resembles that of a rigid plate.

To evaluate the effect of adding a compressible neoprene layer, the soil displacement along the boundary (i.e., at the interface between the soil and the wall or the soil and the compressible layer) was measured. The soil displacement was compared to that measured from the model simulating field conditions (Figure C.9). The results indicate that adding a compressible layer at the interface between the laboratory box and the soil mobilizes more vertical soil displacement than in the case where the soil is directly interacting with the rigid steel wall. Adding a compressible soil layer will therefore result in soil displacement values closer to those encountered in the field.

The distribution of effective stress under the rigid loading plate was compared to that under the flexible plate, as shown in Figure C.10. It was noted that the addition of a compressible layer does not affect the stress distribution. The rigid and compressible models, however, adequately predict the stress distribution compared to field conditions.

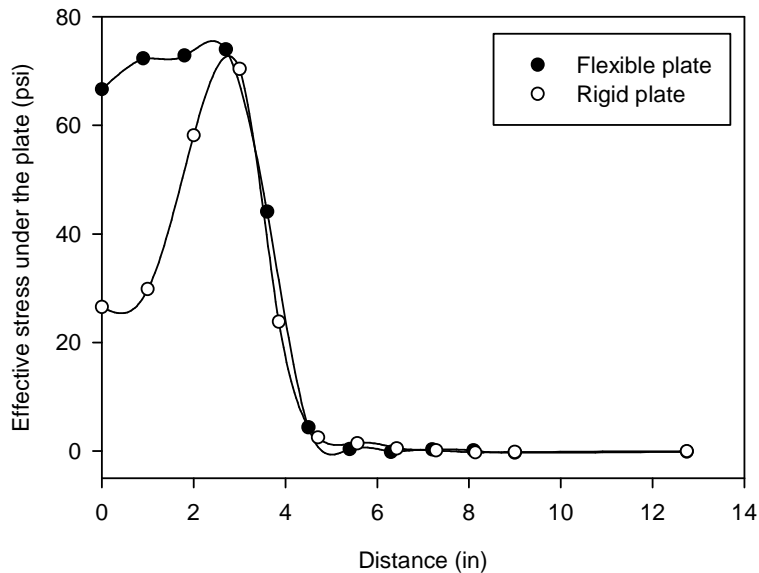


Figure C.7. Effective stress distribution under flexible and rigid plates

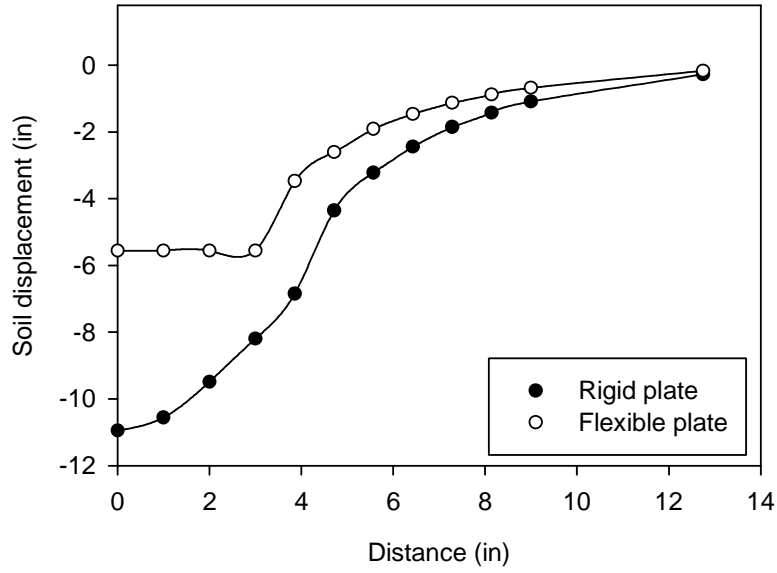


Figure C.8. Soil displacement resulting from applying a static load over rigid and flexible plates

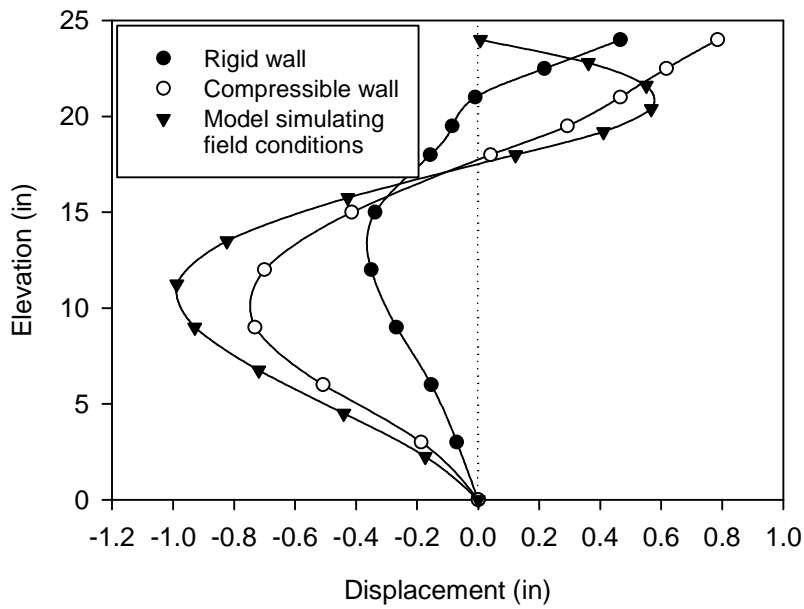


Figure C.9. Vertical soil displacement measured at the model boundary

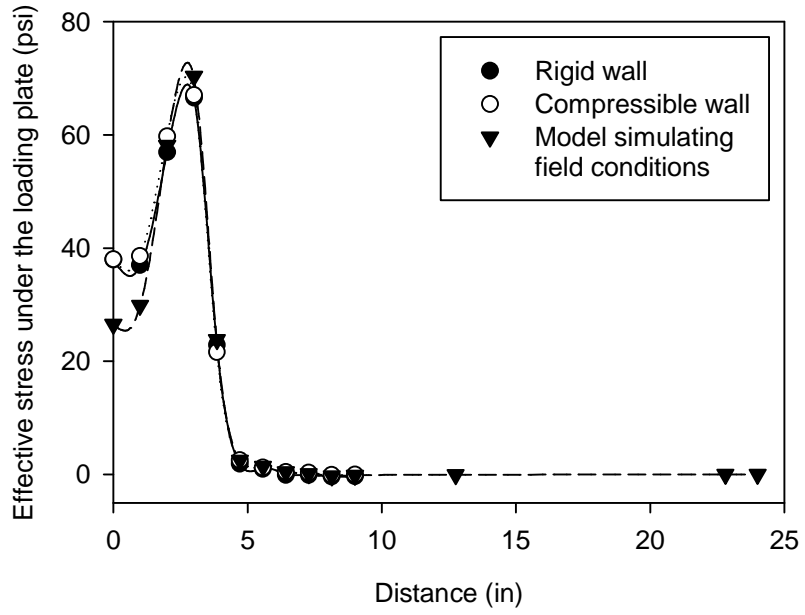


Figure C.10. Effective stress distribution for the finite element models